A STUDY OF A TRANSCRITICAL MULTI-STAGE CARBON DIOXIDE HEAT PUMP

AYMAN G. M. IBRAHIM

A Thesis submitted for the degree of

Doctor of Philosophy

Department Of Mechanical Engineering
University Of Strathclyde
Glasgow, UK

January 2004

Declarations of Author's Rights

Dedication

To my daughters:

Khadeja and Aa'isha

ABSTRACT

The author believes CO_2 to be a promising future refrigerant due to the threat to the HFCs of restriction or elimination posed by legislation planned in many countries. This thesis addresses the feasibility of using reciprocating compressors in a transcritical CO_2 heat pump working in cooling and/or heating modes through the use of computer modeling. A detailed simulation model of a reciprocating compressor is combined with semi-detailed gas cooler, evaporator and internal heat exchanger models to produce complete cycle model of systems having one and two stages of compression. Measured data from the open literature for CO_2 compressors and single-stage heat pumps was used to validate the models.

Piston ring-cylinder leakage and valve dynamics are included in the compressor model. The influence of ring-cylinder clearance on heat pump performance is investigated as is the influence of heat pump running conditions on valve dynamics.

Prior to this study, there were no models known to the author for CO_2 heat pumps which incorporate a detailed simulation of the compression process. Furthermore, there were no models for CO_2 heat pumps incorporating multi-stage compression. This study provides insight into the manner in which a CO_2 heat pump might perform in both cooling and heating modes for running conditions representing summer and winter.The models are believed to be of value to other research workers, plant designers and plant operators.

As a result of this study, useful techniques have been provided for the design and manufacture of environmentally safe and energy efficient heat pump systems; it is hoped that they will make a positive contribution to the reduction of effects harmful to the environment and its inhabitants in the future.

ACKNOWLEDGEMENT

Thanks are due to Allah before and after.

The author wishes to express his sincere gratitude to Dr. John Fleming for his supervision, expert advice and guidance throughout the work.

The author is particularly indebted to his country, Egypt, for the financial support during this work.

The author also wishes to express his deep appreciation to his parents and his wife who supported and encouraged him eagerly.

Thanks go to anyone else who has given help either explicitly or implicitly.

CONTENTS

LIST OF FIGURES

LIST OF TABLES

NOMENCLATURE

The following symbols are used in this thesis, and are defined where they first appear in the text. Some symbols have been assigned more than one meaning, but it will be evident from the context.

Symbol	Description	Unit
<u>Latin Letters</u>		
A	area	m^2
A_f	flow area of valve gap	m^2
A_F	valve equivalent (effective) force area	m^2
A_p	piston cross sectional area	m^2
A_v	valve surface area	-
A_Ω	cylinder wall surface area	-
c_p	specific heat at constant pressure	J/kg K
c_v	specific heat at constant volume	J/kg K
C_D	pressure drag coefficient	-
C_f, K	flow or discharge coefficient	-
C_{oil}	oil correction factor	-
C_{stick}	sticktion coefficient	-
COP	coefficient of performance	-
d_p	valve port diameter	m
D	diameter	m
D_S	diameter of suction line	m
E	energy	J
EER	energy efficiency ratio	Btu/hr W
F, f	friction coefficient	-
f_h	hydraulic drag coefficient	-
f_i	inertia drag coefficient	-

F_0	spring pre-load	N
F_g	gas force	N
F_{stick}	sticktion force	N
Fr	Froude number	-
g	gravitational acceleration	m/s^2
G	mass flux	$kg/m^2 s$
h	specific enthalpy (or heat transfer coefficient or height)	J/kg (or W/m^2 K or
k	spring stiffness (or thermal conductivity)	N/m (or N/m K)
l	length of connecting rod	m
L	piston ring width	m
L_S	length of suction line	M
$LMTD_i$	log mean temperature difference of section/segment	K
m	mass	kg
M	total mass of the refrigerant released	kg
n	polytropic index	-
N	compressor speed	rpm
Nu	Nusselt number	-
P	pressure	kPa
Pr	Prandtl number	-
PW	power	W
q	cooling/heating effect	J/kg
q_0	throttling loss	J/kg
q_{wall}	heat flux density through tube wall to fluid	J/m^2 K
Q	heat (or cooling/heating capacity)	J (or W)
r	crank radius	m
R	gas constant (or thermal resistance or viscous damping coefficient)	J/kg K (or K/W or N s/m)
Re	Reynolds number	-
s	specific entropy	J/kg K
SVR	swept volume ratio	-
t	time (or HTF temperature)	s (or ^{0}C)
T	temperature	K (or ^{0}C)

T_m	thermodynamic average heat rejection temperature	K
u	specific internal energy (or characteristic velocity)	J/kg (or m/s)
U	overall heat transfer coefficient	W/m^2 K
v	specific volume	m^3/kg
V	volume	m^3
w	specific work	J/kg
w_g	swirl velocity	rad/s
W	work	J/kg
We	Weber number	-
x	refrigerant vapor quality	-
X_{tt}	Lockhart-Martinelli parameter	-
y	compressor valve displacement	m
y_0	maximum valve lift	m
z	piston displacement	m
Z	head	m

Greek Letters

α	amount of CO_2 released in generating electricity	kg CO_2 / kWh
β	energy consumption of the system during its whole lifetime	kWh kg/m^3
γ	isentropic exponent	-
Δ	change in	-
ε	effectiveness	-
η	efficiency	-
θ	angular displacement	rad
λ	ratio of crank radius to connecting rod length	-
μ	dynamic viscosity	N/m
ξ	local pressure drop	-
ρ	density	kg/m s
σ	surface tension	-
Φ	two phase multiplier	-
Ω	crank angular speed	rad/s

Subscripts

act	actual
av, m	average
c	compressor (or gas cooler)
ch	cylinder head
cl	clearance
cv	convective (or control volume)
d	down stream (or discharge)
D, dis	discharge
dvc	discharge valve close
dvo	discharge valve open
e	evaporator (or equivalent)
elec	electrical
h	isenthalpic
hx	heat exchanger
i	inlet
ind	indicated
l	leakage (or liquid)
LO	liquid only
mech	mechanical
nb	nucleate boiling
o	outlet
p	piston
r	refrigerant
s	isenthalpic (or suction)
S, suc	suction
svc	suction valve close
svo	suction vale open
th	theoretical
TP	two-phase
u	upper stream
v	vapor

Superscripts

.	time rate of change
-	mean value

LIST OF ABBREVATIONS

BWR	Benedict-Webb-Rubin
CFC	Chlorofluorocarbon
COHEPS	CO_2 Heat Pump Systems
CSD	Carnahan-Starling-DeSanits
DGWP	Direct Global Warming Potential
ECS	Extended Corresponding States
ECU	Environmental Control Unit
EXV	Electronic Expansion valve
FCHV	Fuel Cell Hybrid Vehicle
HC	Hydrocarbon
HCFC	Hydrochlorofluorocarbon
HFC	Hydrofluorocarbon
HP	High Pressure
HPWH	Heat Pump Water Heater
HTF	Heat Transfer Fluid
HVAC	Heating Ventilation Air Conditioning
ICEC	International Compressors Engineering Conference
ID	Indoor
IDGWP	Index of Direct Global Warming Potential
IDLH	Immediately Dangerous to Life or Health
IEA	International Energy Agency
IHX	Internal Heat Exchanger
IPCC	Intergovernmental Panel on Climate Change
LP	Low Pressure
LXV	Level-control Expansion Valve
MBWR	Modified Benedict-Webb-Rubin
OD	Outdoor
ODP	Ozone Depletion Potential

RACE	Refrigeration and Automotive Climate under Environmental Aspects
SCHX	Subcooling Heat Exchanger
TDC	Top Dead Center
TEWI	Total Equivalent Warming Index
TLV	Threshold Limit Value
TR	Ton of Refrigeration (= 12000 Btu/hr)
TXV	Thermostatic Expansion valve
VCC	Vapor Compression Cycle

Chapter 1

Introduction

1.1 General background

Refrigeration and heat pumping play an important role in modern human life. They not only offer a comfortable and healthy living environment but also offer great advantages in severe weather conditions. The accelerated technical development and the economic growth of most countries during the last century have produced severe environmental problems. We have recognized the fact that man-made products, while contributing to human comfort, have side effects which threaten our health as a result of harming the environment by causing ozone depletion and global warming. The desire to limit man-made climate change is the major driving force for the technical innovation and future development of the refrigeration and heat pumping industry.

1.1.1 Refrigerants and environmental impacts

The impact of refrigerants on the environment can be divided into the following points (Steimle et al. 1999a):

1. Toxicity to human beings and animals
2. Influence on biological and genetic areas
3. Odours
4. Flammability and explosiveness
5. Direct impact on the global warming
6. Total energy due to plant construction, operation and refrigerant manufacture.
7. Possible influence on the ozone-layer

Over the years more than 50 chemical substances have been used as refrigerants in compression type refrigeration and heat pump systems, with varying degree of success. The very first machines, as developed by Perkins in 1834 and later Harrison

1856 used ether (or "a fluid for cleaning printing types"), which was neither safe nor particularly suitable for the purpose. More appropriate compounds, carbon dioxide CO_2, ammonia NH_3 and sulphur dioxide SO_2, were introduced in the 1870s and 1880s, and dominated the trade for a substantial period (Lorentzen 1994a).

In the early 1920s concerted efforts were made to find substitutes of the commonly used toxic refrigerants: ammonia, sulphur dioxide, methyl chloride, etc. Charles Kettering and Thomas Migley finally succeeded in inventing chlorofluorocarbons (CFCs) in 1928 as suitable refrigerants. Halocarbon, CF_2Cl_2 (CFC-12), took over much of the market from 1932 on. After the Second World War only one of the old refrigerants, ammonia, was still used extensively in large industrial systems, all other fields were completely dominated by the new refrigerants which were primarily CFCs and hydrochlorofluorocarbons (HCFCs).

CFCs and HCFCs were belived to be incapable of causing harm to life, were very stable, non-toxic and non-flammable.

1.1.1.1 Ozone Depletion Potential

The first major environmental concern to strike the refrigeration and heat pumping industry was due to depletion of the ozone layer as the result of the emission of man-made chemicals into the atmosphere. The first evidence that man-made chemicals containing chlorine destroy the earth's ozone layer was discovered by scientists as early as in the 1970's. Rowland and Molina (1974) presented the theory that the halocarbons could be broken up by sunlight in the stratosphere to release chlorine which united with ozone thus removing it as a protective barrier which prevented ultra-violet radiation, dangerous to life, from reaching the earth surface. Subsequently, an extensive worldwide programme of stratospheric ozone monitoring confirmed the existence of a pattern of depletion which is most pronounced over the Antarctic during springtime. It took more than a decade before this state of affairs was accepted as a proven fact.

1.1.1.2 Global Warming

The second major environmental concern is global warming. Global warming arises because of the greenhouse effect. The frequency distribution of the radiation from the sun closely approximates that from a black body at a temperature of about 5800 K. The spectrum wavelengths range from the less than 1 nm to hundreds of meters; the peak in the spectrum is in the visible region at about 500 nm. When solar radiation (1360 W/m^2) arrives at the earth, about 30% is reflected back into space and most of the remainder passes through the atmosphere to the ground. This heats up the earth, which then behaves approximately as a black body, radiating energy with a spectral peak in the infrared. This infrared radiation cannot pass through the atmosphere because of absorption by water vapor, carbon dioxide and the other infrared absorbers. As a consequence, heat energy is trapped and the temperature at the surface of the earth is higher than it would be without the insulating blanket of the atmosphere.

Global warming is a good thing in itself and allows life to exist in all its varieties. The concern is that man's activities are increasing the concentration of carbon dioxide and other greenhouse gases in the atmosphere, so causing the amount of absorbed infrared radiation to increase, and leading to increased atmospheric temperatures and consequent long-term climate changes.

There are two types of global warming effect. The first one is the Direct Global Warming Potential (DGWP) due to emission of refrigerants into the atmosphere. The second is the Indirect Global Warming Potential (IDGWP) due to emission of CO_2 by consuming the energy, which is obtained by combustion of fossil fuels. The combined effect of these two global warming potentials is called the Total Equivalent Warming Impact (TEWI). The GWP of a refrigerant is not the proper criterion to use in judging the impact of a refrigeration or heat pump system on global warming. The main reason is that in most countries most of the global warming due to refrigeration and heat pump systems (including air-conditioning) is due to the CO_2 released during the production of the electricity required for its

operation. A much better criterion for a refrigerant in a particular system is the TEWI (Steimle et al. 1999a):

$$TEWI = GWP \times M + \alpha \times \beta$$

where, GWP GWP of the fluid, relative to CO_2 (GWP CO_2 = 1)

M total mass of the refrigerant released (kg)

α amount of CO_2 released in generating electricity (kg CO_2 / kWh)

β energy consumption of the system during its whole lifetime (kWh)

The TEWI is directly dependent on how electricity is produced i.e.:

- if all energy comes from hydraulic power generation, $\alpha = 0$
- if electric power derives from fuel, α is around 0.6 - 0.8 kg CO_2 / kWh (depending on the types and efficiencies of the power stations)

Governmental response has been to accept that the man-made global warming issue is real, and to set targets for reducing greenhouse gas emissions. The target has been established by the United Nations Intergovernmental Panel on Climate Change (IPCC), founded in 1988. They are to be found in their reports from a series of Earth Summits and Global Warming Conferences at Sundsvall, Rio de Janeiro, Berlin, Kyoto and Buenos Aires, in 1990, 1992, 1995, 1997 and 1998, respectively (see the IPPC website at www.ipcc.ch). The targets are couched in terms of reducing greenhouse gas emissions to 1990 levels by some date after 2000.

The Koyto Agreement (1997) was established to reduce emissions of global warming gases. As shown in Table 1.1, greenhouse warming occurs when the carbon dioxide is released mostly from the burning of fossil fuels (oil, natural gas and coal). The release of other gases such as methane CH_4, nitrous oxide N_2O, ozone O_3, CFCs, HCFCs and water vapor also contribute (Hartmann 1994).

The direct contribution of HCFCs to global warming is smaller than that of CFCs but still much larger than that of natural refrigerants. The relative contributions of DGWP and IDGWP in different applications are shown in Table 1.2 (Cavallini 1996)

Table 1.1 Contribution of gases to the greenhouse effect (%)

Gases	CO_2	CH_4	N_2O	O_3	CFCs and HCFCs	H_2O
Man-made gases in 1988	52	22	16	2	8	-
Natural greenhouse effect	23	2	2	3	-	70

Table 1.2 DGWP and IDGWP portion in different applications (%)

Application	Household Refrigerator	Automotive a/c	Retail Refrigerator	Unitary a/c	Commercial Chiller
DGWP	4	30	44	10	2
IDGWP	96	70	56	90	98

As can seen in this table, IDGWP is much larger than DGWP. IDGWP results from burning fossil fuels to generate energy. Policies to reduce global warming force industries to develop technologies that will reduce energy consumption. Therefore, it is important to develop alternative refrigerants which have lower DWGP and lower, or at least equivalent IDGWP.

1.1.2 Natural refrigerants as alternatives

Presently, the most pressing research issue in the field of refrigeration and heat pumping systems is the search for new and environmentally acceptable working fluids which can replace the CFCs and HCFCs. Most of the substances considered are new synthetic compounds, namely pure hydrofluorocarbons (HFCs) and binary/ternary HFC blends. Even though these new compounds are extensively tested with regard to toxicity, flammability etc., they are synthetic and not natural. Consequently, widespread use of these fluids will always include a risk of unforeseen global environmental effects, as has already been experienced with CFCs and HCFCs. Moreover, the HFCs are already known as relatively strong greenhouse gases (Greenhouse Warming Potential ranging from 1300 to 3800 for the most common HFCs). The environmental effects of selected refrigerants are shown in Table 1.3 (McMullan 2002).

Table 1.3 Environmental effects of refrigerants

Refrigerants		ODP (CFC-11 = 1)	DGWP (CO_2 = 1)
CFCs	CFC-11	1	3800
	CFC-12	1	8100
	CFC-114	0.8	9300
HCFCs	HCFC-22	0.055	1700
	HCFC-123	0.02	90
	HCFC-124	0.022	480
	HCFC-141b	0.11	630
HFCs	HFC-134a	0	1300
	HFC-245fa	0	900
	HFC-134	0	1300
	R-407C (HFC-32/125/134a)	0	1600
	R-410A (HFC-32/125)	0	1900
Natural Refrigerants	Air (R-729)	0	0
	Water (R-718)	0	0
	Carbon Dioxide (R-744)	0	1
	Ammonia (R-717)	0	0
	Propane (HC-290)	0	3
	Butane (HC-600)	0	3

This has prompted researchers worldwide to consider the development of new refrigerants and/or the investigation of refrigerants occurring naturally in the environment. However, the development of chemically manufactured fluids to be used as refrigerants may result in the same dilemma the world currently faces with several fluorocarbons based refrigerants. There is no possible way of knowing the long term environmental or health impact of synthesised refrigerants with absolute certainty. The use of substances which are found naturally in the biosphere as a refrigerant eliminates the need for such speculation.

It is nothing new that synthetic chemicals, which are foreign to nature, cause unexpected problems when they are released into the environment. Chlorine destroys the ozone layer; fluorine by comparison gives very stable molecules, which contribute to global warming. Hydrogen in the molecule gives less stable structures and leads to flammable fluids. Toxicity in this group of chemicals only occurs with molecules including chlorine. An alternative strategy is to apply naturally occurring and ecologically safe substances, such as air, water, nitrogen, the noble gases, hydrocarbons, ammonia and carbon dioxide. As a result, all uncertainties and potential negative effects on the global environment of direct release will be eliminated. However, the growing acceptance of the TEWI as the measure of a working fluid's contribution to global warming also takes into account the plant energy efficiency which is influenced by the working fluid. Consequently, the main challenge when applying natural working fluids is to build safe and reliable systems that are able to compete with conventional HFCs systems with regard to energy efficiency and first costs.

There are several refrigerant candidates in the group of natural substances, such as air, water, nitrogen, hydrocarbon, ammonia and carbon dioxide. Many of these are already in use but could be used more within the present applications, and also extended into new applications. Other substances have been used in the past but should be looked at closer since the technology in the refrigeration and heat pumping industry, e.g. knowledge of materials, production methods etc. has changed since they last were used.

Annex 22 of the International Energy Agency (IEA) implemented a three year project, " Compression Systems with Natural Working Fluids", in 1995. In this program, natural refrigerants such as ammonia, hydrocarbons, carbon dioxide, water and air are being studied (Stene 1996). These natural refrigerants have a low or zero DGWP, zero ODP and no adverse environmental effects, as shown in Table 1.4 (Lorentzen 1995).

Table 1.4 Characteristics and properties of some refrigerants

Refrigerants	CFC-12	HCFC-22	HFC-134a	R-717	R-290	R-744
Natural Substance	No	No	No	Yes	Yes	Yes
ODP	1	0.05	0	0	0	0
GWP	7100	1500	1200	0	0	1
TLV[1]	1000	1000	1000	25	1000	5000
IDLH[2]	50000	-	-	500	20000	50000
Amount per room vol.[3] (vol.% / kg m^{-3})	4/0.2	4.2/0.15	-	-	0.44/ 0.008	5.5/0.1
Flammable or Explosive	No	No	No	Yes	Yes	No
Flammability Limits in Air (vol. %)	-	-	-	15.5/27	2.2/9.5	
Toxic/irritating decomposition products	Yes	Yes	Yes	No	No	No
Approx. Relative Price	1	1	3-5	0.2	0.1	0.1
Molar Mass	120.92	86.48	102.03	17.03	44.1	44.01
Vol. Refri. Capacity[4] at 0 ^{0}C (kJ/m^3)	2740	4344	2860	4360	3870	22600

[1] TLV: Threshold Limit Value, The refrigeration concentration limit in air for a normal 8-hour workday, will not cause an adverse effect in most people.

[2] IDLH: Immediately Dangerous to Life or Health, Maximum level from which one could escape within 30 minutes without impairing symptoms or any irreversible health effects.

[3] Maximum refrigerant Charge in relation to refrigerated room volume.

[4] Enthalpy of evaporation divided by saturated vapor volume.

1.2 Revival of carbon dioxide

1.2.1 Historic view

Application of Carbon dioxide as a refrigerant is not a new idea. CO_2 was first solidified in 1835 by the French physicist Thilorier and used as cooling medium (dry ice) (Strommen et al. 1999). Though the Evans-Perkins process, upon which modern refrigerators and heat pumps are based, was developed in 1834, it wasn't until 1866 that the American Thaddeus S.C. Lowe first harnessed carbon dioxide for ice

production. Following a period of further development, the first documented carbon dioxide compressor was built by Windhausen in 1880. Other landmark uses of carbon dioxide refrigeration include the first marine installation of a carbon dioxide plant by J&E Hall in 1890 and the first continuous production of carbon dioxide refrigerating equipment in the United States by Kroeschell Bros. of Chicago in 1897 (Pettersen 1995).

Not only were carbon dioxide machines growing in popularity in the late 1800s, but also improvements were continually being made to the basic cycle. J&E Hall demonstrated that the efficiency of the vapor compression process could be improved through the use of two-stage compression. In 1905, Voorhees developed what is now known as the multiple effect cycle, which involves a separation of liquid and vapor at an intermediate stage in the expansion process (Lorentzen 1994a).

The advent of refrigeration and heat pumping in the late 1800s had an enormous impact on numerous industries. At the time, carbon dioxide was the only refrigerant used. Ammonia and sulphur dioxide machines enjoyed a level of popularity, but generally only in industrial applications due to their toxicity and/or flammability. No such hazards are inherent in carbon dioxide apart from care needed in confined spaces. For that reason food-related industries and places of human occupancy (theatres, hospitals, restaurants, etc.) used carbon dioxide refrigerators/heat pumps almost exclusively. Though they used technology primitive by today's standards, carbon dioxide machinery functioned satisfactorily and generally pleased those who purchased it. However, engineers' desire to improve system efficiency led to the development of fluorocarbons in the 1930s. Cycles which employed fluorocarbons had substantially lower heat rejection pressures than those of carbon dioxide (requiring less compressor work, which in turn led to better efficiency). Considered to be non-toxic to humans and harmless to the environment, fluorocarbons quickly replaced carbon dioxide as the refrigerating fluid of choice. Furthermore, unfortunate aspects of carbon dioxide such as lower cooling capacity, and reduced COP at higher ambient temperature were reported later when carbon dioxide was compared with

other refrigerants. As a result, Carbon dioxide machinery was phased out and has not been mass-produced since.

1.2.2 Advantageous aspects of carbon dioxide as a refrigerant

Carbon dioxide is a substance whose properties are very well known. It exists naturally in the biosphere and has already been used as a refrigerant. In addition to these highly desirable features, carbon dioxide has several advantages such as:

1. ODP is zero.
2. Non-flammable and non-explosive.
3. Non-toxic and non-irritating decomposition products.
4. Excellent thermodynamic properties.
5. The price is a fraction of today's available refrigerants.
6. Greatly reduced compression ratio compared with conventional refrigerants.
7. Compatibility with normal lubricants and common machine construction materials.
8. Simple operation and service, no recycling required, very low price.
9. Carbon dioxide cycle components are smaller and lighter than those of conventional refrigerants due to operation at high density.

In the field of synthetic substances, it appears that no further choices remain. Only the natural substances are available, namely: ammonia, hydrocarbons, air, water and carbon dioxide. Given the toxic and/or flammable nature of ammonia and the hydrocarbons, the poor efficiency of air and limited range of applications of water, many research workers around the world have pinned their hopes on carbon dioxide, a benign fluid if simple precautions are taken.

The major problem with carbon dioxide as a refrigerant is caused by its relatively low critical temperature of 31 ^{0}C. As the critical temperature is approached or exceeded, a loss of efficiency occurs when compared with conventional phase change substances. However, given the very large pressure differences in CO_2 compressors, this is compensated to some extent by an improved compressor performance as a result operating at a low pressure ratios natural for carbon dioxide.

Pearson (1999) reported that isentropic efficiency is reduced at high pressure ratio because the compressor geometry cannot be optimised. Objective comparisons between reciprocating and screw compressors with R-717 at different pressure ratios were presented by Villadsen (1985). Isentropic efficiency of both compressors decreased when the pressure ratio was increased. Similar behaviour was reported by Fleming et al. (1999) for R-134 reciprocating compressor. For CO_2 compressors, the above trend was verified experimentally through the work of many researchers, e.g. Pettersen (1997), Neksa et al (1998), Neksa et al. (1999), Dorin and Neksa (2000), Ohkawa et al. (2002), Baumann (2002), Hubacher et al. (2002), Süss (2002) and Försterling et al (2002).

One way to improve efficiency is by staged compression and expansion. Another tempting solution lies in recovering work from the expansion using a suitable device needed to re-establish the low temperature state of the refrigerant.

Carbon dioxide is a greenhouse gas. However, when used as a refrigerant, the quantities are small. Table 1.3 shows that its effect is minute compared to that of halocarbons. In practice, gas will be used which is already available as a waste product in quantity from other activities. Its release into the atmosphere is delayed by its use as a refrigerant. This is in principle good for the environment, like planting a tree to bind carbon for a period of time. With regard to personal safety, CO_2 is a safe refrigerant, provided that the well-known procedures for using it in confined spaces are followed. In the case of accidental loss of a large quantity, a good ventilation system is required in order to prevent the concentration rising above 5.5%, the level at which it becomes dangerous to humans. Halocarbons are also dangerous when released into a confined space; suffocation can result from the displacement of air and essential organs like the heart are adversely affected by large concentrations.

The high pressure levels in carbon dioxide plant can be handled safely by normal professional engineering competence (maximum pressures: halocarbon plant 30 bar, carbon dioxide 140 bar). However, reduced weight and size are potential advantages. Pressurised carbon dioxide gas within the system can also be applied as a fire

extinguisher in case of fire. The inner volume of carbon dioxide plant is also decreased according to the high density compared to halocarbon systems. So the energy released i.e. inner gas volume multiplied by the gas pressure in a rupture should not be much higher than for plants with today's refrigerants.

1.2.3 Recent work on carbon dioxide

Following its neglect as a refrigerant for virtually half a century, carbon dioxide was revived at the beginning of the 1990s by Scandinavian research groups (Lorentzen et al. 1993, Pettersen et al. 1994, Neksa 1994). Triggered by their publications, numerous research groups all over the world started research efforts utilizing carbon dioxide as a refrigerant. A vast research activity has been provoked and about 20 research areas have been investigated (Fleming 2003). The areas chosen for research effort reflect the opinions of publishing authors as to which are most promising.

Research on carbon dioxide cycles is mainly carried out for water heater heat pumps, and for a/c in residential and mobile systems. Water heating is a very promising application as the temperature rejection of the carbon dioxide cycle takes place over a temperature range, called the temperature glide, matching the water side better than a conventional cycle. Carbon dioxide could be an appropriate refrigerant for mobile a/c where the size and weight of components are under tight constraints. The high volumetric heat capacity of carbon dioxide compared with current refrigerants is an advantage. Utilization of carbon dioxide in commercial refrigeration and large scale heat pumps has received detailed attention. Promising results were obtained by using carbon dioxide as a secondary fluid or cascaded with other refrigerants (Pearson 2003).

Fundamental work has focused on the measurement and determination of heat transfer and pressure drop correlations for carbon dioxide. Also, a search for suitable gas coolers for the transcritical cycle was reported. This is particularly challenging in the supercritical region close to the critical point where the refrigerant properties change rapidly. Finally, the compression process of carbon dioxide and lubrication behaviour have received careful consideration due to higher pressure differences

compared with conventional refrigerants and the importance of compressor efficiency to cycle performance.

Despite vigorous research, the use of carbon dioxide in the market is still relatively small. Recently, IEA has launched Annex 27 (1999), " Selected issues on CO_2 as a working fluid in compression systems", in an attempt to bring CO_2 technology closer to commercialisation.

1.3 Scope and objectives

Recognition of the role of chlorine in stratospheric ozone depletion, and the determination that CFCs were the primary source of chlorine in the stratosphere, led to the Montreal Protocol and subsequent measures to ensure that the changeover to non-ozone depleting substances is achieved as quickly as possible. Subsequently, attention turned to global warming and once again the halocarbon refrigerants have become targets because of their extremely high global warming potentials. However well the primary objective of limiting the contribution of refrigeration to ozone depletion has been achieved, it is very important to keep things in perspective with regard to global warming which is a separate issue. We must weigh the relatively small contribution arising directly from the working fluid against the much larger contribution from energy consumption for most applications.

To satisfy comfort conditioning of any kind (cooling or heating) by the use of heat pumps, the heat pump has to be capable of meeting demands which vary greatly as dictated by seasons, summer to winter; time, day to night and by the need for a quick pull-down of temperature, in the case of mobile air conditioning for example. Assuming an equal effectiveness in achieving comfort, the heat pump energy consumption will have to be judged against competing systems by its total performance over a standard 12-month period or other appropriate work or life cycle period.

The work reported here includes the development of a computer model for transcritical carbon dioxide heat pump cycles working in cooling and/or heating mode. The focus in this work is on the performance of a conventional reciprocating compressor and its influence on the overall performance of the heat pump.

The motivation for this work was inspired by the belief that the first carbon dioxide compressors to become commercially available will be conventional reciprocating compressors. Delaying action until scrolls etc. are available would, the author believes, delay the introduction of carbon dioxide systems and thereby grant time to the developers of systems using synthetic refrigerants in which to strengthen their grip on their (currently overwhelming) market share. The author believes that a world-wide ban on synthetic refrigerants is unlikely, hence carbon dioxide systems will have to compete in the market in the normal way except of course in the (probably) few countries that ban synthetics. In such countries the success of carbon dioxide will be guraanteed.

1.3.1 Scope

This thesis addresses the feasibility of using a reciprocating compressor for a transcritical carbon dioxide heat pump working in cooling and/or heating mode through the use of computer modeling. This was accomplished by developing computer models describing the performance of the components which constitute a transcritical vapour compression carbon dioxide cycle (hereafter called the transcritical CO_2 cycle). These component models were combined into an overall cycle model which simulate the performance of a transcritical CO_2 cycle. The thermodynamic predictions of the overall cycle model were then validated by comparing its performance to published experimental data. Once validated, the overall cycle model was used to simulate the operation of a CO_2 heat pump working in cooling and/or heating modes.

A complete cycle model, which predicts energy consumption reasonably well for a wide range of operating conditions is needed. Clearly, a detailed compressor simulation was required in addition to the cycle model, given that a comprehensive

design tool needs both. It's worth noting that phase change heat exchanger design, despite being a long-established activity, still depends on calculations of wide uncertainty, ± 30% being not uncommon. The industry has become skilled in dealing with such uncertainties. Given the inaccuracy of the calculation for the heat transfer components, the tolerance on the cycle predictions will be wide. But as already stated this is also true of models for competing HFCs systems so judgment is likely to play an important part in ranking for selection.

Hence, it would be wise to give careful consideration to the effort required to achieve highly sophisticated gas cooler and evaporator models; the improvements in accuracy achieved may be small, given the inherent uncertainties in heat transfer calculations. In the work reported here, time constraints left the author with little choice. Semi-detailed models for the gas cooler and the evaporator were unavoidable. In any case, the focus of the work reported here was on the design of a compressor suitable for varied running conditions.

It was not an intention to establish an optimum transcritical CO_2 cycle. The first objective was to explore the performance of a CO_2 heat pump using a reciprocating compressor and working in cooling and/or heating mode throughout the year. Another aim was to uncover the potential of a multi-stage compression process for the transcritical carbon dioxide cycle.

This study provides insight about how a CO_2 heat pump might perform in both cooling and heating mode. Moreover, insight was gained concerning potential two-stage compressor design/modeling problems specific for the transcritical CO_2 cycle. Once an application is chosen the determination of a suitable design for the appropriate range of pressure, temperature and energy demand can be proposed. The variation within these running conditions constitutes the duty profile. A start can then be made on the first trial design, perhaps a plant optimised to suit the most common running conditions (the design point). The behaviour of the heat pump as predicted by the cycle and compressor models, if judged to be satisfactory at the design point,

can then be examined at off-design conditions so that a judgement may be made regarding its general acceptability.

1.3.2 Objectives

Prior to this study, there were no CO_2 heat pump models which simulate the compression process using a detailed reciprocating compressor model. Furthermore, there were no CO_2 heat pump models incorporate two-stage compression. Therefore, this study focused on the evaluation of CO_2 as a working fluid for heat pump working in cooling and/or heating mode and utilize double stage compression technique. The objectives of this study include:

- The development of a detailed simulation tool for transcritical CO_2 system.
- The evaluation of CO_2 two-stage compression transcritical systems and the provision of design tools and guidance for designers.

To accomplish these objectives, sub-objectives had to be reached:

- *Component modeling.* A detailed model of the compressor was developed and validated by comparing its output with published measured data. Semi-detailed models of the evaporator and gas cooler were developed. Simpler models for the expansion process and the internal heat exchanger were presumed. A reciprocating compressor was chosen for the reasons given earlier, e.g. it is likely to be available earlier than other types.
- *The overall transcritical cycle model.* A transcritical CO_2 cycle model with one compression stage was developed by combining the individual component models. Available data representing the performance of a prototype CO_2 residential environmental control unit (ECU) and mobile a/c were used for model validation by imposing the same geometric and environmental conditions on the cycle model and comparing the model results with prototype cycles performance results.
- *Overall transcritical CO_2 single-stage cycle model parametric study.* A parametric study was conducted using the validated CO_2 cycle model for typical conditions for residential ECU operation.

- *Modification of the transcritical CO_2 cycle model for use with multi-stage compression with intercooling.* A review of multi-stage options and possible configurations was conducted. The transcritical CO_2 cycle model was modified to simulate operation with two-stage compression. The two-stage model was used to investigate the performance of systems of this kind.

1.4 Structure of present work

The outline of the the thesis is almost in the same sequence as the sub-objectives described in the former section:

Chapter 2 gives information on the transcritical CO_2 cycle. The range of current CO_2 applications in the field of refrigeration and heat pumping is also presented.

In order to begin properly modelling an efficient CO_2 system, the potential improvements to be derived from transcritical CO_2 cycle were investigated in chapter 3. Also, the research work of this field was reviewed.

Chapter 4 describes the development of a detailed reciprocating compressor simulation model. The model validation and parametric study are also included.

Chapter 5 describes the transcritical CO_2 cycle model which was developed by combining the individual component models. A parametric study followed the model validation against published experimental data.

A two-stage transcritical CO_2 cycle is presented in chapter 6. The multi-staging alternatives were screened and an intercooling technique was selected based on proposed applications. The performance map of the multi-stage system is developed for different operating conditions and is believed by the author to be of value to those whishing to develop heat/cooling systems.

Conclusions and the future work are outlined in chapter 7.

Chapter 2

Transcritical CO_2 Cycle

The objective of the current chapter is to introduce CO_2 as a modern refrigerant in the refrigeration and heat pumping industry. It is divided into three sub-chapters. In the first sub-chapter, the basics of the transcritical CO_2 cycle and its characteristics are presented. A review of the literature concerning the current applications of CO_2 as a modern refrigerant in refrigeration and heat pump systems will be reported in the second sub-chapter. The last sub-chapter will summarize the recent work in CO_2 systems and draw conclusions relevant to the next chapter, chapter 3 which deals with scope for improvements.

2.1 Basics of transcritical CO_2 cycle

2.1.1 Fundamentals

Figure 2.1 shows schematically the main components of a transcritical CO_2 cycle and Figure 2.2 illustrates the cycle process on a P-h diagram. As shown in Figure 2.1, the basic transcritical CO_2 cycle consists of a compressor, a gas cooler, an expansion valve and an evaporator. The transcritical cycle is composed of the same four basic processes that make up the vapor compression cycle (VCC) upon which CFCs and HCFCs are based: compression (1-2), heat rejection (2-3), expansion (3-4) and heat absorption (4-1). The only process which differs from the current conventional VCC is the supercritical heat rejection process. The critical temperature of CO_2 is 30.98 ^{0}C and the critical pressure is 73.83 bars. At high ambient temperatures, in order for CO_2 systems to reject heat to the atmosphere, the temperature (and pressure) of CO_2 will be higher than the critical temperature (and pressure) during the heat rejection process. Consequently, instead of a constant temperature two-phase heat rejection process which occurs with fluorocarbon refrigerants, heat is expelled from CO_2 during a supercritical process. Therefore, a CO_2 system will have to operate in a transcritical cycle most of the time.

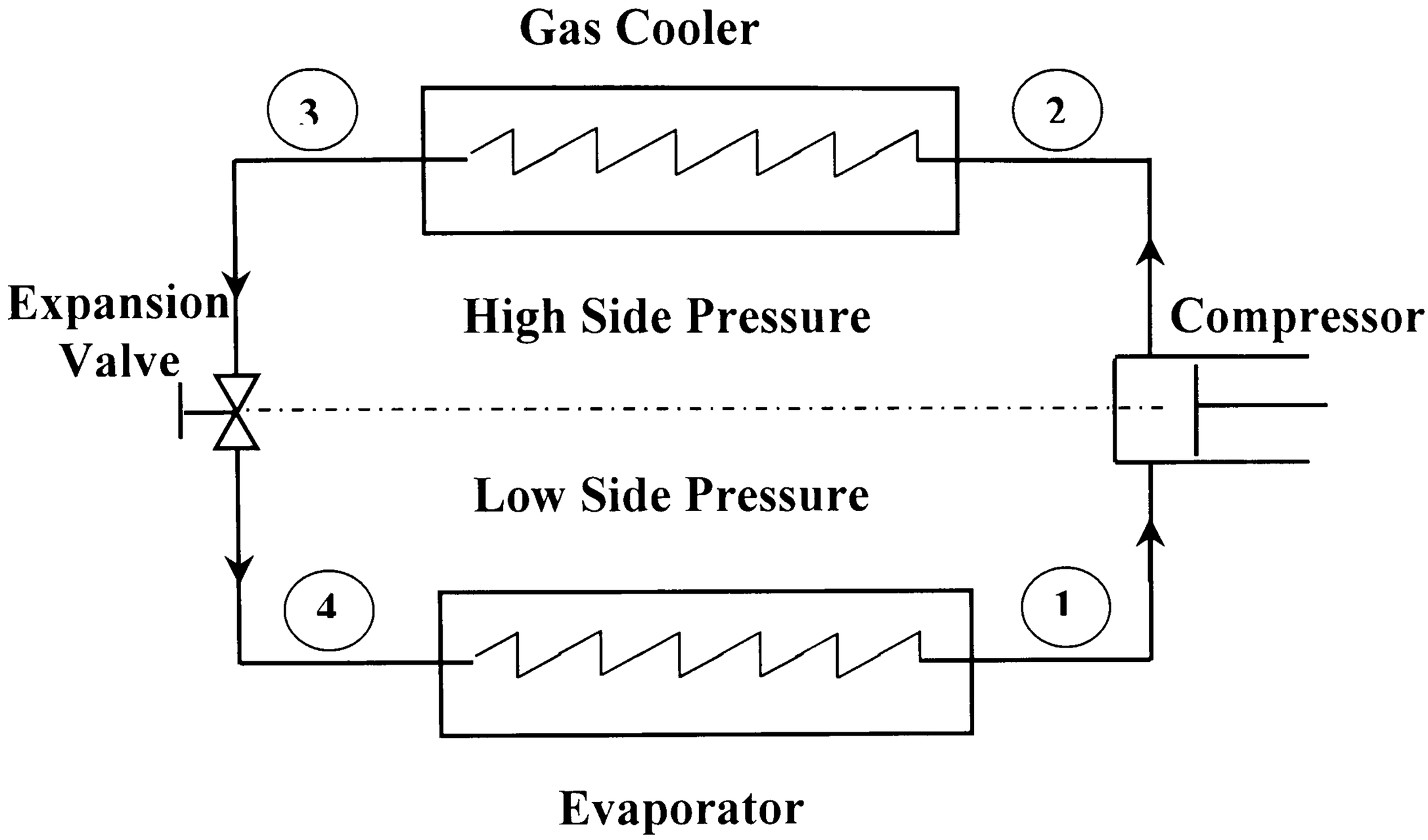

Figure 2.1 Scheme of a basic transcritical CO_2 cycle

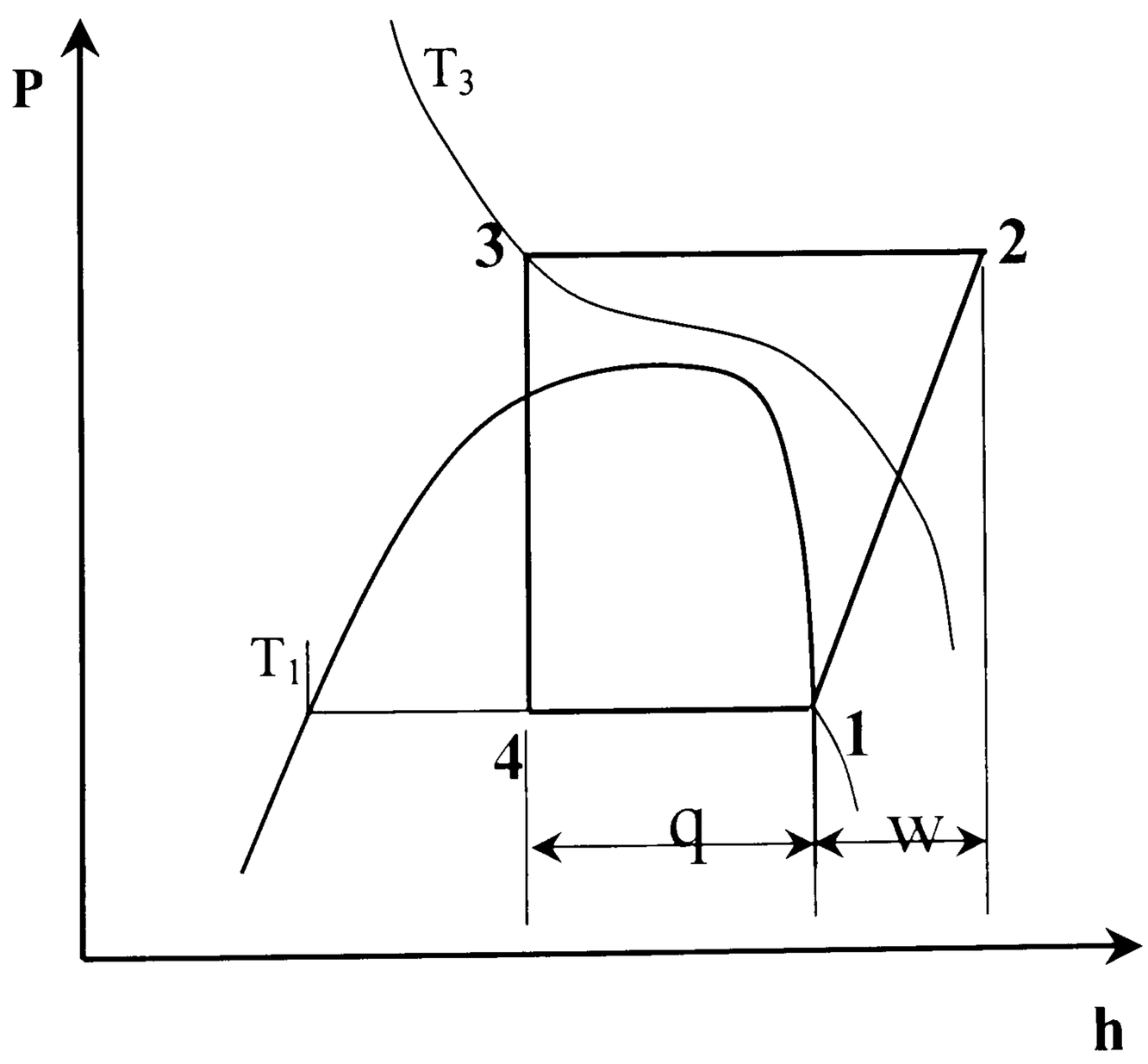

Figure 2.2 P – h diagram of a basic transcritical CO_2 cycle

In the transcritical cycle, the low side conditions will generally remain subcritical. At supercritical pressures a saturation condition does not exist. During the gas cooling process, the CO_2 does not experience a phase change as seen in the two-phase region. However, it is reasonable to say that carbon dioxide changes from a "vapor-like" to a "liquid-like" fluid in the gas cooler. As the carbon dioxide moves through the gas cooler its thermophysical properties change enormously, the rate of change reaching a maximum in the region immediately above the critical point.

Table 2.1 Basic refrigerants properties at –15 ^{0}C

Refrigerant	HCFC -22	HFC -134a	HC -290	R-744	R-717	R-410A
Molecular Weight, kg/kmol	86	102	44	44	17	73
Critical Temperature, ^{0}C	96	101	97	31	133	73
Critical Pressure, bar	49.77	46.67	42.36	73.83	113.53	51.74
Saturated Pressure at –15 ^{0}C, kPa	296	164	292	2288	236	471
Pressure/Temperature Sensitivity, kPa/K	11	7	10	68	10	17
Liquid Specific Heat, kJ/kg K	1.15	1.29	2.41	2.19	4.53	1.41
Vapor Specific Heat, kJ/kg K	0.7	0.82	1.65	1.39	2.42	0.81
Ratio of Vapor Specific Heats	1.27	1.16	1.2	1.76	1.36	1.25
Liquid Density, kg/m^3	1331	1341	549	1008	658	1284
Vapor Density, kg/m^3	13	8.3	6.5	60.6	2.0	19.2
Heat of Vaporization, kJ/kg	214	210	394	268	1313	230
Ratio of Liquid Specific Heat to Heat of Vaporization, 1/K	0.005	0.006	0.006	0.008	0.003	0.006
Liquid Thermal Conductivity, W/m K	0.104	0.102	0.115	0.13	0.552	0.124
Vapor Thermal Conductivity, W/m K	0.092	0.01	0.015	0.015	0.026	0.01
Liquid Viscosity, μPa.s	2540	3463	1469	1397	2234	2079
Vapor Viscosity, μPa.s	110	103	72	142	89	111

Table 2.1 summarizes some of the key thermophysical properties of CO_2 and other common refrigerants at a temperature of –15 ^{0}C, chosen to be representative of evaporators (Charles 1997). Based on data of Table 2.1 CO_2, in particular, is characterised by:

1. Low critical temperature, 40 K – 100 K lower than others listed.
2. High pressure, 14 times as high as HFC-134a and nearly five times as high as R-410A.
3. High vapor density, about 30 times as high as R-717 and 3 times as high as R-410A.
4. High saturated liquid and saturated vapor specific heats, not as high as HC-290 or R-717 but higher than HCFC-22, HFC-134a or R-410A.
5. High vapor specific heat ratio, 25% - 50% higher than the others listed.
6. Moderately high latent heat of vaporization, less than R-717 but comparable to others.
7. High saturation pressure/temperature sensitivity, up to 10 times as high as the others listed.

These attributes have important influences on CO_2 cycle performance and system design. Low critical temperature means that heat rejection will most likely not involve two-phase condensation but will rather occur at a temperature above the critical and will resemble a single-phase process. High pressure and density reduce the diameter requirements for pipes and vessels. High specific heats generally improve heat exchanger effectiveness. High vapor specific heat ratio has a negative effect because it raises the work of compression. High latent heat of vaporization means potentially less refrigerant flow for a given cooling requirement. High saturation pressure/temperature sensitivity results in high line pressure drops and high flow velocities and heat transfer coefficients for given saturation temperature changes.

2.1.2 Transcritical cycle characteristics

Compared to conventional refrigerants, the most remarkable property of CO_2 is the low critical temperature of 30.98 ^{0}C. Heat rejection will, in most cases, take place at

supercritical pressure, causing the cycle to be "transcritical", i.e., with subcritical low-side and supercritical high- pressure side. In a transcritical vapor compression system, the high- pressure side is independent of temperature, and the selection and adjustment of high- pressure side therefore represents a new variable that affects capacity and COP. Other features of the single-stage transcritical CO_2 cycle to be discussed in the following are: high pressure side, high throttling loss, heating capacity and COP characteristics, importance of gas cooler refrigerant exit temperature, compressor efficiency, improved heat transfer coefficients, compactness of equipment, high pressure drops and adaptation to heating and heat recovery applications.

2.1.2.1 High Pressure Side

The pressure at which heat is rejected in a conventional VCC is determined by the condensation temperature, which is primarily determined by the heat sink temperature. The same cannot be said for the transcritical cycle since there is supercritical heat rejection over a range of temperature instead of two-phase heat rejection at constant refrigerant temperature.

Figure 2.3 shows the influence of high-pressure side variation on specific cooling capacity (q), specific compressor work (w) and COP, assuming constant evaporating temperature (T_1) and gas cooler exit temperature (T_3). The heat rejection pressure influences both the compressor work and amount of heat which can be absorbed by the evaporator. For a fixed gas cooler exit temperature, as the heat rejection pressure increases from the critical pressure, the heat which can be absorbed by the evaporator increases due to the fact that the refrigerant specific enthalpy exiting the gas cooler decreases, reducing the specific enthalpy entering the evaporator. In addition, as the heat rejection pressure increases from the critical pressure, the work required to drive the compressor also increases. As a function of heat rejection pressure, the heat absorbed by the evaporator increases faster than the work required to drive the compressor, hence the COP increases. A heat rejection pressure exists at which the COP reaches a maximum, and then begins to fall.

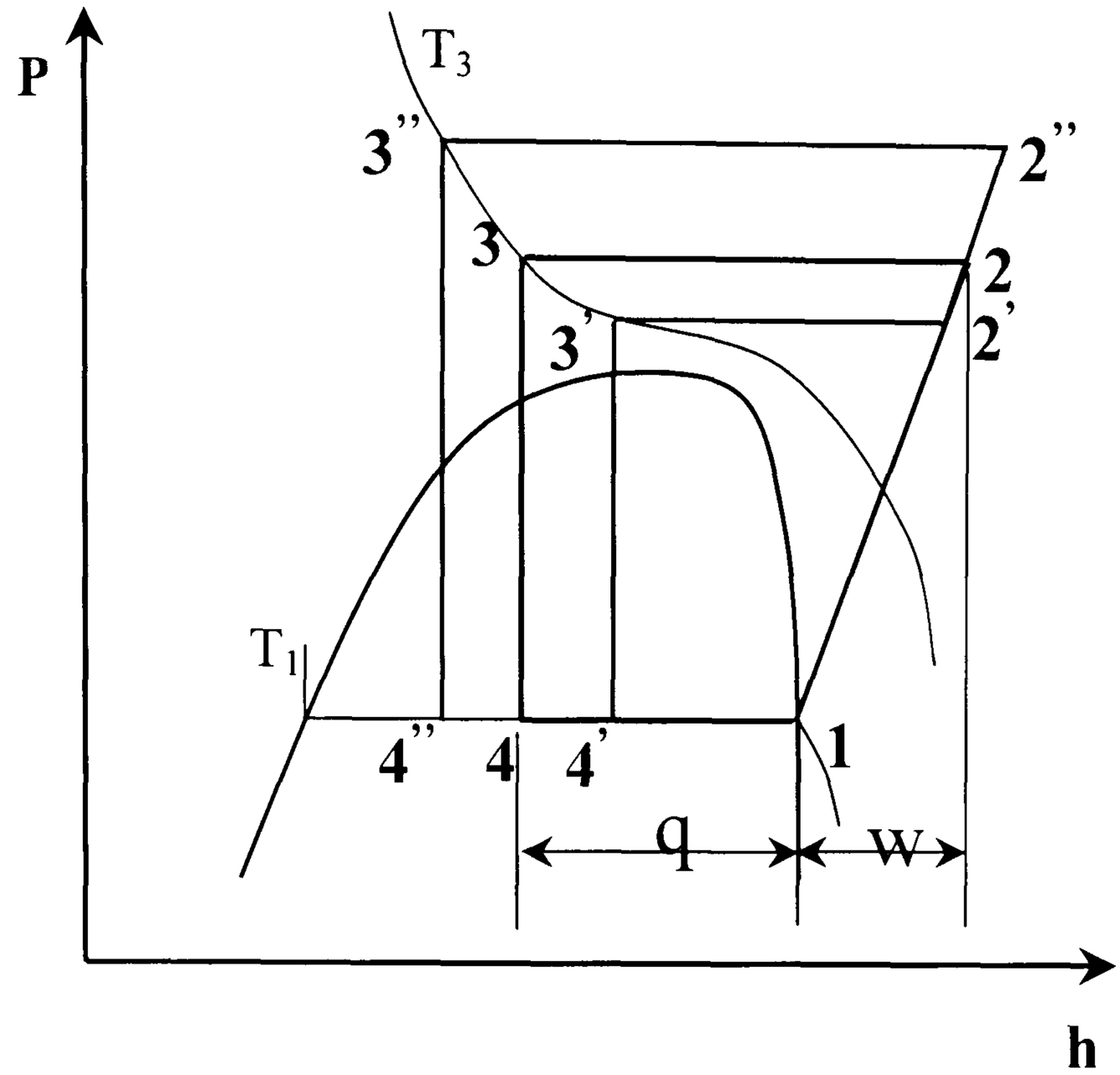

Figure 2.3 Effect of high pressure side

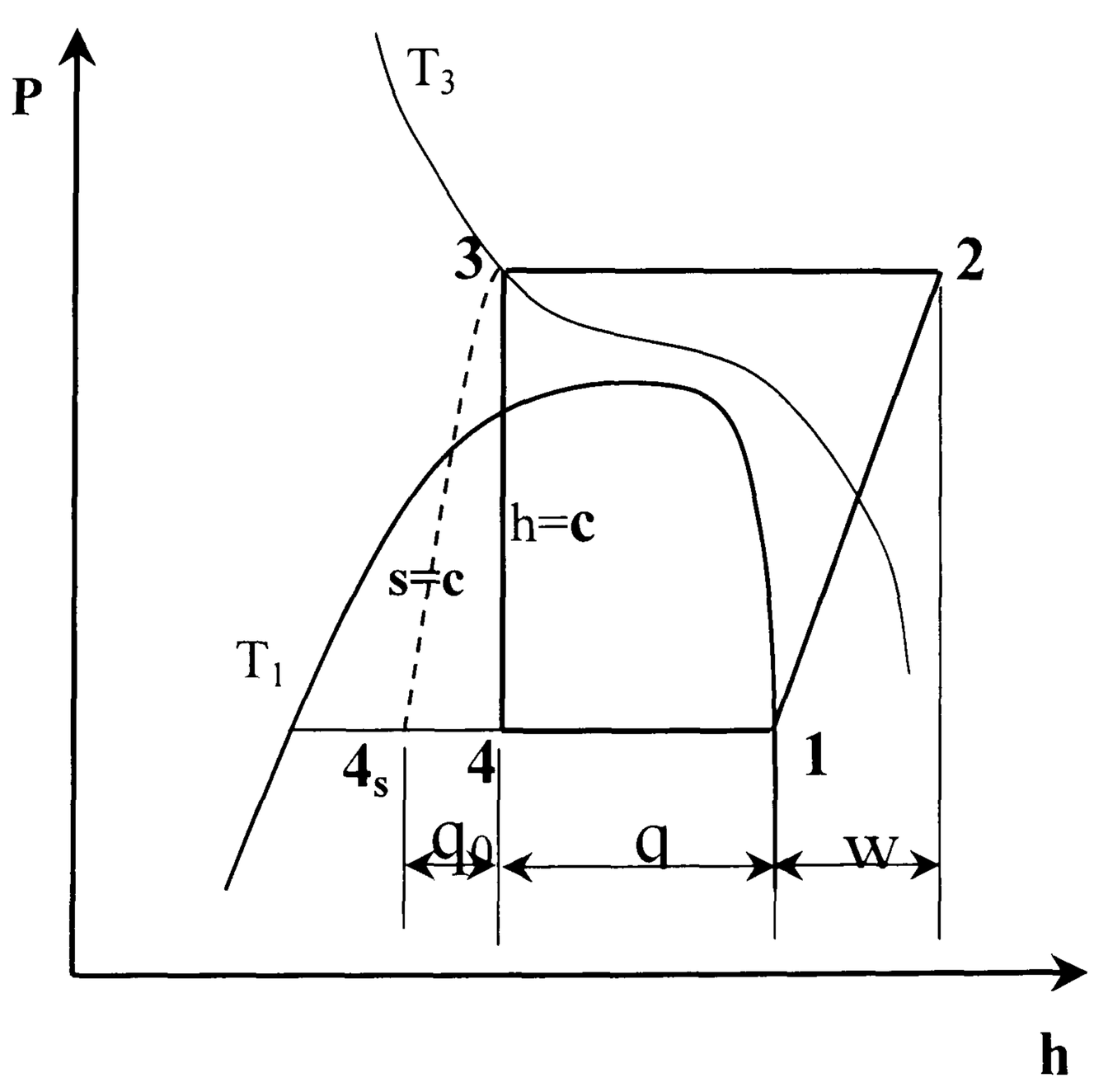

Figure 2.4 Throttling loss in a transcritical CO_2 cycle

The cooling COP reaches a maximum at an optimum gas cooler pressure. For cooling operation, the location of this pressure is mainly determined by the gas cooler exit temperature T_3. Similar tendencies can also be observed for heating COP.

2.1.2.2 High Throttling Loss

Figure 2.4 illustrates the throttling loss for the transcritical CO_2 cycle. Due to the considerably higher specific heat of liquid carbon dioxide in this near-critical region, the throttling loss (q_0) is significantly higher. The throttling loss becomes smaller at low heat rejection temperature and in particular when the CO_2 heat rejection temperature becomes subcritical.

2.1.2.3 Heating Capacity and COP Characteristics

In heating mode operation, the CO_2 system obtains a maximum COP at a particular pressure for a given evaporating temperature. By raising the pressure above this level, the heating capacity may be increased or maintained if the evaporating temperature is reduced. Despite the reduced COP, the overall efficiency of heating may then be increased in dual systems using supplementary electrical heaters due to reduced supplementary heat.

Another feature of the transcritical CO_2 cycle is the relatively weak influence on heating capacity and COP of the evaporating temperature, which enables the CO_2 system to maintain a higher heating capacity at low ambient temperature (Pettersen 1997).

Transcritical hot water heat pumps are able to provide high water supply temperatures, and the COP is not sensitive to the maximum water temperature. When the temperature of the hot water delivered varies from 60 ^{0}C to 80 ^{0}C, the reduction in COP is only about 15% (Neksa et al. 1998c).

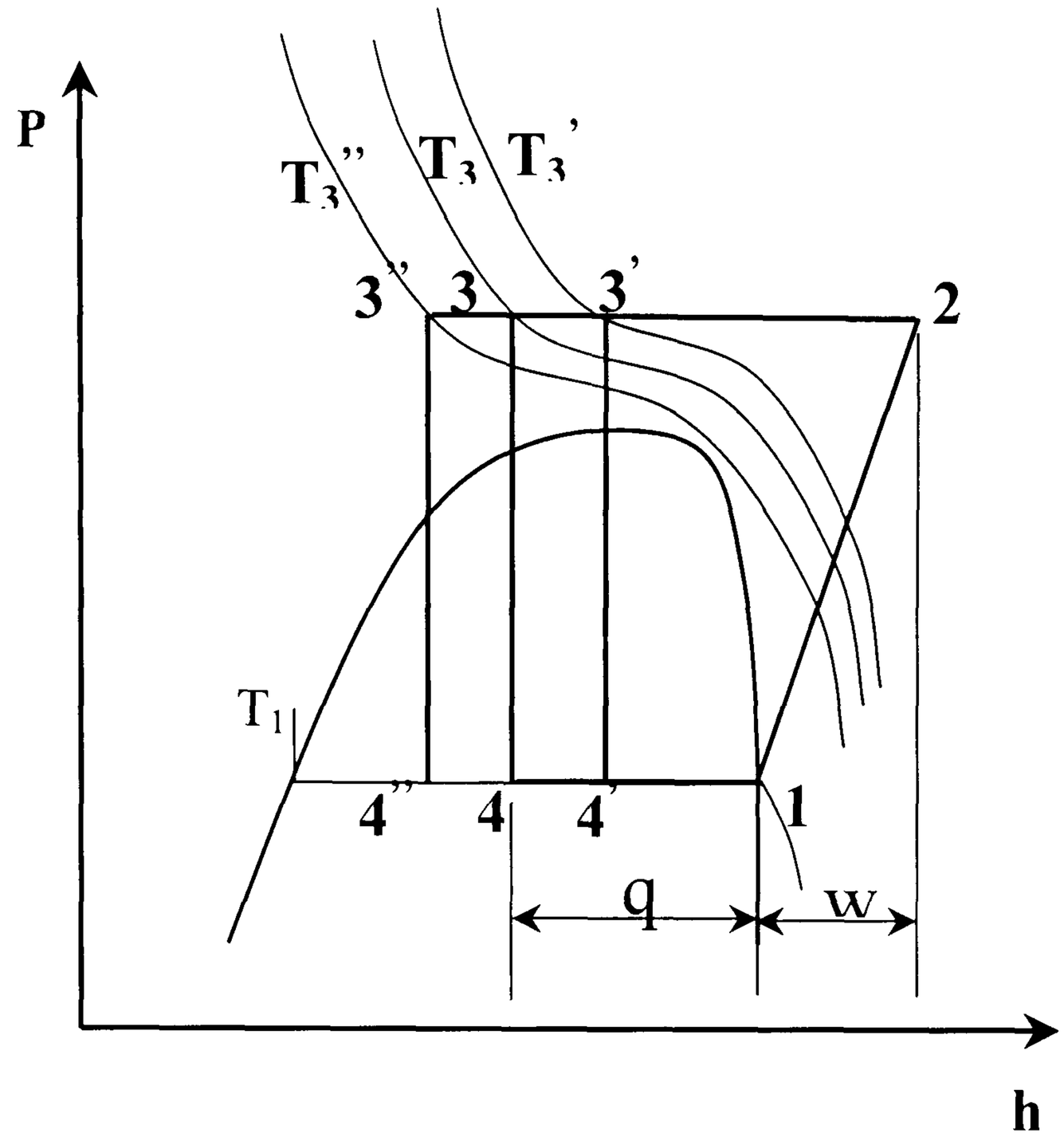

Figure 2.5 Effect of gas cooler refrigerant exit temperature

2.1.2.4 Gas Cooler Refrigerant Exit Temperature

The great importance of obtaining as low temperature as possible at the gas cooler outlet should be emphasized. The throttling loss depends on the gliding heat rejection temperature; the COP of a CO_2 system is more sensitive to the gas cooler refrigerant exit temperature than are systems with common refrigerants. A close temperature approach is desirable and practical in CO_2 gas coolers and contributes significantly to practical COP improvement as shown in Figure 2.5.

2.1.2.5 Improvement In The Compressor Isentropic Efficiency

Compressors in CO_2 systems will operate at high mean effective pressure and with large pressure differentials, but the pressure ratios will be quite low. The reduced pressure ratio contributes to good compressor performance.

The effect on efficiency of valve pressure drops is likely to be low in a CO_2 compressor, even though the gas density and the associated valve pressure drops will be high. This is because the valve pressure drops are a smaller fraction of the pressure difference in a CO_2 compressor than in compressor compressing a conventional refrigerant.

The volumetric capacity of CO_2 is around 5-10 times higher than for the common refrigerants due to higher gas densities. This opens the possibility for smaller compressors, even though the structure is thicker. Dorin (2000) also indicates the possibility of running semi-hermetic CO_2 compressors at 3000 rpm, which of course would give a very compact compressor for a given capacity.

2.1.2.6 Improved Heat Transfer Coefficients

A number of factors contribute to the efficient heat transfer reported for CO_2, among them favourable fluid properties, high mass flux and small tube diameters.

For a given heat transfer duty, a CO_2 heat exchanger will be smaller in volume than a heat exchanger for conventional refrigerants. The effective air-side surface will be higher in the CO_2 coil because less fin area is removed by the refrigerant tubes. Also, the fin pitch can be reduced for the same air-side pressure drop. Similar principles will apply to CO_2 heat exchangers based on other tube geometries, e.g., multiport extrusions. Less heat exchanger volume will be occupied by refrigerant, e.g. heat transfer tubes and headers/manifolds, and the airflow resistance caused by refrigerant tubes will be reduced, thereby allowing larger air-side surface and more efficient heat transfer.

Owing to the high operating pressures of gas cooler and evaporator, the large pressure gradient associated with a large mass flux can be tolerated for both. Furthermore, due to high sensitivity of saturation pressure/temperature of CO_2, pressure drops that are 7-10 times higher may be allowed in a CO_2 evaporator, for the same drop in saturation temperature. As a consequence, CO_2 evaporators may be

designed for considerably higher mass flux with the benefit of more efficient heat transfer than for conventional refrigerants.

Because of the higher densities, higher thermal conductivity, lower viscosity, higher specific heat, smaller tube diameters, and the favourable saturated temperature/pressure relationships of CO_2, refrigerant side heat transfer coefficients will be higher than for conventional refrigerants. This could allow the evaporating temperatures to be slightly higher for CO_2 than for conventional refrigerants for the same cooling capacity. Improvements in the gas cooler performance could likewise allow a closer approach between the CO_2 exit temperature and the entering air temperature than for conventional refrigerants.

Minimum burst pressure requirements will be in the order of 100 bar for the CO_2 evaporator and 400 bar for the gas cooler, corresponding to between 2.5 and 3 times the maximum operating pressure and pressure relief setting.

2.1.2.7 Compactness Of Equipment

Low-side refrigerant line diameters are typically reduced by 60% - 70% compared to HFC systems due to the higher vapor density and flow velocity. Similar reductions will also apply for the high-side piping dimensions. Assuming that a wall thickness similar to that in the corresponding HFC system of equal capacity, the pressure capability will be sufficient for CO_2 due to the reduced refrigerant line diameter.

For the same reasons, the compressor displacement is reduced by 80% - 85% for a given capacity. Compressor and heat exchanger size and weight reductions seem possible due to the reduced refrigerant-side volumes and smaller heat transfer surfaces (Pettersen 1997).

2.1.2.8 Adaptation To Heating And Heat Recovery Applications

The CO_2 cycle is well adapted to heating requirements with gliding temperature. The CO_2 temperature glide during heat rejection in this process is ideal for heating of service water from around 10 ^{0}C to 70 – 80 ^{0}C. By proper counter flow heat

exchanger design (e.g., double tube units) and by adjustment of the high-pressure side, varying temperature requirements can be met.

Even in direct air heating, the CO_2 system may have advantages due to its ability to supply reduced air flow rates at high temperature, thereby avoiding draft problems.

2.1.2.9 High Pressure Drops

Heat exchanger pressure drops are five to ten times higher than for conventional refrigerants. This influences the pressure/temperature relationship. At 0 ^{0}C, for instance, conventional refrigerants such as HCFC-22 and HFC-134a have a pressure drop of around 0.1 bar per degree K temperature loss, while a CO_2 evaporator with the same temperature drop has to be designed for 0.9 bar pressure drop.

2.2 Recent advances in CO_2 systems

A patent filed by Prof. Gustav Lorentzen in 1990 in which he described the transcritical process with its implied capacity control mechanism, initiated the revival of CO_2 as a modern refrigerant. CO_2, thanks to its negligible DGWP and other attractive features, may become an important refrigerant in the near future. This part provides a review of the literature concerning the recent advances in CO_2 systems. The results of investigations concerning the various applications of CO_2 are presented. The following review of work done in this field shall be divided according to the application areas and will be based mainly on:

- The latest reviews papers on CO_2 of Fleming (2003) and Kruse (1999).
- The overview papers of current activities in the field of CO_2 systems by authors such as Neksa (1998a and 2002), Halozan (2000), Rieberer (1999), Pettersen (1995) and Lorentzen (1994c).

2.2.1 Transport refrigeration and mobile air conditioning

After Lorentzen (1990) had presented his idea, Lorentzen et al. (1993) and Pettersen (1994) reported on the theoretical and experimental investigations of a CO_2 system for automotive air conditioning. They came to the conclusion that CO_2 is the ideal

working fluid for automotive air conditioning systems as it has hardly any negative impact on the environment. In experimental investigations it has been shown (Lorentzen and Pettersen 1993 and McEnaney et al. 1999) that the COP of CO_2 prototype automotive air conditioning systems may well compete with a traditional CFC-12 system regarding capacity, efficiency, installation costs, weight, dimension. Furthermore, its TEWI should be better.

Pettersen and Skaugen (1994) investigated the initial idea of the patent cycle further and stated from their measured and simulated results that in order to maintain the COP maximum, the high pressure side should follow nearly linearly the gas cooler outlet temperature. Concerning capacity control, they stated that high pressure side control seems not to be a promising option for capacity enhancement or part load capacity reduction. They recommended that the capacity control should therefore be based on conventional principal of compressor control.

A detailed report on aspects of an experimental investigation of the components of the car air conditioning system with CO_2 was given by Holst (1996).

Wertenbach (1997) reported on the European RACE (Refrigeration and Automotive Climate under Environmental Aspects) project involving five major automakers and four component manufactures. He showed first test results and requested further development concerning weight and efficiency because the measured COP fell around 15% below the HFC-134a equivalent. The first experimental experiences were gathered and the possibility of applying CO_2 as a refrigerant in automotive air conditioning systems was believed to be proved. Preliminary results of this RACE project showed minor disadvantages regarding the COP of the CO_2 system; questions concerning safety, dynamic behaviour, weight reduction, production costs and reliability were raised as requiring further attention.

Bullard and Hrnjak (1997) discussed CO_2 and HFC cycles for mobile air conditioning and described together with the authors Yin et al. (1998), an experimental comparison of transcritical CO_2 versus HFC-134a cycles. Experimental

results of investigations on automotive air conditioning systems were presented by McEnaney et al. (1998 and 1999). They concluded that at idling conditions the system provided approximately equal capacity at extremely high temperatures but that its COP fell 10% short of a chosen baseline system. However, at outdoor ambient temperatures below 40 ^{0}C, the CO_2 system COP exceeds that of the HFC-134a baseline system by 40% or more.

Also, the above-mentioned authors Wertenbach (1998) and Gentner (1998) made an environmental evaluation of an automobile air conditioning system with the CO_2 versus HFC-134a as refrigerant. They concluded that CO_2 systems have a high potential to reduce global warming caused by vehicle driving, without reducing comfort, and that those systems can be applied only if worldwide acceptance is achieved.

Fujiwara (1998) compared automotive air conditioning systems with HFC-134a, propane and CO_2 from an environmental point of view and came to the conclusion that only a minor and perhaps temporary TEWI advantage for the CO_2 system can be achieved since HFC-134a compressors have a larger potential for efficiency improvement.

Preissner et al. (2000) presented experimental results for prototype CO_2 and HFC-134a automotive air conditioners. Their major findings were that the capacity of the CO_2 system ranged from 13% lower to 20% higher as compared with the HFC-134a system, and the COP of the CO_2 system ranged from 11% to 23% lower as compared with the HFC-134a system. The major difference between this study and that of McEnaney et al. (1998) is that the HFC-134a heat exchangers had similar technology to the CO_2 heat exchangers, i.e. micro channel type, and an internal heat exchanger was employed in the HFC-134a system, not just in the CO_2 system as in the previous study.

Hirao et al. (2000) reported the development of an air conditioning system using CO_2 for automobiles. In their study, they suggested that the high-pressure control system

in parallel with an improved scroll compressor and high efficiency gas cooler could maximize COP in the CO_2 automobile air conditioning system. The system utilizing these components achieved a COP equal to or higher COP than that of the comparative HFC-134a system.

Boewe et al. (2001) investigated the contribution of an internal heat exchanger to CO_2 cycle performance. They found that the internal heat exchanger had a substantial effect, increasing the cycle efficiency by up to 25% because of the relatively high loss caused by expansion from a different state point in the basic transcritical cycle.

Most recently, Toyota's fuel cell hybrid vehicle (FCHV) was introduced to the market in December 2002. It utilizes CO_2 as a refrigerant in its air conditioning system (Fleming 2003).

A favourable aspect of the application of CO_2 as a refrigerant in automotive air conditioning systems is the possibility of heating the interior with the gas cooler since a range of high temperatures can be achieved. A similar proposal has been made by Hafner et al. (1998). Simulation results indicate that the CO_2 HVAC system is a competitive total solution for modern vehicles, with a high COP and heating and cooling capacity under all climatic conditions.

Experimental studies of the heating mode of operation of prototype CO_2 automobile air conditioning systems were reported. The first results were presented by Bullard and Hrnjak (2000) and Giannavola et al. (2000). Data were presented for moderately cold weather. Ambient temperatures were varied in the range $-10\ ^0C$ to $20\ ^0C$ with compressor speed at 950 rpm representing idling condition. Heat rejection was done in the supercritical region and ambient air was dehumidified using a glycol coil to minimize risk of frost formation on the evaporator. The reported heating COP ranged from 2.5 up to 4 for higher ambient temperatures.

Hafner (2000) tested a prototype CO_2 air conditioning system in heating mode. The heating capacity was between 2 and 6 kW at an ambient temperature of $5\ ^0C$ and -5

^{0}C and the relative humidity was 80%. Frost formation on the exterior heat exchanger surface was the limiting factor of the system. The air flow through the exterior heat exchanger was blocked after 15–20 minutes of operation. He suggested controlling the evaporation pressure with a variable displacement compressor to delay the formation of frost.

Besides the application of CO_2 for car air conditioning systems, Kohler (1995) discussed the application of CO_2 as a refrigerant for bus air conditioning. He presented a prototype system with compressor and heat exchanger components for laboratory measurements. In follow-up papers, Kohler et al. (1997 and 1998) presented measurements on a bus system utilising a newly designed compressor. They reported that prototype test rigs showed a comparable or even better COP than traditional systems. Moreover, the efficiency of the new compressor was found to be very high.

Later, Tegethoff et al. (1999) developed a dynamic simulation to predict the transient behaviour of a CO_2 air conditioning system for buses. The simulation results of the model and the experimental data were in good agreement.

Quack and Kraus (1994) presented CO_2 investigations for railway refrigeration and air conditioning. They showed that the use of an expansion machine in combination with a special cycle configuration shows a remarkable COP improvement when the minimum gas cooler achievable temperature is 45 ^{0}C.

A completely different application of CO_2 in the field of transport refrigeration is the application of CO_2 to reefer containers. Simulating this application Kauffeld (1998) stated that reefer CO_2 systems have a theoretical potential for replacing HFC-134a systems when the advantage of a higher efficiency compressor and the smaller influence of pressure drops in the heat exchangers are taken into consideration.

Jakobsen (1999) investigated, theoretically and experimentally, the utilization of an innovative hot water driven ejector to improve the performance of a transcritical CO_2

system especially for reefer applications. Experimental results showed that the ejector system would increase the COP at a sea water temperature of 34 ^{0}C by around 80% at design conditions.

2.2.2 Water heating

Lorentzen and Neksa (1994) favoured hot water heat pumps and other applications where large temperature glides in pipe networks are advantageous. They stated that CO_2 is especially efficient in hard working conditions with low heat source temperatures and high temperature requirements at the hot side of the process. This application was considered for evaluation in another European research project called COHEPS (CO_2 Heat Pump Systems) with the participation of research institutes and industry from four countries. Enkemann and Kruse (1997) reported on their part of the project, the development of a CO_2 heat pump for retrofitted hydronic hot water heating systems, and predicted a seasonal performance factor of 3.2 for Berlin if the water flow rate could be halved, to provide a larger temperature difference between supply and return water temperatures. Concerning capacity control, they discussed the combination of a capacity controlled compressor together with inverter speed control.

Neksa et al. (1997, 1998b and 1998c) presented a CO_2 prototype system with experimental results and showed that the process is very suitable for domestic water heating heat pumps. With the system they investigated, a COP of 4.3 was measured if water was heated from 9 ^{0}C to 60 ^{0}C at an evaporation temperature of 0 ^{0}C. With this installation it was possible to achieve water temperatures up to 90 ^{0}C. Similar conclusions were drawn by Rieberer et al (1997a and 1998a) whose results showed that a COP higher than 5 can be achieved when heating water from 10 ^{0}C to 60 ^{0}C. However, the COP drops significantly with rising gas cooler inlet temperatures, leading to the recommendation that reheating of hot water cooled down by poor insulation and circulation losses has to be avoided.

The above-mentioned statements were supported by various authors, for example Hwang et al. (1997a, 1998b and 1999) who reported on a water heating heat pump

and an improvement in the COP of 10% above an equivalent HCFC-22 system. Chumak et al. (1996) also supported these statements. Furthermore, Heyl et al. (1997) reported on the applications of CO_2 for heat pumps with large temperature glides and experimentally investigated those systems. For a system with a heating capacity of 18 to 26 kW, the measured COP was between 3.5 and 4 when heating water from 10 ^{0}C to 60 ^{0}C, depending also on favourable running conditions for the compressor with a low-pressure ratio.

Later, Lemke (1999 et al.) developed a new kind of stratified tap-water storage system that takes advantage of the temperature glide in the CO_2 gas cooler for water heating.

The feasibility of a transcritical CO_2 heat pump for high temperature heating was investigated theoretically by White et al. (2002). They incorporated in their model performance data from a prototype CO_2 heat pump which was constructed for heating water up to 65 ^{0}C. Model prediction showed that the hot water temperature could be raised from 65 ^{0}C to 120 ^{0}C with reductions in heating capacity and COP of 33% and 21%, respectively.

With a laboratory heat pump system Saikawa et al. (1997 and 1998) gained knowledge of the dynamic behaviour and control of heat pump water heaters. They recommended controlling such a system with an electronic expansion valve and an inverter motor-driven compressor. A dynamic simulation of a CO_2 heat pump was developed by Skaugen et al. (1998). Good qualitative agreement between experimental results and model predictions were reported.

Recently, several papers have been published reporting the development of CO_2 heat pump water heaters either for residential use Saikawa et al. (2000), Mukaiyama et al. (2000) and Kusakari et al. (2001) or large-scale application Zakeri et al. (2000). Also, Fleming (2003) reported on residential CO_2 heat pump water heaters in the Japanese market. These units are produced by Denso, Sanyo and Daikin companies.

2.2.3 Residential ECU

Aarlien et al. (1996), as well as Pettersen et al. (1997) reported on the application of a CO_2 ECU and compared the results with commercial HCFC-22 units, remarking that further improvements of the efficiency of the CO_2 system are achievable. Aarlien (1998) experimentally achieved an improvement of the heating COP of a CO_2 test rig of 3% to 14% compared with HCFC-22 reference systems, while the cooling COP was 0.5% to 14% lower.

Also, Bullard and Hrnjak (1997) discussed CO_2 and HFC cycles for residential ECU and described together with the authors Yin et al. (1998), an experimental and modelling comparison of transcritical CO_2 versus R-410A cycles. Experimental results of investigations on a residential ECU were presented by Beaver et al. (1998) for the cooling mode operation and by Richter et al. (2000) for the heating mode operation. They concluded that for the cooling mode the CO_2 system provided approximately the same COP at lower outdoor ambient temperatures (27 ^{0}C) but that its COP fell 10% short of the baseline system at higher outdoor ambient temperatures (35 ^{0}C). Tests were performed at equal capacity and equal fan power. In the heating mode, the CO_2 system operates with a slightly lower COP, but its higher capacity at lower outdoor temperatures reduces the need for (expensive) backup heating capacity, typically electric resistance heaters.

Recently, various prototypes of transcritical CO_2 ECU have been developed and tested for the U.S. Army. Further details are given here under the heading of ' military applications' section 2.2.5.2.

2.2.4 Commercial refrigeration

Pearson (1993) described the first use of liquid CO_2 as a volatile secondary refrigerant with an ammonia supermarket refrigeration system. Later, Lorentzen (1994b) presented for the application of CO_2 in commercial refrigeration the idea of using a one-stage CO_2 cycle to provide the low temperatures on the one hand and to produce on the other hand favourable hot water with the gliding temperatures of the transcritical process on the high-pressure side.

Enkemann and Arnemann (1994) investigated CO_2 as a secondary refrigerant. They concluded from their experiments that CO_2 is an ideal choice as a secondary fluid in low temperature commercial refrigeration since it is applicable in practice with conventional components and the temperature differences and pressure drops are much lower than for conventional coolants. Hesse (1996) discussed CO_2 as a secondary refrigerant in comparison with conventional brines. Also Rolfsmann (1996 and 1998) reported on the application of CO_2 as a secondary refrigerant in a supermarket which has been run without problems. Later Rolfsmann (2002) presented an analysis of important parameters and the collection of experiences with over 40 installations using CO_2 as a secondary coolant in Sweden.

Looking at the application of CO_2 in commercial systems, Ferreira et al. (1996) reported on theoretical investigations of the application of CO_2 as a secondary fluid in comparison with its application as a refrigerant in a cascade system. From experimental and theoretical investigations, comparative COP for CO_2 systems were obtained (Ferreira 1997). In a further study, Ferreira (1998) investigated the exergetic losses of supermarket systems with CO_2 as refrigerant. The losses are greater in the gas cooler and the economizer than in their HCFC equivalent. However, the increased compressor efficiency offsets these losses.

Brendeng (1997) also considered a NH_3/ CO_2 cascade system to be less costly than a two-stage ammonia plant. Also, Eggen et al. (1995, 1998) reported on their theoretical investigation of commercial refrigeration with ammonia and CO_2 as working fluids in three configurations: namely with CO_2 as a secondary refrigerant, with CO_2 as a low temperature working fluid in a cascade system and with CO_2 as a sole refrigerant. The power consumption is practically identical for the two NH_3/ CO_2 systems but the swept volume of a CO_2 compressor is only 10% of that of low-pressure ammonia compressors. Therefore NH_3/CO_2 cascade refrigeration plant is very promising provided that the compressor and other components are available for CO_2 as refrigerant. Comparing all systems with an R-404A commercial refrigeration system, the seasonal performance with air-cooling is similar for all systems. The cooling water mass flow rate for the two-stage CO_2 system water-cooling is only

10% of that needed for the condenser of a conventional system. When the gain from water heating is taken into account, power consumption can be reduced 10%.

A similar attempt to apply CO_2 in this field is described by Neksa et al. (1998a) who referred to two systems for water-cooling and air conditioning. The water cooling system may lead to considerable energy savings compared with conventional systems using heat recovery for tap water and space heating, whereas the air cooled system has direct heat recovery for the shopping area when space heating is required. The system can compete with conventional systems concerning the energy consumption for refrigeration.

Recently, there are several plants worldwide which utilize CO_2 as a low temperature working fluid in cascade systems or as secondary refrigerant, for example Christensen (1999) in Denmark, Steimle et al. (1999b) in Germany, Kim et al. (2002) in Korea, Taylor (2002) in USA and Pearson (2001) and Blackhurst (2002) in UK.

Sasaki et al. (2002) reported the design and construction of 40 TR water chiller which uses CO_2 as the sole refrigerant. A single-stage oil injected rotary screw compressor was used. They mentioned that the system functioned well, with only slight mechanical vibration and noise. Starting and shutting down were smoothly controlled automatically. The COP of this system was not high compared with similar types. It did not exceed 2.0 because it was used where cooling demand required coolant at only $-10\ ^0C$.

2.2.5 Miscellaneous

2.2.5.1 Food Processing

Yarrall et al. (1998) reported on the simultaneous use of the cold and warm side. A heat pump and a prototype system for the food processing industry were constructed, where refrigeration at $0\ ^0C$ and a heating of water to $90\ ^0C$ were required. Under these conditions, the total COP was measured to be about 5. Furthermore Yarrall et al. (1999) investigated the heating COP across a range of operating conditions, before and after the addition of oil to the system. The optimum heating COP of the

prototype was about 3 in most trials, but increased to 3.2 when operating the compressor at part load with no oil in the system.

2.2.5.2 Drying and Dehumidification

A future application of CO_2 system is seen in drying processes introduced by Steimle (1997) and Schmidt et al. (1998 and 1999). In terms of COP, and especially if temperatures above 70 ^{0}C are required, the CO_2 system has advantages compared with the HFC-134a.

2.2.5.3 Military Applications

Beside the use of CO_2 for civil applications, there were recently reports by Patil (1998, 1999) and Manzione (1998) about military interest in this refrigerant, as it has an extra ordinarily high volumetric refrigeration capacity, enabling use of very compact units. Since it does not need recovery procedures, servicing is much easier, a feature which makes it particularly attractive for military use.

Culter et al. (2000) designed and built a prototype transcritical CO_2 ECU for the U.S. Army. Details of the system design were presented but test results were not available.

Later, Connaghan (2002) investigated experimentally a breadboard model of CO_2 U.S. Army ECU. The unit was tested under a high outdoor ambient temperature range, namely from 32.2 ^{0}C up to 51.7 ^{0}C, while indoor conditions were 32.2 ^{0}C and 50% relative humidity. Discharge pressures ranged from 10 to 13 MPa when stable conditions were maintained. Higher discharge pressures increased evaporator capacity at all conditions and generally increased COP. The greatest evaporator capacity measured was 11.3 kW.

Also, Manzione et al. (2002) evaluated experimentally a transcritical CO_2 using an open compressor in a packaged unitary military ECU. The results showed that the CO_2 ECU did not perform well as the HCFC-22 military standard ECU. The conclusion drawn was that the viability of CO_2 as refrigerant for military ECUs is still uncertain and further design improvements are necessary.

2.2.5.4 Liquefaction

Zhang et al. (1998) investigated theoretically CO_2 for R-502 substitution in low temperature commercial and CO_2 liquefaction systems.

2.2.5.5 Air Heating

Rieberer et al. (1998b) reported on the application of a CO_2 system for a low energy house with a controlled ventilation system. Based on the results of a simulation a COP between 5 and 10 is expected.

2.3 Summary

Since the revival of CO_2 as a refrigerant initiated by Prof. Lorentzen, the interest in CO_2 has increased immensely during the last decade. Due to the low critical temperature of CO_2, the VCC is required to be transcritical for many applications. As was discussed earlier, the theoretical disadvantage in COP CO_2 has when compared with HFCs systems is reduced and in some cases eliminated by a number of practical factors such as potentially better CO_2 compressor efficiency and favourable heat transfer properties.

Investigations have shown that the field of application is very large. A number of promising applications of CO_2 systems have been identified. The first application of CO_2 concerned automotive air conditioning systems for which intensive development work has been done mainly in the European RACE project. It was successfully finished and the prototypes built work well, although a few questions remain to be resolved regarding safety, dynamic behaviour, reduction of weight, production, cost and reliability. Reliability is of great importance in auto marketing. The second field where the application of CO_2 as a refrigerant is very promising is that of water heating systems where a high temperature glide is desirable. Here, CO_2 offers interesting possibilities for the most commonly demanded temperatures. Various prototypes have been built and successfully operated within the European COHEPS project framework. In Japan, three companies have market such systems successfully (Fleming 2003). With regard to commercial refrigeration, CO_2 is a promising

candidate either as a volatile secondary refrigerant or in cascade with ammonia for multi-stage plants. Several plants were built and are functioning in a satisfactory manner worldwide. Furthermore, very promising results exist for CO_2 application in residential ECUs (Aarlien 1998). It can be said that the CO_2 systems are encouraging. Moreover, a heat pump dryer with CO_2 has good prospects (Kruse et al. 1999).

In conclusion, the CO_2 systems introduced to date show promising results in different applications. However, more work requires to be done to gain improvements in the performance of the existing CO_2 systems. To apply CO_2 to area currently served by conventional refrigerants, design improvements are required. Scope for transcritical CO_2 cycle improvement is discussed in the following chapter.

Chapter 3

Scope For Transcritical CO_2 Cycle Improvements

The preceding chapter has shown that CO_2 has the potential to be used as a competitive refrigerant for a number of applications. Though many researchers published promising results, the performance of the single-stage CO_2 cycle when compared to that of the conventional HFC refrigerants is still inferior for most applications. The transcritical CO_2 cycle is receiving strong consideration in reduced weight and volume applications, such as automotive a/c and military ECU. In both applications, system improvements may be necessary to meet the goal of the reduction of weight and volume while maintaining the same or achieving higher system efficiency than the existing HFC systems.

Previous publications have discussed the theory and performance of CO_2 cycles (Neksa 1994, Robinson and Groll 1996, Pettersen 1997 and Bullock 1997). The low critical temperature of CO_2 gives a theoretical cooling COP in simple VCC operation that is 30-50% lower than that of other common refrigerants, and a greater difference at high heat rejection temperatures. In practice, however, a number of cycle design changes are capable of reducing or even eliminating these theoretical differences in performance. A correct evaluation of CO_2 in relation to conventional fluids should take into account all the important differences in properties and characteristics as well as their effect on component efficiency and system behaviour. These factors include compressor efficiency; heat transfer and temperature characteristics in evaporators; supercritical-pressure gas coolers; pressure drops; capacity characteristics; and the influence of varying operating conditions and climate. Results of many investigations indicate that the energy efficiency of CO_2 systems may exceed that of conventional refrigerants if the unique properties of CO_2 are exploited with the objective of improving efficiency.

In general, there are a number of possibilities for modifying the transcritical CO_2 cycle to reduce or eliminate the negative effects of throttling and high heat rejection temperature. These modifications include: improvement of the compression efficiency, internal heat exchanger arrangements, improvement of heat exchanger design, expansion with work recovery, cofluid arrangements etc. Further, CO_2 systems need new control techniques, particularly in relation to the high pressure side. Cycles capable of gaining efficiency improvements are required to be the objects of investigation and models must be constructed accordingly. The objective of this chapter is twofold. The first is to explore the potential for improvement of transcritical CO_2 systems. The second is to review the research work of this field and to draw conclusions for the direction and detailed reporting of the work of the author.

3.1 Minimizing compression losses

Owing to the fluid properties of CO_2, much higher pressures occur when applying CO_2 as a refrigerant in a compression process as compared with the conventional refrigerants. However, the heating and/or cooling capacity per unit volume of CO_2 is higher than for conventional refrigerants. Recently, CO_2 has been considered as refrigerant for several different applications as reported in the preceding chapter. However, the most important task will be the design of efficient, reliable, and, in the case of transport applications, compact/lightweight compressors. Moreover, the optimized design should minimize compression loss, valve throttling loss, refrigerant internal leakage, suction gas heating. Consequently, it is necessary to develop new compressors or modify existing ones to meet the required demands. When modifying existing ones, the main procedure is to decrease the cylinder diameter in accordance with the greater volumetric capacity of CO_2 to ensure that the bearing forces created by the cylinder pressure remain nearly the same in order to be able to use a conventional drive mechanism such as the crankshaft and connecting rod with their existing bearings. Later, with the use of hermetic compressors, the electric motor could be nearly the same size as that for HFC refrigerants. However, due to much higher suction pressure, a stronger shell would be needed.

Factors such as high operating pressure, small displacement, low pressure ratio and large pressure differential are in favour of reciprocating machines, although other types may also be considered in particular for larger systems. Several theoretical studies investigated the possibility of applying the scroll (Fagerli 1998a and 1998b), vane (Fukuta et al. 2000) and rolling piston (Collings et al. 2002) compressors for CO_2 compression; gas forces are not seen by these authors as a problem but design attention to internal clearance is needed to reduce internal leakage to a reasonable level.

A reciprocating compressor with relatively small cylinder bore and long stroke has the advantage of limiting the forces on the drive system and offers the best possibility of avoiding internal leakage. Nevertheless, good shaft seal design with minimum leakage and high reliability is also needed.

Potentially high impact velocities are a danger with conventional flapper valve designs in small CO_2 compressors. Mechanically operated valves of the sliding/rotating type may offer advantages, in particular since pressure ratio variations and therefore losses by over/under-compression will be small. However, greater mechanical complexity is a penalty.

Internal leakage losses in valves and as piston blow-by could be a problem with the high-pressure differentials in CO_2 compressors. However, everything is smaller in a CO_2 compressor, so owing to reduced valve circumference in the CO_2 machines, the valve leakage losses are not affected as much by the larger pressure differentials as might be expected. The main volumetric losses are due to clearance volume re-expansion, suction gas heating and leakage past piston rings.

For domestic water heating, CO_2 systems with single-stage compression have been shown to be competitive with the state of the art existing systems (Fleming 2003). In some applications two-stage compression will however be advantageous due to operational constraints, for instance for reducing the discharge temperature,

minimizing internal leakage, or in order to achieve higher efficiencies via intercooling.

Earlier, Lorentzen (1995) reported that a large gain in efficiencies could be achieved in low temperature applications using a two-stage compressor with external sub-cooling. One may imagine that an extra heat exchanger area is needed, but actually less heat exchanger area may be the result due to a higher COP resulting from heat rejection at intermediate pressure rather than at high pressure.

A way of increasing the efficiency of the process further is by sub-cooling the high-pressure gas/liquid before throttling, by means of heat exchange with gas throttled to intermediate pressure (Lorentzen 1995). He reported that the COP could be increased by 30% and the volumetric capacity by about 40% at an evaporation temperature of –35˚C and an ambient temperature of 30˚C. By controlling the mass flow to intermediate pressure this can also be used as a means of capacity control, however with a certain loss in efficiency.

The first CO_2 compressor applied to verify the idea of using CO_2, as a primary refrigerant presented by Professor Lorentzen was an old double acting CO_2 reciprocating compressor. This compressor was designed and manufactured by Sabroe A/S in 1927 and the nominal speed was 320 rpm. The efficiency was not high, but it served to show that the process was workable and to verify a mathematical model/simulation program developed for the process (Neksa et al. 1997).

Later, a complete CO_2 automobile a/c prototype system was designed for this purpose (Lorentzen et al. 1993 and Pettersen 1994). A prototype reciprocating compressor with 3 cylinders and wobble plate drive mechanism was designed and built. The cylinder diameter was 18.5 mm, stroke 31.9 mm and the total swept volume was 26 cm^3. Each piston was equipped with one piston ring. However, the new CO_2 system showed a competitive performance when compared with conventional CFC-12 and HFC-134a units. Details of the performance of the CO_2 compressor were not given.

In order to achieve high compressor efficiencies, measurements on test rigs and comparative studies are of great importance. Several compressors have been developed for CO_2 systems and a number of prototype compressors of various types exist. In the following a comprehensive review on the state of the art technology with respect to CO_2 compressor development is given.

The following review of work shall be divided according to the number of compression stages: single or multi-stage, and the type of compressor: open, semi-hermetic or hermetic. In this connection a review of investigations have addressed the important issue of selecting a lubricant for optimal performance. Lubricant behaviour could be one of the key issues, as the right choice of lubricant/refrigerant mixture must also be considered to be part of CO_2 compressor design. A review of studies regarding the selection of a lubricant for CO_2 compressors will be presented.

3.1.1 Single-stage compressors

Compressors for refrigeration and heat pumping applications are manufactured in three types of design: open, semi-hermetic or bolted hermetic and welded shell hermetic. Open type compressors are those in which the shaft extends through a seal in the crankcase for an external derive. Hermetic compressors are those in which the motor and compressor are contained within the same casing, with the motor shaft integral with the compressor crankshaft and the motor in contact with the refrigerant. Ammonia compressors are manufactured only in open design because of the incompatibility of ammonia and hermetic motor materials. A semi-hermetic compressor (bolted, accessible, or serviceable) is a hermetic compressor of bolted construction amenable to field repair. Meanwhile the open type compressors are applied for mobile a/c and large-scale commercial systems, hermetic and semi-hermetic type compressors are more convenient for residential HPWH and ECU units. Here, the single-stage compressor will be further sub-divided into a high-pressure category for transcritical operations and a low pressure category for the low pressure stage of cascade systems.

3.1.1.1 High-pressure Compressors

3.1.1.1.1 Open

Several open-type reciprocating CO_2 compressors have been developed during the last 10 years. Early investigations focused on the modification of existing HFC-134a compressors to use with CO_2 as described by Kohler et al. (1995) who experienced problems at first with the discharge valves which had larger pressure losses; as a consequence, the second model was fitted with ring plate valves (Kohler et al.1997). The compressor had two cylinders, each with swept volume of 60 cm^3 and was designed and built by Bock GmbH. For a suction temperature between 7 ^{0}C and 12 ^{0}C, a suction pressure of 34 bar, and a pressure ratio range of 2.7 to 3.6, a volumetric efficiency of 88% and isentropic efficiency of 79% were maintained over the range of pressure ratios. The prototype compressor was installed in a city bus. In a further stage of development, conversion to an even more optimised design with an aluminium housing is planned (Kohler et al. 1998). Decreasing the piston diameter leads to design constraints caused by lack of space for a piston pin; the piston force acts now on a very small bearing. Therefore, further optimisation of this construction element was necessary.

The design of new compressors was carried out especially for automotive a/c based on the experience with high pressure hydraulic machinery. From these experiences in the European RACE project a wobble plate compressor was built for compressing CO_2 with a angle modulation of the wobble plate (Wertenbach et al. 1997). Jörgensen (1998) reported on the optimisation of this wobble plate compressor regarding how its self-adjusting capacity modulation depends on the suction pressure. In his paper, simulations were introduced to calculate the optimal inclination angles.

Süss and Kruse (1996, 1997 and 1998) investigated thoroughly the above-mentioned reciprocating type and the wobble plate type compressor to which they contributed within the RACE project in the field of optimum design for capacity modulation. They summarized theoretical and experimental research results on these compressors and showed that the fluid properties of CO_2 are rather favourable for the energetic

performance of a compressor thanks to the low pressure ratio. Because of the high pressure difference, leakage has a rather strong influence so the best suited for CO_2 compression are those compressors with a good sealing device and a small leakage gap area. They showed that the reciprocating compressors with a small number of cylinders are much more suitable than the rotating compressors.

Also, Neksa et al. (1997) reported on the development of a reciprocating compressor with a swept volume 8.48 m^3/h. The compressor has a single cylinder and runs at speeds of 700 – 1200 rpm. The measurements of compressor efficiencies as a function of pressure ratio were presented. With a suction pressure of 35 bar, the compressor achieved a volumetric efficiency ranging from 76% up to 88% and an isentropic efficiency averaging 78% as the pressure ratio varied from 2.0 – 4.0.

The company Mitsubishi Heavy Industries has developed a high-pressure, open type scroll compressor for automobiles. A description of this development can be found in Hirao et al. (2000). Experimental published results reported a COP equal to or greater than a comparator HFC-134a system. Compression efficiency was measured to be 76% at a speed of 2400 rpm.

Försterling et al. (2002) presented experimental results of different compressor types developed for mobile applications: a 7 cylinder swash plate compressor with a pressure controlled and a path-controlled valve system from Obrist Engineering GmbH and a second generation two-cylinder reciprocating compressor from Bock GmbH. The swash plate compressor with path control is derived from a hydraulic pump for mobile applications. In contrast to common swash plate compressors the cylinders rotate with the pistons. The swash plate is fixed and the shaft and the cylinders rotate. It is possible to vary the displacement by adjusting the swash plate angle. As the cylinders rotate the cylinders are pressed by the exerted gas forces against the fixed port plate. A movement from one dead center to the next constitutes one complete stroke during which a volume of gas, corresponding to the piston area and the stroke, is either sucked in or discharged via the suction or discharge area in the port plate. The swash plate compressor with path control showed a nearly

constant value over the whole speed range while the efficiency for the compressors with a pressure controlled valve system was reduced by higher valve losses. At relatively low compressor speed of 1000 rpm, both pressure controlled compressor types achieved a 10% to 20% higher isentropic efficiency than the path controlled type and the efficiency of the reciprocating compressor was about 5% higher than the swash plate compressor. The authors reported that at higher speeds similar efficiencies were observed. Concerning the volumetric efficiency, all three compressors showed very similar results. The authors concluded that the path-controlled principle is an interesting option to achieve good efficiencies over a wide range of compressor speed, which is needed for mobile applications.

Mayekawa Manufacturing Co., Ltd developed a twin-screw compressor for air conditioning systems in the range of 40 TR (Sasaki et al 2002); it is oil injected with a volumetric delivery of 63 m^3/h, a speed of 2950 rpm and, although originally designed for natural gas, was modified for high-pressure CO_2 usage. A detailed compressor performance was not available.

Sanden LuK Co. developed a new swash ring variable displacement CO_2 compressor for mobile application (Sakamoto et al. 2000, Parsch et al 2002 and Fagerli 2002). Measurements indicated that the CO_2 automotive a/c system would cool adequately and, in most situations, consume considerably less fuel than HFC-134a systems. The authors reported that the mass production of the new compressor would begin in 2005.

3.1.1.1.2 Semi-hermetic

The high pressure in the crankcase, maximum 80 bar at standstill, make a hermetic or semi-hermetic design preferable, thus avoiding the shaft seal. The compressor developed by Neksa et al. (1999) is the first semi-hermetic compressor and probably the compressor nearest to serial production within the commercial sector. Neksa et al. (2000) and Dorin et al. (2000) reported on the development of a series of semi-hermetic reciprocating compressors with swept volumes in range of 0.5 – 12.6 m^3/h. The compressor series consists of single and two stage compressors with two cylinders, running at nominal speeds of 2900 rpm. The measurements of compressor

efficiencies as a function of pressure ratio were presented. At a pressure ratio of 2.6, overall isentropic and volumetric efficiencies were 69% and 77% respectively for the single stage compressor rated at suction tube conditions.

Saikawa et al. (2000) and Kusakari et al. (2001) also reported development of a semi-hermetic scroll compressor produced by the company Denso, which originally serves a HPWH with 4.5 kW heat output. However, no details were available for the performance of the compressor.

Most recently, Baumann et al. (2002) reported on a small oil-free semi-hermetic CO_2 compressor. They investigated the feasibility of an oil free semi-hermetic reciprocating compressor for supercritical heat pump water heating applications. The suction gas was heated up by the motor windings and in the crankcase quite strongly by about 70 K and in the cylinder head almost 20 K. They reported an isentropic efficiency up to 70% which is comparable with a conventional oil lubricated compressor.

3.1.1.1.3 Hermetic

Adolph (1994) was first who to convert an HCFC-22 compressor to a CO_2 compressor by using the former piston as crosshead and adding on top of that piston another one of smaller diameter together with a mating cylinder with suction and discharge valves. The reported experimental results at a suction temperature of 11 ^{0}C, a suction pressure of 3.42 MPa and over a pressure ratio range of 2.5 – 3.0; the volumetric efficiency varied from 53% - 44% and the isentropic efficiency averaged 38% (Heyl et al 1997). The poor behaviour was believed to be due to the compressor construction. The compressor was only built for the feasibility study and trial investigations of CO_2 in railway a/c.

Fagerli (1996a, 1996b and 1997) reported a similar conversion for an even smaller HCFC-22 hermetic compressor without a crosshead piston design but changing the original cylinder and piston to smaller sized components. The measured compressor efficiencies were up to 85% and 40% for volumetric efficiency and isentropic efficiency, respectively at a pressure ratio of 2.6, a suction temperature of 10 ^{0}C, a

suction pressure of 35 bar and a speed of 2900 rpm. Hwang et al. (1998a) also developed a laboratory prototype of a hermetic compressor. In experimental studies, it was found that internal leakage has to be considered closely and further design changes were recommended.

Most recently, Süss (2002) reported on the development of low capacity reciprocating hermetic compressor from Danfoss A/S. A traditional refrigerant hermetic compressor was adapted to the requirements of the transcritical CO_2 process. Tests exceeded more than 1300 hours with individual compressors at various operating conditions up to 160 bar as the high pressure. For a constant suction pressure of 40 bar and 10 K superheat, volumetric efficiency values between 70% and 80% and isentropic efficiency values of around 50% were measured. The author reported that the compressor design study is ongoing, with the goal of improving the performance.

A prototype hermetic scroll compressor for CO_2 systems in the range of 2.5 - 5 kW was reported to be under development by the company Matsushita (Hasegawa et al. 2000). It was evaluated experimentally by varying the operating speed between 30 and 50 Hz by means of an AC inverter. The experimental results indicated that the volumetric efficiency and the compression efficiency improved as operating speed and the pressure difference between suction and discharge increased. At an operating speed of 48.2 Hz, a suction pressure of 3.93 MPa and a discharge pressure of 9.49 MPa, the volumetric efficiency was 86.4% and the compression efficiency was 47.1%. However, they reported that the compression efficiency of the CO_2 scroll compressor was substantially lower than that of their HFC-410A scroll compressor. In the development process Hiwata et al. (2002) investigated the relationship between the compressor efficiency and the oil injection rate to the compression chamber. The experimental results showed that up to 5% improvement in COP could be obtained by optimising the oil injection rate and decreasing the leakage loss of refrigerant from the compression chamber.

Daikin Industries, Ltd., developed a hermetic swing compressor for a heat pump water heating application (Ohkawa et al. 2002). They optimised the design of an HFC-410A compressor for minimization of leakage by reducing the clearance 50% and adopting high viscosity oil. Also, they reviewed the thickness of parts that receive a large pressure difference. After a compressor durability test of 2000 hours the HPWH unit was launched into the market in February 2002.

3.1.1.2 Compressors for cascade systems

Industrial contributors were most prominent in reporting experimental work in CO_2 compressors for the low-pressure stage of cascade system. Braendgaard (1996) published test results on an industrial reciprocating compressor from Sabroe Refrigeration A/S for a CO_2/NH_3 cascade system and stated much higher efficiencies than HCFC–22 and R-717. Also, Renz (1999) gives a description of semi-hermetic reciprocating and screw compressors from Bitzer International.

3.1.2 Multi-stage compressor

Unlike single-stage CO_2 compressors, very few two-stage prototype CO_2 compressors were reported to be in development. Also, little design detail and performance data are reported in the open literature.

3.1.2.1 Open

An automobile two-stage compressor based on the swash plate design was developed by the company Denso (Inagaki et al. 1997). A two-stage compression was chosen to increase the cooling capacity and COP. Performance improvement up to 15% in COP and 7% in cooling capacity compared with single stage compression were recorded at 35 ^{0}C outside temperature. They reported measured volumetric and compression efficiencies of 75% and 70% respectively at a swept volume ratio of 0.86 and a speed of 1800 rpm.

3.1.2.2 Semi-hermetic

Neksa et al. (2000) and Dorin et al. (2000) described the development of semi-hermetic two-stage compressors. They presented the measured volumetric and

isentropic efficiencies for a prototype two-stage compressor with a swept volume of 2.7 m^3/h at 1450 rpm while varying the total pressure ratio. The 1st stage discharge gas is cooled to 20 ^0C, the superheat of the suction gas being 10 K. The efficiencies were compared to those of the single-stage machine and the isentropic work of the single stage process was used as a reference. An overall isentropic efficiency at 80 bar high pressure of 52% was achieved at an evaporation temperature of –45 ^0C, increasing to 60% at an evaporation temperature of –30 ^0C. The discharge gas temperature was reduced from about 150 ^0C to 130 ^0C at the same condition. They reported that compared to the use of a single-stage compressor, an increase of more than 20% in COP could be expected at an evaporation temperature –35 ^0C.

3.1.2.3 Hermetic

Lately, Tadano et al. (2000) reported on the development of a rotary two-stage hermetic compressor for small capacities (750 W) from the company Sanyo. The compressor was designed to operate between low pressures of 3 to 4 MPa and a high pressure of 10 MPa. The compressor displacement was 2.633 cm^3. The intermediate pressure was selected to be 5 to 6.5 MPa. Several tests were performed as a function of motor frequency, superheat and pressure ratio. The authors reported an isentropic efficiency of up to 88%. However, this efficiency did not include motor and shell losses. A durability test over 1000 hours was performed.

Most recently, another two-cylinder two-stage rotary hermetic compressor was developed by Techmseh Products Company (Dreiman and Bunch 2003). The compressor runs at nominal speed 3600 rpm (60 Hz) and has a swept volume 16.11/11.62 cm^3, 1st and 2nd stage, respectively. Compressor performance indices, such as the volumetric and isentropic efficiency were not given.

3.1.3 Lubricants for compressors

The selection of a lubricant for the CO_2 compressor could have a major impact on the reliability and performance of the system. The high compressor discharge temperature, high operating pressure, exceptional supercritical operation and the

acidic nature of CO_2 in the presence of moisture present a challenge in terms of selecting a lubricant for the long-term reliability of CO_2 systems.

The discharge temperatures are much higher than in cycles using conventional refrigerants. Depending on the particular compressor design, this may lead to unusually high lubricant temperatures. High temperatures reduce lubricant viscosity and therefore lubricants of high ISO viscosity may be required. Also, high pressure leads to compressors with small displacement and thus limits the space and the dimensions of bearings for certain compressors. This high-pressure difference and the resulting geometry limitations lead to very high mechanical bearing loads and place exceptional film strength requirements on the lubricants. High discharge temperature and high bearing loads will require the selection of lubricants which are characterized by high thermal stability.

Furthermore, Seeton et al. (2000) reported that supercritical CO_2 is an excellent solvent. This solvency may cause excessive lubricant dilution, producing a working lubricant without sufficient viscosity to perform effectively. In general, for good solubility, highly polar fluids may be required. However, the more conventional lubricants such as mineral oils or alkyl benzenes may be favoured to offset thinning of the lubricant resulting from dissolved CO_2.

At the beginning of the last century, CO_2 systems utilized glycerine/water mixtures and later mineral oils as lubricants (Seeton et al. 2000). Recently, Hesse and Spauschus (1996) investigated lubricants for CO_2 systems. They reported that many of lubricants are possible candidates for CO_2 VCC. Some soluble lubricants have been identified as candidates for possible application with CO_2. However, due to high pressure, compressor bearing loads are high and high temperature, property data for CO_2 / lubricant systems are needed for proper design. Olsen (1996) investigated the chemical reaction between the lubricant and CO_2. He stated that minor problems with chemical stability might occur in comparison with CFC systems.

Later, Li et al. (2000) evaluated various lubricant chemistries for their interactions with CO_2. Critical properties of a refrigeration lubricant, including miscibility, stability, solubility, working viscosity and load carrying capability have been summarized and the differences among lubricants highlighted. Seeton et al. (2000) also discussed lubricants for compressors and measured the solubility, lubricity and miscibility of CO_2 with a number of synthetic lubricants.

In further study, Li et al. (2002) evaluated the most suitable candidates in compressor tests to compare the performance of different lubricant chemistries. Potential applications include transcritical operations as well as CO_2/NH_3 cascade systems. The base lubricant chemistries used in the compressor or system tests included polyalphaolefin (PAO), polyol ester (POE), polyalkylene glycol (PAG) and alkylnaphthalene (AN). A series of tests to evaluate the performance of a transcritical CO_2 cycle for three different lubricants was conducted using an 11 kW stationary heat pump system. The three lubricants tested cover a wide range of chemical structure, density and miscibility/solubility with CO_2 and had the same viscosity. Results showed that all three types of lubricants afforded peak performance at about the same refrigerant charge. All three lubricants also gave the same level of performance, COP = 2.78. They reported that this interesting finding is in contrast to experience gained with HFC systems and is worthy of further investigation. It appears that the properties and/or operating characteristics of CO_2 have neutralized some of the effects of lubricant properties under the test conditions. The tests of CO_2/NH_3 cascade system showed similar results. The CO_2 cycle in this system was entirely sub-critical and had a screw compressor rated to 4 MPa maximum discharge pressure. Li et al. (2002) concluded that various lubricants could successfully lubricate CO_2 compressors.

Another aspect is oil retention characteristics in CO_2 air conditioning systems. Lee et al (2002) studied experimentally oil retention and pressure drop characteristics due to the presence of oil in CO_2 air conditioning systems. Moreover, lubricants' property requirements may change with an extremely reduced flow cross-section in new heat exchanger designs for transcritical CO_2 systems.

3.2 Minimizing throttling losses

The relatively high throttling loss for CO_2 detracts considerably from the advantages of this refrigerant in a simple system. Compared with conventional VCC the potential room for improvement in the transcritical cycle is much greater because evaporator inlet qualities often exceed 50% and the resulting irreversibility is correspondingly large (Robinson and Groll 1997).

Also, due to the considerably higher specific heat of liquid carbon dioxide in this near-critical region, the throttling loss is significantly higher. The throttling loss becomes smaller at low heat rejection temperature, and in particular when the CO_2 heat rejection temperature becomes sub-critical.

The throttling loss can be reduced by a number of well-known methods. One method is to recover useful work by the addition of an expander in place of a simple throttling valve. Another method is to use an internal heat exchanger. Further details are given below.

3.2.1 Expander

The CO_2 process can be improved by the recovery of useful work from an expansion machine instead of the expansion valve especially when the gas cooler outlet temperature is rather high. Figure 3.1 illustrates a VCC using an expander instead of a conventional expansion valve and Figure 3.2 presents the cycle on P – h diagram. A work recovery expansion device, typically a high speed turbine, is essential for a gas cycle to provide cooling. In VCC however, it is currently only applied in large units. A transcritical VCC being operated partially in the 2-phase region and partially in the supercritical region has a larger performance potential with an expander than a conventional VCC. In other words, the throttling losses to be avoided with an expander are significantly larger for the transcritical CO_2 cycle than with a conventional VCC.

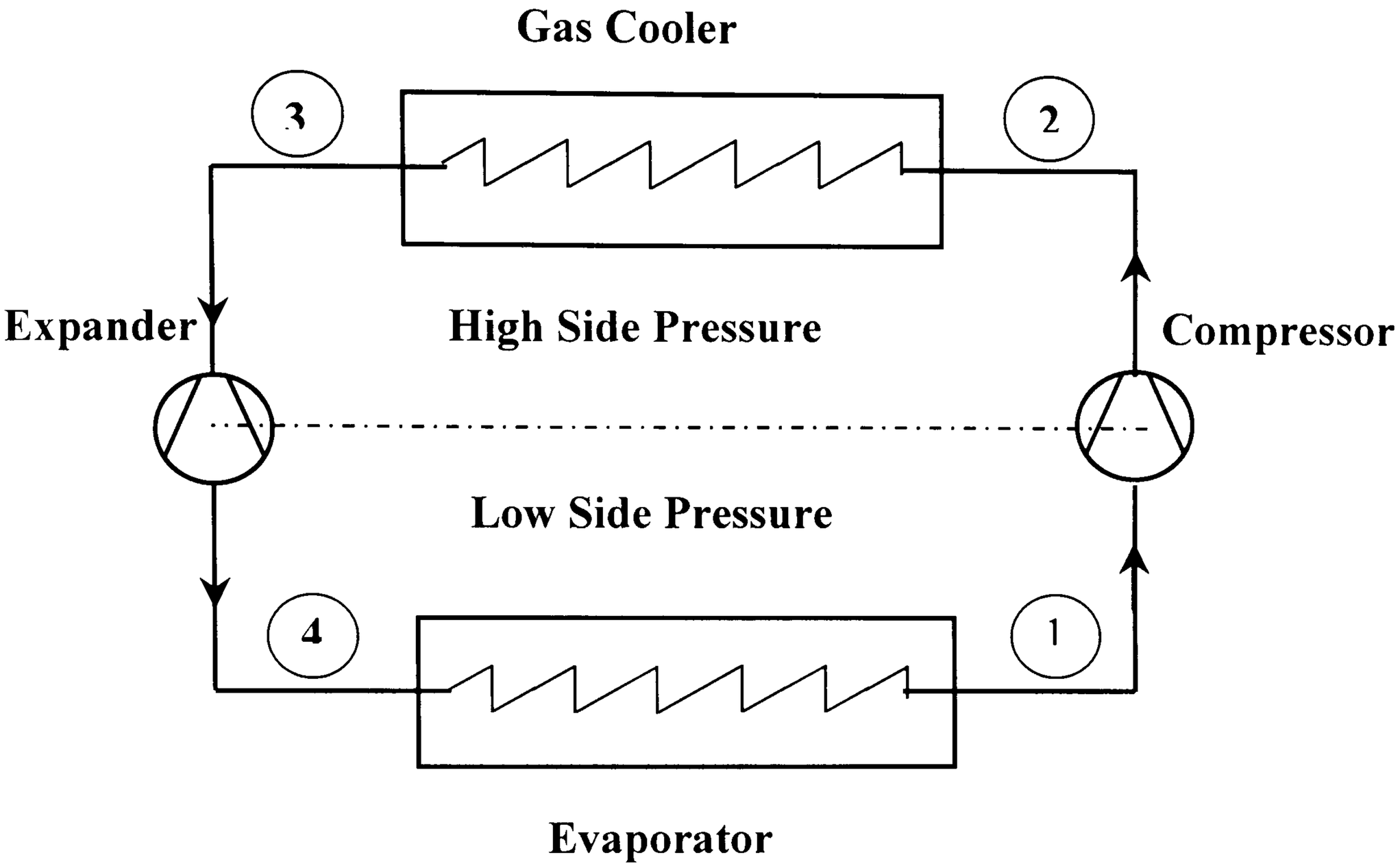

Figure 3.1 A scheme of VCC using expander

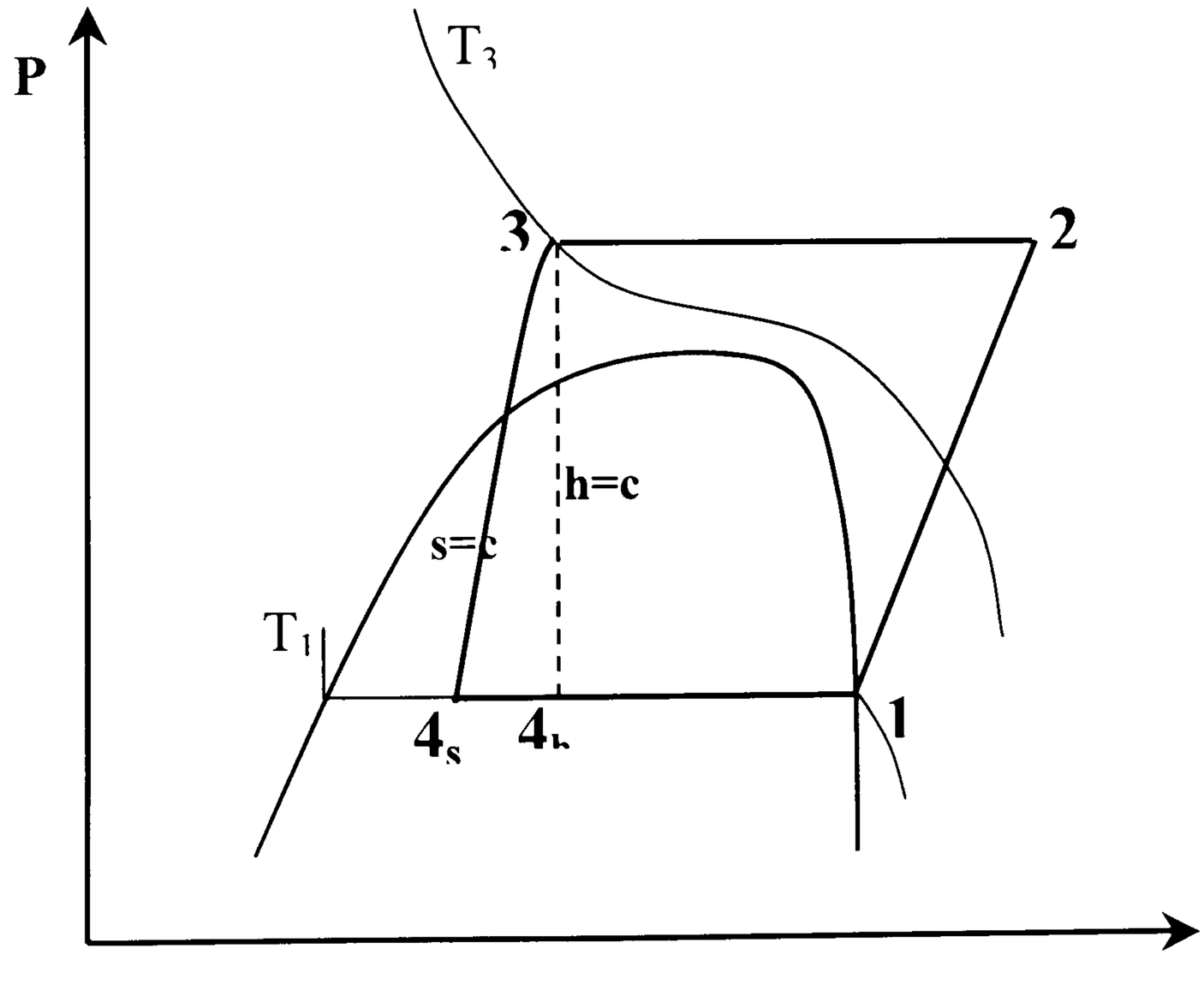

Figure 3.2 A transcritical CO_2 cycle using expander

Quack and Kraus (1994) in particular have dealt with this technology and recommended a free piston expander unit for smaller systems. By application of such an expander compression unit, it would be possible to achieve (based on theoretical investigations) a COP which is comparable to HFC cycles. A further step in this direction is described by Heyl et al. (1998 and 1999). He predicted for the above-mentioned expander compressor unit a transfer of 78% of the expansion work to the compression of the low-pressure gas.

In addition, a prototype piston – cylinder work output expansion device in an experimental transcritical CO_2 cycle was designed and tested by Baek et al. (2002a). They reported that the use of a work output expansion device increased the system performance by up to 10%.

Another research group, Robinson and Groll (1997), reported on the possibility of the application of an expansion turbine and also found theoretical improvements of the same magnitude. Applying such a device simultaneously with an internal heat exchanger in the CO_2 cycle should be avoided, as the expansion energy from low temperatures is very low.

A vortex tube expansion device was proposed by Li et al. (2000). They compared its theoretical performance with a conventional isenthalpic expansion valve and work output expansion devices for a transcritical CO_2 cycle. Based on simulation results, the maximum increase in COP using a vortex tube or expansion work output device, assuming ideal expansion processes, is about 37% compared to the COP of an isenthalpic expansion process. Considering a more realistic efficiency for the expansion work output device of 0.5, the increase in COP is about 20%. In order to achieve the same improvement in COP using a vortex tube expansion device, its efficiency has to be about 0.38. They reported that the COP using a vortex tube expansion device increases as the effectiveness of the internal heat exchanger increases.

For applications where the temperature after the high pressure heat exchanger is still rather high, such as for an ambient cooled gas cooler in automotive air conditioning, a combined compressor – expander may be a promising device to improve the energetic efficiency of the CO_2 process. A combined compression – expansion machine based on this principle with a vane (Driver 1999, Fukuta et al. 2001), scroll (Huff et al. 2002b) and twin-screw (Stostic et al. 2002) options were investigated.

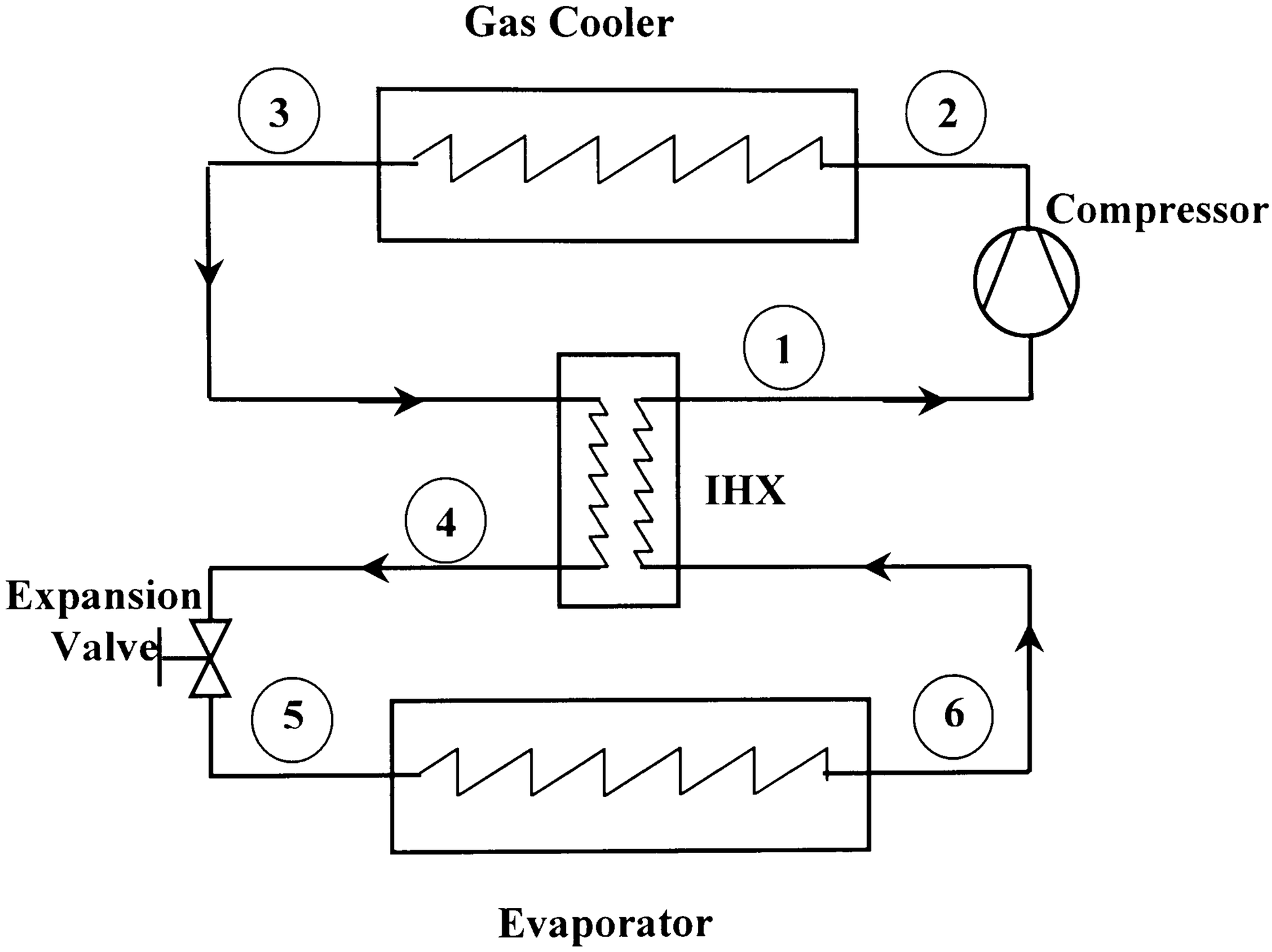

Figure 3.3 A scheme of basic VCC with IHX

3.2.2 Internal heat exchanger

In general, the use of an internal heat exchanger (IHX) may improve the cooling COP and prevent loss of capacity at high ambient temperatures. Figure 3.3 shows the use of an IHX in a basic VCC. The improvement in COP by internal heat exchange is mainly due to the reduction of throttling loss resulting from cooling of the refrigerant before throttling.

An IHX provides a considerable enhancement; in CO_2 systems without an IHX, the capacity and COP optimised discharge pressures are far apart. The IHX reduces both and brings them closer together, creating opportunities for using less precise or simpler control systems and strategies (Boewe et al 2001). Moreover, the potential suction line pressure drop penalty is less severe for CO_2 due to the higher operating pressure and low viscosity.

A disadvantage is the increased compressor discharge temperature. Another undesirable effect is the heat rejection loss. Figure 3.4 illustrates the thermodynamic average temperature of heat rejection ($T_m = \frac{\Delta h}{\Delta s}$) for CO_2. The gliding heat rejection temperature in the supercritical region results in a high T_m. The heat rejection loss increases as the average heat rejection temperature becomes higher.

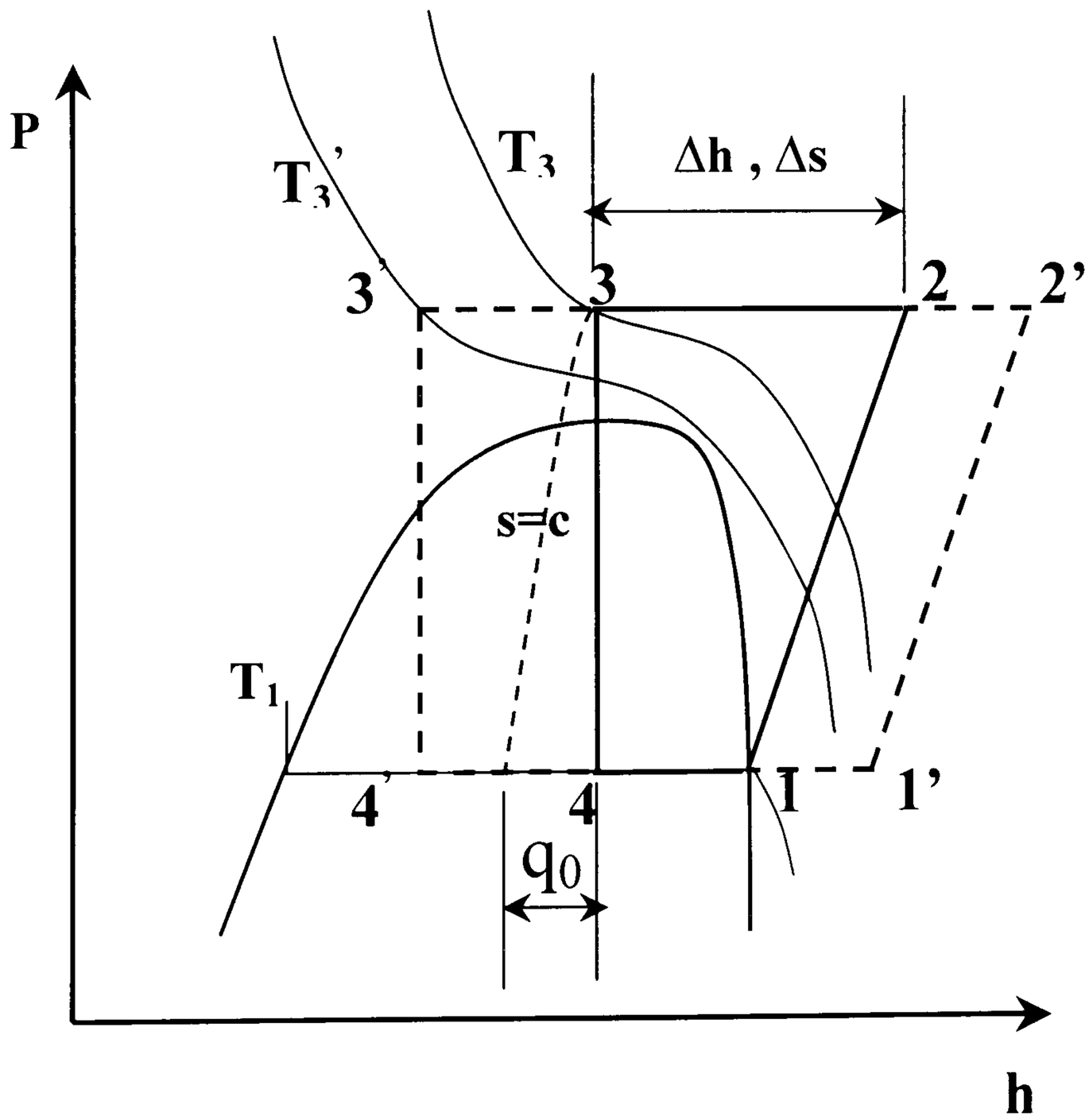

Figure 3.4 IHX and thermodynamic average heat rejection temperature T_m

Lorentzen et al. (1993) designed a CO_2 system with an IHX. The IHX guaranteed a superheated vapour at the inlet of the compressor. They reported that in the simple cycle operation, the theoretical COP of carbon dioxide is generally less than half of the CFC-12 figures at higher heat rejection temperatures. Internal heat exchange improves the level to between 55% and 75% of the CFC-12 COP. The effect of internal heat exchange is small at low heat rejection temperatures.

Similar conclusions were drawn by Boewe et al. (2001) whose results showed the influence of the IHX on system performance to be significant, increasing COP up to 25%. The optimal design of IHX was guided by the trade-off between the heat exchanger effectiveness and suction pressure drop.

3.3 Heat exchanger design

The properties of CO_2 differ considerably from those of conventional refrigerants and this has a major impact on heat exchanger design and optimization. A successful introduction of CO_2 technology depends on the development of efficient and compact components with low weight, good reliability and low cost. As discussed earlier, CO_2 heat exchangers are designed for high refrigerant mass flux and the use of small diameter tubes or extruded flat microchannel tubes. Also, refrigerant side heat transfer coefficients are higher than with conventional refrigerants and reduced internal surface areas can therefore be achieved. In the following, several peculiarities should be considered for performance improvement and optimization of CO_2 heat exchangers.

3.3.1 Construction

In general, smaller tube diameters and longer circuits should be chosen for CO_2 due to the good heat transfer, the high volumetric capacity and the small temperature loss associated with a given pressure drop. Ordinary tube-and-fin designs can be made for the high pressure required for CO_2. Pettersen et al. (1998) theoretically and experimentally investigated various constructions for CO_2 heat exchangers. They found that microchannel heat exchangers give the

best performance and concluded that the heat exchangers in CO_2 processes have advantages regarding energetic performance, weight and size compared to HFC heat exchangers.

3.3.2 Gas cooler temperature profile

In gas cooler designs, the refrigerant temperature gradient must be taken into consideration. Gas coolers have significant refrigerant-side temperature gradients, and negative effects due to internal conduction through fins, headers, or connectors will have to be avoided by careful deign. Otherwise, a problem of thermal short circuit due to conduction through the fins from hot tubes to cold tubes could occur and lead to high refrigerant exit temperature (Garimella 2003).

3.3.3 Gas cooler temperature approach

The gas cooler temperature approach is an extremely important parameter affecting the CO_2 cycle since COP is very sensitive to the gas cooler outlet state. In an actual cycle, the refrigerant temperature at the gas cooler exit changes with different operating conditions and a good design can bring it closer to the ambient temperature, i.e. a lower temperature approach.

Minimizing the gas cooler exit temperature is important to the performance of the transcritical CO_2 system for three reasons. First is the effect on system capacity, which is maximized by rejecting the maximum amount of heat to the surroundings before entering the internal heat exchanger. The system capacity can be maximized by reducing the difference between the refrigerant temperature at the gas cooler exit and the approach air inlet temperature, while keeping the refrigerant side pressure drop in the gas cooler to a minimum. The internal heat exchanger also increases capacity, but at the cost of higher compressor work caused by suction gas heating. Therefore it is desirable to reject heat to the surroundings directly from the gas cooler.

Second, minimizing the gas cooler exit temperature will reduce the optimum gas cooler pressure and consequently minimize the throttling loss. Due to the high

throttling loss, the positive effect of lowering the minimum heat rejection temperature is much higher for CO_2 than for other for other common refrigerants.

Third is the effect on compression power, reducing the optimal operating pressure by minimizing gas cooler exit temperature will reduce compressor power.

3.3.4 Conversion from cross-flow to counter-flow

Interest in CO_2 as a refrigerant has recently led to the development and testing of several prototypes. In liquid-to-refrigerant heat exchangers, double-tube counter flow (Rieberer et al. 1997a) or shell-and-tube (Schonfeld et al 1997 and Hwang et al. 1997c) concepts offer high-pressure capability and high efficiency.

In air-to-refrigerant heat exchangers, several prototypes (Skaugen 2000 and Yin et al 2000), all of cross-flow design, were developed. The temperature profile for supercritical heat rejection gives the possibility of designing a counter-flow gas cooler having reduced face area and larger depth and smaller air flow rate. The surface areas had to be increased in the counter-flow unit. This will gave about 20% larger core volume and a similar increase in mass (Pettersen et al. 1998). A multi-slab, counter-flow arrangement, gas cooler design was proposed by Bullard et al. (2002). The new design offers better performance than the commonly used multi-pass design. For a given gas cooler volume, the new design can have 11% higher gas cooler capacity. The predicted approach temperature difference is reduced from 6.9 K to 3.6 K. For a residential ECU, a counter-flow indoor heat exchanger could operate with a very low air low rate in heating mode. This would reduce draft and increase comfort of heating due to warmer air entering the room.

3.3.5 Refrigerant distribution in evaporator

CO_2 has a lower liquid/vapour density ratio than conventional refrigerants. This may give fewer problems of distribution in CO_2 evaporators, since the two-phase flow is likely to behave more homogeneously than with low-pressure conventional refrigerants. Installation of a venturi-type distributor with a capillary tube to each circuit will assure a satisfactory distribution of the two-phase flow in the

conventional type heat exchangers. The use of a microchannel heat exchanger would solve this problem (Pettersen et al. 1998).

3.3.6 Burst pressure

Minimum burst pressure requirements will be in the order of 300 bar for the CO_2 evaporator and 400 bar for the condenser, corresponding to between 2.5 and 3 times the maximum operating pressure and pressure relief setting. Smaller tube diameters would meet the burst pressure requirements for given constrains on heat exchanger dimensions, weight and pressure drop.

3.3.7 Dehumidification and water drainage

In addition to cooling, the evaporator in an air conditioning system is designed for dehumidification. The higher evaporator surface temperature of CO_2 units compared with HFC/HCFC units might not necessarily give lower dehumidifying capacity due to a larger air-side area and lower temperature drop on the refrigerant side (Pettersen et al. 1997). However, careful design of fin geometry to drain condensed water and to minimize water retention is required.

3.3.8 Other issues

Several issues should be considered to improve CO_2 heat exchangers design, including frosting behaviour of outdoor heat exchangers and the influence of lubricants on refrigerant side heat transfer and pressure drop. However, experimental data and more test results for complete heat exchangers are needed than are currently available to the author.

3.4 Control system

An important factor to consider when operating at supercritical high-side conditions is the selection and control of the pressure, which is a variable parameter. Since the high pressure side affects both the capacity and COP, the determination of a favourable level and control of the pressure is necessary.

A reasonably priced and efficient system for capacity regulation and high pressure side control must therefore be developed. This task also includes the determination and development of a favourable strategy for high pressure side regulation, including the use of the pressure measurement for capacity control.

3.4.1 High pressure control

The expansion valve in a traditional vapour compression refrigerating cycle is a mass flow rate control which conforms to the operational constraints set by the other main components of the circuit. Indeed, it cannot set the pressures but it can maintain a pressure difference and associated mass flow rate. Given that the fluid pressure at saturation is linked to the temperature in the wet vapor region and thus to the cycle equilibrium determined by the energy rates of the compressor and those of the two heat exchangers (evaporator and condenser), it follows that the valve only has to keep constant the pressure difference between the evaporator and the condenser. It can be seen that for cycle control the evaporator or condenser pressure must also be controlled. The condenser pressure can be set by setting the mass flow rate of the condenser coolant. The combination of a condenser pressure combined with an expansion valve pressure drop determines the evaporator pressure and hence temperature. Many control schemes are in use.

In a transcritical cycle the function of the expansion valve is different; importantly such a cycle has one freedom degree more which is the pressure of the gas cooler which is not related to the heat transfer conditions: the upper cycle pressure is therefore a parameter which must be controlled, ideally optimized. The common type of valve used in this cycle is basically a back-pressure valve; the valve stem is operated by the upstream pressure, which, in opposition to an adjustable spring, acts on a bellows rigidly linked to the stem itself; the valve keeps the gas cooler pressure constant, since it responds to an increase in upstream pressure by enlarging the flow area to reduce the upstream pressure, i.e. by making conventional use of negative feedback.

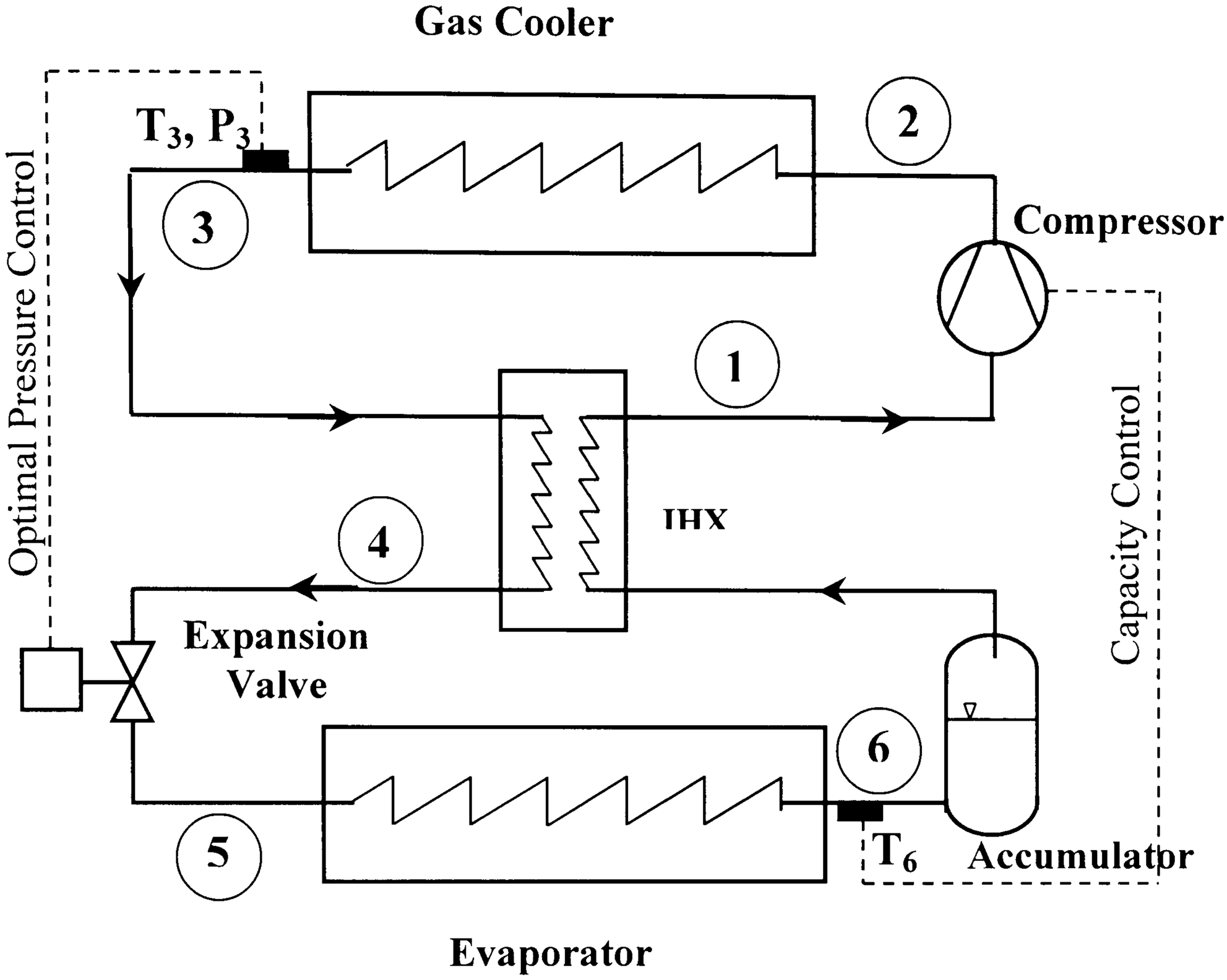

Figure 3.5 A scheme of control system.

In principal a refrigerant reservoir has to be included in order to make operation at the optimum heat rejection possible. The back pressure valve is effective in controlling the upper cycle pressure, but it is not able to fulfil the intrinsic function of the expansion valve in a common refrigerating cycle, that is feeding the evaporator with the correct refrigerant flow rate with regard to the thermal exchange. A possible solution consists in loading the circuit with a suitable mass of refrigerant as to keep a liquid receiver, placed downstream the evaporator, partially flooded by liquid. This liquid is saturated and vapor continuously evolves from it as new vapor comes in from the evaporator to maintain steady state. In this arrangement the evaporator will not be dry at its exit.

Lorentzen et al. (1993) designed a CO_2 system with an accumulator to fulfil this requirement. The accumulator will guarantee an optimum refrigerant charge in the CO_2 system components. The scheme of the CO_2 cycle control system is shown in Figure 3.5.

Rieberer et al. (2000) investigated experimentally some possible CO_2 systems: a system with an accumulator, a system without an accumulator and a system using an intermediate pressure vessel. They reported that for applications without a large variation of the heat source temperature, a superheat controlled system without accumulator means a more cost efficient solution and possible problems with the oil return are eliminated.

However, charging the system has to be done carefully because overcharging results in high discharge pressure. On the other hand, the efficiency may suffer where undercharging or leakage occur. Furthermore, possible pressure peaks during start-up should be considered when designing such a system. The two stage throttling system is a combination of the system which allows an optimum control of the high side pressure and the system above, free of oil return problems. But a problem of this system is vessel size. It has to be large enough in order to serve as a refrigerant reservoir (with liquid level) during the whole period of operation. In case of a too small vessel, the refrigeration enters the second throttle as a two-phase mixture which may result in a strongly superheated evaporator outlet.

Casson et al. (2003) presented a new expansion system. The system has a two stage throttling of the refrigerant, as does a system proposed in Rieberer et al. (2000), that differs from the one here illustrated due to using, as the first stage, a back-pressure valve. Here, the first stage of the expansion is performed by a differential valve, used when it is necessary to impose a definite pressure drop between two sections of a plant. The second stage is performed by a common thermostatic expansion valve.

The operating mode of such new system has been analysed by means of simulation (Casson et al. 2003); its feasibility has been verified with tests on a pilot plant which confirmed the results obtained from the simulation model.

For the purpose of the optimisation and control of a transcritical CO_2 system, it is of interest to obtain a correlation of the optimal heat rejection pressure in terms of appropriate parameters. For a theoretical cycle, Inokuty's graphical method can be used to find the optimal heat rejection pressure (Pettersen and Skaugen 1994). However, this method cannot be used to analyze more practical cases in which the optimal heat rejection pressure may be affected by the efficiency of the compressor.

Pettersen and Skaugen (1994) stated from their measured and simulated results that in order to maintain the COP at a maximum, the high side pressure should follow nearly linearly the gas cooler refrigerant outlet temperature. A simple high side pressure control strategy based on detection of the refrigerant temperature at the gas cooler outlet and a linear temperature/pressure relation has been devised. They applied a backpressure regulator as throttling valve.

Later, Liao et al. (1998 and 2000) found a theoretical correlation to calculate the optimal high pressure as a function of both the gas cooler refrigerant outlet temperature and the evaporator temperature. In order to assure that the system can be operated at the optimal heat rejection pressure, he suggested a control method that simultaneously adjusts both the speed of compressor and the throttling valve setting.

Also, Kauf (1999) introduced a control function that determines the optimum high pressure with help of a simulation model. He developed a control function based on refrigerant temperature at the gas cooler outlet. This function is used to adjust the high pressure so that the system can run with a COP that deviates from the maximum value by less than 5.8%.

Recently, Howard (2002) analysed optimal high side pressure through a consideration of real gas properties. He identified non-dimensional parameters that

combined with system observations to derive high side pressure optimisation. These observations are the outlet temperatures of the gas cooler and evaporator, the system mass flow rate, evaporator load, existing compression ratio and at least one internal heat exchanger outlet temperature. An alternative formulation of the model is provided that accounts for compressor efficiency and utilizes compressor power consumption instead of system pressure ratio.

The optimisation and control of high side pressure in transcritical CO_2 cycles with an expander was investigated by Huff et al. (2002a). Theoretical study showed that the CO_2 expander cycle has an optimum high side pressure and the variable expander speed was the best option for optimising high side pressure. They reported a near optimum COP for a wide range of operating conditions with suitable constant ratio of expander speed to compressor speed.

3.4.2 Capacity control

Pettersen and Skaugen (1994) stated that high side pressure control seems not to be a promising option for capacity enhancement or part load capacity reduction. They recommended that the capacity control should therefore be based on conventional principles of compressor control such as cycling clutch and variable compressor displacement.

Enkemann et al. (1997) discussed the combination of a capacity controlled compressor together with inverter speed control. Saikawa et al. (1997 and 1998) recommended controlling with an electronic expansion valve and an inverter motor driven compressor.

3.5 CO_2 - cofluid cycle

A practical concern with the transcritical CO_2 cycle is its extremely high operating pressures. The pressure in the gas cooler increases with ambient temperature and may exceed 120 bar when ambient temperature reaches 45 ^{0}C (McEnaney et al.

1999). The environmental friendliness of CO_2 refrigerant can be retained with reduced operating pressure and improved efficiency by introducing a second fluid (cofluid) into which CO_2 can absorb. Resorption and desorption of CO_2 from solution replace condensation/gas cooling and evaporation of pure CO_2. These processes occur at significantly lower pressures near those of HFCs while retaining adequate capacity. A scheme of CO_2 – cofluid system and its cycle plot on P–h diagram are shown in Figure 3.6 and 3.7 respectively.

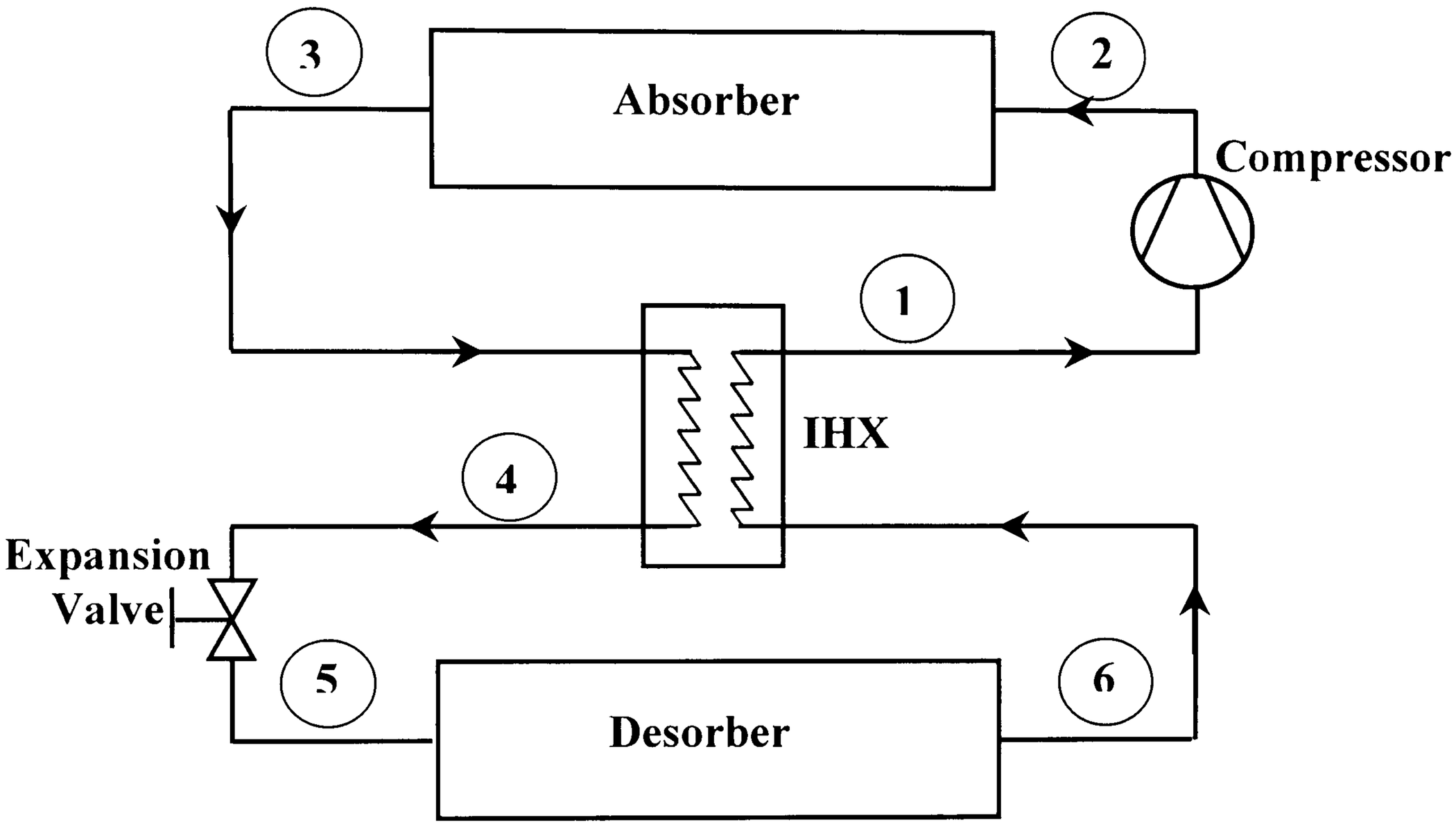

Figure 3.6 A CO_2 – cofluid system

The concept of adding a cofluid to the refrigerant is not new, the first related patent was published in 1895 (Mozurkewich et al. 2002). Interest in this technology has increased because of its potential environmental benefits, and several pilot facilities have been built, e.g. Stokar and Trepp (1987), Groll (1995) and Seeton et al. (1999). The typical hardware configuration is the so-called vapour compression cycle with solution circuit.

Groll (1995 and 1997) has presented a simplified cycle model for this configuration and applied it to a CO_2 – acetone working fluid mixture. He compared simulations with experimental results and showed that a discrepancy of 2.5% could be achieved.

showing that useful simulations could be carried out for air conditioning and refrigeration applications. For both of them, the maximum COP predicted could be greater than the conventional VCC if the plant maximum pressure is increased to 5 MPa. Also, Park et al. (1998) reported on cascade system with a mixture of CO_2 and HFC-134a. They found that results from experimental and theoretical investigations did not match and that the measured overall COP of the prototype test rig was rather low.

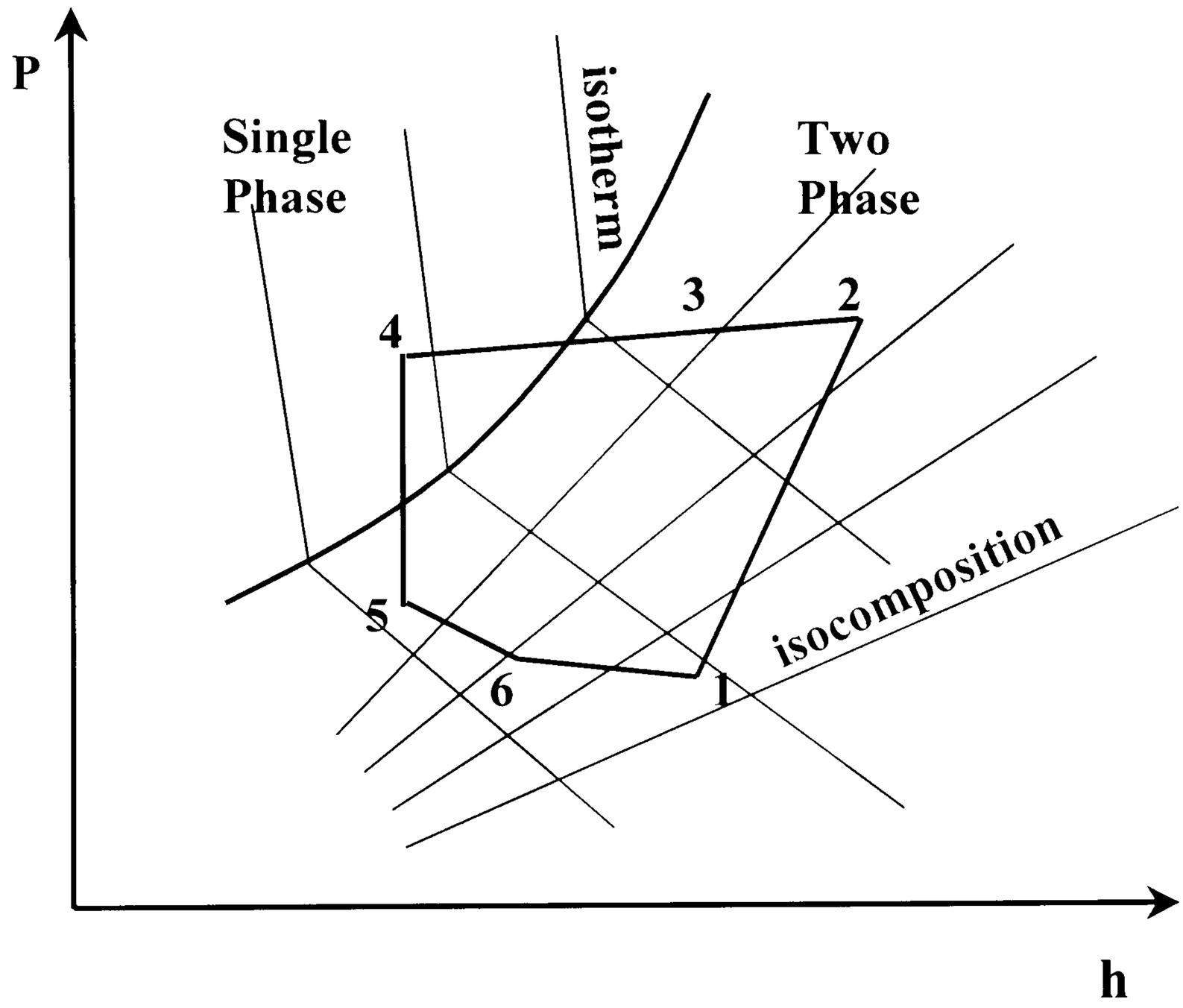

Figure 3.7 CO_2 – cofluid cycle on P – h diagram

Recently, Seeton et al. (1999) and Meyer et al. (2000) described a cofluid cycle that eliminates the separate solution circuit by wet compression of the CO_2 and cofluid simultaneously in a compliant scroll compressor. Performance under conditions relevant to automotive air conditioning was demonstrated. Poor performance was recorded at medium to high compressor speed, i.e. more than 1000 rpm, while capacity is fairly flat with changes in speed. The wet compression system has the advantage that the hardware and control requirements are comparable to the current HFC-134a vapour compression system.

In parallel work, Mozurkewich et al. (2002) described a cycle model for the CO_2 – cofluid refrigeration system with wet compression. The cycle model was used to assess the dependence of cycle performance, operating under environmental conditions representative of automotive air conditioning, on the equilibrium properties of the CO_2 – cofluid mixture, as well as on the relative proportions of CO_2 and cofluid. Results indicated that the two most important determinants of the cycle performance are the vapour pressure of CO_2 over the particular cofluid and the enthalpy associated with the transfer of CO_2 from vapour into the cofluid. Also, the results illustrated that among the four CO_2 – cofluid mixtures considered, CO_2 – acetone is expected to have the highest performance.

Meyer et al. (2000) reported that the challenges for the CO_2-cofluid system are: need of special design of IHX to maintain efficiency, need of cofluid with higher CO_2 heat of solution and production issues such as charging/servicing of the co-fluid system and an undecided control strategy and required hardware.

3.6 Summary

The potential for improvement of the transcritical CO_2 cycle was discussed. Recognizing the transcritical feature of CO_2 cycle, the improvement of the individual components is believed by the author to be the first approach to increasing the cycle performance while keeping the cycle simple. The following options were presented:

1. The improvement of the compressor efficiency shows a large benefit.
2. The reduction of the gas cooler approach temperature results also in a large benefit.
3. Taking into consideration that an optimum refrigerant pressure at heat rejection exists, the CO_2 system has to be designed to allow the adjustment of the gas cooler pressure to the optimum value.

Considering the advanced CO_2 cycle, the following options were presented:

1. Two-stage compression with intercooling will reduce compression loss and lower work input.

2. Owing to the high throttling loss, the CO_2 cycle COP will be greatly improved by an IHX or the use of expansion machinery to usefully recover work.
3. The low pressure CO_2-cofluid system operates at 35 bar maximum which is only a little higher than current HFC systems.

Although an expander will generally lower work input due to work recovery, it is costly and therefore most suitable for large capacity units. Also, a new control strategy is required based on matching expander speed with compressor speed and/or design of an integrated compressor – expander device (Huff et al. 2002b). On the other hand, the addition of an IHX which lowers throttling loss, is easier to implement and gains COP improvements up to 25% (Lorentzen et al. 1993 and Boewe et al. 2001).

Although higher in cost the two-stage compression system will be favoured due to, for instance, a low discharge temperature, reduced internal leakage and higher compression efficiencies. Moreover, it allows the use of an IHX.

Theoretical and experimental research results on the CO_2-cofluid system showed that further improvement in COP, developments to optimise components and a search for new and improved cofluids are required (Meyer et al. 2000).

A two-stage compressor combined with an IHX shows high improvement potential. Thus, the work reported here is focused on a two-stage compression system. In the following chapters the implementation of a two-stage compressor in a transcritical CO_2 cycle is discussed.

Chapter 4

Design Study Of A CO_2 Compressor

CO_2 as a natural, non-flammable and non-toxic substance is attractive as an alternative refrigerant to take the place of conventional high global warming synthetic refrigerants. However, successful CO_2 technology depends mainly on obtaining a competitive energy performance.

The compressor is the heart of the heat pump cycle. It compresses the refrigerant to a higher pressure by the use of work from an electric motor or engine. The performance of a CO_2 heat pump depends to a major extend on the efficiency of the compressor. The compressor determines the power consumption of the heat pump cycle and the state of the gas at the inlet of the gas cooler. As discussed earlier, the CO_2 cycle has unique characteristics. Selection of the compressor type requires the consideration of the characteristics of CO_2, in particular the high pressures and pressure differences at which it must operate. Further, a CO_2 compressor model has to be able to predict the performance accurately in the light of parameters affecting compressor performance. For a heat pump compressor, the main performance criteria which affect the overall performance of the heat pump are: volumetric efficiency, compression efficiency, compression power, discharge temperature and mass flow rate or capacity. Reliability and service life are affected by valve dynamics, which are also considered.

In this chapter, selection of the compressor type was made with consideration for such characteristics. Next, a detailed modeling for the compressor working process is developed. The compressor model described here is the main building block for the transcritical CO_2 heat pump simulation model. The influences of different design and operating parameters on the compressor performance including valve dynamics are discussed at the end of the chapter.

4.1 CO_2 compressor technology selection

Compressors can be classified broadly into two types: positive displacement types and turbo or roto-dynamic types. The positive displacement compressor compresses gas by reducing volume. The turbo compressor compresses gas by imparting the momentum energy and then diffusing to higher enthalpy level. Positive displacement type compressors are applicable to smaller capacities and higher pressure ratios than turbo types. The turbo compressors could be radial, axial or mixed. The positive displacement compressors can further be classified as reciprocating and rotating compressors.

Important features of CO_2 compressors are as follows: (1) high refrigerant density, (2) the volume per unit capacity is about 1/3 that of a HFCs compressor and (3) the high working pressure of the transcritical CO_2 cycle, typically more than 100 bar. Therefore, the positive displacement type compressors seem to be a good choice for CO_2 compression processes in general, and definitely for smaller systems.

A conventional reciprocating compressor has been chosen for this study because the author believes that this type will be the first type to be both technically successful and widely available to CO_2 system designers. This will enable the earliest possible introduction of CO_2 systems to the market. The early introduction is important because the competition provided by HFC systems can only be increased by delay, given the continuing improvement of HFC systems.

Work on different compressor types is to be found in the open literature. For example among the physical characteristics influencing the performance of CO_2 reciprocating compressors, leakage past the piston rings has been identified to have the major impact (Süss and Kruse 1997). Therefore, it is desirable to minimize the length of the leakage gaps and to apply an efficient sealing technique. The lowest leakage rates are achieved by making use oil-lubricated machines with seals sliding along the cylinder wall, e.g. piston rings. Accordingly, compressors without seals are not a promising option for the application in CO_2 compression processes. Only higher production

accuracy than is currently available or larger capacities may make these compressors viable.

The work of various authors highlights the importance of good gas sealing and bearing design. For example Stosic et al. (2002) reported on huge bearing forces for a twin-screw compressor when applied to CO_2 compression. They suggested the use of a combined compressor-expander to eliminate the axial force and reduce the radial bearing loads. Also, Fukutta et al. (2000) reported that leakage loss is the dominant factor in the performance of the vane compressor and clearance height is a critical design parameter. The need of advanced design such as a two-stage vane compressor or a compressor–expander combination was suggested. Furthermore, Fagerli (1998a and 1998b) supported these statements in his feasibility study of compressing CO_2 as working fluids in scroll compressors. The experimental measurements of CO_2 scroll compressors revealed a lower performance than that of an HFC-410A scroll compressor (Hasegawa et al. 2000).

Thus, for technical in addition to strategic reasons the choice of reciprocating piston type compressors is a good one, mainly trunk and axial piston machines. Reciprocating compressors are widely used in a lot of engineering applications. Beside other features such as: availability, a rather small leakage gap and ease of modification for the higher pressure difference, they are simple in principle and can accept wide variations in suction and discharge conditions. Their flexibility is combined with the minimum power per machine volume over a wide operating range (Süss and Kruse 1997).

As leakage has a strong influence, best suited for CO_2 compression are those reciprocating compressors with a small leakage gap area and a good sealing device such as piston rings. Also, to minimize the internal leakage the sealing length has to be short, pushing the concept towards a cylinder with a rather long stroke-to-bore ratio. The disadvantage of this concept is the little space left to apply valves with a sufficient flow area. However, the proper design of plenum chambers ensures that

the pressure losses inside a CO_2 compressor have a rather small influence on the isentropic and volumetric efficiencies of the compressor.

In this respect, theoretical and experimental research results of Süss (2002) concluded that reciprocating compressors with a small number of cylinders are much more suitable. Furthermore, CO_2 compressors should have a rather large stroke-to-bore ratio compared with conventional designs for HFC refrigerants. He expected an optimal performance around a stroke-to-bore ratio of 1.2 to 1.6, which is untypically large for a process with such a low-pressure ratio. Nevertheless, this recommendation is based on considerations regarding cylinder leakage. Regarding the driving mechanisms, the piston pin bearing was found to be the most critical as rather large forces occur there.

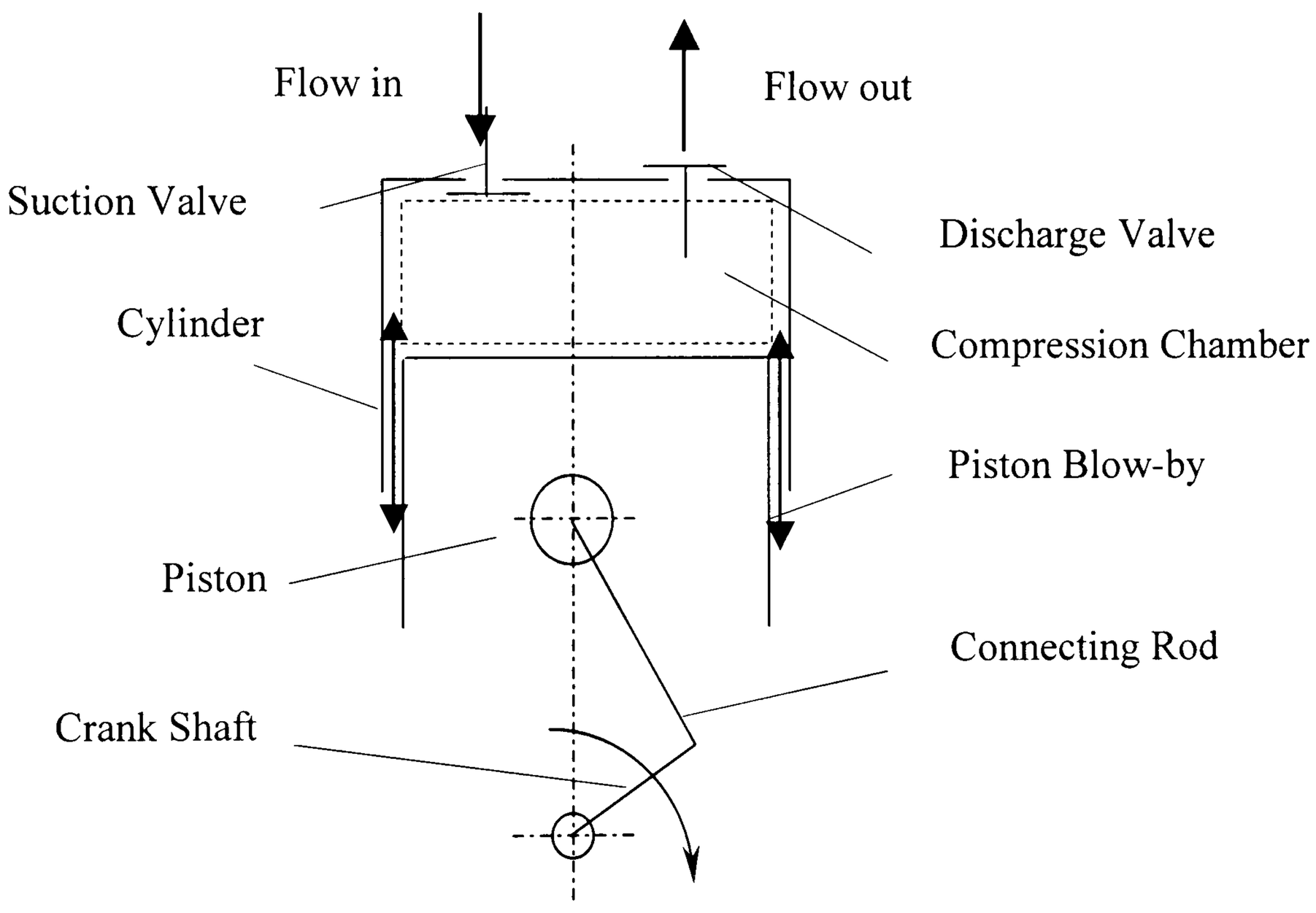

Figure 4.1 Scheme of reciprocating compressor, physical model

Based on the above discussion, a reciprocating compressor was chosen for this study. Figure 4.1 shows the physical model of a reciprocating compressor. In the following section, the corresponding mathematical model will be developed.

4.2 Mathematical model

Various modelling methods have been developed for reciprocating compressors. In general, mathematical modelling applies standard engineering formulations to describe mathematically the basic processes occurring in the compressor. Mathematical modelling is not an end in itself but is a step towards simulation and optimization. Simulation could be defined as the prediction of performance with given inputs or simultaneous solution of performance characteristics. In general, simulation is used when it is not possible or uneconomical to observe the real system.

In the past 30 years a large number of compressor models have been presented in the open literature and at scientific conferences. These models cover many different types of compressors and modelling purposes. An important source of works on compressor models is the proceedings of the International Compressor Engineering Conferences (ICEC) at Purdue. It is argued that the models found in the ICEC-proceedings are representative of the general development within this area of research.

The literature is examined with reference to the modelling needs of a heat pump compressor model. This is best done by breaking down the problem of modelling the compressor into its various components. Based on the findings of such a review, development of heat pump compressor model can be undertaken with the following criteria:

- The accurate prediction of all essential performance variables
- Simplicity with respect to mathematical formulation and programming
- Minimum requirement of empirical coefficients

The compressor mathematical model consists of a number of sub-models which describe the processes taking place within a compressor cylinder. The sub-models involved can be classified as follows:

- Crank mechanism kinematics
- Compression chamber thermodynamics

- Heat transfer
- Mass flow rate
- Leakage
- Valve dynamics
- Thermophysical properties of working fluid
- Performance criteria

4.2.1 Crank mechanism kinematics model

It is necessary to know the instantaneous cylinder volume in order to determine the mass and thermodynamics state of the refrigerant inside the compressor cylinder. The cylinder volume is derived from the kinematics of crank mechanism. Cylinder volumes can be expressed as a function of crank angle. In this model it was assumed that the compressor runs at a constant angular speed. This condition can be approximated closely in practice by fitting a flywheel to the compressor shaft.

The instantaneous piston displacement and cylinder volume are given respectively by:

$$z(\theta) = r\left(1-\cos\theta\right)+l\left(1-\sqrt{1-\lambda^2\sin^2\theta}\right) \qquad \text{Eqn 4.1}$$

and $$V_{cv} = V_{cl} + A_p\left\{r\left(1-\cos\theta\right)+l\left(1-\sqrt{1-\lambda^2\sin^2\theta}\right)\right\} \qquad \text{Eqn 4.2}$$

where, θ angular displacement of crank angle measured from TDC (rad)

λ r/l (-)

r crank radius (m)

l connecting rod length (m)

V_{cl} clearance volume (m^3)

A_p piston cross sectional area (m^2)

The derivative of the cylinder volume is required for determining the state of the refrigerant inside the cylinder and is obtained by differentiating Eqn 4.2 with respect to the crank angle as follows

$$\frac{dV_{cv}}{d\theta} = A_p r\left(\sin\theta+\frac{\lambda\sin\theta\cos\theta}{\sqrt{1-\lambda^2\sin^2\theta}}\right) \qquad \text{Eqn 4.3}$$

4.2.2 Compression chamber thermodynamics model

4.2.2.1 Literature Review

In the literature three major methods are employed to predict the thermodynamic behaviour of the refrigerant inside the compression chamber.

4.2.2.1.1 Polytropic process

In the first method a simple polytropic process is assumed:

$$Pv^n = const. \qquad \text{Eqn 4.4}$$

where, P pressure (kPa)

v specific volume (m^3/kg)

n the polytropic index (-)

The value of the polytropic index can vary according to the assumption made for each process in the cycle (Soedel 1972). In general, the value of n was determined using a trial and error procedure, based on a comparison of analytical and experimental results. The temperature T is calculated at each step by utilizing the ideal equation of state.

4.2.2.1.2 First Law of Thermodynamics

The second and the most popular method employs the utilization of the First Law of Thermodynamics in its rate form. Taking the compression chamber enclosure of Figure 4.1 as the boundary of a control volume, the rate form of the energy equation for the compression chamber can be written as:

$$\frac{dE_{cv}}{dt} = \frac{dQ_{cv}}{dt} + \frac{dW_{cv}}{dt} + \sum \frac{dm_i}{dt}\left(h_i + \frac{V_i^2}{2} + Z_i g\right) - \sum \frac{dm_o}{dt}\left(h_o + \frac{V_o^2}{2} + Z_o g\right) \qquad \text{Eqn 4.5}$$

where, $\frac{dE_{cv}}{dt}$ rate of change of energy inside the control volume (W)

$\frac{dQ_{cv}}{dt}$ rate of heat transfer to the control volume (W)

$\frac{dW_{cv}}{dt}$ rate of work done on the control volume (W)

$\frac{dm_i}{dt}$, $\frac{dm_o}{dt}$ rate of mass flow rate entering and leaving the control volume (kg/s)

h_i, h_o specific enthalpies of inlet and outlet stream (J/kg)

$\frac{V_i^2}{2}$, $\frac{V_o^2}{2}$ specific kinetic energy associated with inlet and outlet streams (J/kg)

$Z_i g$, $Z_o g$ specific potential energy associated with inlet and outlet streams (J/kg)

One of the major simplifications made in many models which adopt the energy equation approach is to use of the ideal gas equation of state to calculate the thermodynamic properties of the working fluid, e.g. Squarer et al. (1972), Hamilton (1974), Brablik (1974), Prakash and Singh (1974), Maclaren et al. (1974), Scheideman et al (1978), Kim et al. (1984), Lee et al. (1984), Sun et al. (1995), Manepatil et al. (1998) and Arzano-Daurelle et al. (1998). A small number of publications concern models which make use of real gas equations of state, e.g. Röttger and Kruse (1976), Ng et al. (1980), Meyer et al. (1990), Todescat et al. (1992), Cavallini et al. (1996) and Corberán et al (2000).

4.2.2.1.3 Solution of conservation equations

In this method the motion of the fluid is accounted for by solving the Navier-Stokes equations as well as the energy equations. The main difference between this third method and the second is its ability to predict spatial variations in the properties within the control volume and the ability to predict heat transfer without recourse to empirical correlations. This method is well illustrated by Chong and Watson (1976) and Recktenwald et al. (1986). Recently, Rigola et al. (1996) developed a numerical simulation model for the thermal and fluid dynamics analysis of hermetic reciprocating compressors.

4.2.2.2 Model Development

The criteria for a compressor model suitable for heat pump use are that it should be able to predict overall performance accurately and, if possible, does not absorb excessive amounts of computer time.

A polytropic approach is simple to use and require less computational time, however errors can arise in the prediction of cylinder temperatures (Prakash and Singh 1974).

Moreover, in polytropic process no account is made for piston leakage. Both heat transfer and piston leakage affect the pressure/crank angle trace and thus any derived value of the polytropic index would include 'both' these effects. Keeping in mind, the need to monitor the internal leakage of CO_2 compressors, the polytropic approach does not seem to be attractive.

Based on the foregoing literature review, the recommendations of Fleming et al. (2001) and due to the transcritical operation of CO_2 heat pump, method 2 employing real equations of state will yield a good compromise between predictive accuracy and required computing power. In deriving the mathematical model for compression chamber thermodynamics the following conditions are imposed:

(1) Uniform properties exist throughout the compression chamber.

(2) Kinetic and potential energy contributions may be ignored compared with enthalpies and $\frac{dE_{cv}}{dt}$ terms.

(3) Constant crank angular speed Ω.

(4) The pressure inside the plenum chambers remained constant throughout the whole compressor cycle.

Taking the compression chamber enclosure of Figure 4.1 as the boundary for the control volume. Neglecting potential and kinetic energies, the rate form of energy equation for the compression chamber may be developed as following:

$$\frac{dQ_{cv}}{dt} = \frac{dE_{cv}}{dt} + \frac{dW_{cv}}{dt} + \frac{dm_o}{dt} h_{cv} - \frac{dm_i}{dt} h_i \qquad \text{Eqn 4.6}$$

where, $$\frac{dE_{cv}}{dt} = \frac{d(m_{cv}u_{cv})}{dt} = m_{cv}\frac{du_{cv}}{dt} + u_{cv}\frac{dm_{cv}}{dt} \qquad \text{Eqn 4.7}$$

and the work term can be written as:

$$\frac{dW_{cv}}{dt} = P_{cv}\frac{dV_{cv}}{dt} \qquad \text{Eqn 4.8}$$

Letting the specific internal energy u be a function of temperature T and specific volume v, so $u = u\ (T, v)$

Hence, $\frac{du_{cv}}{dt} = (\frac{\partial u_{cv}}{\partial T})_v \frac{dT}{dt} + (\frac{\partial u_{cv}}{\partial v})_T \frac{dv_{cv}}{dt}$ Eqn 4.9

Substituting from Eqn 4.7 to Eqn 4.9 into Eqn 4.6 gives

$$\frac{dT}{dt} = \frac{1}{m_{cv}(\frac{\partial u}{\partial T})_v}\left\{\frac{dQ_{cv}}{dt} - m_{cv}(\frac{\partial u_{cv}}{\partial v})_T \frac{dv_{cv}}{dt} - u_{cv}\frac{dm_{cv}}{dt} - P_{cv}\frac{dV_{cv}}{dt} + \frac{dm_o}{dt}h_{cv} - \frac{dm_i}{dt}h_i\right\}$$

Eqn 4.10

Since $v = \frac{V}{m}$

So, $\frac{dv_{cv}}{dt} = \frac{1}{m_{cv}}\left(\frac{dV_{cv}}{dt} - v_{cv}\frac{dm_{cv}}{dt}\right)$ Eqn 4.11

From definition of enthalpy $h = u + Pv$

Hence, $u_{cv} = h_{cv} - P_{cv}v_{cv}$ Eqn 4.12

Substituting Eqn 4.11 and 4.12 into Eqn 4.10 yields

$$\frac{dT}{dt} = \frac{1}{m_{cv}(\frac{\partial u_{cv}}{\partial T})_v}\left\{\frac{dQ_{cv}}{dt} - \left((\frac{\partial u_{cv}}{\partial v})_T + P_{cv}\right)\left(\frac{dV_{cv}}{dt} - v_{cv}\frac{dm_{cv}}{dt}\right) - h_{cv}\frac{dm_{cv}}{dt} + h_i\frac{dm_i}{dt} - h_{cv}\frac{dm_o}{dt}\right\}$$

Eqn 4.13

Since for a single component vapour, $(\frac{\partial u_{cv}}{\partial T})_v = c_v$ Eqn 4.14

and $\frac{\partial u}{\partial v} + P = T\frac{\partial P}{\partial T}$, refer to Maxwell relations (Cengel and Boles 1994) Eqn 4.15

Substituting Eqn 4.14 and 4.15 into Eqn 4.13 yields

$$\frac{dT}{dt} = \frac{1}{mc_v}\left\{\frac{dQ_{cv}}{dt} - T\frac{\partial P}{\partial T}\left(\frac{dV_{cv}}{dt} - v_{cv}\frac{dm_{cv}}{dt}\right) - h_{cv}\frac{dm_{cv}}{dt} + h_i\frac{dm_i}{dt} - h_{cv}\frac{dm_l}{dt}\right\}$$ Eqn 4.16

where, $m = \frac{V_{cv}}{v_{cv}}$ Eqn 4.17

$$\frac{dm_{cv}}{dt} = \frac{dm_i}{dt} - \frac{dm_o}{dt} - \frac{dm_l}{dt}$$ Eqn 4.18

For constant crank speed, $\theta = \Omega t$

Hence $d\theta = \Omega\, dt$ Eqn 4.19

Eqn 4.16 can be expressed in terms of crank angle as

$$\frac{dT}{d\theta} = \frac{1}{mc_v}\left\{\frac{dQ_{cv}}{d\theta} - T\frac{\partial P}{\partial T}\left(\frac{dV_{cv}}{d\theta} - v_{cv}\frac{dm_{cv}}{d\theta}\right) - h_{cv}\frac{dm_{cv}}{d\theta} + h_i\frac{dm_i}{d\theta} - h_{cv}\frac{dm_l}{d\theta}\right\} \quad \text{Eqn 4.20}$$

To solve for P and T, a second relationship between pressure and temperature is needed and is obtained by letting the pressure P be a function of temperature T and specific volume v,

$$P = P(T, v)$$

Hence, $$\frac{dP}{d\theta} = \frac{\partial P}{\partial T} \times \frac{dT}{d\theta} + \frac{\partial P}{\partial v} \times \frac{dv_{cv}}{d\theta} \quad \text{Eqn 4.21}$$

The two principal unknowns involved in Eqn 4.20 and 4.21 are T and P of the cylinder contents. The partial derivatives and the enthalpies are determined from the refrigerant property subroutine, while $\frac{dv_{cv}}{d\theta}$ is obtained from Eqn 4.11 and 4.19. The calculation of mass flow rates and rate of heat transfer will be shown in the following sections. Eqn 4.20 and 4.21 are two simultaneous first order differential equations with T and P as unknowns and can be integrated numerically to obtain values of P and T at chosen intervals of crank angle.

4.2.3 Heat transfer model

4.2.3.1 Literature Review

The heat transfer in compressor occurs in four parts. The first part is suction gas heating in the suction line. The second is heat transfer from the discharge gas to the suction gas through the cylinder head wall and valve plate. The third is indirect heating; due to pressure increase inside the cylinder, the temperature of the working fluid increases. The fourth is regenerating heat transfer from the discharge gas to the cylinder/piston wall then from the cylinder/piston wall to the suction gas. Until recently, most mathematical models neglected the effect of heat transfer on the compressor performance. There are debates and contradictory opinions regarding to the significance of heat transfer influence on the compressor performance. There are

two reasons for the diverse conclusions. The first reason is the complexity of the phenomenon. Different experiments or different models have different results. The second is the differing scope of the evaluation. Some studies only focused on the regenerative heat transfer between the gas and cylinder wall. Others attempted an evaluation of the overall heat transfer effect.

In his work, Brok et al. (1980) disputed the findings of Adair et al. (1972) and developed a model to account for heat transfer effects which incorporated a modified version of the Adair's (referred to from now on) correlation. They concluded that heat transfer effects were not so dominant as described by Adair and gave a value of 2.5% as the maximum impact on volumetric efficiency or power requirement for the worst operating conditions. They came to the conclusion that the inclusion of heat transfer in compressor modelling did not greatly improve the model.

Later, Gerlach and Berry (1989) reported a systematic study of heat transfer effects in a reciprocating compressor. They divided it into direct and indirect heating effects. They used a wall heat transfer correlation similar to that of Adair to model regenerative heating in their overall compressor simulation model and arrived at heat transfer loss estimates by force fitting measured discharge temperature data. They also measured the capacity loss due to heat transfer by monitoring the capacity right from the instant the compressor was started until the system attained a steady state. They noticed a capacity loss as high as 10%. Their results indicate that heat transfer plays a very important role in achieving efficient operation of reciprocating compressors. Their conclusion of a large impact of heat transfer on volumetric efficiency was confirmed by Shiva Prasad (1992a, 1992b) in his detail investigations for developing a quick and direct analytical method for estimating the effect of suction gas heating on capacity loss.

Shiva Prasad (1998) gave a good review of the works on heat transfer in reciprocating compressors. He reported that the work of modelling heat transfer inside the cylinder itself was initially focussed on engines and started with the early dimensional models formulated by Nusselt (1923) and Eichelberg (1938). Those

models had inherent scaling problems and hence gradually gave way to dimensionless models proposed by Annand (1963) and Woschni (1967). The dimensionless models were mere adaptations of the Reynolds number – Nusselt number formulations commonly used in pipe flows and hence lacked representation of the physics of flow inside cylinders.

In the compressor field investigations by Adair et al (1972), Brok et al. (1980) and Liu et al. (1984) adapt a dimensionless model. Also, there have been attempts by some investigators like Chong and Watson (1976), Recktenwald et al. (1986) and Keribar and Morel (1988) to use the mathematical models of the conservation equations for extracting the proper velocity and length scales of fluid motions and incorporating them in dimensionless heat transfer models.

On a more fundamental basis, several studies have questioned the applicability of the simple Newton's law of cooling to a basically oscillating flow with large amplitude pressure variations. The possible existence of a phase difference, i.e. in time, between the heat flux and the temperature gradient for such a flow was recognized first by Pfriem (1943). He solved a simplified form of the one-dimensional energy equation and derived an expression for the complex Nusselt number, which could account for this phase difference. Later, Lee (1983) included the effect of turbulence by introducing a turbulent thermal diffusivity into his definition of the Peclet number. Also, Lawton (1987) proposed a new correlation for the gas/wall Nusselt number, again with reference to engines. Later, Kornhauser and Smith (1994) revised the complex Nusselt number model to cover the low and high ends of the Peclet number range.

However, Shiva Prasad (1998) reported that in spite of serious doubts about the ability of Newton's law of cooling to predict instantaneous heat transfer rates, its use is likely to continue due its simplicity. Also, Fagotti et al. (1998) reported that probably the simplification of no phase shift has been widely assumed to gain the benefit of dealing with simpler correlations. The experimental difficulties of

installing thermometers with adequate time response to measure directly the in-cylinder process, also inhibits progress in this work.

As discussed above, there have been many investigations concerning development of heat transfer correlations for the complex unsteady flow which exists inside the cylinders of reciprocating compressors. As far as cylinder passages, valve chambers and passages are concerned, virtually no special correlations are available. Although the flow could be considered as steady and hence appear simpler, the complexity of practical geometries excludes direct applicability of available standard correlations developed for laboratory type flows.

No detailed discussions of heat transfer to the suction pipe were found in the literature although there are several references to it (Squarer et al. 1972, Hiller and Glicksman 1976 and Scheideman et al 1978). Prakash and Singh (1974) used the Dittus-Boelter (1930) correlation, widely used to evaluate heat transfer in inner duct turbulent flow.

The valve passage-ways consists of the holes formed in the valve plate through which the working fluid moves when passing in and out of the cylinder. The valve-passage ways are generally of small cross-sectional area especially of hermetic compressors. There is a little data or comment on this heat transfer arrangement. Most of mathematical models did not even consider it. The importance of valve passage-way heat transfer is therefore uncertain.

4.2.3.2 Model Development

From the above discussion it can be seen that considerable uncertainty still exists as to the magnitude of heat transfer rates encountered within compressors and the suitability of existing correlations. However, from the work of Gerlach and Berry (1989) and Shiva Prasad (1992a, 1992b), it seemed necessary to this author to include cylinder heat transfer in the compressor model.

Two methods have been employed by various investigators to characterize the velocity field, these accompany two quite distinct modelling methods discussed in section 4.2.3.1 Adair et al. (1972), Brock et al. (1980) and Liu et al. (1984) have used a single average value for the characteristic velocity taken from the average swirl velocity. This results in the computation of a single value heat transfer coefficient for all the cylinder surfaces. On the other hand, Chong and Watson (1976), Recktenwald et al. (1986) and Keribar and Morel (1988) determined the spatial velocity field to compute the local heat transfer rates.

Fagotti et al. (1994) have analysed the most important correlations proposed in the literature to determine the gas-to-wall heat transfer through a pragmatic approach, of unknown accuracy. The correlations proposed by Annand (1963) and Adair et al. (1972) led to the best results, the latter with slightly lower precision. Both Annand's and Adair's correlations are widely used in reciprocating compressor simulations like those of Parakash and Singh (1974), Röttger and Kruse (1976), Todescat et al. (1992) Giovanni et al. (1996) Arzano-Daurelle (1998) and Manepatil et al. (1998). Hence, both correlations will be considered here.

Annand (1963) proposed the following correlation for internal combustion engines

$$Nu = A\,Re^{b} \qquad \text{Eqn 4.22}$$

where, A and b are experimentally determined. The author suggests values around 0.7 for both constants. He also mentioned the possibility of considering Peclet number Pe instead of Reynolds number; this procedure is considered here.

Adair et al. (1972) determined the correlation below, originally for compressors

$$Nu=0.053\,Re^{0.8}\,Pr^{0.6} \qquad \text{Eqn 4.23}$$

where, the characteristic velocity in the Reynolds number is

$$u = \frac{D_e}{2} w_g \qquad \text{Eqn 4.24}$$

where, D_e is the equivalent or characteristic diameter and defined as

$$D_e = \frac{1.5 \times \pi D^2 \times z(\theta)}{\pi D \times z(\theta) + 2\pi (D/2)^2} \qquad \text{Eqn 4.25}$$

and w_g is the swirl velocity and defined as

$$w_g = 2w(1.04 + \cos(2\theta)) \qquad \text{where, } \frac{3\pi}{2} < \theta < \frac{\pi}{2}$$

$$\text{or } w_g = w(1.04 + \cos(2\theta)) \qquad \text{where, } \frac{\pi}{2} < \theta < \frac{3\pi}{2} \qquad \text{Eqn 4.26}$$

The heat transfer in the compressor cylinder $\frac{dQ_{cv}}{d\theta}$ in Eqn 4.20 can be expressed as

$$\frac{dQ_{cv}}{d\theta} = \frac{hA\Delta T}{\Omega} \qquad \text{Eqn 4.27}$$

where, h heat transfer coefficient (W/m^2K)

A heat transfer area (m^2)

ΔT temperature difference between cylinder wall and refrigerant inside the cylinder (K)

Ω angular speed (rad/s)

The heat transfer area is obtained as following

$$A = A_p + A_{cl} + A_\Omega \qquad \text{Eqn 4.28}$$

where, A_p , piston area $= \frac{\pi D_p^{\,2}}{4}$

A_{cl} , clearance volume surface area $= 4\frac{V_{cl}}{D_p}$

$$A_\Omega = \pi D_p z(\theta)$$

The wall temperature T_w is assumed to be constant throughout the compressor cycle and is taken to be approximately equal to the mean value of the suction and discharge temperature. Alternatively, it could be calculated using the correlation developed by Liu et al. (1984) as following

$$T_w = 24.32 + 0.7191T_S + 5.64\frac{P_D}{P_S} - 17.936\frac{z(\theta)}{D_p} + 14.183(\frac{z(\theta)}{D_p})^2 \qquad \text{Eqn 4.29}$$

The rate of heat transfer in suction line is calculated as

$$Q_S = h_S A_S (T_{ch} - T_S) \qquad \text{Eqn 4.30}$$

The correlation used to calculate heat transfer coefficient in the suction line was that for a turbulent flow in a pipe quoted by Dittus-Boelter (1930) in the following form

$$h_S = 0.023\, Re^{0.8}\, Pr^{0.4} \frac{k}{D_S} \qquad \text{Eqn 4.31}$$

The suction line heat transfer area is obtained as following

$$A_S = \pi\, D_S L_S \qquad \text{Eqn 4.32}$$

where, D_S diameter of suction line (m)

L_S length of suction line (m)

T_{ch} is assumed to be cylinder head temperature and calculated using the correlation developed by Liu et al. (1984) as following

$$T_{ch} = 13.64 + 0.1791 T_S + 11.235 \frac{P_D}{P_S} \qquad \text{Eqn 4.33}$$

Due to the lack of information relating to transient heat transfer in valve passages of small surface area, the heat transfer effect in the valve passage-way will not be considered here. Also, the author believes the influence to be small.

4.2.4 Mass flow rate model

4.2.4.1 Literature Review

The literature on this subject is vast. Various expressions are used in computing the mass flow rate through valves according to the assumptions made. The majority of models assumed one-dimensional flow through an orifice. In some models (Yu et al. 1986 and Dechamps et al. 1988) the flow is treated as a two-dimensional flow in a diffuser. A steady flow model has predominated. However, a few considered unsteady flow condition like Böswirth (1984, 1990 and 1996).

In general, the model applied for one-dimensional steady state flow through the valves was derived for upstream stagnation conditions and neglected change of potential energy. The First Law of Thermodynamics was applied to account for compressible, adiabatic and isenropic flow. Further, this equation could be expressed in terms of enthalpy differences for a real gas (Röttger et al. 1976, Scheideman et al. 1978, Ng et al. 1980, Sun et al. 1995) or by using an isentropic exponent in an ideal gas model (Sodel 1972, Prakash and Singh 1974, Arzano-Daurelle et al. 1998, Yanagisawa et al. 1999, Corberán et al. 2000). The flow equation based on the Bernoulli equation would be sufficient as long as the flow is treated as

incompressible. The flow in the incompressible flow approach could be viscid (Böswirth 1984 and 1990) or inviscid, i.e. isothermal (Lorentzen 1955, Blankespoor and Touber 1972, Bredesen 1974, Mars et al. 1979, Liang et al. 1991 and Xin 2000).

Most expressions however utilize an effective force area which assumes that the valve behaves as a simple single orifice of varying diameter. The resulting mass flow rate equation was thus a function of the valve system geometry and the valve lift.

$$\frac{dm}{d\theta} = K\ A(y)\ f(\Delta P) \qquad \text{Eqn 4.34}$$

where $\frac{dm}{d\theta}$ the mass flow rate through the valve

K the orifice or discharge coefficient

$A(y)$ the flow area and will depend on the geometry of the valve seat and port

$f(\Delta P)$ a function of pressure difference across the valve derived from the flow model chosen

K and $A(y)$can be combined for simplicity to give the effective flow area, $A_f(y)$. The effective flow area is a function of valve lift while the valve moves towards its stop. The area is often linearly proportional to valve lift until $y \approx 0.2\ d$, where d is the effective radius of the port (see Ferreira et al. 1986). There is then normally a non-linear section until the effective area saturates at a value equal to the port area. At this point, the influence of the valve is negligible.

Schwerzler and Hamilton (1972) attempted to develop an analytical expression for the effective (sometimes called equivalent) flow area for ring valves. The derived expression represents the restriction of flow area as a combination of simple orifices connected in parallel and/or series. The flow coefficients for each orifice are determined from published values on incompressible flow through general configurations similar to the particular restriction in question. But, from the literature published after the above paper it would appear that few compressor models have employed this analytical method. Most mathematical models used empirical

coefficients for effective flow area. Some regarded the flow coefficient as a function of valve lift. The majority however regarded it as being independent of valve lift.

4.2.4.2 Model Development

The following assumptions are made concerning flow through valves:

- Flow may be treated as one-dimensional flow through an orifice.
- Instantaneous, unsteady, flow rates can be computed from a steady state flow analysis.
- Potential energy terms are neglected.
- Upstream conditions may be regarded as stagnant. This is because the upstream cross sectional area is large compared to that of the valve.
- The proportion of time when sonic vapour velocities through the valve occur is negligible compared to the total time when the valve is open. Thus no analysis for sonic flow is necessary and in all conditions, sub-sonic flow expressions may be employed. White (1994) assumed that Mach number equal to 0.3 is the upper limit where incompressible flow may be considered to occur. This assumption is valid for well-designed valves with large effective flow areas. For such valves sonic flow is likely to occur only when valve excursion from the seat is small and it is assumed that this condition only exists for a very small proportion of the total valve open time.

Based on Bernoulli and continuity equations, the flow equation applied for both the mass flow into and out of the cylinder is

$$\frac{dm}{d\theta} = \frac{C_f}{\Omega} A_f \sqrt{2\rho_d \Delta P} \qquad \text{Eqn 4.35}$$

where, C_f, flow coefficient (-)

A_f, flow area of valve gap, $= \pi\, d_p\, z(\theta)$ (m^2)

ρ_d, down-stream density (kg/m^3)

ΔP, gas pressure difference (kPa)

d_p, valve port diameter (m)

Here, The flow coefficient for both the suction and discharge valves are assumed to be constant throughout the range of valve openings and pressure ratios found in the flow processes and obtained from the data available in the literature and/or based on experience of the users.

4.2.5 Leakage model

4.2.5.1 Literature Review

There are two different paths of gas leakage out of (or into) the compression chamber: leakage past the piston, i.e. piston blow-by and leakage between valves and their seats. For valve leakage, it is necessary to distinguish between the leakage when the valve is at rest on its seat, held down by pressure e.g. static leakage and the leakage when the valve is doing its job in the cylinder i.e. dynamic leakage or back flow.

Piston blow-by loss of reciprocating compressors takes the gas back to the suction side. It is dependent mainly upon the clearance gap which is itself a function of wear and temperature. The significance of piston leakage is reduced for pistons with rings where the leakage rate in the range of 2 - 4% of the mass flow rate (Jacobs 1976), compared with values up to 12% for plug pistons (Ferriera et al. 1984). This later figure, applying to the most common type of piston in small hermetic compressors must be regarded as significant. Besides the loss of capacity, leakage out of the compression chamber back to the suction side is equivalent to a loss of the energy which is required to compress the gas to that pressure, when the leakage occurs.

Leakage through the clearance between the piston and the cylinder has been considered in a number of studies. Various piston blow-by formulae have been established. Smith (1961) used the simple momentum and continuity equations to calculate the leakage mass flow rate for the plug piston of a small refrigeration compressor. Brown and Pearson (1963) presented an empirical linear relationship between piston leakage and mean differential pressure based on their experimental work on a single cylinder, reciprocating compressor fitted with a piston having one ring. Imaichi et al. (1978) used the Navier-Stokes equations to derive an expression

for the approximate mass escape through the clearance between the plug piston and the cylinder wall. Similar expressions were developed by Scott and Davis (1978) and Bukac (2000). Jacobs (1976) developed analytical and experimental techniques for evaluating piston blow-by loss for an HCFC-22 ring type, two cylinder compressor. He assumed an isothermal expansion past the piston ring. Experimental work showed that the model provided successful predictions. Later, Ferriera et al. (1984) evaluated the leakage past plug pistons. Two mechanisms for leakage are suggested; direct leakage (vapour) and indirect leakage which occurs when oil in which refrigerant is dissolved is scraped off the cylinder wall into the crankcase when the pistons descends. Fairly complex expressions are derived for the two mechanisms. Close agreement between theory and experiment is achieved for radial clearance less than 10 μm after which the theory significantly under predicts the losses. Mass leakage is found to vary between 0.5 and 12% of the total mass flow rate over the experimental range of operating conditions. But, due to the complexity of the derived expressions, they are unlikely to be commonly used for leakage modelling of plug pistons. Finally, Liu et al (1986) studied the sealing characteristics of piston rings and lubrication oil effects on an air reciprocating compressor. Their expression accounted for three possible paths of gas through the rings: rings and the surface of the cylinder, rings and bottom of piston slot and end gaps of rings. An oil sealing coefficient was introduced to take account of the oil sealing effect.

4.2.5.2 Model Development

Hughes et al. (1972) performed tests on a special rig to examine the magnitude of leakage past closed valves. In the test rig the valve seats were oiled to simulate real operating conditions and a constant supply of high pressure air was supplied to the valve. At a pressure ratio of 4, the effective leakage area was found equal to 0.65% of the valve area (undefined, but it is assumed that the port area is meant). This is quite a small cross-sectional area which would depend upon the type of valve seat and oil used. In the absence of other substantiation of this figure static valve leakage will not be considered here. Only the leakage past the piston is considered for two reasons:

(1) Due to the large leakage area of the gap between the piston and the cylinder, its negative influence on the compressor performance is more likely to exceed that of valve leakage.

(2) The back flow calculation is likely to be inaccurate here since gas pulsation effects in the suction and discharge lines have been ignored. Also, the time interval of delay in valve closing could be neglected compared with the total time interval of valve opening. The delay in valve closing results mainly from the oil stiction force which delays the departure of the valve from the stop.

The model developed here is based on the same assumptions made by Jacobs (1976) for flow past rings, namely the flow can be regarded as isothermal and incompressible. The latter approximation can be made only if the velocity of the vapour in the circumferential clearance gap is much less than the sonic speed in the vapour.

Referring to Jacobs (1976), the rate of leakage past the rings is

$$\frac{dm}{dt} = \left\{ \frac{2(\pi D)^2 h^3 (P_u^{\,2} - P_d^{\,2})}{F \times L \times RT_u} \right\}^{1/2} \qquad \text{Eqn 4.36}$$

where, D diameter of piston (m)

h equivalent distance between ring and cylinder due to the irregular surface (m)

P_u upstream pressure (kPa)

P_d downstream pressure (kPa)

F friction factor (-)

L ring width (m)

T_u upstream temperature (K)

R gas constant (J/kg K)

The radial clearance space can be modelled as a duct of rectangular cross-section of width equal to the circumference of the piston, length equal to ring height and

thickness equal to the effective radial clearance. A correction factor, C_{oil}, of 0.7 is used to account for oil films on piston and cylinder walls that occupy a fraction of the space, as suggested by Liu et al. (1986). The friction factor for laminar flow in a duct of rectangular cross-sectional area is equal to *96/Re.* Thus, Eqn 4.36 can be rearranged to give the piston leakage rate as:

$$\frac{dm}{d\theta} = C_{oil} \frac{(\pi D)h^3(P_u^{\ 2} - P_d^{\ 2})}{24 \times \Omega \times \mu_u \times L \times P_u v_u} \qquad \text{Eqn 4.37}$$

4.2.6 Valve dynamics model

Considering a single cycle it is possible to see the motion of the valves and the way in which they affect the performance of the compressor. When the cylinder pressure drops below the suction pressure, the suction valve does not immediately open because of oil stiction caused by oil on the seat and in most designs there may also be a spring pre-load preventing immediate movement. This delay in opening causes additional indicated cylinder work. During this delay a considerable pressure differential across the valve can build up so that when the valve finally opens it is rapidly driven to the stop by the differential pressure acting on the effective force area. The acceleration of the valve is determined by the valve mass, the force exerted by the pressure differential, the spring constant and the damping of the valve as it moves through the working fluid. The mass flow rate through the valve during suction depends upon both the pressure drop across the valve and the effective flow area. The pressure drop across the valve during suction necessitates work being done during suction. Once fully open the valve may bounce on its stop. Valve return begins when the spring force exceeds the pressure difference force, but may be delayed further by oil stiction on the valve stop. Since the stop/valve contact area is considerably less than the seat/valve contact area, oil stiction forces are less upon valve closure. As a result, a smaller pressure differential across the valve is developed and hence a smaller returning force exerted. This reduced pressure differential and consequent force acting on the valve to return it is partially responsible for the valve flutter often observed upon closure. Reverse flow through the valve may occur, reducing efficiency and mass flow rate. A similar description may be advanced for the discharge valve.

Since the study of self-actuating valves is fairly advanced, the literature review is intended to assess the existing simple methods of valve modelling with the aim of developing a model which would describe valve behaviour sufficiently to enable accurate predictions of the overall performance of the compressor including valve dynamic behaviour.

4.2.6.1 Literature Review

The literature on valve modelling is vast. There are three main types of models. First, there are models where the valve is treated as a mass-spring-dashpot system. Essentially it is dealing with a system with one degree of freedom. Second, there are models which treat the valve as a beam which may flex and exhibit resonant behaviour, thus allowing it to have two degree of freedom (Corberán et al. 2000). The third method allows the valve three degrees of freedom (Machu 2001) and is normally based on the finite element method, e.g. Sodel (1972), Hamilton (1974), Friley and Hamilton (1976) and Griner et al (1980). As a general rule the last two methods, but in particular the third, are used exclusively by valve designers to examine induced stresses and impact velocities.

Simple models of compressors do not even consider the dynamic motion of the valves but rather use an expression for volumetric efficiency to determine mass flow rate (Karll 1972). Other models regard the valves as opening in a step-wise fashion. Brablik (1974) regards the valves as opening instantaneously as soon as the pressure difference across them reverses. Squarer et al. (1972) also assume instantaneous opening and closing of the valves but this is regarded as occurring after a specified pressure drop across the valve has developed. They also allow for valve delay upon closing by regarding the suction valve to remain open until a certain angle after BDC and the discharge valve remaining open until a certain angle after TDC. These delay angles are found from experimental data. Hiller and Gliksman (1976) model the delay in the suction valve closure as a decrease in effective displacement and the delay in discharge valve closure as an increase of the effective dead space volume. The method of Brablik (1974) would not be very successful for most real compressors where valve delay on the opening and closing exists while the method

of Squarer et al. (1972) and Hiller and Glicksman (1976) require extensive experimental data over the whole range of operating conditions.

Most compressor models apply Newtons Second Law to the valve with the restriction that it behaves one-dimensionally, e.g. Blankespoor and Touber (1972), Prakash and Singh (1974), Röttger and Kruse (1976), Scheideman et al. (1978), Ng et al. (1980), Sun et al. (1995), Giovanni et al (1996), Manepatil et al. (1998), Arzano-Daurelle et al. (1998), Xin et al. (2000). Further empirical coefficients may be involved in the valve model, namely coefficients of pressure drag, damping and oil stiction. Little specific information has been published on these coefficients although work on coefficients of restitution and damping was reported. To survey the information would be difficult task since authors seldom define fully the coefficients used.

When the valve is in motion between the stops it is subject to a damping force as it moves through the working fluid. Most models account for viscous damping by the inclusion of a term in the valve equation of motion where the damping force is made proportional to the valve speed. The damping force is the greatest when the valve velocity is highest. The constant of proportionality is derived from experiment, e.g. Woollatt (1972), Röttger and Kruse (1976) and Scheideman et al. (1978), and may also be a function of lift, e.g. Blankespoor and Touber (1972).

Oil stiction is the phenomenon whereby a valve is delayed by the adhesive effects of oil present on seat or stop. Stiction constitutes an additional force which must be overcome before movement occurs. Clearly it is related to the quantities and properties of the oil present as well as the cross-sectional contact area. Oil stiction can reduce the mass flow rate by delaying the closure of both the inlet and outlet valves thus allowing reverse flow through the valve. This affects the suction process by permitting the working fluid back out of the cylinder and the discharge process by allowing it back into the cylinder. Oil stiction generated delay in valve opening creates additional unwanted cylinder over and under-pressure work. At the ideal time the valve should open, the pressure drop tending to open the valve becomes positive

and increases very rapidly. Once the force is enough to release the valve from the seat, it is high enough to accelerate the valve moving element very rapidly, causing a very high impact velocity. Opening and closing delays are likely to differ from each other and from valve to valve.

Little research appears to have been conducted on oil stiction. Giacomelli and Giorgetti (1974) undertook extensive investigations into oil stiction on ring valves. They note that the problem increases for higher rpm compressors since the delay time, which remains fairly constant, represents an ever-increasing proportion of the cycle time. Further works on the oil stiction of ring valves were presented by Bauer (1990) and Stehr (2001). Also, Brown et al. (1975), Fleming et al. (1983) and (Khalifa and Liu 1998) studied the influence of oil stiction on compressor reed valve performance.

It was decided to develop an equation of motion which would include all the most important behavioural features which affect overall compressor performance. The main requirement is the knowledge of when the valve opens and closes, and by how much. This is determined by oil stiction, valve inertia, spring constant and pressure drop along with the effective force area.

4.2.6.2 Model Development

Newton's Second Law was applied to establish a force balance on the valve to derive an equation for the dynamic valve motion. Assuming a valve to be a damped spring-mass system having a single degree of freedom, the equation of valve motion formed a second order differential equation:

$$m_{ve}\frac{d^2y}{dt^2} + R\frac{dy}{dt} + ky + F_0 + F_{stick} = F_g \qquad \text{Eqn 4.38}$$

where, m_{ev} equivalent mass of the valve (kg)

y valve displacement (m)

R viscous damping coefficient, $= 2\, m_{ev}\, \Omega\, \zeta$ (N s/m)

k spring stiffness (N/m)

F_{stick} stiction force (N)

F_0 pre-load on the valve (N)

F_g gas force (N)

Eqn 4.38 can be expressed non-dimensionally and in terms of crank angle. Thus in terms of crank angle,

$$\Omega = \frac{d\theta}{dt} \qquad \text{Eqn 4.39}$$

using the chain rule of differentiation,

$$\frac{dy}{dt} = \frac{dy}{d\theta} \times \frac{d\theta}{dt} \qquad \text{Eqn 4.40}$$

Substitute Eqn 4.40 into Eqn 4.39 gives

$$\frac{dy}{dt} = \Omega \frac{dy}{d\theta} \qquad \text{Eqn 4.41}$$

Similary,

$$\frac{d^2y}{dt^2} = \Omega^2 \frac{d^2y}{d\theta^2} \qquad \text{Eqn 4.42}$$

Eqn 4.38 can now be re-written as:

$$\frac{d^2y}{d\theta^2} = \frac{1}{m_{ve}\Omega^2}\left(A_F(y)\Delta P - \Omega R \frac{dy}{d\theta} - ky - F_0 - F_{stick} \right) \qquad \text{Eqn 4.43}$$

Eqn 4.43 can be reduced to two simultaneous first order differential equations. One of the equations described the valve lift and the other described the valve velocity.

Letting $\frac{dy}{d\theta} = Y$ Eqn 4.44

then $\frac{dY}{d\theta} = \frac{1}{m_{ve}\Omega^2}\left(A_F(y)\Delta P - \Omega R Y - ky - F_0 - F_{stick}\right)$ Eqn 4.45

The real valve system has multi-degree of freedom but the model developed here was only able to deal with one degree of freedom. So an equivalent valve mass was calculated. There might be several methods of calculating valve mass. The method applied here was the same used by Xin et al. (2000). He assumed the reed valve equivalent mass is the sum of the valve mass and one third of the spring mass. For the ring-type valve, the equivalent valve mass takes two thirds of the valve mass.

For reed type valves, the spring stiffness is determined by the valve material and the thickness and width of the reed valve. For the small excursions in lift experienced the valves can be generally regarded as obeying Hooke's law. In ring type valves, the valve spring is used to close the valve in time. That is, before the dead centre (when the piston reverses direction). If the spring is too light, the valve will close late and will then be slammed shut by the reverse gas flow. If the spring is too stiff, the gas force cannot hold the valve fully open.

Frequently, valves are assembled, intentionally or because of tolerance chaining, so that the valve is pushed against its seat. It is believed that this initial force or pre-load helps to improve sealing and prevents rebound of the valve from its seat. On the other hand, it also delays valve opening that results in a bigger spike on the cylinder pressure.

The gas flow through the valve produces a gas force which determines the valve movement together with other forces. The gas force depends on the pressure difference across the valve and the effective force area. Eqn 4.46 was employed to describe the gas force

$$F_g = A_F(y)\Delta P = C_D A_v \Delta P \qquad \text{Eqn 4.46}$$

where, A_F equivalent (effective) force area (m^2)

ΔP pressure difference across the valve (kPa)

C_D pressure drag coefficient (-)

A_v valve surface area (m^2)

The product of the pressure drag coefficient and the valve surface area is called the effective force area. The pressure drag coefficient may be calculated or measured. The effective force area, a function of valve lift and working fluid flow direction, is defined simply as the force exerted on the valve divided by the pressure difference across it. Clearly, it is related to the total surface area of the valve, the port area, the surrounding geometry and the direction of flow. When the valve is closed, the effective force area is simply equal to the valve port area, but after it opens this alters since the whole plate area is then exposed to the fluid flow.

Schwerzler and Hamilton (1972) developed an analytical expression for the effective force area for ring valves. Knowledge of the effective flow area is required. Fairly good predictions were achieved for seven different ring valves analysed. Not many models utilized this analytical method, instead most assumed the equivalent force area, which is a function of valve lift and can be found experimentally, e.g. Röttger and Kruse (1976) and Ng (1980). It was assumed that experimental data acquired from steady state flow conditions could be applied to conditions in the compressor where the flow is changing. Published experimental data is still fairly scarce. Trella and Soedel (1974) and Ferreira et al. (1986) presented data for example.

Since valve types vary significantly and there are no available formulae to correlate data relevant to different valve configurations, like the flow coefficient, the pressure drag coefficients for both the suction and discharge valves are assumed to be constant throughout the valve movement.

Stiction is accounted for in various ways. The simplest approach is to introduce a time delay in the valve dynamic model, e.g. Maclaren and Kerr (1969) and Squarer et al. (1972). Most, however employ empirical coefficients and treat it as an additional force term in the dynamic equation, e.g. Blanespoor and Touber (1972) and Bukac (2002). More sophisticated models provided solutions of the thin film, low Reynolds number Navier-Stokes equations for simple valve geometries subjected to time-varying pressure differences (Khalifa and Liu 1998).

Eqn 4.47 is used in order to employ the stiction force in valve model

$$F_{stick} = C_{stick}\, k\, y_0 \qquad \text{Eqn 4.47}$$

where, C_{stick} stiction coefficient (-)

y_0 maximum valve height (m)

The stiction coefficient for the valve seat is not the same as that for the valve stop.

4.2.7 Thermophysical properties

In general, knowledge of the thermophysical properties is essential for the evaluation of refrigerants and the design of equipment using them. There are many models

commonly used to calculate the thermodynamic properties of refrigerants. Mclinden et al. (1997) presented a detailed review of the most commonly used models for alternative refrigerants including carbon dioxide. For pure refrigerants, the virial. cubic, Martin-Hou, Bendict-Webb-Rubin and Helmholtz energy equations of state and the extended corresponding states (ECS) models were presented. Guilpart et al. (1998) used a curve fitted polynomial approach to develop computer subroutines for rapid evaluation of the main thermodynamic properties of natural refrigerants. However, the range of applicability was very limited for carbon dioxide and would not cover transcritical applications.

In the view of the existence of multiple approaches representing the thermodynamic properties of the alternative refrigerants and their mixtures, a programme working group of IEA – Annex 18 (1999) – entitled: 'Thermophysical Properties of the Environmentally Acceptable Refrigerants' evaluated the available models and recommended formulations as international standards. The Helmholtz model equation of state developed by Span and Wagner (1996) was recommended by Annex 18 as yielding the most accurate thermodynamic properties available for carbon dioxide.

Currently, property databases are widely used for the design and analysis of refrigeration and heat pumping systems. In this work it was decided to employ this approach. The National Institute of Standards and Technology (NIST) Standard Reference Database 23 – REFPROP Version 5.0 (1996) was used to calculate the CO_2 properties. REFPROP is an interactive computer database for the prediction of thermodynamic and transport properties of pure fluids and their mixtures. Mixtures with up to 5 components may be specified from among the 43 pure fluids. Virtually any combination is allowed.

Two models within REFPROP are used for the thermodynamic properties of pure components. The first model is the Carnahan-Starling-DeSantis (CSD) equation of state (DeSantis et al. 1976). The simplicity of CSD equation of state is both its main attribute and major limitation. Because it requires only 6 adjustable coefficients per

fluid, the CSD equation can represent properties quite well over limited ranges, even for fluids with very limited experimental information; it is easily extended to mixtures. But such a simple model cannot represent all of the properties of a fluid over wide ranges of temperature and pressure with high accuracy. The second pure fluid model is the modified Benedict-Webb-Rubin (MBWR) equation of state. MBWR is a highly accurate equation of state discussed in detail by Younglove and Mclinden (1994). This equation can accurately represent thermodynamic properties over wide ranges of temperature and pressure but requires extensive data to fit its 32 adjustable coefficients; it is thus available for only select fluids for which wide-ranging data are available. All mixture properties are calculated with the ECS model of Huber et al. (1994). It is used for fluids with limited data. The ECS model is based on the idea that, with the appropriate scaling of temperature and density, the properties of a fluid can be mapped onto those of a reference fluid.

Transport properties such as viscosity and thermal conductivity are calculated with an ECS model (Ely and Hanley 1981, 1983); this model is also recommended for the thermodynamic properties of mixtures and also for pure fluids when the MBWR model is not available. In the ECS model the properties of a range of related fluids are scaled to a well-characterized reference fluid HFC-134a.

4.2.8 Performance criteria

This section details the equations describing many of the parameters of interest to the compressor performance criteria. In general, the term performance of a compressor means different things to different people in the compressor industry. In the refrigeration and heat pump industry, some of the most common terms used to indicate the compressor performance are system coefficient of performance (COP), energy efficiency ratio (EER). The general definition of COP and EER is the ratio of cooling or heating capacity to the power supplied the system. The difference between these two definitions is the capacity, which are expressed in watts for the COP but Btu per hour for EER. Power supplied is expressed in watts for both definitions. So one has dimensions and the other is dimensionless. These two definitions do not give

any idea of the various energy and mass flow losses occurring in the compressor. Therefore they are not appropriate for compressor performance criteria.

In very general terms, the performance of the machine is an evaluation of the ability of the machine to accomplish the task it has been designed for. In the case of a compressor, its task is to pump the maximum possible quantity of gas from the given suction conditions to the desired discharge conditions with the least amount of energy consumption. Thus, two useful criteria for performance emerge: capacitive performance and energetic performance.

4.2.8.1 Capacitive Performance

The capacitive performance of the compressor relates the actual flow of refrigerant to an ideal flow assuming no losses. Most often the capacitive performance is described by the volumetric efficiency. The volumetric efficiency accounts for many different phenomena: clearance volume re-expansion, pressure drops in valves, internal heating of suction gas, etc. The mathematical definition of volumetric efficiency is given in three ways:

(1) A theoretical or clearance volumetric efficiency $\eta_{v,th}$ based on the ideal compressor cycle which accounts for clearance volume expansion.

$$\eta_{v,th} = 1 - \frac{V_{cl}}{V_{swept}}\left(\left(\frac{P_d}{P_s}\right)^{\frac{1}{\gamma}} - 1\right) \qquad \text{Eqn 4.48}$$

where, γ isentropic exponent (-)

V_{swept} swept volume (m^3)

An indicated volumetric efficiency $\eta_{v,ind}$ based on the actual mass of gas induced per cycle during the interval the suction valve is actually open which accounts for suction gas heating and clearance volume expansion is given by

$$\eta_{v,ind} = \frac{(m_{svc} - m_{svo})v_s}{V_{swept}} \qquad \text{Eqn 4.49}$$

where, m_{svo} cylinder mass at suction valve open (kg)

m_{svc} cylinder mass at suction valve close (kg)

v_s specific volume of gas at suction condition (m^3/kg)

(2) An actual or overall volumetric efficiency $\eta_{v,act}$ based on actual mass of gas delivered through the discharge valve which accounts for blow-by effects, suction gas heating and clearance volume expansion.

$$\eta_{v,act} = \frac{(m_{dvc} - m_{dvo})v_s}{V_{swept}} \qquad \text{Eqn 4.50}$$

where, m_{dvo} cylinder mass at discharge valve open (kg)

m_{dvc} cylinder mass at discharge valve close (kg)

4.2.8.2 Energetic Performance

The energetic performance of a compressor can be described by several different efficiencies comparing the actual power consumption to the power consumption of a reference process; most often a reversible adiabatic, i.e. isentropic, compression process is used as reference for expressing the energy efficiency of a compressor. The compression or indicated efficiency based on indicated work calculated from indicator diagram is described as:

$$\eta_{ind} = \frac{(m_{svc} - m_{svo}) \times \frac{N}{60} \times \Delta h_s}{PW_{ind}} \qquad \text{Eqn 4.51}$$

where, Δh_s specific isentropic compressor work (J/kg)

N compressor speed (rpm)

PW_{ind} indicated power (W)

PW_{ind} is calculated using the equation:

$$PW_{ind} = W_{ind} \times \frac{N}{60} \qquad \text{Eqn 4.52}$$

where, W_{ind} is the indicated cycle work (J/cycle)

The indicated cycle work corresponds to the total area enclosed by the pressure/volume curve. It is calculated by storing the values of cylinder pressure P

and cylinder volume V for each step of the calculation throughout a compressor cycle and evaluating $\int PdV$ by summing the area, PdV, of a number of elemental strips over the whole compressor cycle.

The part of the area enclosed by the curve and below the horizontal line representing the mean suction pressure can be described as the indicated cycle suction work. The indicated cycle suction work, W_{suc}, is calculated by storing the values of cylinder pressure and volume for each step of calculation during the suction stroke and then calculating the area of the indicator diagram below a line corresponding to the nominal suction pressure. In the same way, that part of the enclosed area which is above the mean discharge pressure can be described as the indicated cycle discharge work. The indicated cycle discharge work, W_{dis}, is calculated in a similar way to the suction work. These are the quantities of pumping work which are necessary per cycle in order to induce refrigerant into the cylinder and to discharge it. The necessity for pumping work arises from the pressure losses across the suction and discharge valves.

The average suction pressure $P_{suc,av}$ was calculated using the equation

$$P_{suc,av} = P_s - \frac{W_{suc}}{V_{svc} - V_{svo}} \qquad \text{Eqn 4.53}$$

where, P_s suction pressure (kPa)

V_{svc} cylinder volume at suction valve close (m^3)

V_{svo} cylinder volume at suction valve open (m^3)

Similary, $P_{dis,av} = P_d - \frac{W_{dis}}{V_{dvo} - V_{dvc}}$ Eqn 4.54

where, P_d discharge pressure (kPa)

V_{dvc} cylinder volume at discharge valve close (m^3)

V_{dvo} cylinder volume at discharge valve open (m^3)

A common practice regarding calculation of the aforementioned compressor efficiencies for hermetic and semi-hermetic compressors is to refer the refrigerant properties to the compressor shell inlet. In a more profound compressor rating,

compressor efficiencies are also calculated with reference to the cylinder inlet. The influence of the suction gas heating caused by the compressor motor and cylinder head and warm parts are omitted in the last case.

4.3 Computer simulation

The simulation of the compressor involves many mathematical sub-models which are coupled to each other. For instance, the valve behaviour is governed by the pressure differential across it and these pressures are calculated by the compression chamber thermodynamic model which in turn depends upon the valve model, heat transfer, piston blow-by and crank mechanism kinematics models. Thus, the implementation of the simulation requires the simultaneous solution of several differential equations.

A generalized computer simulation program was developed. The computer program was written in Visual C++® 6.0 and calculates the conditions in a compressor cycle using small increments of crank angle $\Delta\theta$. The program is initialised at the chosen starting position $\theta = 0^0$, the piston at TDC where the cylinder pressure is taken as a trial value to be equal to the discharge pressure P_d while the cylinder temperature T_d is obtained assuming that compression is isentropic from the suction condition T_s and pressure P_s to the discharge pressure. The compression chamber thermodynamic equations, Eqn 4.20 and 4.21, are solved by the Runge-Kutta procedure, over a small increment of crank angle $\Delta\theta$ to predict new values of cylinder pressure P_c and temperature T_c. At each crank angle, the cylinder pressure P_c and temperature T_c are now known hence, by using the REFPROP database the other properties such as specific enthalpy, specific entropy and specific volume can be obtained, together with their partial derivatives. The cylinder volume is calculated uniquely for each crank angle (Eqn 4.2) and knowing the appropriate value of specific volume, the mass contained in the cylinder can be calculated. During opening and closing of the suction or discharge valve, the valve dynamic equations, 4.44 and 4.45, are solved to obtain the valve lift and the corresponding valve velocity. The mass flows through the valves and piston blow-by are calculated using Eqn 4.35 and 4.37, respectively. The cylinder heat transfer is obtained from Eqn 4.27. After completion of the first

compressor cycle calculation, the discharge valve may not close at starting point, θ $=0^0$, indicating that the chosen starting conditions were in error. The computation for the cycle is repeated using a revised starting condition and typically three cycles of computation are required to produce a converged solution.

At the end of the third cycle of computation several parameters of interest, e.g. mass flow rate, volumetric efficiency, compression efficiency, compression work and power and various losses are calculated. Variables such as cylinder pressure, temperature, specific volume, enthalpy, entropy, valve displacement and velocity are stored in files and can be used for plotting and further processing. A flow chart giving the sequence of operations in the compressor simulation program is shown in Figure 4.2.

4.3.1 Main program

The main program deals with the compression chamber thermodynamic model. As simultaneous solutions of several sub-models are required, six subroutines as listed below were incorporated in the main program: (1) kinematics model of crank mechanism, (2) mass flow through valves model, (3) cylinder heat transfer model, (4) valve dynamics model, (5) piston blow-by model and (6) Runge-Kutta model. The main program comprises of three main segments:

(a) Input and setting initial conditions

(b) Simulation

(c) Output

4.3.1.1 Input Data and Setting of Initial Conditions Segments

The input data required could be classified under the following categories: (1) geometrical description (2) initial conditions (3) empirical information. The main program starts by reading parameters which describe the working fluid, the operating

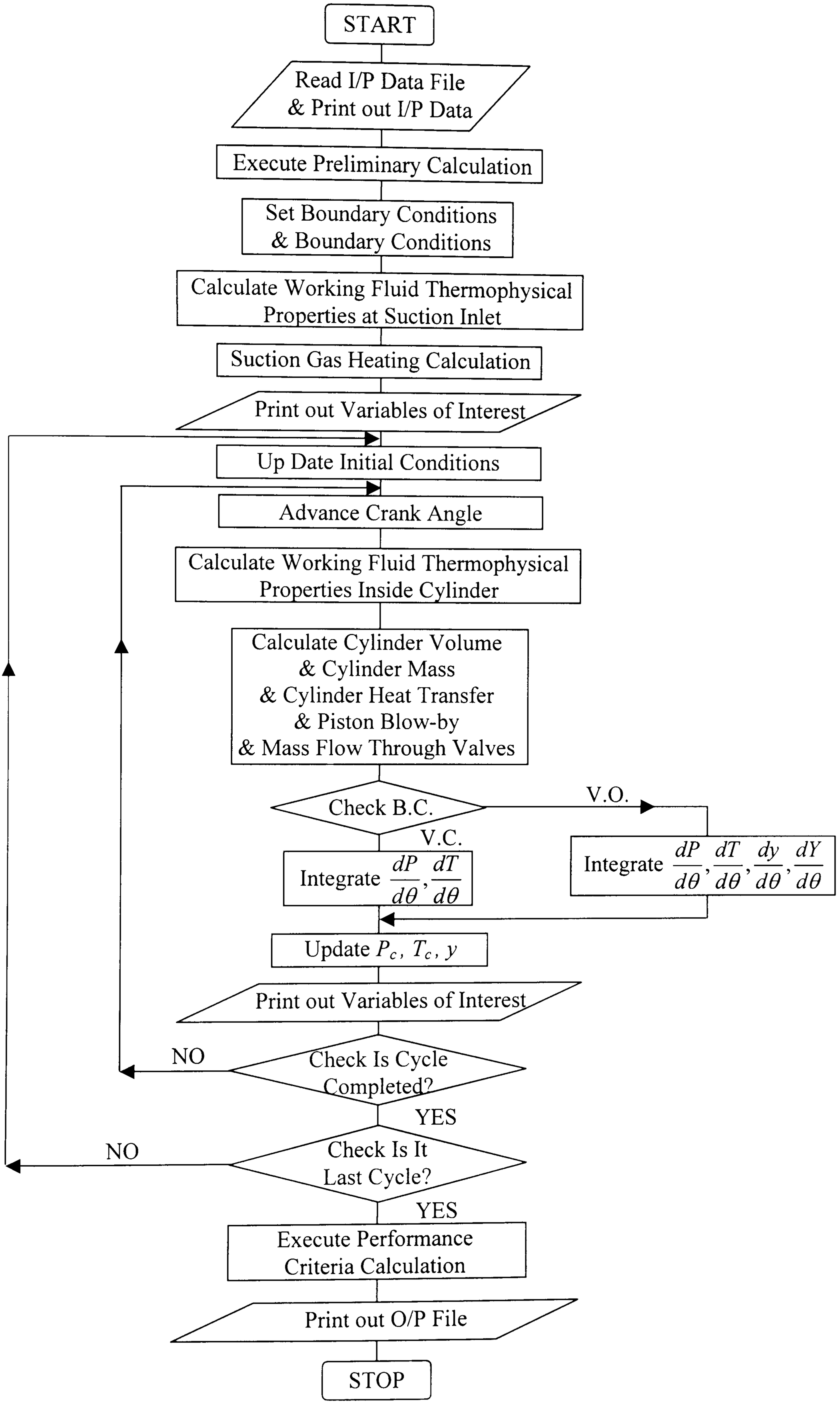

Figure 4.2 Flow chart of compressor simulation program

conditions, step size $\Delta\theta$, total number of cycles to be computed, the compressor geometry and the valves empirical coefficients. A list of the input parameters and variables is given in Appendix A. The input data is printed out to provide a cross check on input values.

The calculation of the suction gas heating in the suction line is followed the preliminary geometric calculations and initialisation of the REFPROP database. In the setting of the initial conditions, the piston is assumed to be at the TDC position at the start of the calculation, the cylinder pressure and temperature are assumed to be the pressure and temperature of the discharge line obtained from the operating conditions and the valves are fully closed.

4.3.1.2 Simulation Segment

The simulation of the compressor cycle is essentially a repeated simultaneous solution of a number of initial-value boundary condition problems. The simulation starts with the assumption that the initial pressure and temperature of the refrigerant in the cylinder when the piston is at its TDC are equal to those of the discharge condition. The REFPROP subroutines are called to determine all the other properties of the refrigerant in the cylinder. Calculation of the instantaneous mass inside the cylinder is followed by calculation of the derivative of specific volume of the gas in the cylinder. Different subroutines are next called to calculate the instantaneous cylinder heat transfer, mass flow through valves and piston blow-by. Derivatives of the cylinder pressure and temperature are integrated numerically by calling the Runge-Kutta subroutine. The conditions in the cylinder are then updated for the next crank angle and the process is repeated till a condition is reached at which the suction valve starts to move. In this case the valve dynamics equations are integrated in addition to the cylinder pressure and temperature derivatives by calling up the Runge-Kutta subroutine. A set of similar circumstances exists when the discharge valve is moving.

4.3.1.3 Output Segment

The program output provides the history of the refrigerant as it flows through the compressor by punching out cylinder temperature, pressure and fluid flow rates. Valve displacements and velocities are also obtained.

In the output segment, the variables which specify the state of the refrigerant at the various parts of the system, the valve displacement and velocities and other variables of interest were printed after each step. At the completion of the last cycle of the simulation, several parameters of interest such as mass flow rate, volumetric and compression efficiencies and various losses are calculated and printed.

4.3.2 Evaluation of thermophysical properties of refrigerant

The REFPROP subroutines were used to evaluate the complete thermodynamic state of the refrigerant at each crank angle. However, The property models are implemented as a suite of Fortran subroutines. The subroutines are written in ANSI-standard FORTRAN 90. As the main program was written in Visual C++® 6.0, a bridge subroutine between REFPROP subroutines and the main program was necessary to interpret different data types such that REFPROP subroutines could recognize it properly. Moreover, the REFPROP subroutines do not give the partial derivatives of pressure $\frac{\partial P}{\partial T}$ and $\frac{\partial P}{\partial v}$ explicitly. Hence, it was necessary to develop a further subroutine which is called to deliver the required derivatives.

4.3.3 Integration of a system of differential equations

Differential equations to be solved are constituted from Eqns 4.20, 4.21, 4.44 and 4.45. They are usually solved by a numerical method. Any of the following methods could be chosen, (1) Runge-Kutta, (2) finite difference or (3) Predictor corrector. In the present work, a 5^{th} order Runge-Kutta method was used. The crank mechanism equation explicitly gives the volume inside the cylinder for a given crank angle. Taken together with equations for the cylinder heat transfer, mass flow through the valves and piston blow-by, a system of simultaneous compression chamber

thermodynamic equations is generated. Thus, the required first order ordinary differential equations to be solved could be represented as follows:

$$\frac{dT}{d\theta} = T(\theta, P, T, y, Y)$$

$$\frac{dP}{d\theta} = P(\theta, P, T, y, Y)$$

$$\frac{dy}{d\theta} = y(\theta, P, T, y, Y)$$

$$\frac{dY}{d\theta} = Y(\theta, P, T, y, Y)$$

The Runge-Kutta subroutine first evaluates the right hand sides of the differential equations. These equations include: one each for the derivatives of cylinder pressure and temperature and two for the valve dynamics. When the subroutine is called, the number of equations to be calculated simultaneously is specified so that the right set of equations is evaluated.

After the solution of the above first order differential equations, the instant pressure and temperature are determined in the cylinder. Consequently, the state parameters of the working fluid inside the cylinder at every instant can be easily determined by using the REFPROP subroutines.

4.4 Validation against published data

It is necessary to establish the extent of the validity of the simulation program which describes valve behaviour and compressor performance. This can best be achieved by comparison between accurate experimental records and those predicted by the simulation program. In order to judge the correctness of the theoretical computation, the validity should be assessed over a wide range of compressor operating conditions and working fluids. For the present work, an assessment was made primarily by comparison of the computed results with experimental results published in the open literature for CO_2 reciprocating compressors.

Five different compressors have been studied for the purpose of verifying the present compressor model:

1. A small hermetic compressor developed by Fagerli (1996) for CO_2 compression.
2. A small open compressor developed by Yanagisawa et al. (2000) for CO_2 compression.
3. A relatively large open compressor developed by Bock GmbH Company and studied by Süss and Kruse (1997).
4. Second version of the Bock GmbH compressor in 3 (Försterling et al. 2002).
5. A relatively large open type R-502 compressor (Boyle 1985).

Comparisons of the actual and predicted performance for the above compressors are given in Figures 4.3 to 4.7. In general the comparisons show fair agreement. It is shown that the simulations of compressors 1 and 2 are reasonably good given that the model is restricted to constant plenum pressures (Figures 4.3a, b and c and 4.4a and b). The constant plenum pressures could also contribute to the lack of pressure pulsations in the simulated cylinder pressures. The agreement for compressors 3 and 4 (Figures 4.5a, b and c and 4.6) is also reasonable. The deviations during the suction and discharge strokes are due mainly to the pressure pulsations which occur in the suction and discharge plenums of the real compressors. A possible explanation of deviations during the expansion and compression strokes is the inaccuracy of the clearance volume value used in the model. The clearance volume is difficult to calculate since geometric details such as the clearances between the piston rings and their grooves and valve internal tolerances are not known. Moreover, the model calculation of heat transfer between the cylinder wall and the gas, having a high uncertainty, could contribute to these deviations.

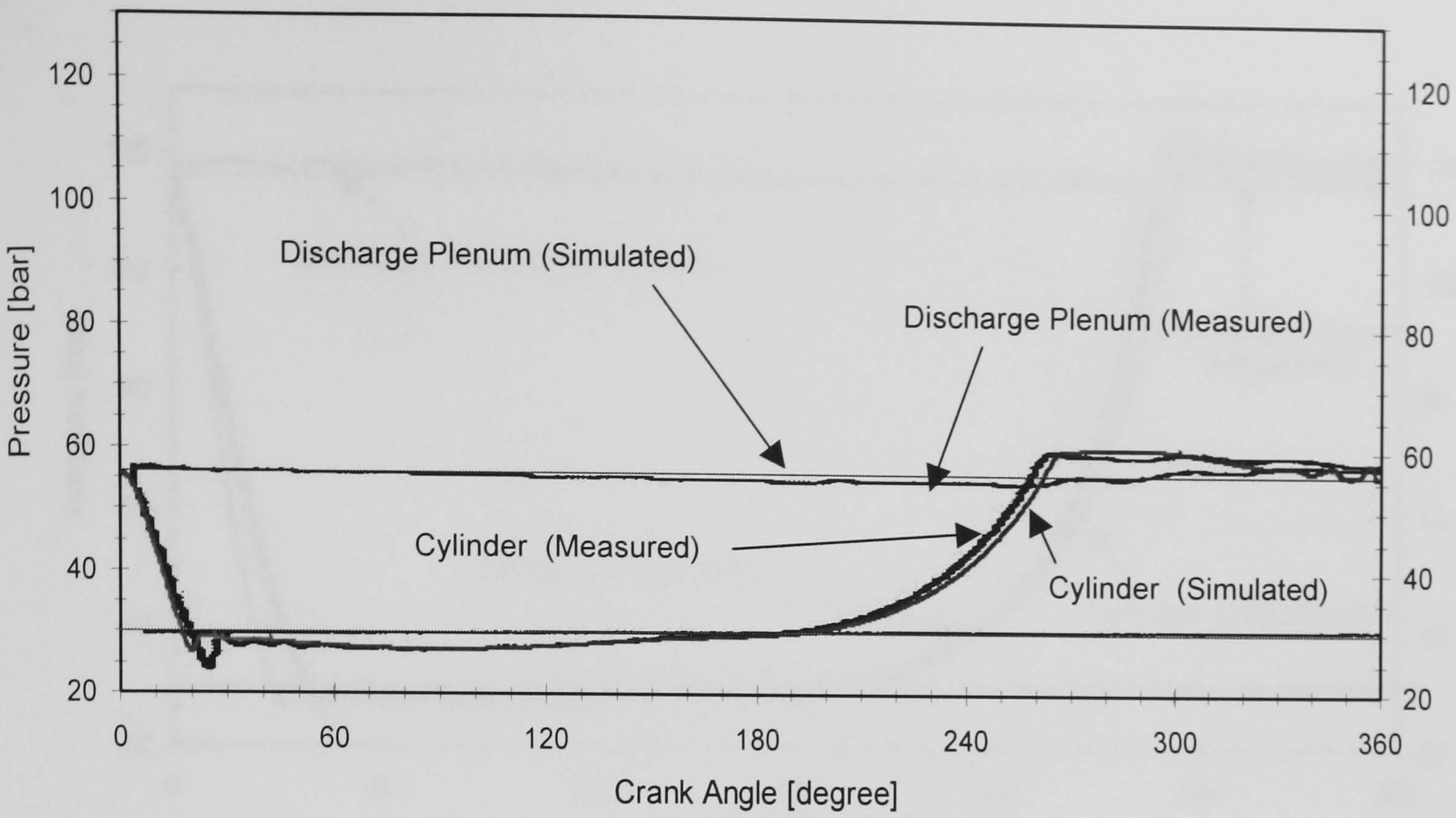

Figure 4.3a Comparison of simulated and measured cylinder pressure Vs crank angle for (Fagerli 1996) CO_2 compressor at 2940rpm, suction pressure 30 bar, discharge pressure 56 bar

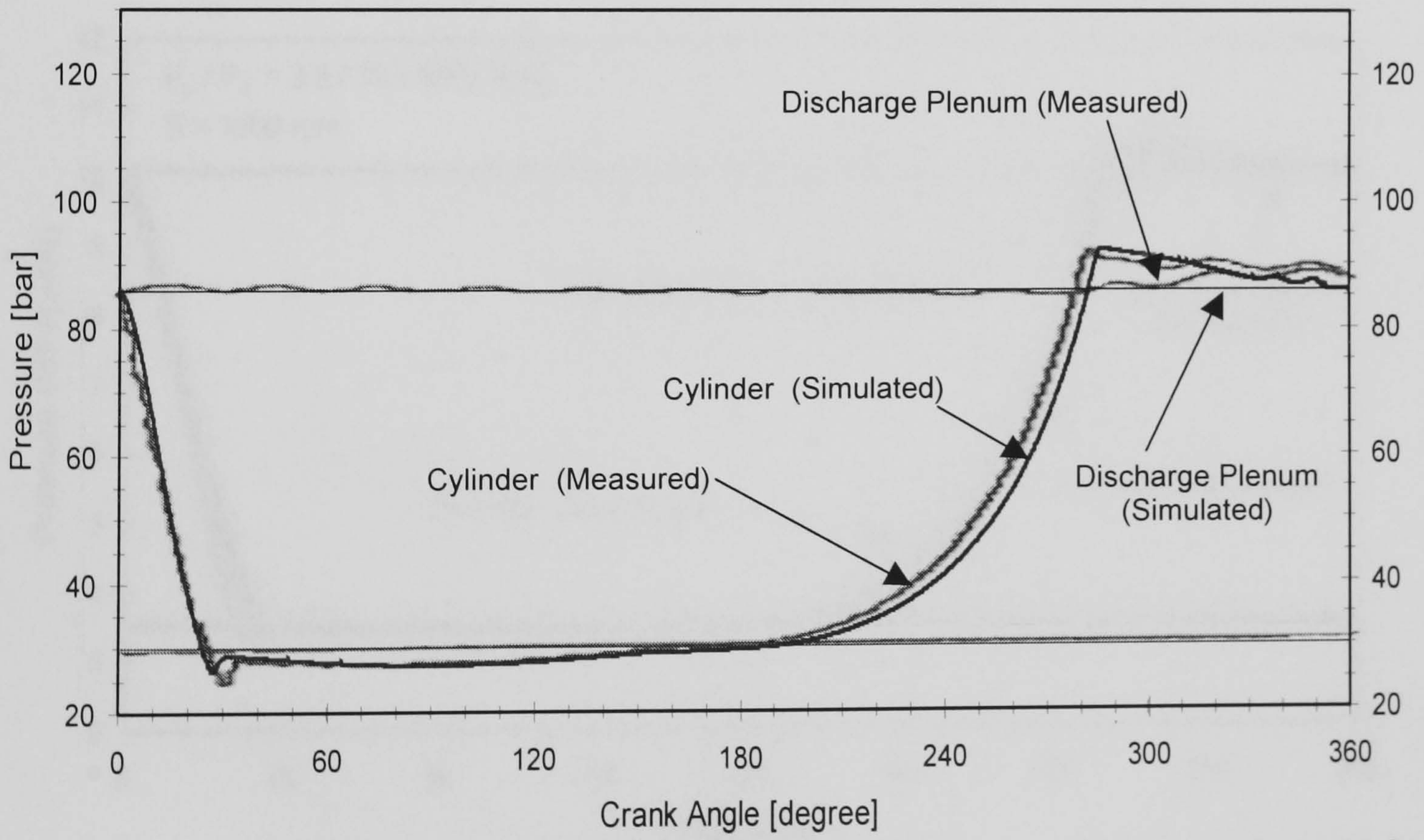

Figure 4.3b Comparison of simulated and measured cylinder pressure Vs crank angle for (Fagerli 1996) CO_2 compressor at 2940rpm, suction pressure 30 bar, discharge pressure 86 bar

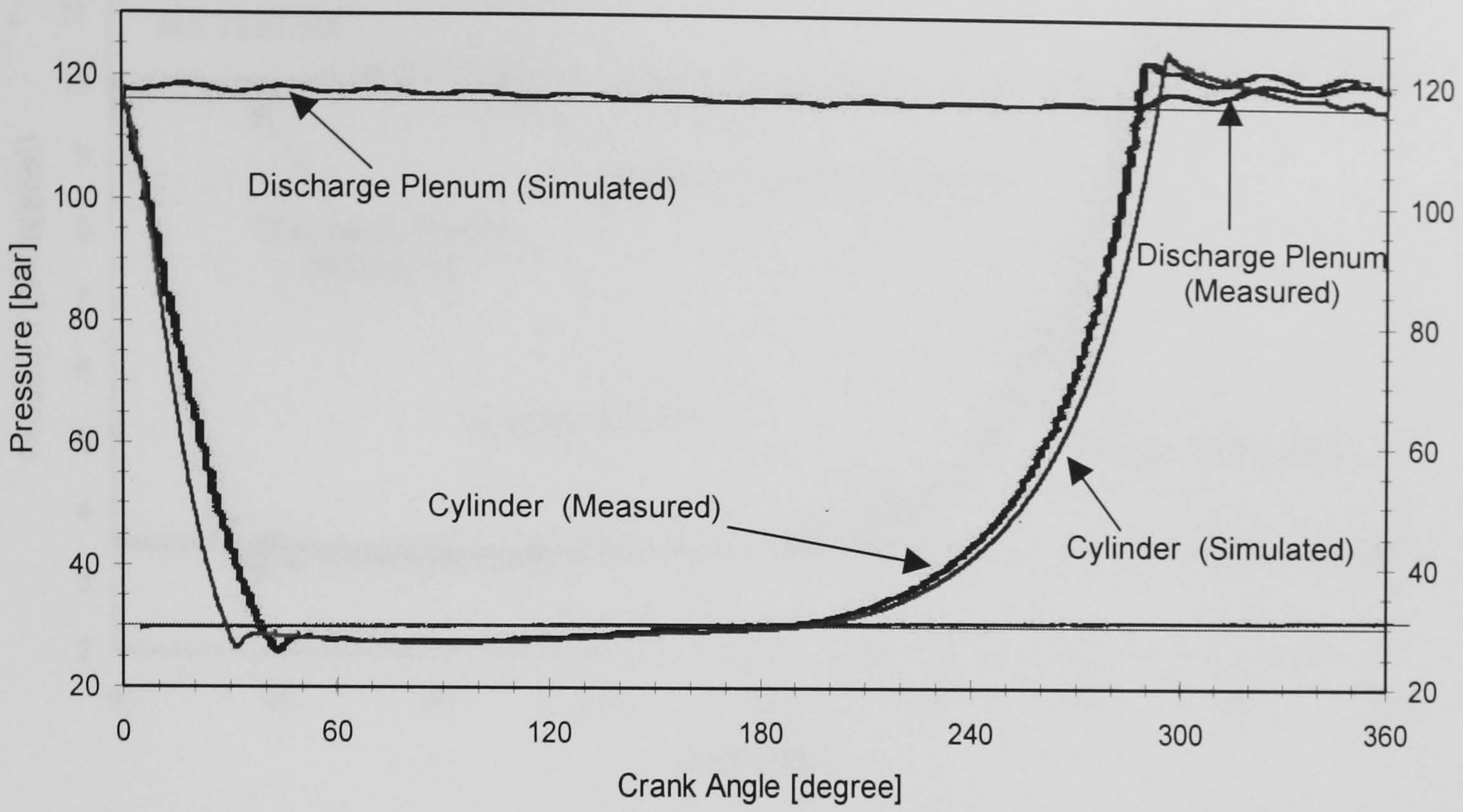

Figure 4.3c Comparison of simulated and measured cylinder pressure Vs crank angle for (Fagerli 1996) CO_2 compressor at 2940rpm, suction pressure 30 bar, discharge pressure: 116 bar

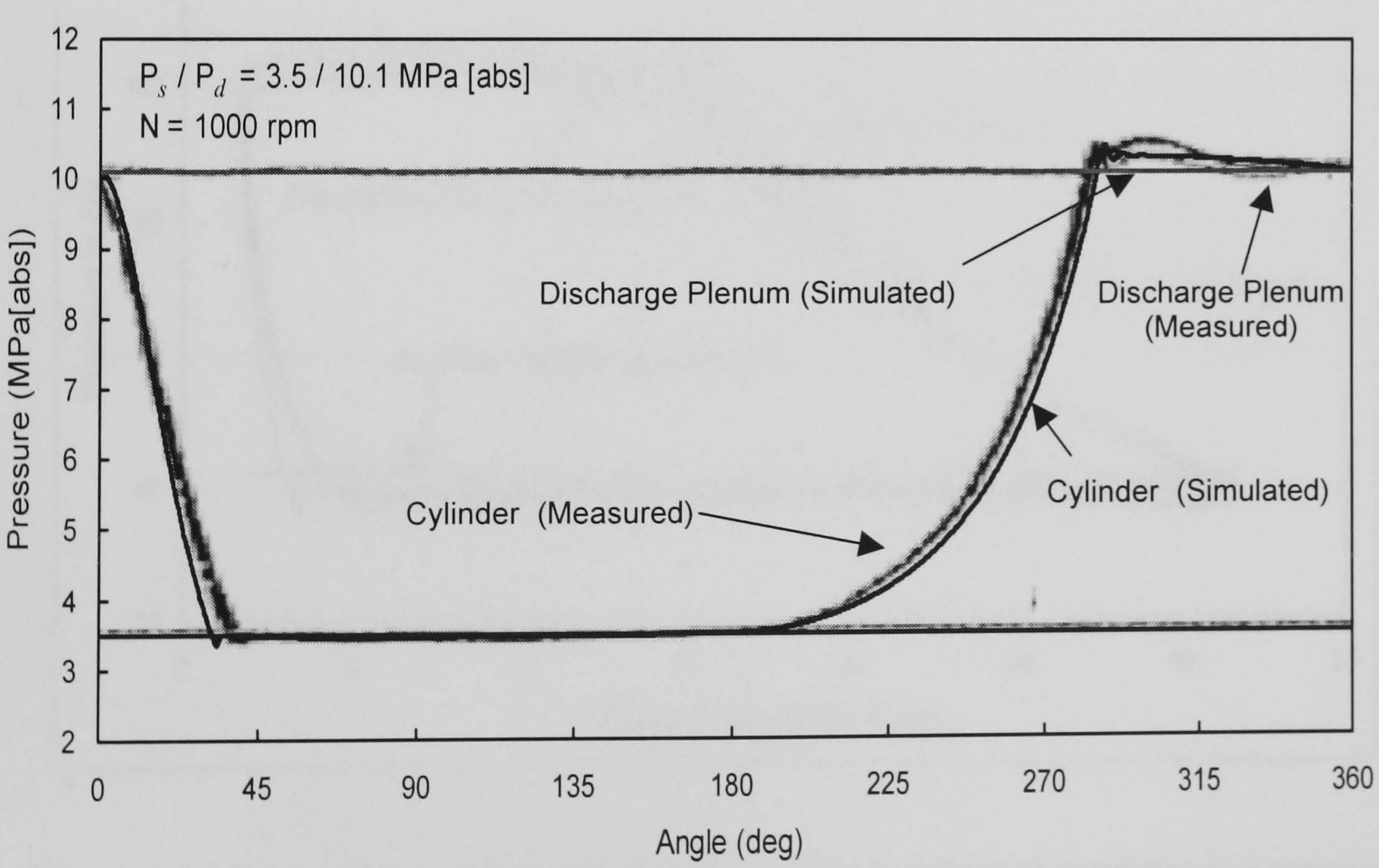

Figure 4.4a Comparison of simulated and measured cylinder pressure Vs crank angle for (Yanagisawa 2000) CO_2 compressor at 1000 rpm

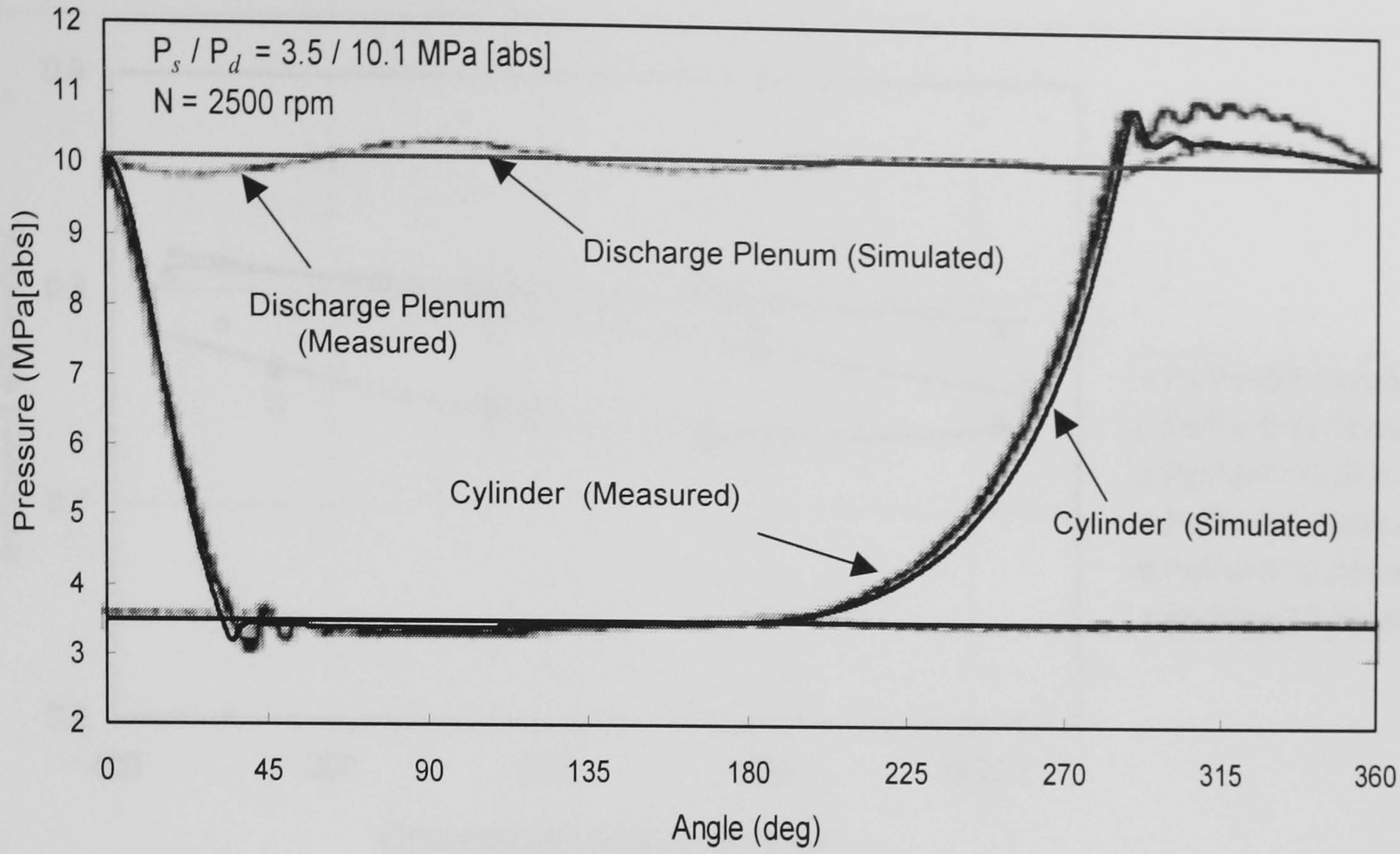

Figure 4.4b Comparison of simulated and measured cylinder pressure Vs crank angle for (Yanagisawa 2000) CO_2 compressor at 2500 rpm

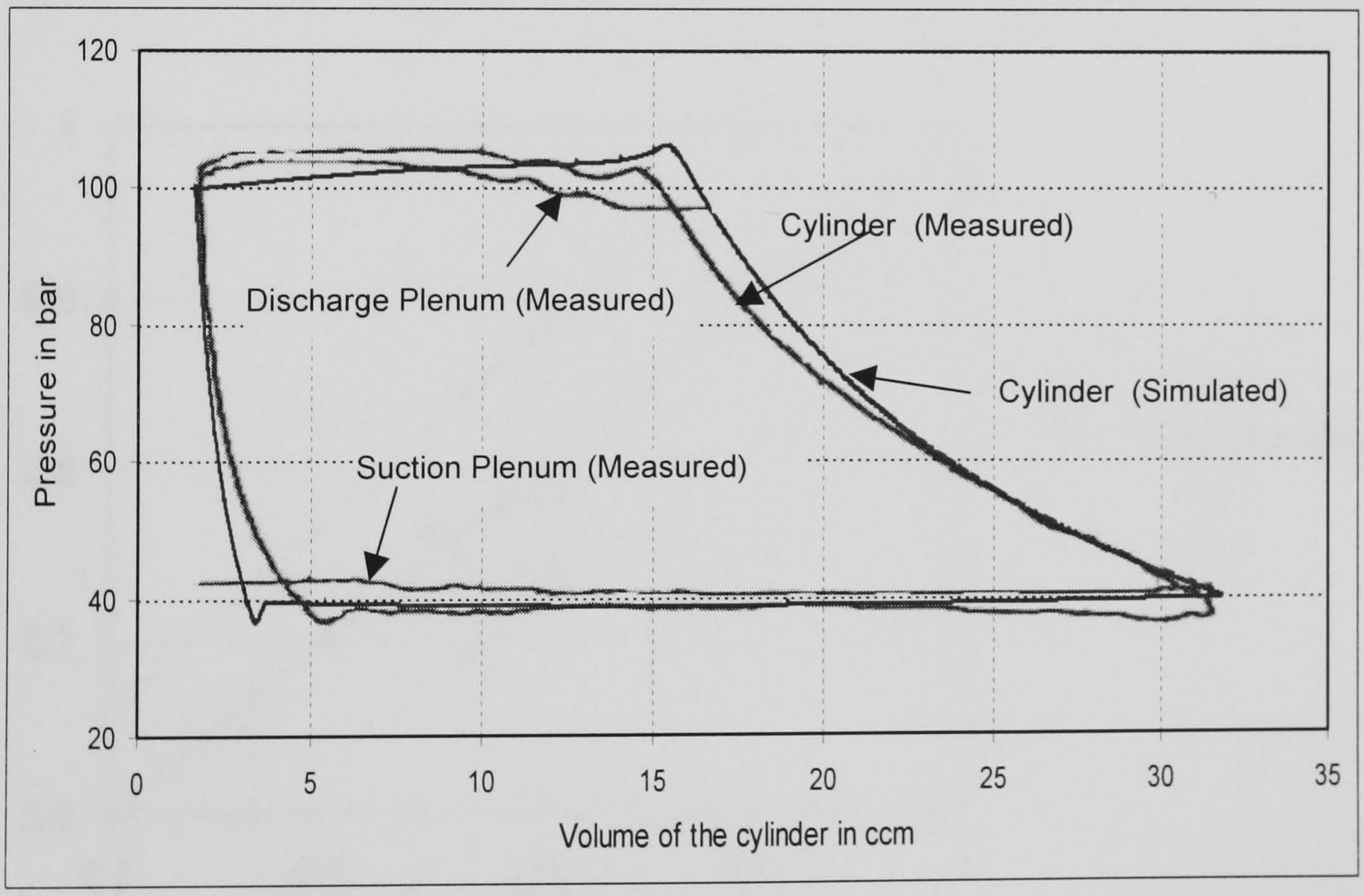

Figure 4.5a Comparison of simulated and measured indicated compression process for (Süss and Kruse 1997) CO_2 compressor at 1226 rpm, suction pressure: 4 MPa, discharge pressure: 10 MPa

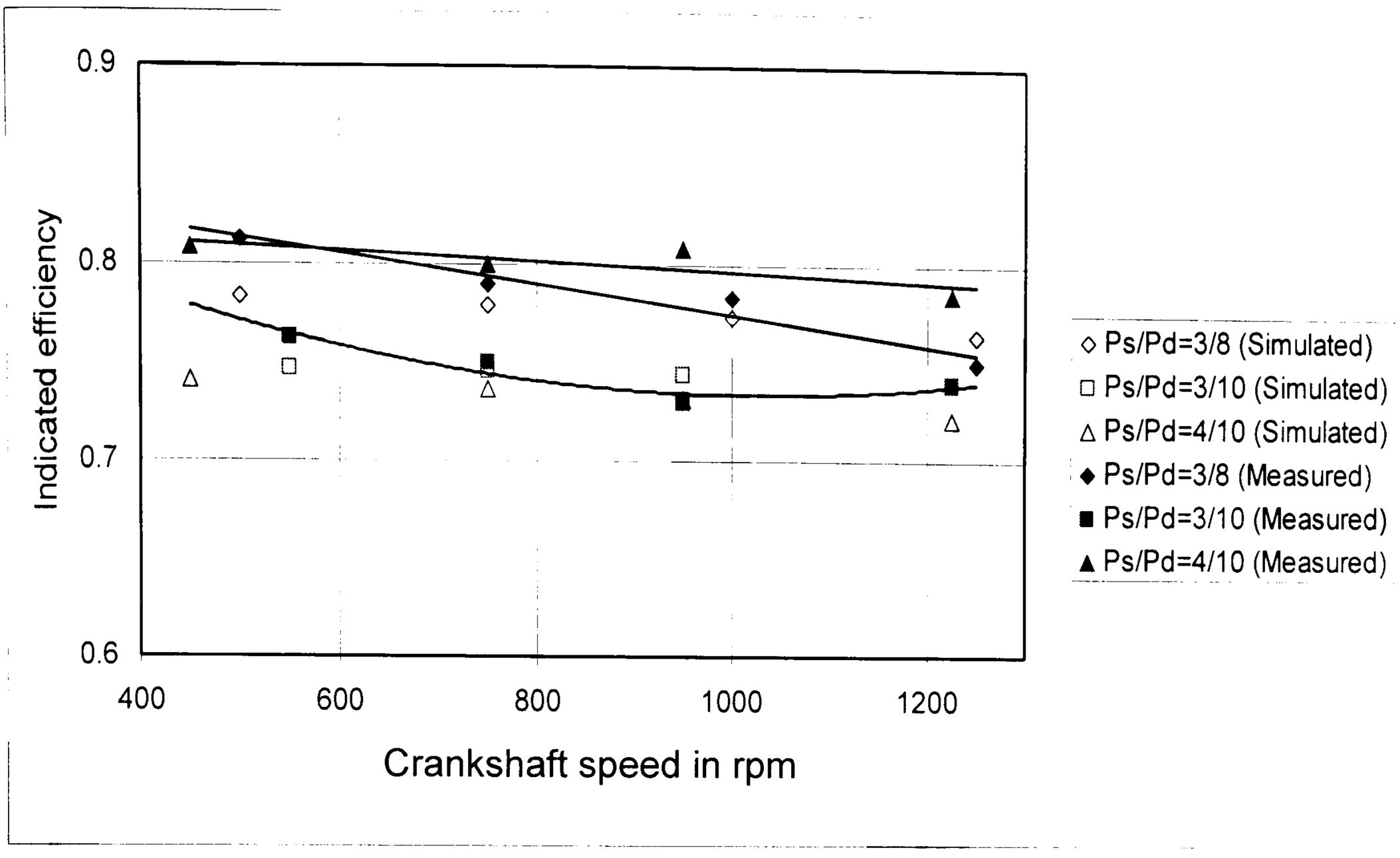

Figure 4.5b Comparison of simulated and measured compressor indicated efficiency for (Süss and Kruse 1997) CO_2 compressor at different speeds and pressure ratios (MPa / MPa)

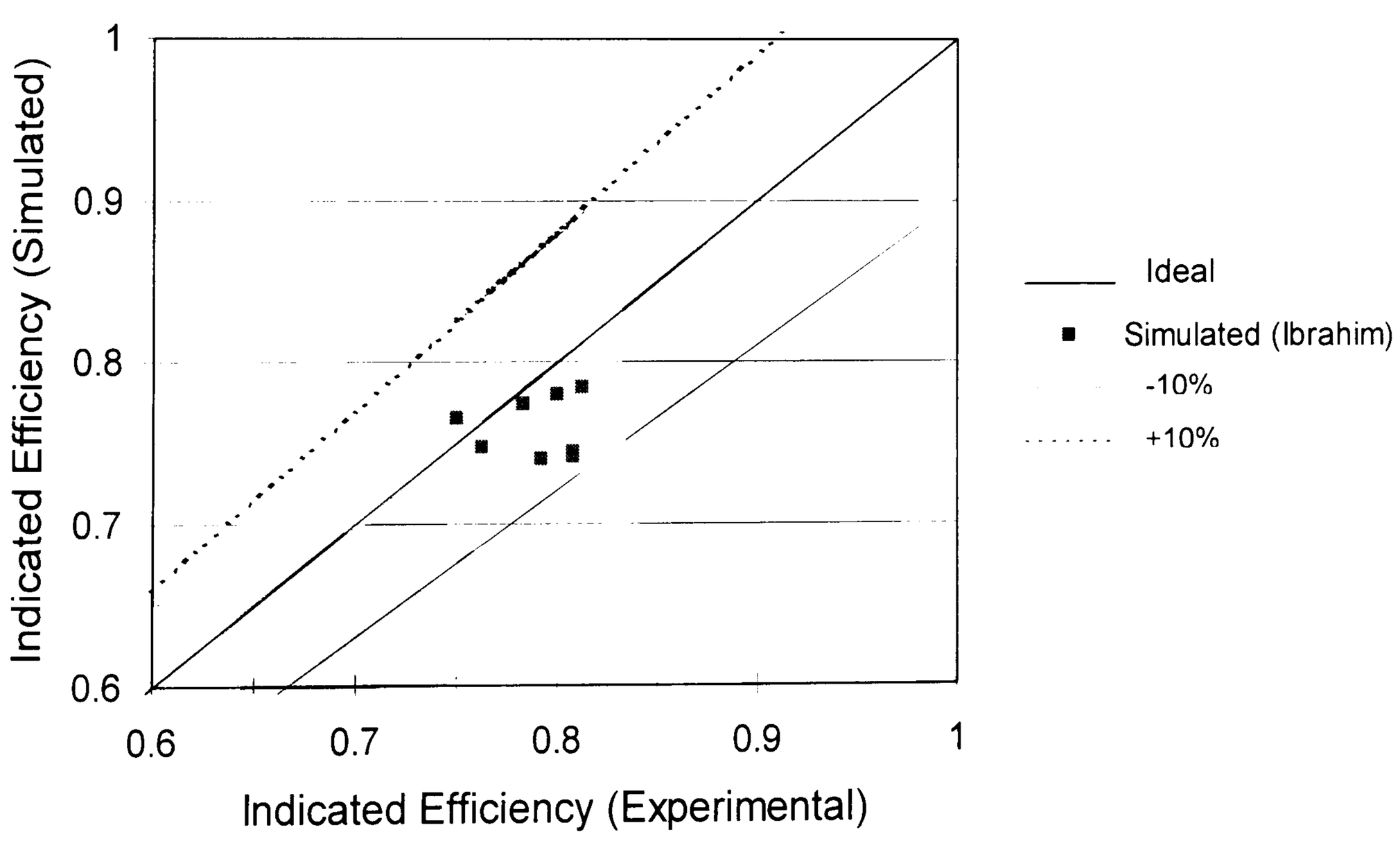

Figure 4.5c Comparison of simulated Vs measured compressor indicated efficiency for (Süss and Kruse 1997) CO_2 compressor

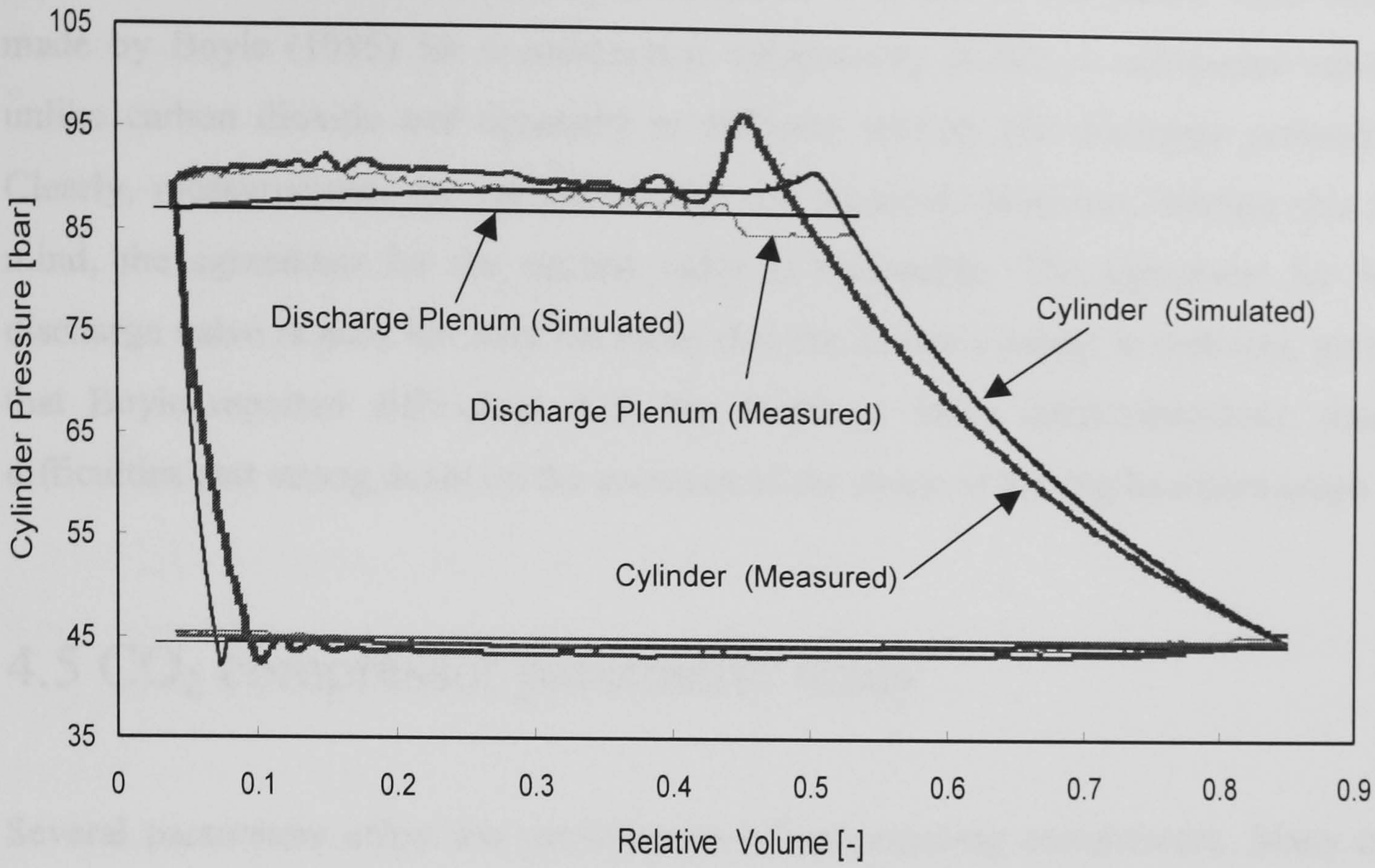

Figure 4.6 Comparison of simulated and measured indicator diagram for (Försterling 2002) CO_2 compressor at 1000 rpm, suction pressure: 45 bar, discharge pressure 87 bar

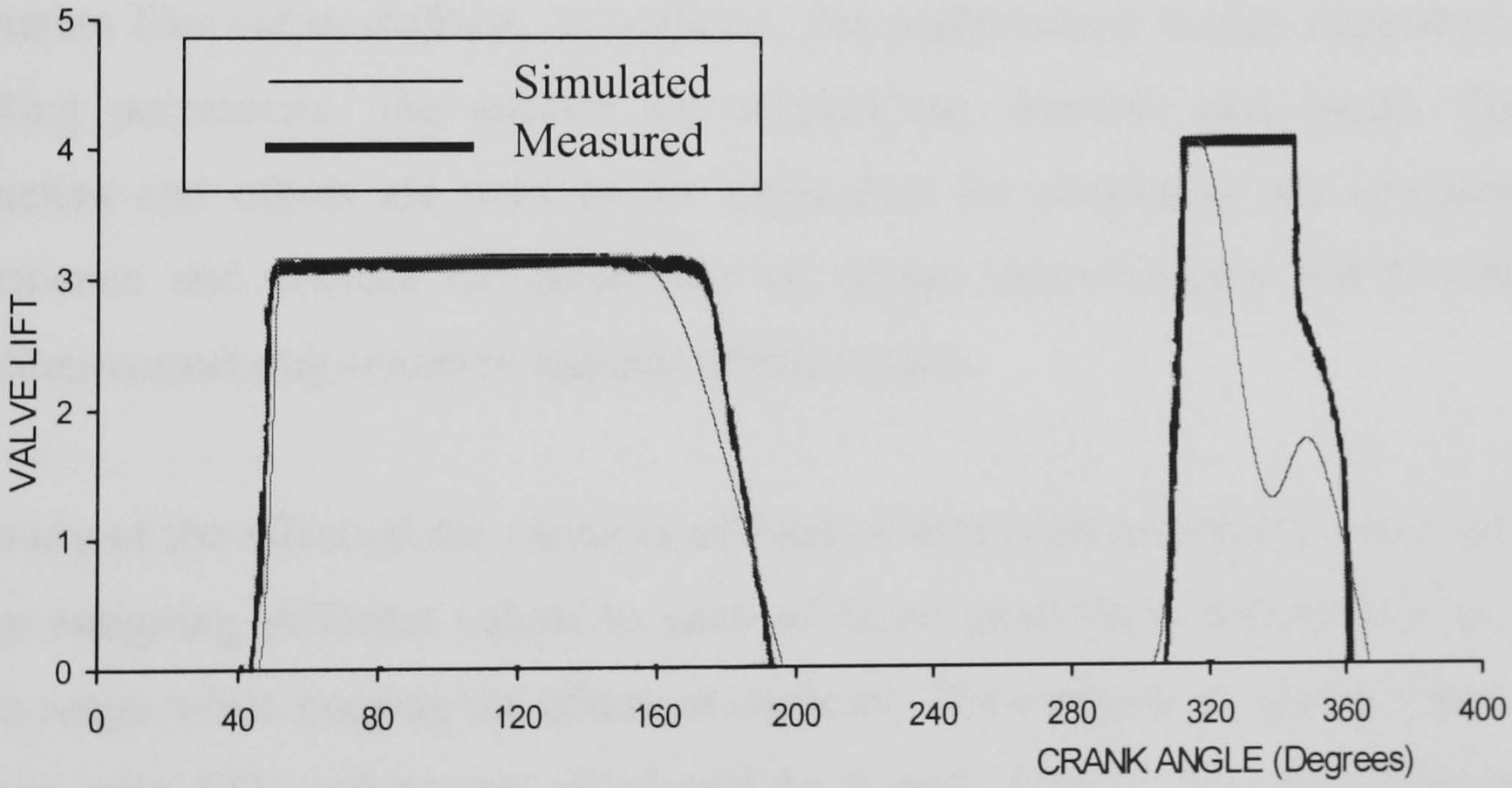

Figure 4.7 Comparison of simulated and measured valve displacement Vs crank angle for (Boyle 1985) R-502 compressor at 1450rpm, suction pressure 7.76 bar, discharge pressure 23.51 bar

The only measurements of valve displacements available to the author were those made by Boyle (1985) for a compressor compressing R-502, a refrigerant totally unlike carbon dioxide and operating at different suction and discharge pressures. Clearly, measurements for carbon dioxide are required. However, bearing this in mind, the agreement for the suction valve is reasonable. The agreement for the discharge valve is poor but may not mean that the author's model is deficient, given that Boyle reported difficulties with the discharge valve instrumentations; these difficulties cast strong doubt on the accuracy of the shape of the displacement graph.

4.5 CO_2 compressor parametric study

Several parameters affect the performance of reciprocating compressors. Many of these effects are quite difficult to estimate experimentally. However, the effects of one parameter may be separated from the others by simulation. In this section the compressor model, developed in sections 4.2 and 4.3 and validated in section 4.4, is used to simulate the effects of common parameters affecting the compressor performance. The compressor performance is dependent on the values of design parameters like valve stiffness. In addition, the performance is also dependent on operating parameters like suction air temperature, pressure and speed. These parameters and others are used in the input data for simulating the compressor performance and provide the possibility of design improvements and to obtain guidelines concerning sensitive features of behaviours.

The study of the effect of the variation of each of these parameters has been carried out by assigning different values to each of these parameters individually in the known range while keeping the others as constant. The compressor studied here is a hermetic type CO_2 compressor developed by Fagerli (1997). The most important characteristics of the compressor and the operating conditions are given in Appendix A. For a heat pump compressor, the main performance criteria affecting the overall performance of the heat pump are: volumetric efficiency, compression efficiency, compression power, discharge temperature and mass flow rate or capacity. In the

present work, both mechanical efficiency and electric motor efficiency are considered as 100% so that the power absorbed by the compressor motor is equal to indicated power. The indicator diagram and valve dynamics were plotted for the variations of every parameter. Valves dynamic behaviour will give an indication of valve and therefore compressor reliability. This has a major influence on the overall heat pump unit reliability.

4.5.1 Design parameters

4.5.1.1 Effect of Suction and Discharge Valve Stiffness

Reed type valves were used in Fagerli compressor; hence the stiffness will depend mainly on reed material, thickness, length and width. Here, the equivalent stiffness for each reed was halved, doubled and tripled to provide trial values. Figures 4.8 and 4.9 show that compressor performance is not much affected by the change of reed stiffness. A high value of stiffness will force the reed to reach its stop later and leave it earlier. Consequently, it may be expected that the time of contact between the reed and its stop be decreased sharply by high values of stiffness. Both valves are affected but the relative effect may be greater for the discharge valve due its briefer opening time. Since valve durability depends on low impact velocities on its stop and seat, these diagrams indicate the importance of the choice of valve stiffness to a long and trouble-free valve life. It should be noted how insensitive the P-v diagram is to the chosen range of valve stiffness.

4.5.1.2 Effect of Suction and Discharge Valve Masses

The valves considered here are very light and respond to changing pressure conditions rapidly. Cylinder pressure changes rapidly as the valve opens and a heavy valve will not be able to react fast enough. The effects of mass change of the valve moving elements are presented in Figures 4.10 and 4.11. It is seen that the influence on compressor performance or valve behaviour is small for the trial variations in valve mass. However, a slight over-pressure caused by slow opening of heavy valves is observed. It is evident that changes to the mass of the valve moving element have small effects on both valve dynamic behaviour and compressor thermodynamic performance. For this machine the valve stiffness is the dominant design parameter.

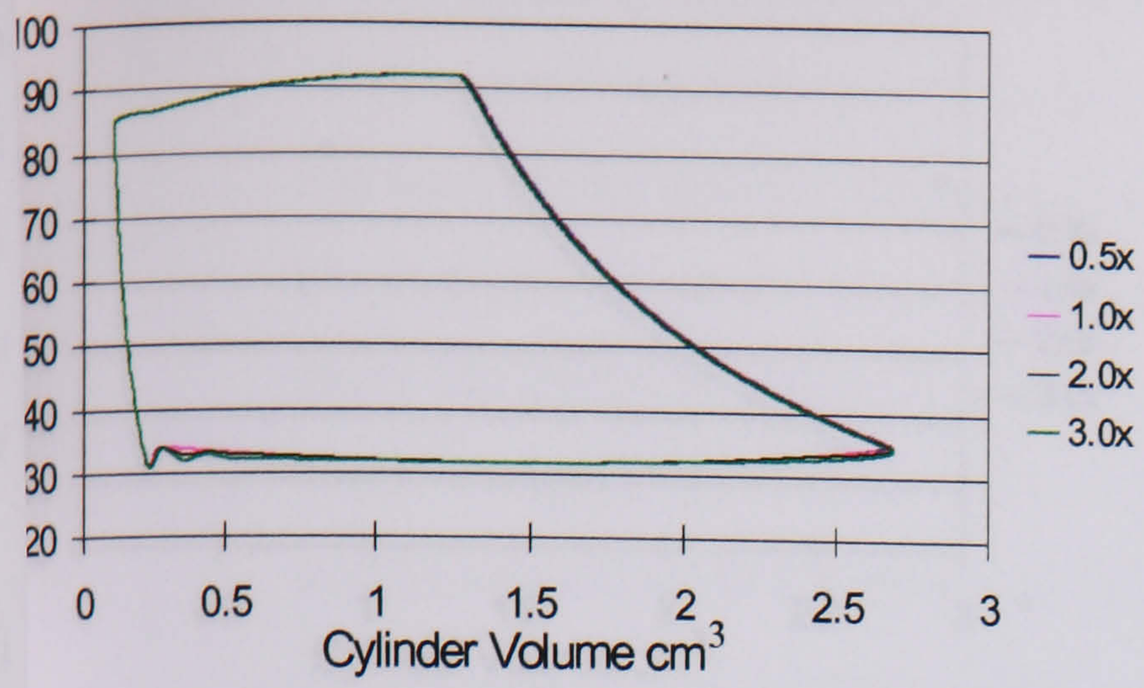

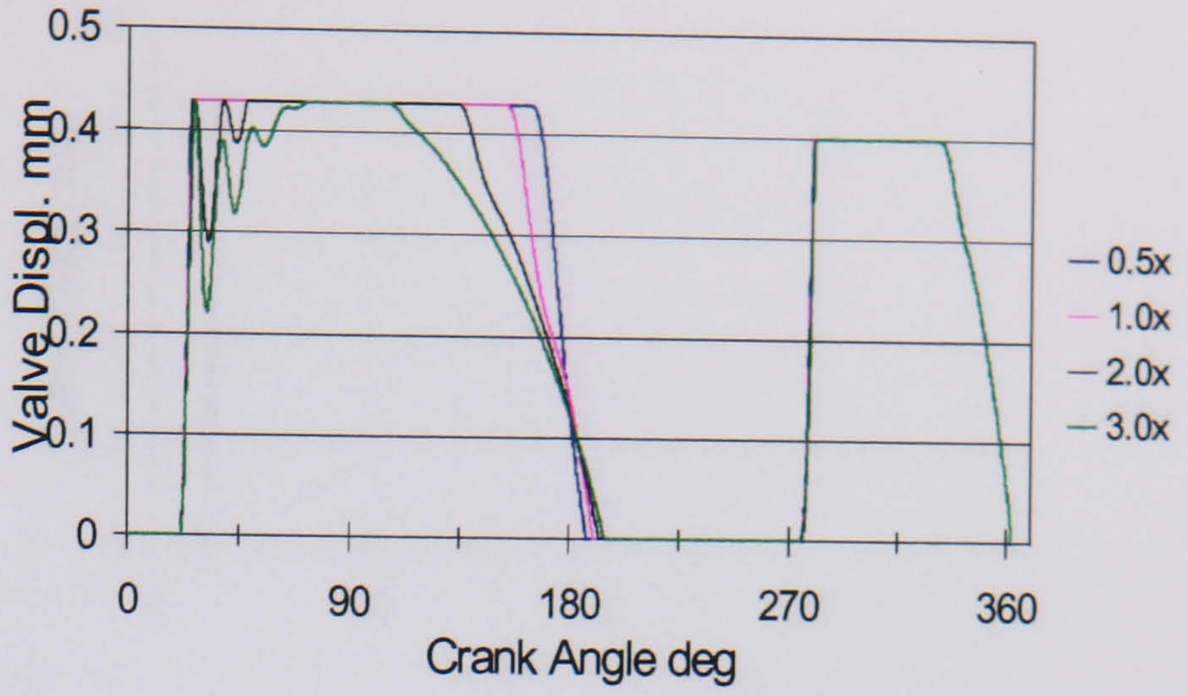

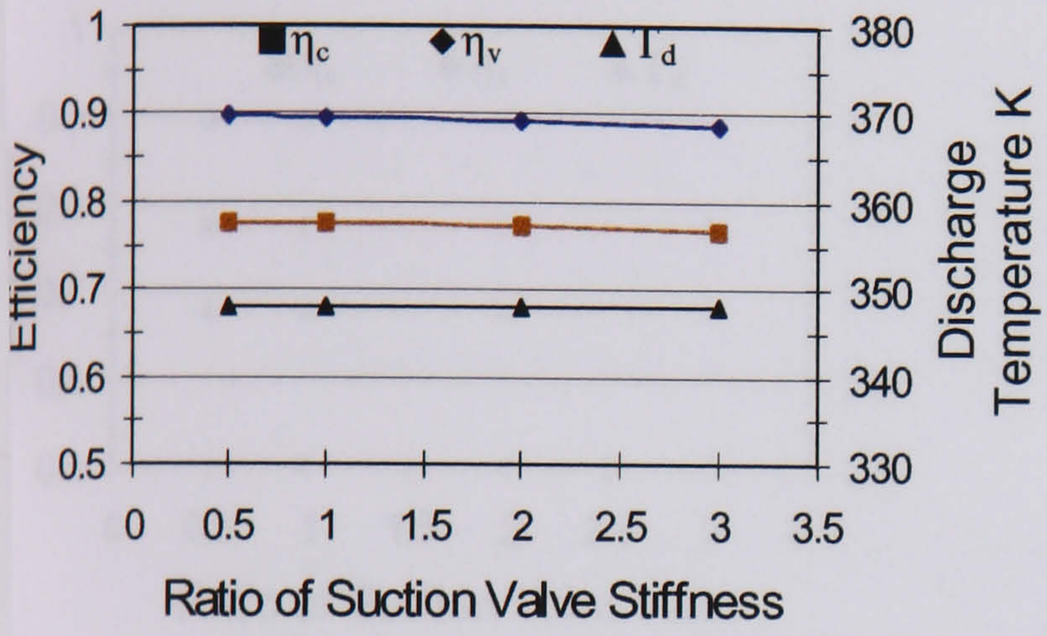

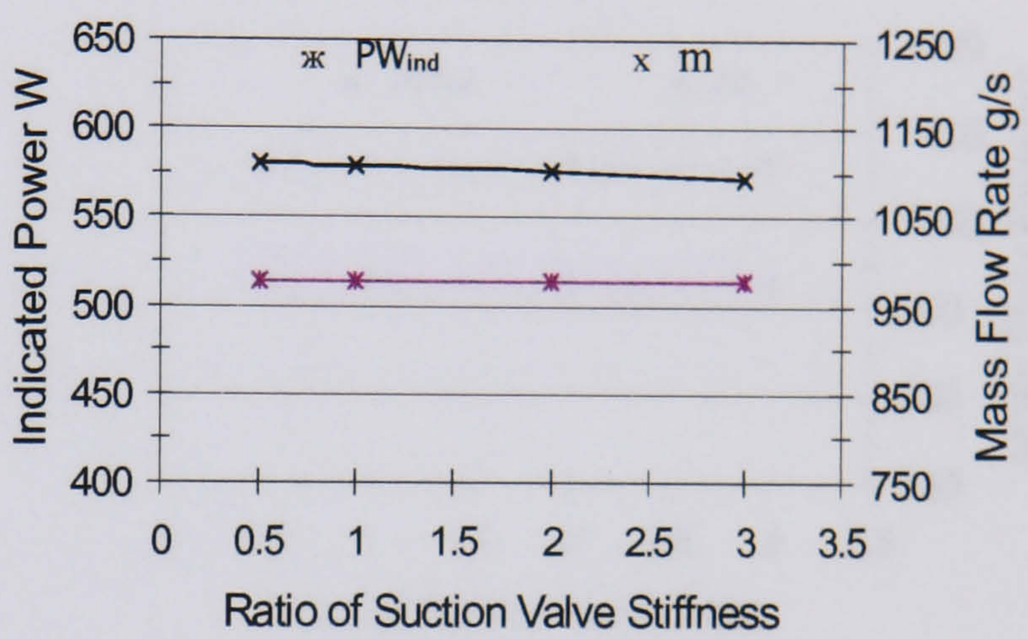

Figure 4.8 Effect of suction valve stiffness variation

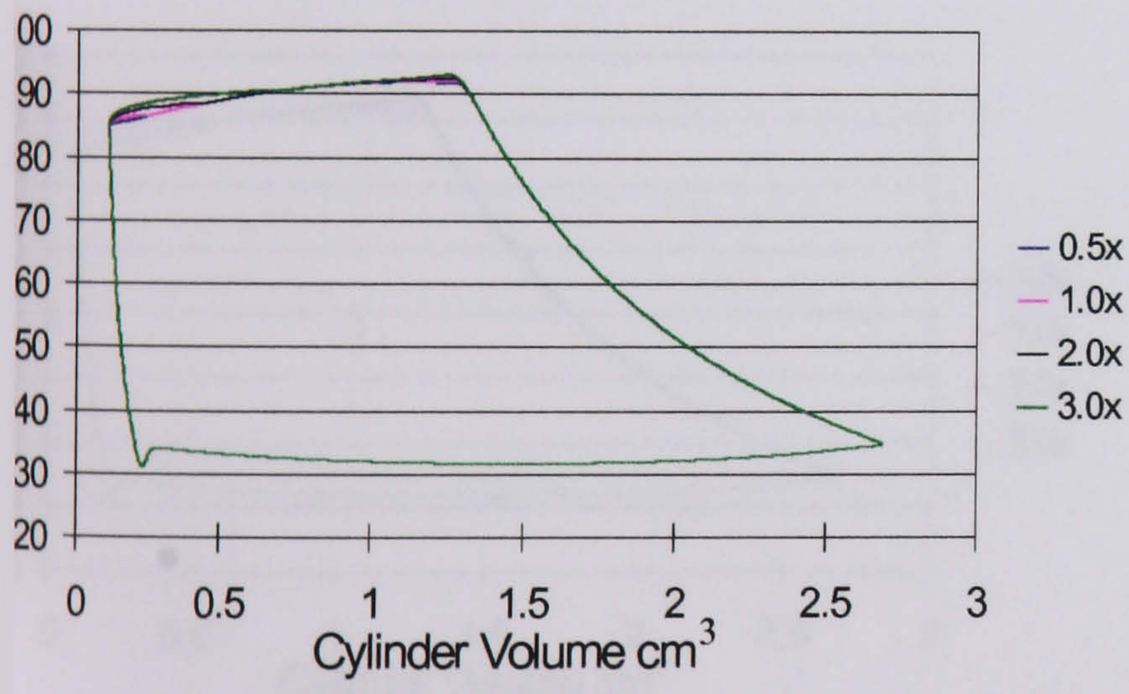

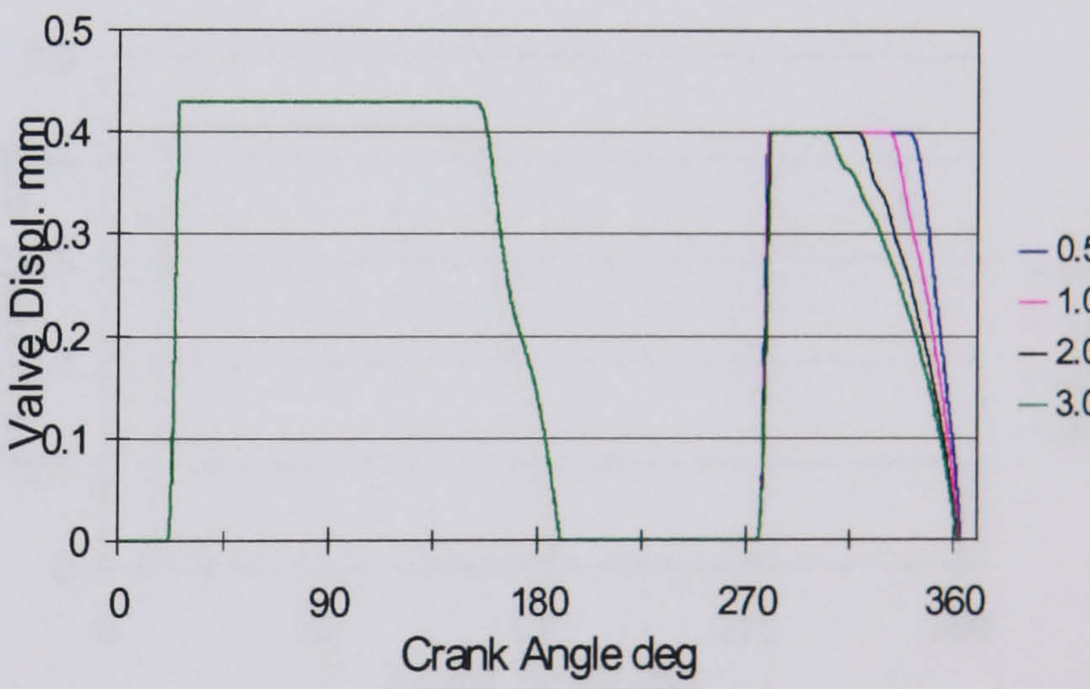

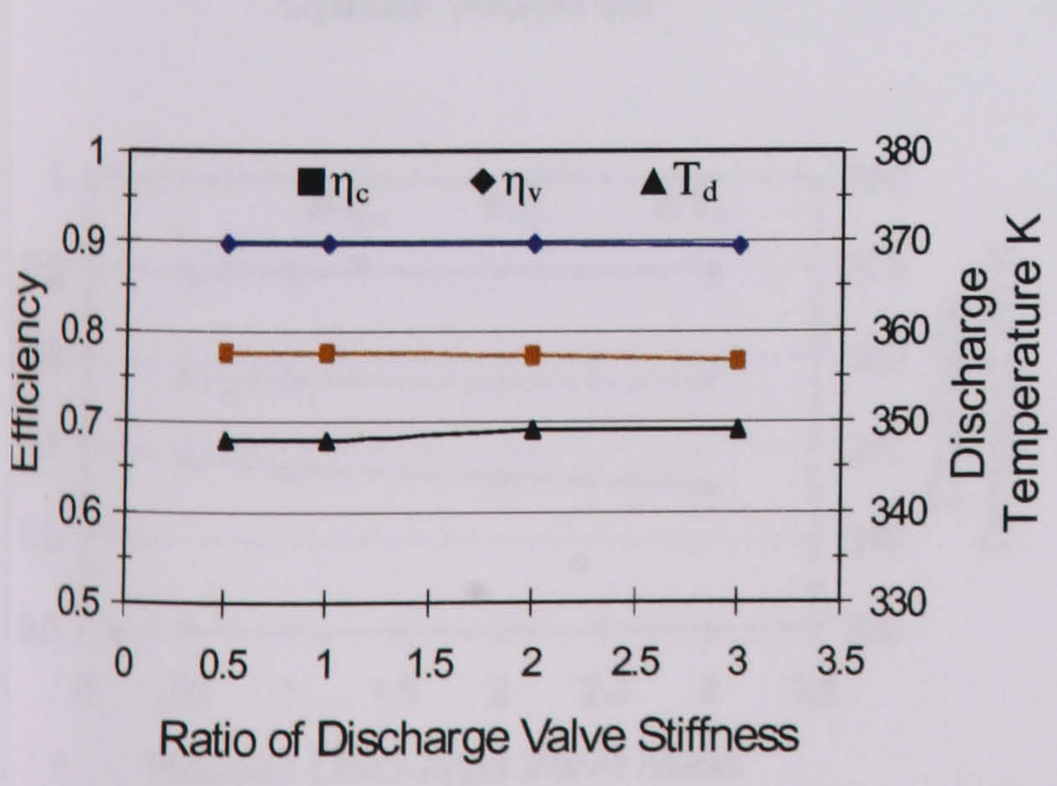

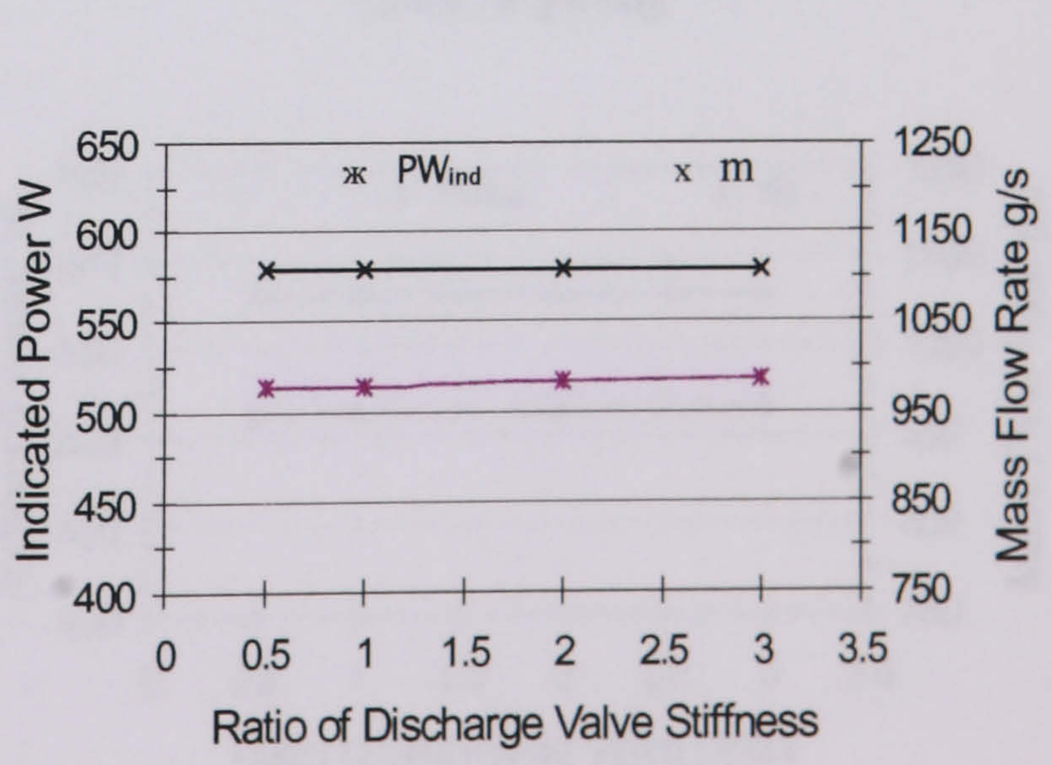

Figure 4.9 Effect of discharge valve stiffness variation

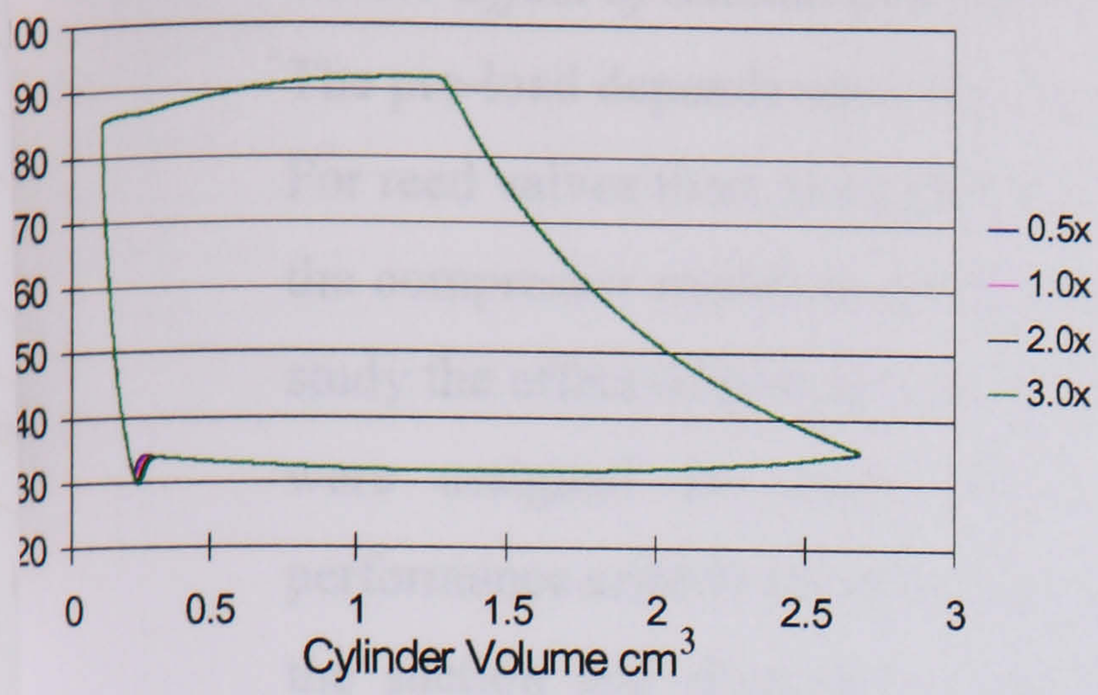

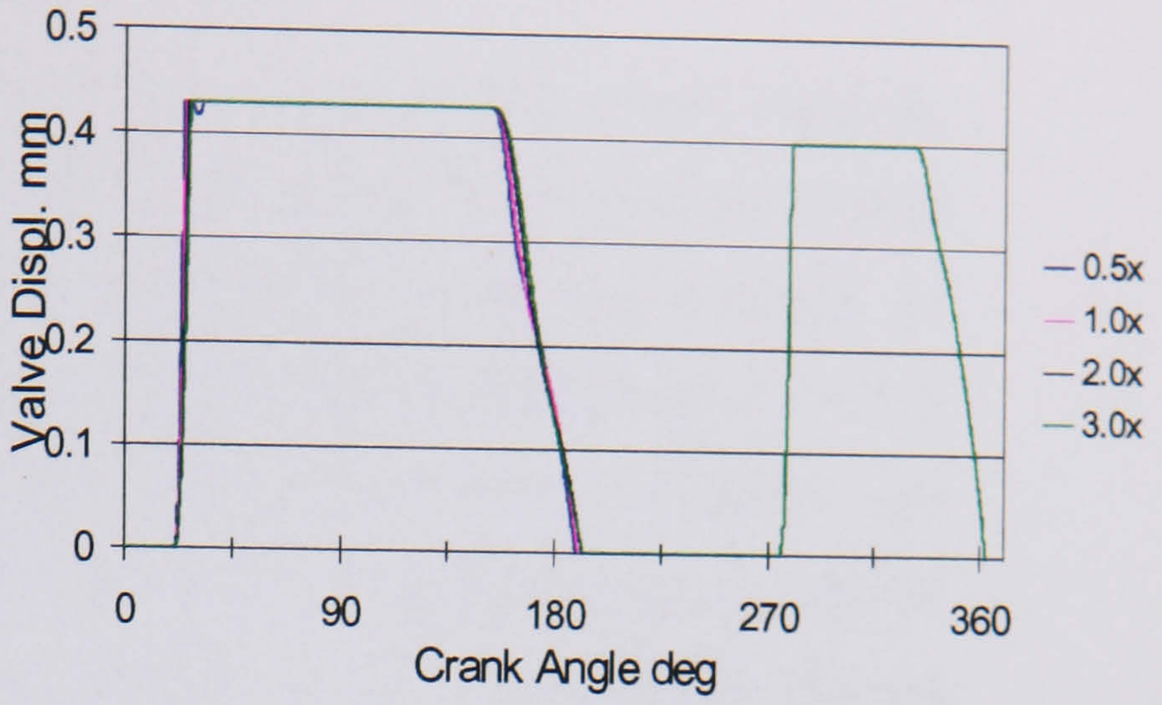

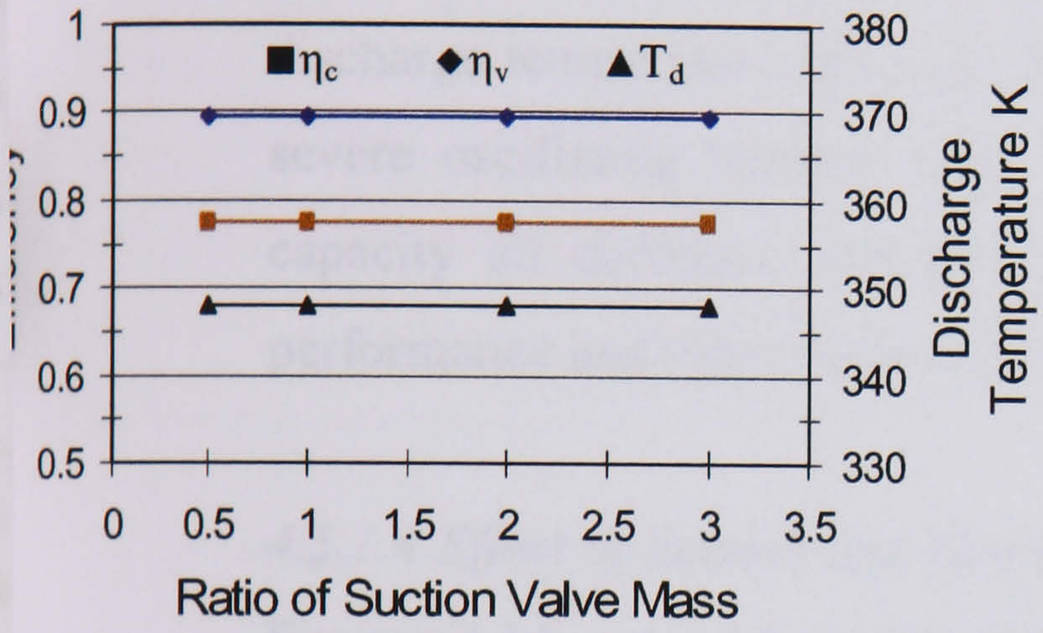

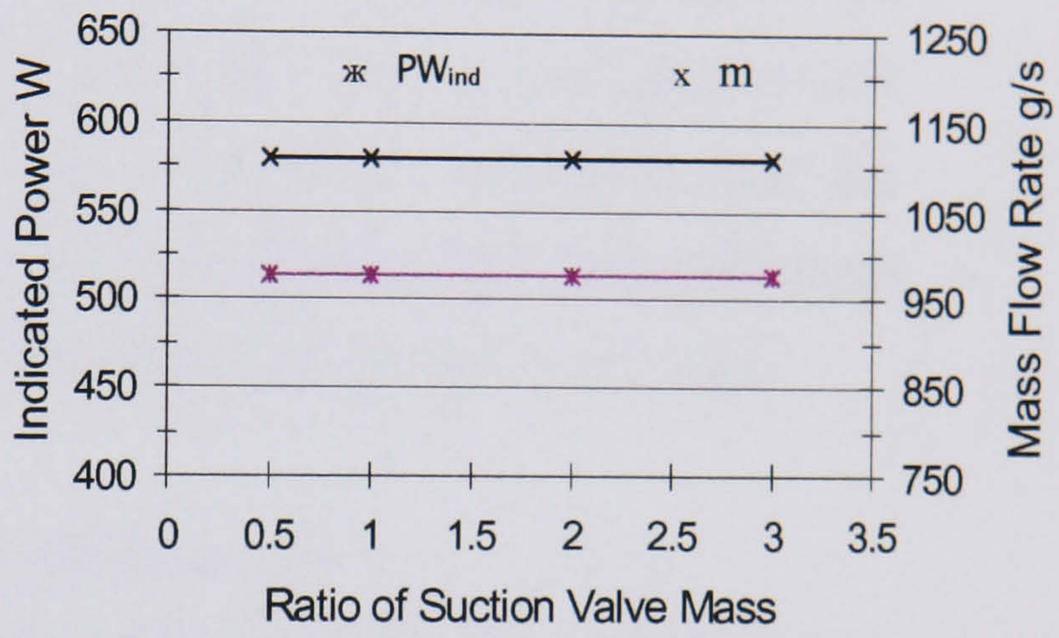

Figure 4.10 Effect of suction valve mass variation

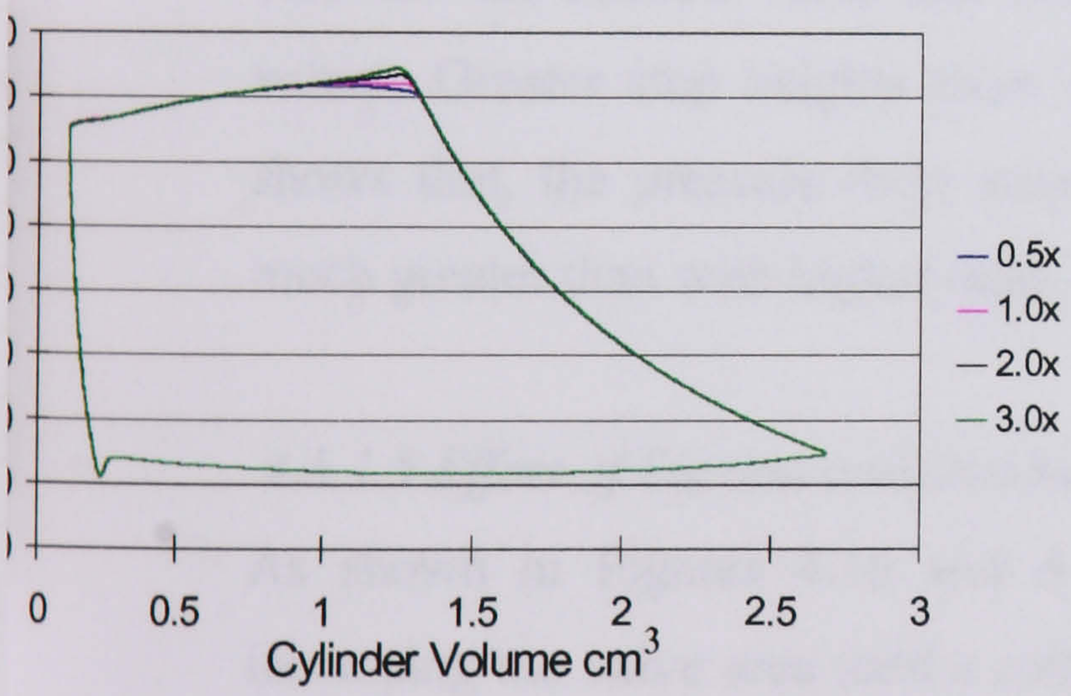

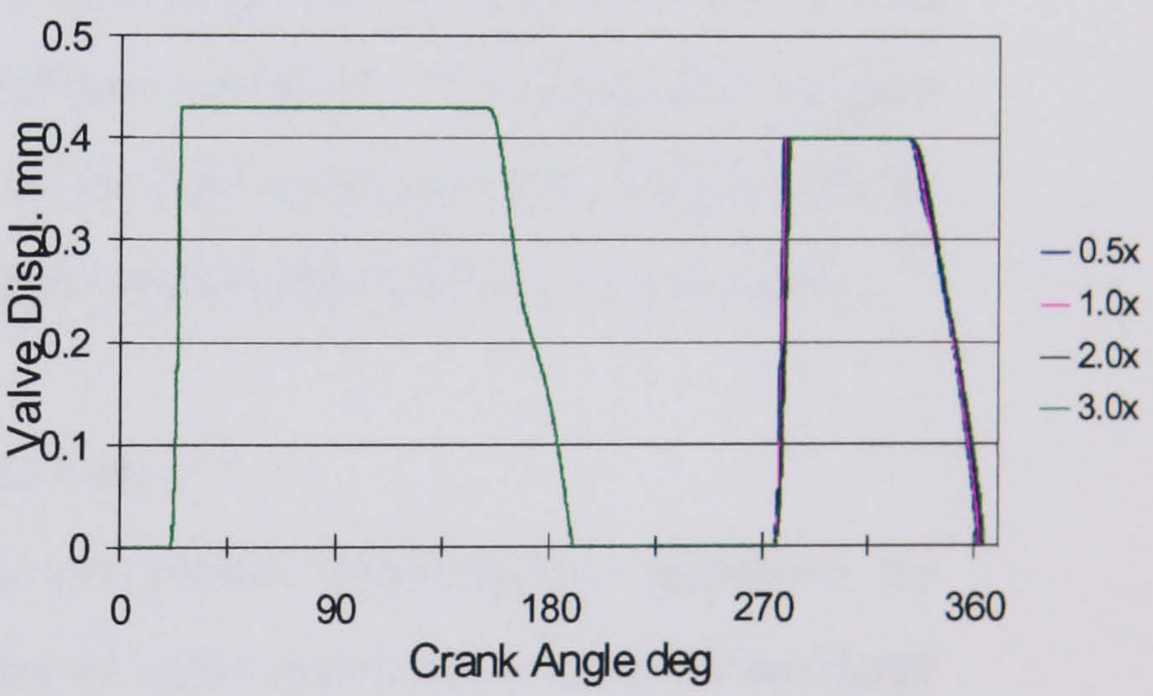

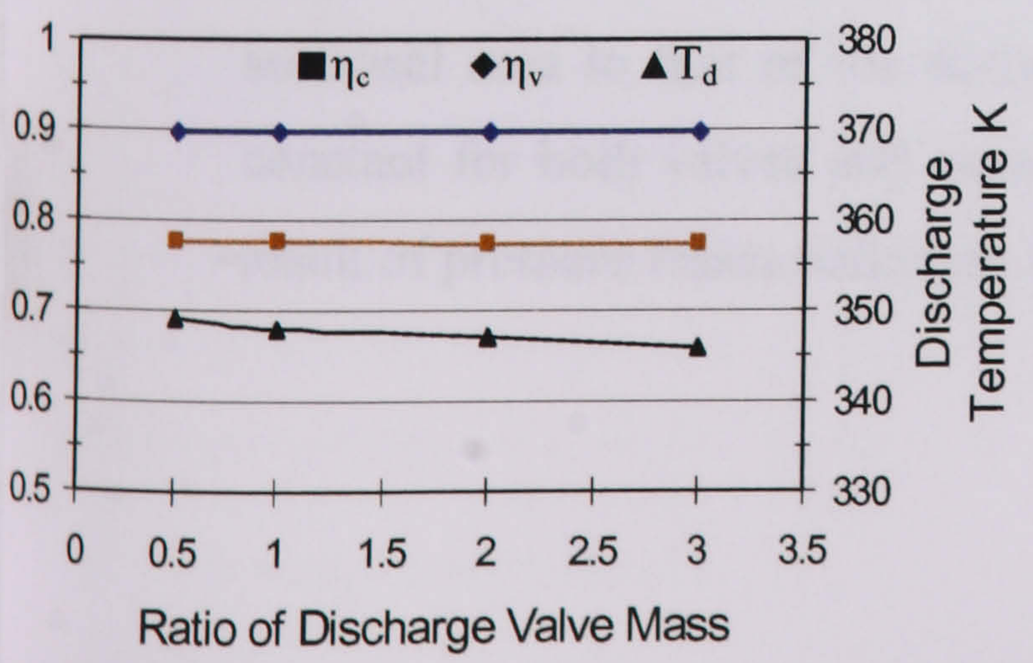

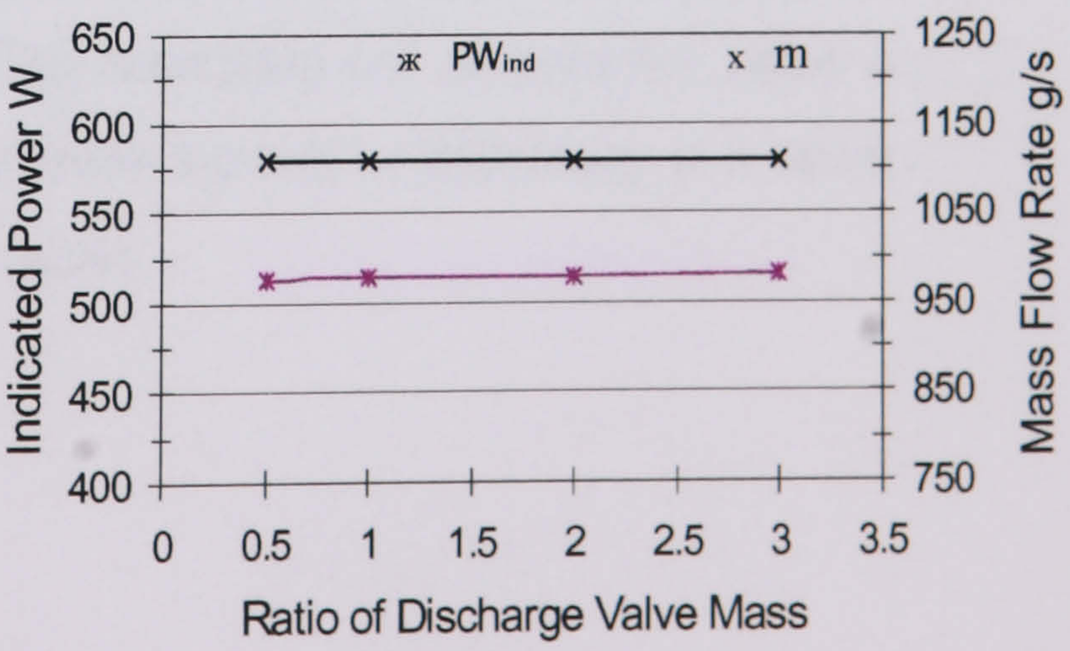

Figure 4.11 Effect of discharge valve mass variation

4.5.1.3 Effect of Suction and Discharge Valve Pre-Load

The pre-load depends upon the stiffness and the initial compression of valve springs. For reed valves there is no pre-load actually. Since the valve dynamics model used in the compressor model is general, the effect of pre-load variations is considered. To study the effect of preload on compressor performance, values in the range 0 to 15 N were assigned for each valve. The cylinder pressure, valve dynamics and performance criteria are shown in Figures 4.12 and 4.13. With the increase in preload the suction and discharge valves opening are delayed. The compression process begins at a lower pressure and the maximum cylinder pressure increases. The discharge temperature has a slight increase in both cases. Both valves experience a severe oscillating motion. The volumetric and compression efficiencies and the capacity all decrease with the increase of pre-load. Compressor thermodynamic performance and valve behaviour are both influenced considerably by pre-load.

4.5.1.4 Effect of Suction and Discharge Valve Maximum Lift

Figures 4.14 and 4.15 present the effect of changing the valve stop height, i.e. the maximum lift. Simulation results indicate that better compressor performance is obtained by increasing the stop height till it reaches maximum at stop height ratio of 1.25 for the suction valve and 1.5 for the discharge valve relative to the design values. Greater stop heights show no significant variation. The indicator diagram shows that, the pressure drop across valves for low values of stop height will be much greater than with higher ones. Discharge temperature indicates no variation.

4.5.1.5 Effect of Suction and Discharge Valve Area

As shown in Figures 4.16 and 4.17, the compressor performance improves by increasing the valve area until a certain value of valve area ratio is attained and kept constant. The valve area ratio is defined as the ratio of the valve equivalent cross-sectional area to that of the design value. This saturation (or asymptotic) value is constant for both valves and equals 1.5. The improvement of efficiency is a direct result of pressure losses reduction across the valves.

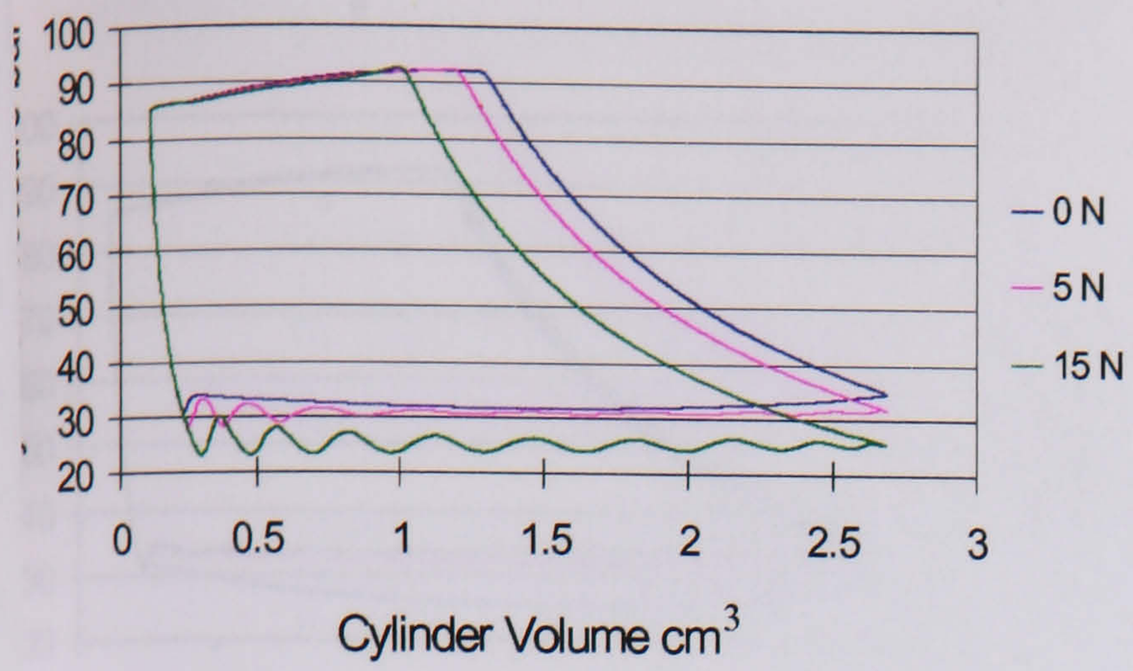

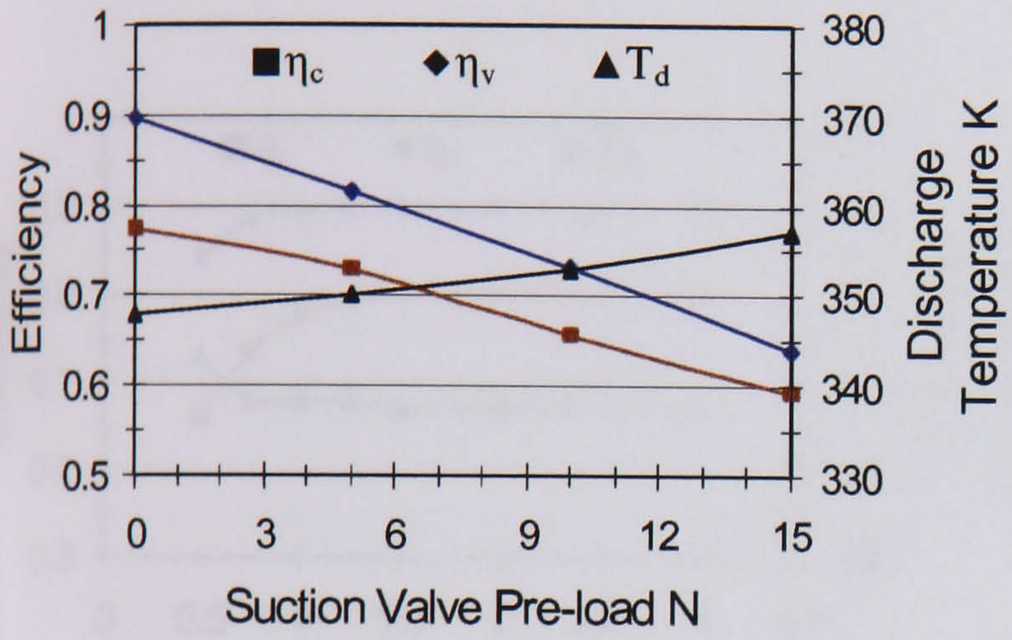

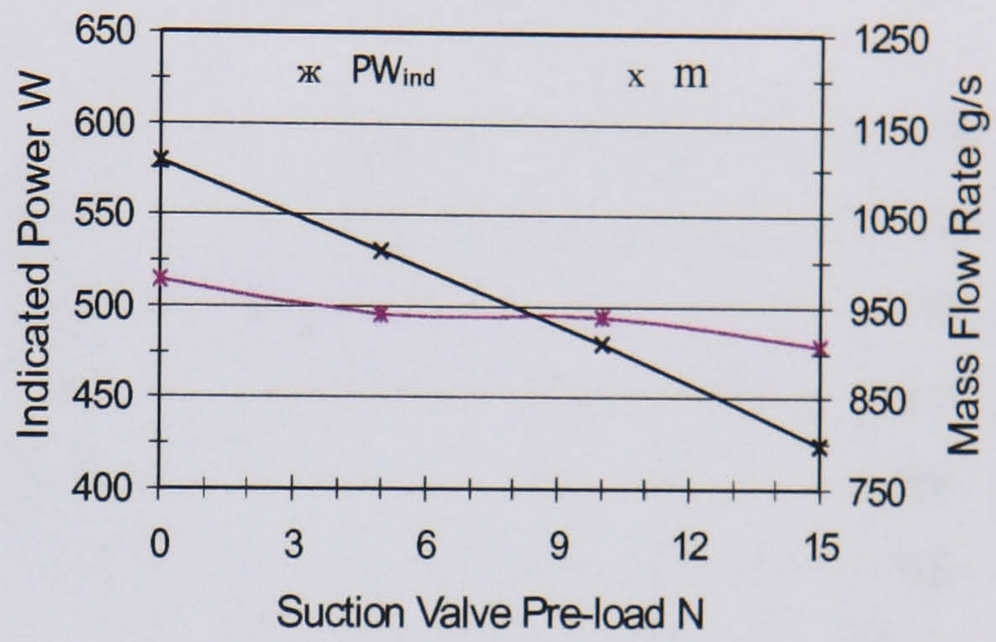

Figure 4.12 Effect of suction valve pre-load variation

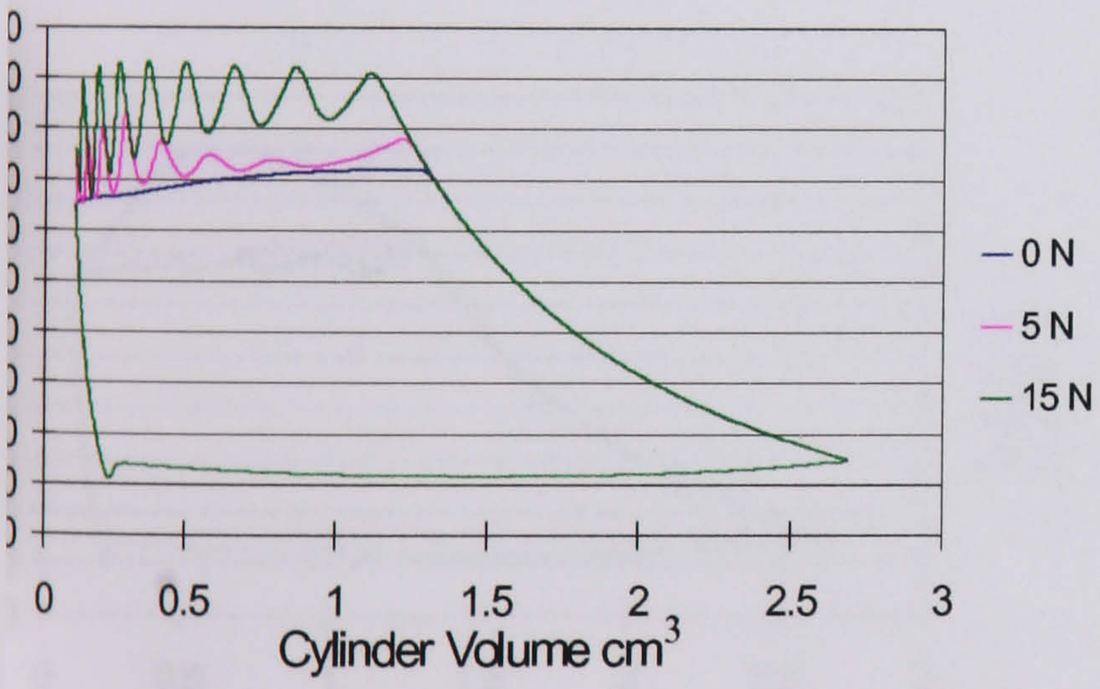

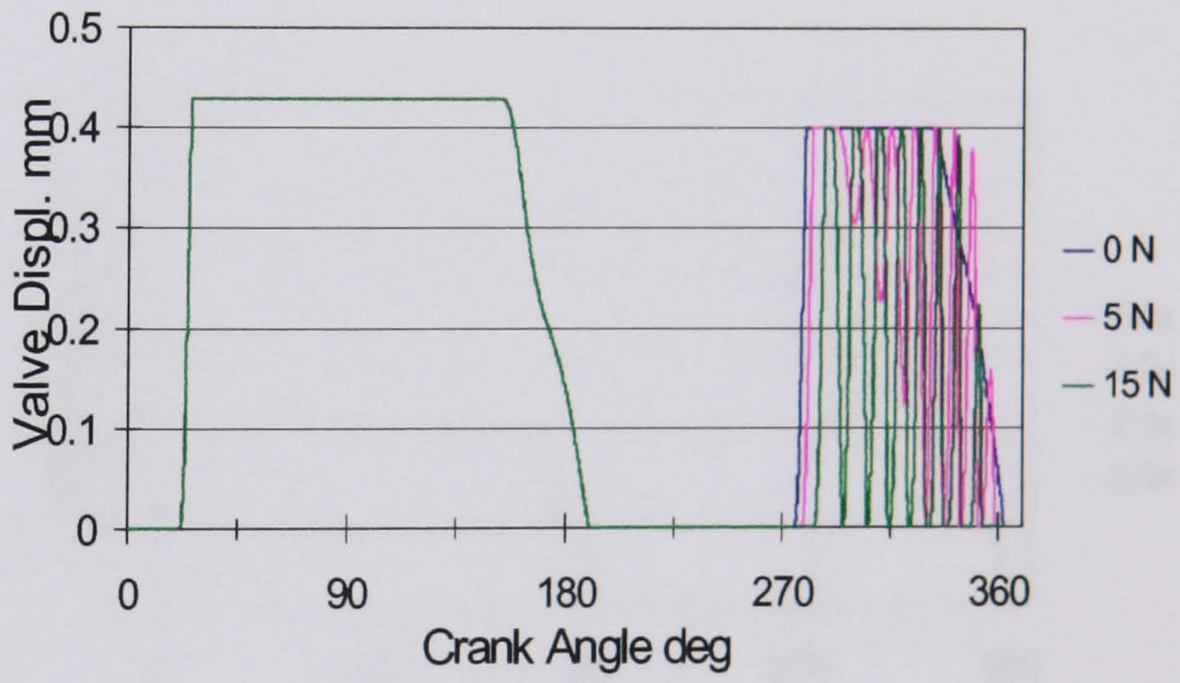

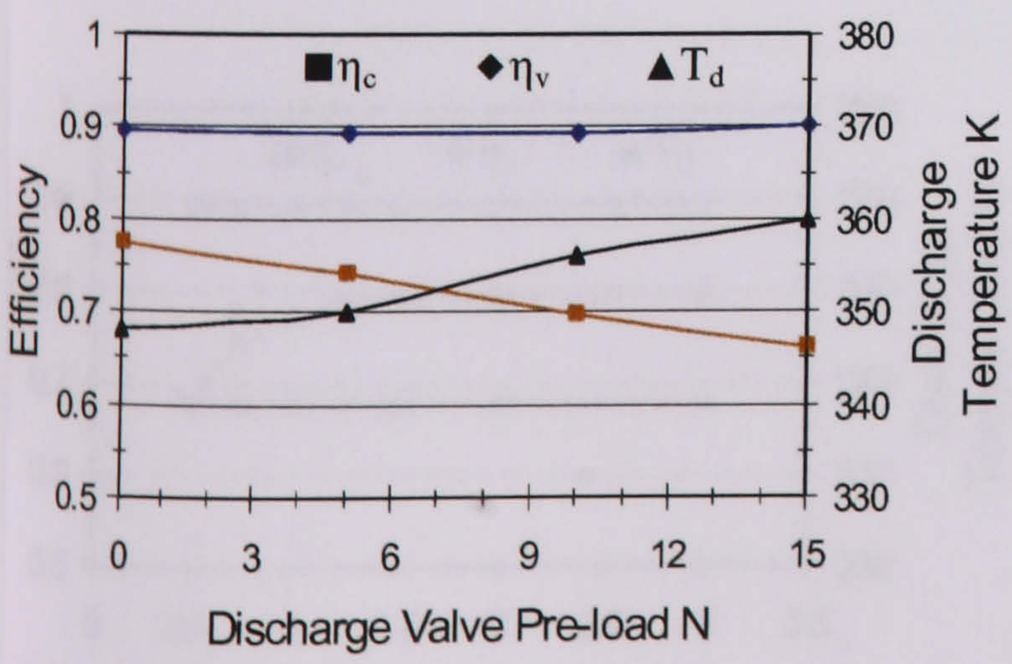

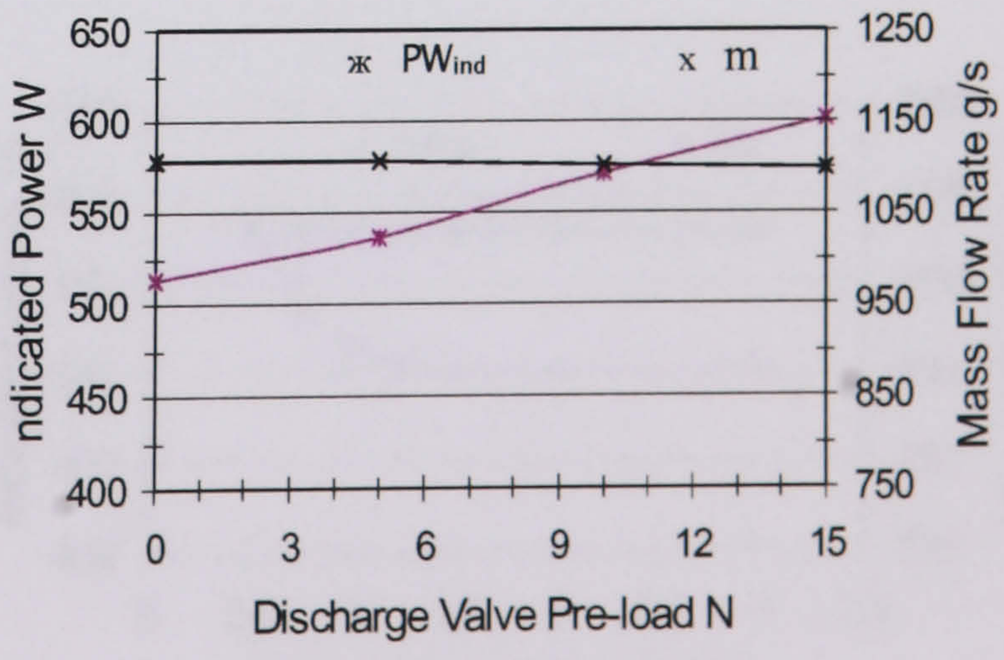

Figure 4.13 Effect of discharge valve pre-load variation

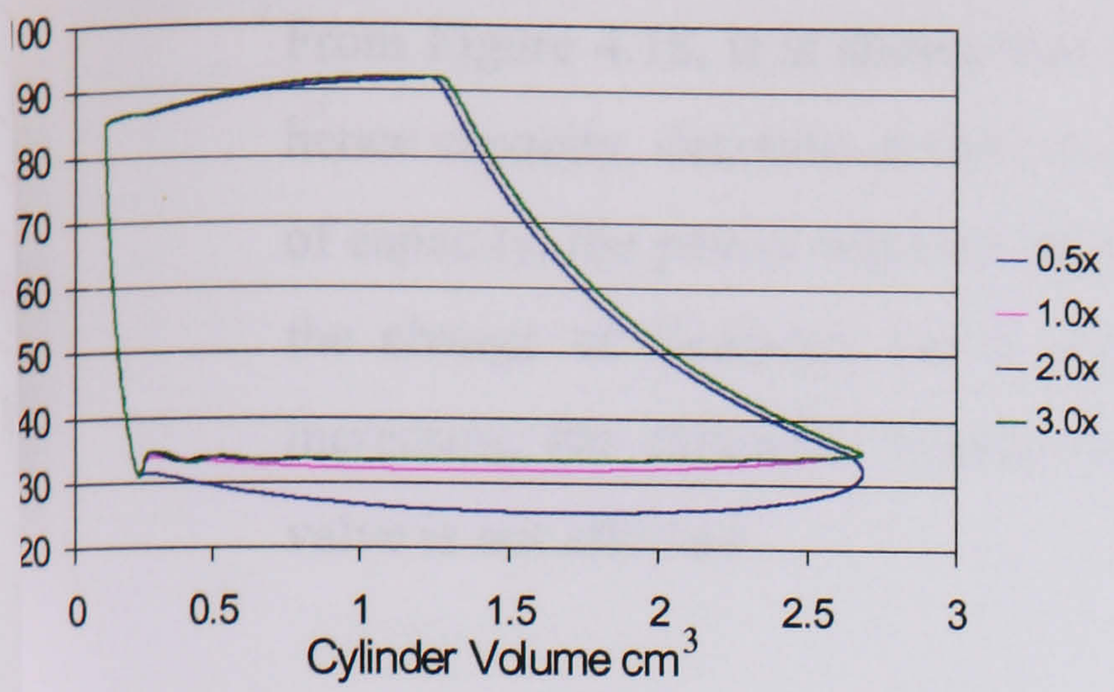

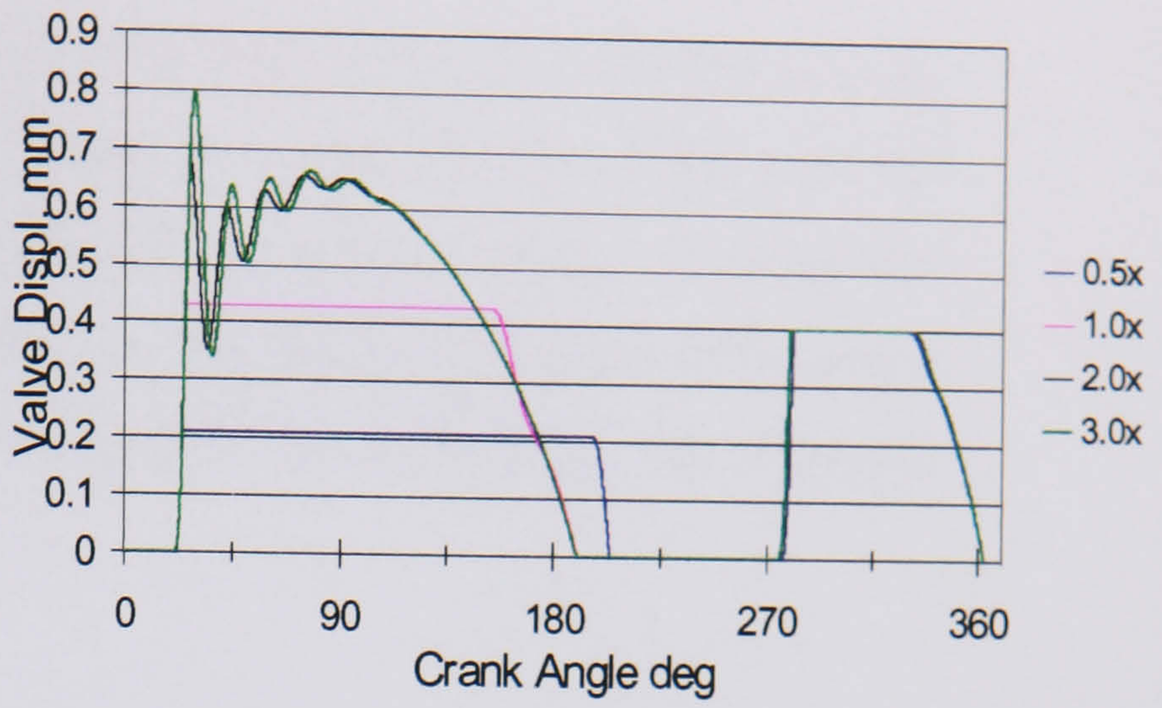

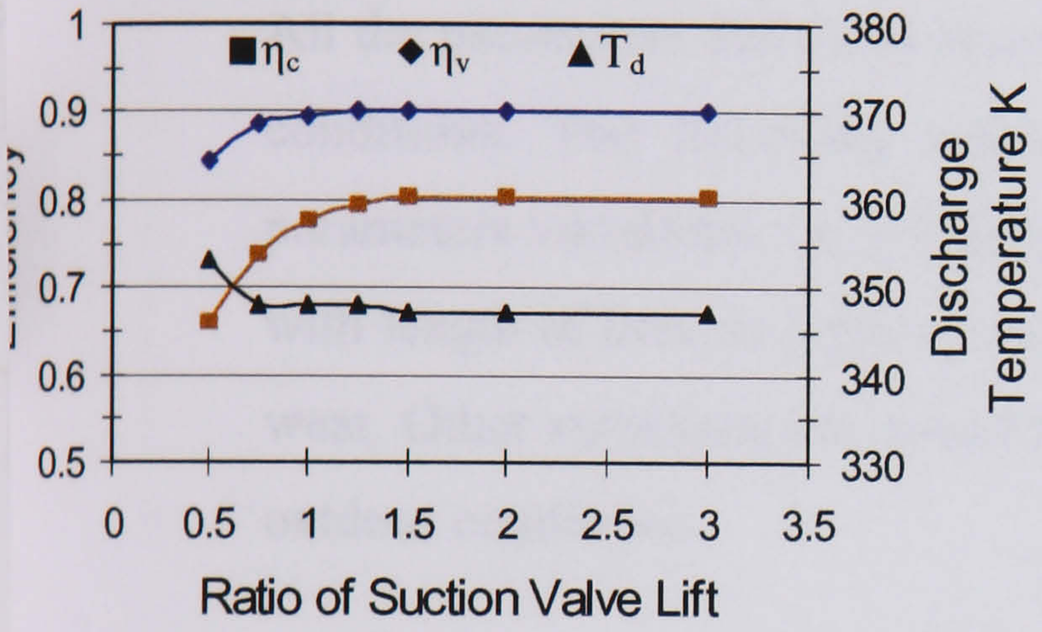

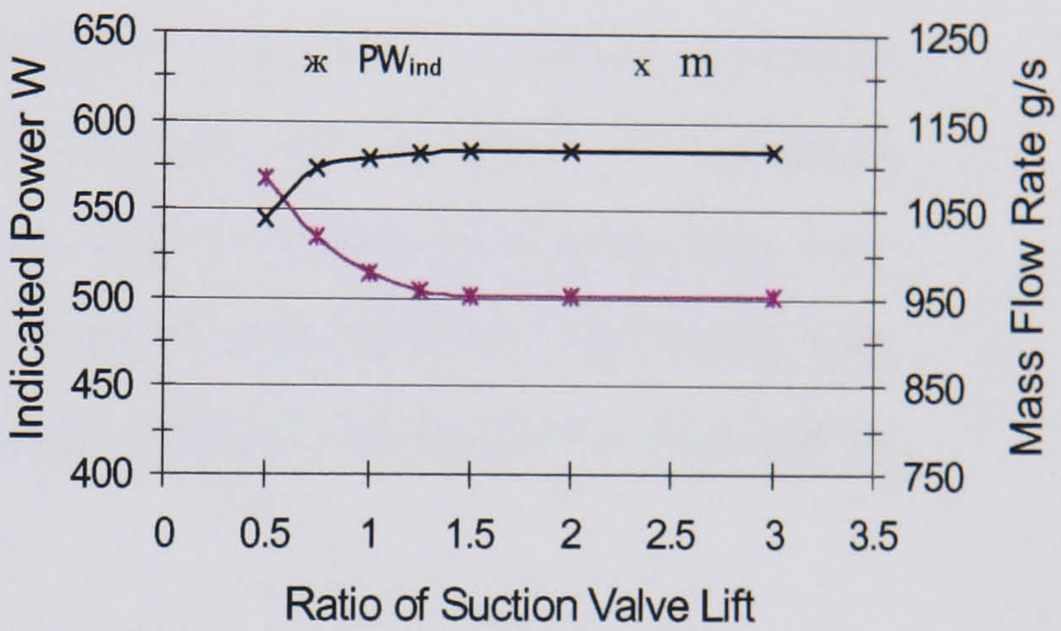

Figure 4.14 Effect of suction valve maximum lift variation

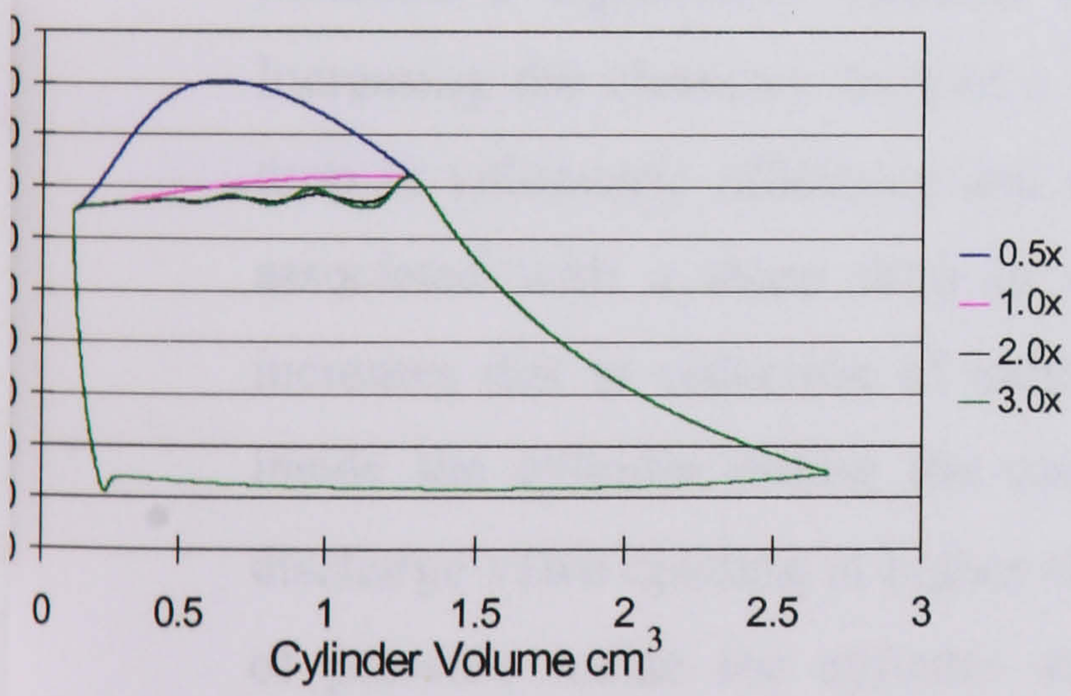

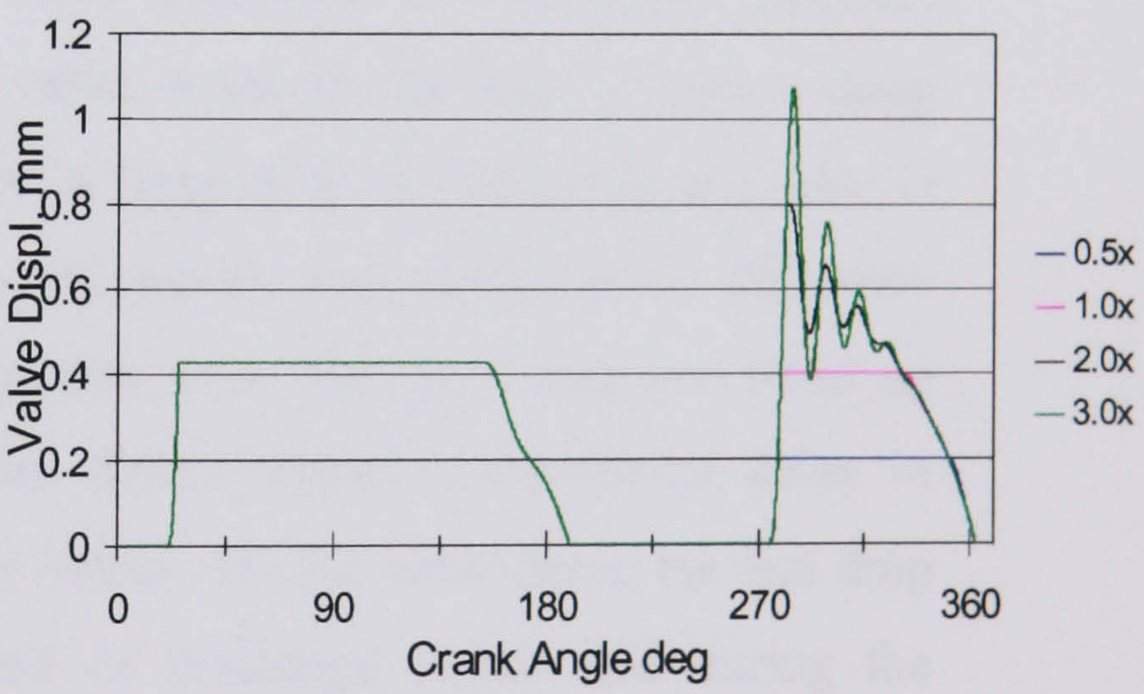

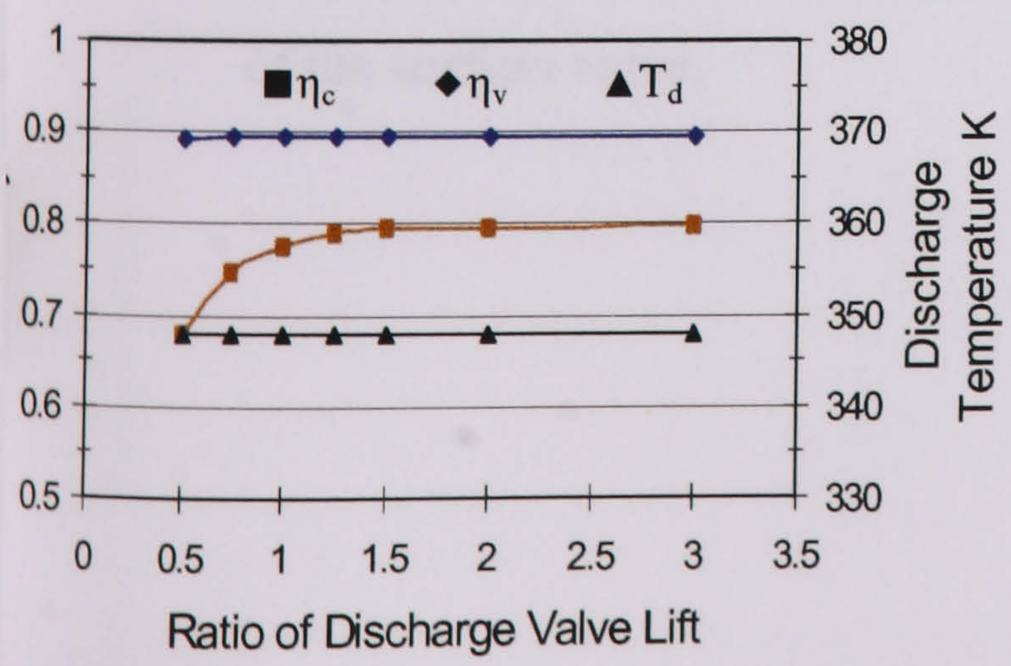

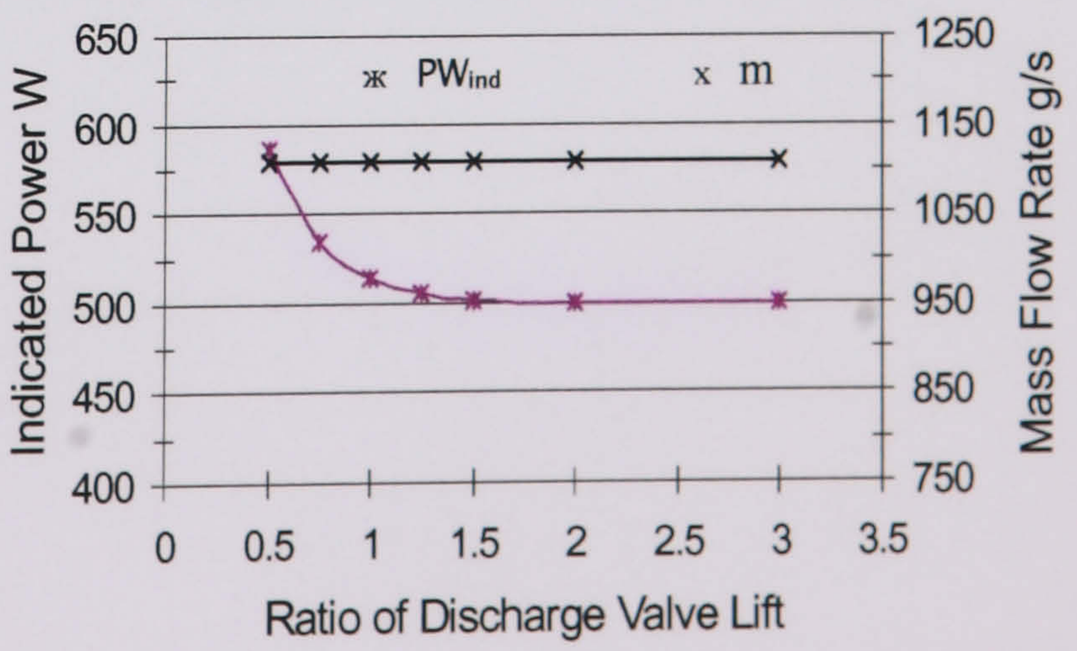

Figure 4.15 Effect of discharge valve maximum lift variation

4.5.1.6 Effect of Clearance Volume

From Figure 4.18, it is shown that the volumetric and compression efficiencies and hence capacity, decrease as the clearance volume increases. Due to a slight decrease of capacity, the power required remains approximately without change. It seems that the change of clearance has a small effect on the discharge temperature. While increasing the clearance volume delays the suction valve opening, the discharge valve is not affected.

4.5.2 Operating parameters

All the parameters discussed above were simulated at constant, i.e. design, operating conditions. The following subsections will consider the influence of operating parameters variations, i.e. off design conditions. Some of these parameters may vary with length of time in service, such as piston ring-cylinder clearance increasing with wear. Other variations are caused by load demand changes influenced for example by outdoor conditions.

4.5.2.1 Effect of Piston Ring-Cylinder Clearance

The effect of different piston ring-cylinder clearances is presented in Figure 4.19. It indicates a significant variation in the valve dynamics and indicator diagram. Increasing the clearance beyond a certain value, 6 μm in this case, causes a sharp drop in volumetric efficiency and capacity. A large drop in compression power is associated with a sharp drop in capacity. However, the compression efficiency increases due to reduction of indicator diagram area. The slow pressure build up inside the cylinder during the compression stroke causes a significant delay in discharge valve opening at higher clearance values. On the other hand, the fast drop of pressure inside the cylinder at the end of discharge stroke and during the expansion stroke yields an early closure of the discharge valve and an early opening of the suction valve.

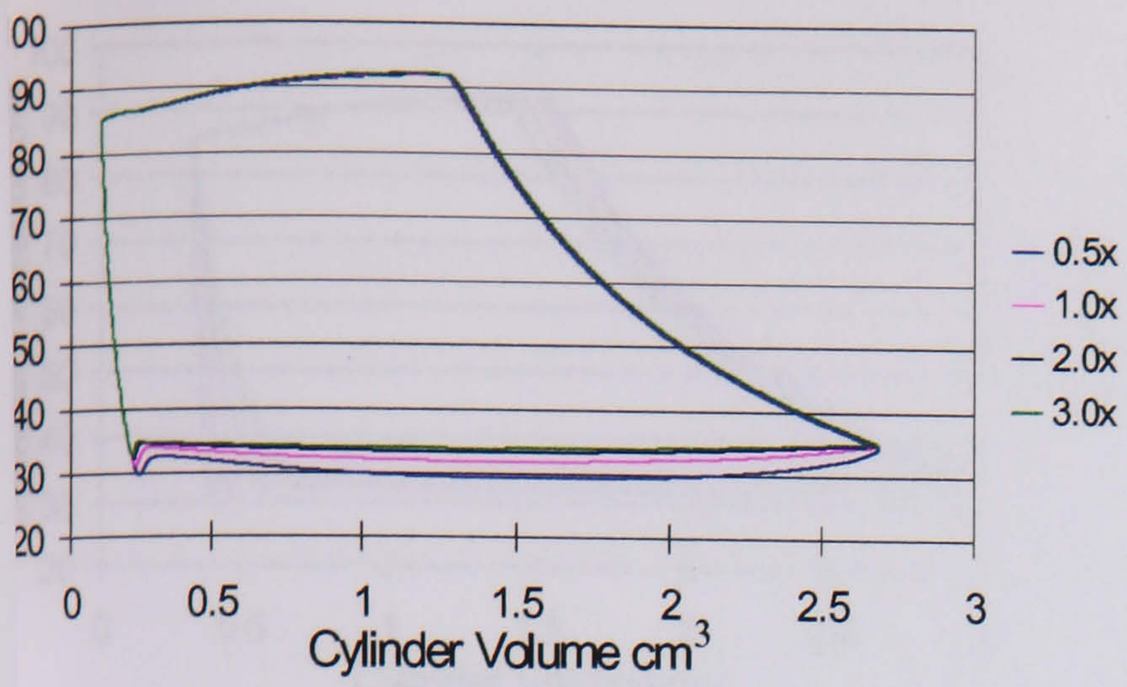

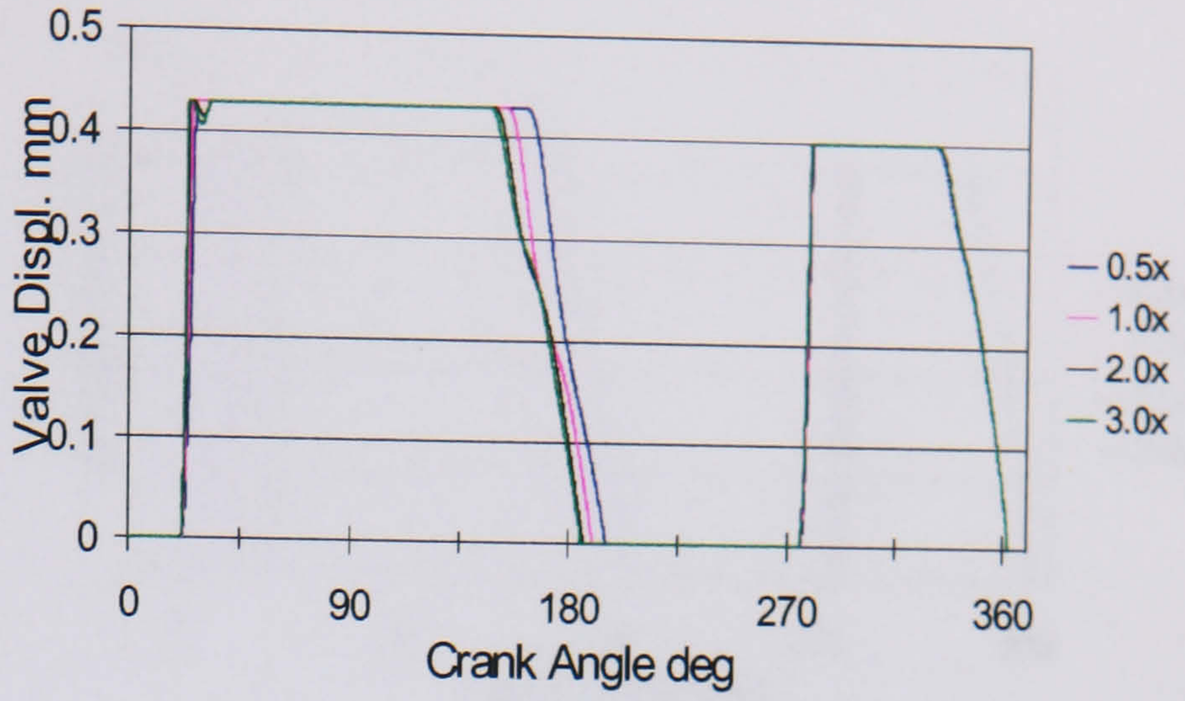

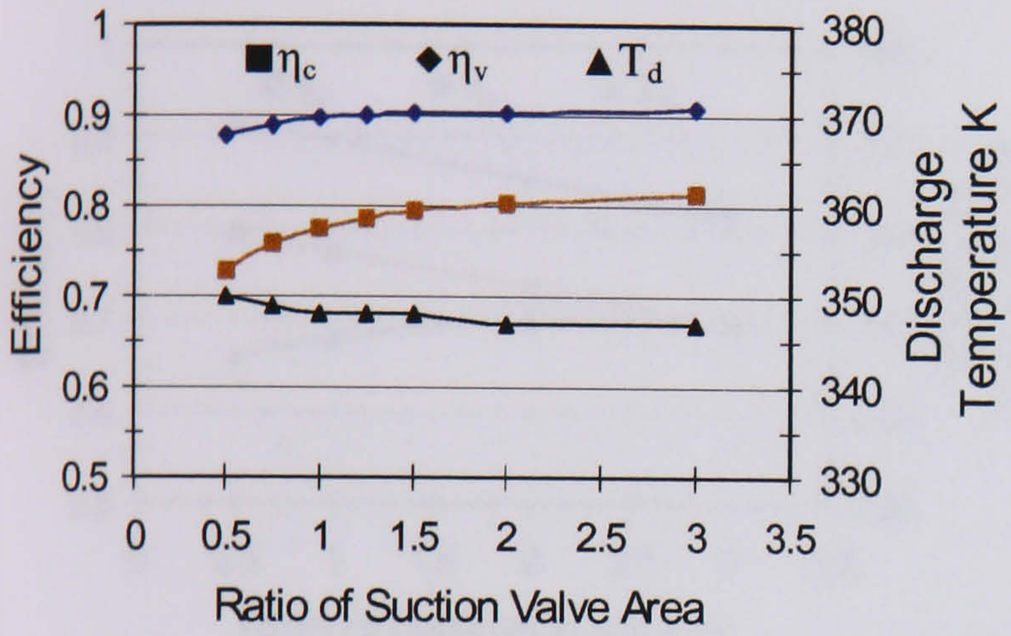

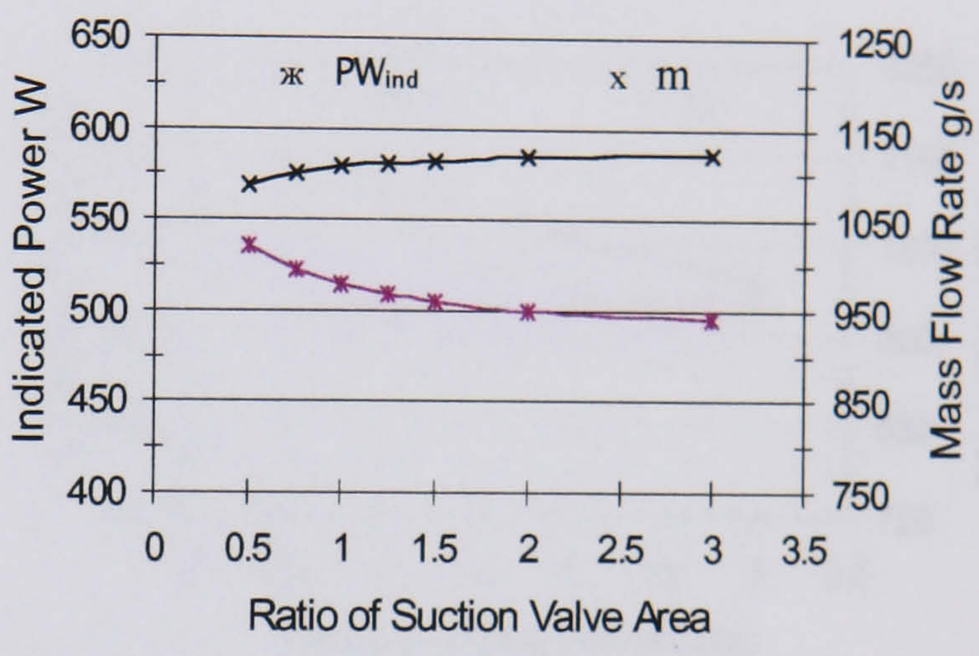

Figure 4.16 Effect of suction valve equivalent surface area variation

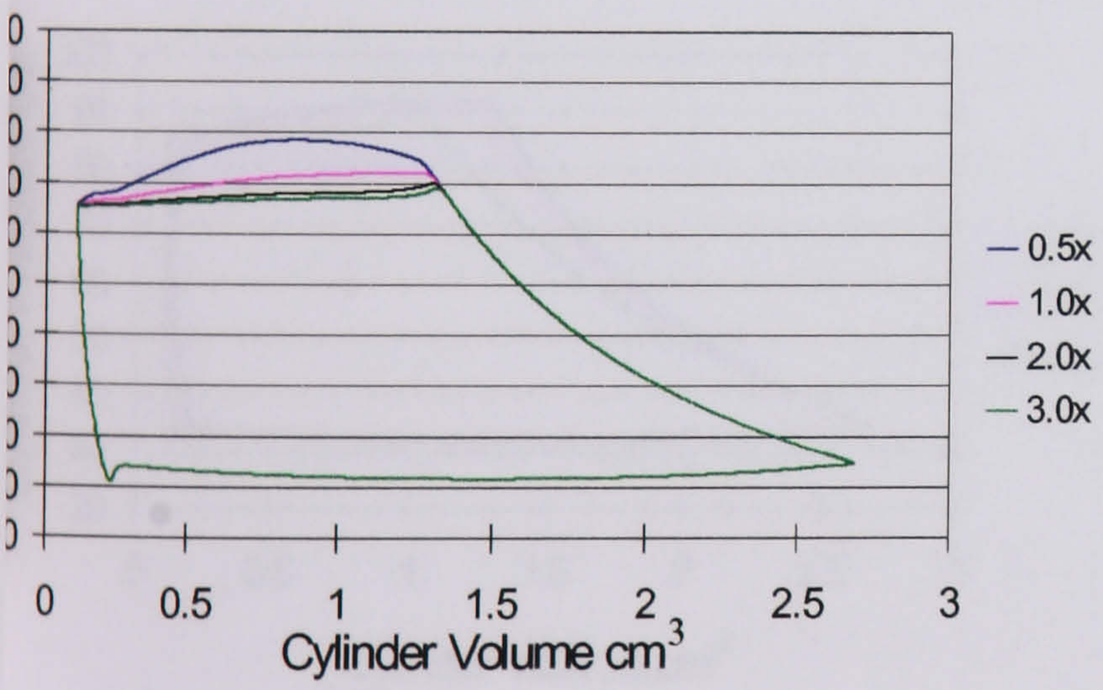

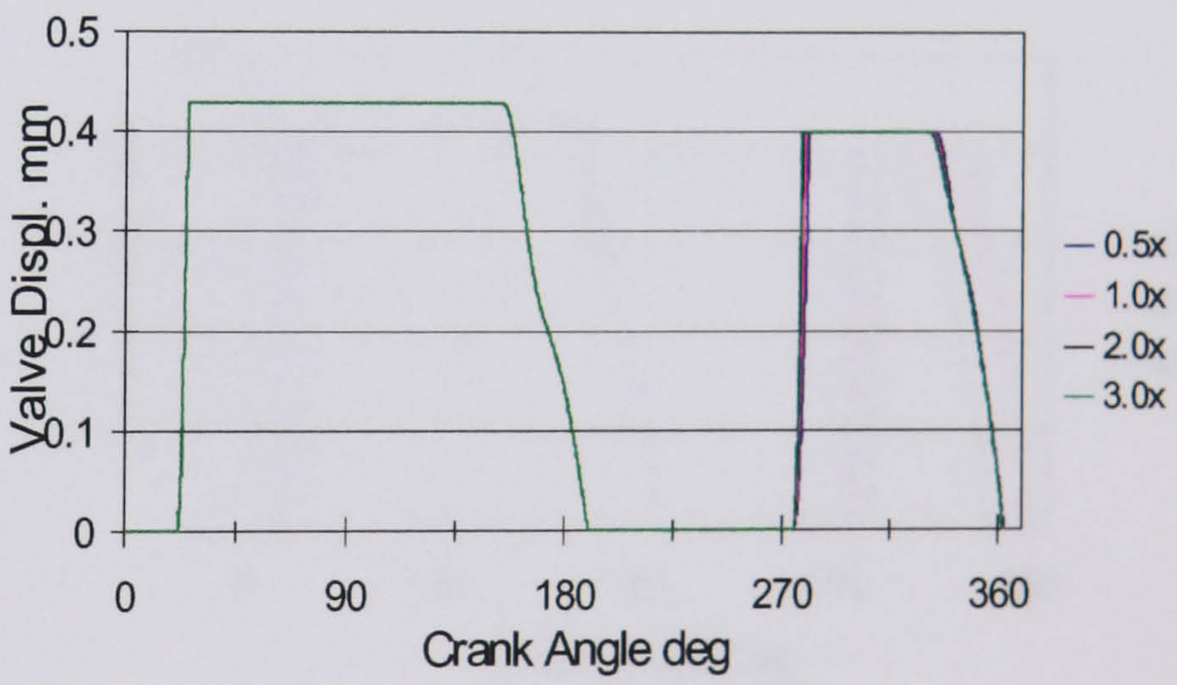

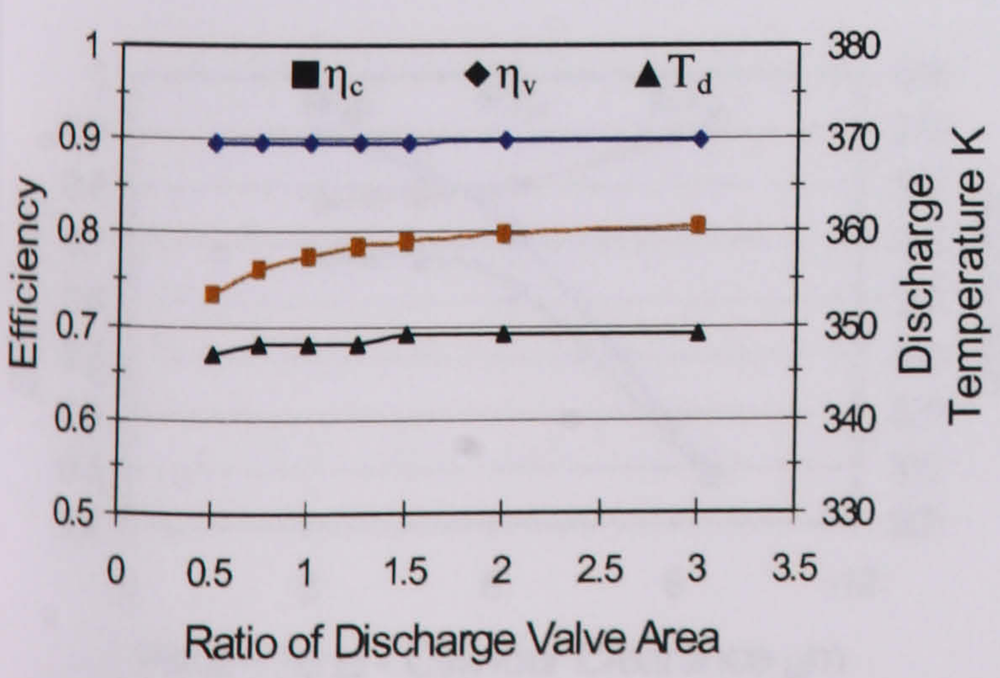

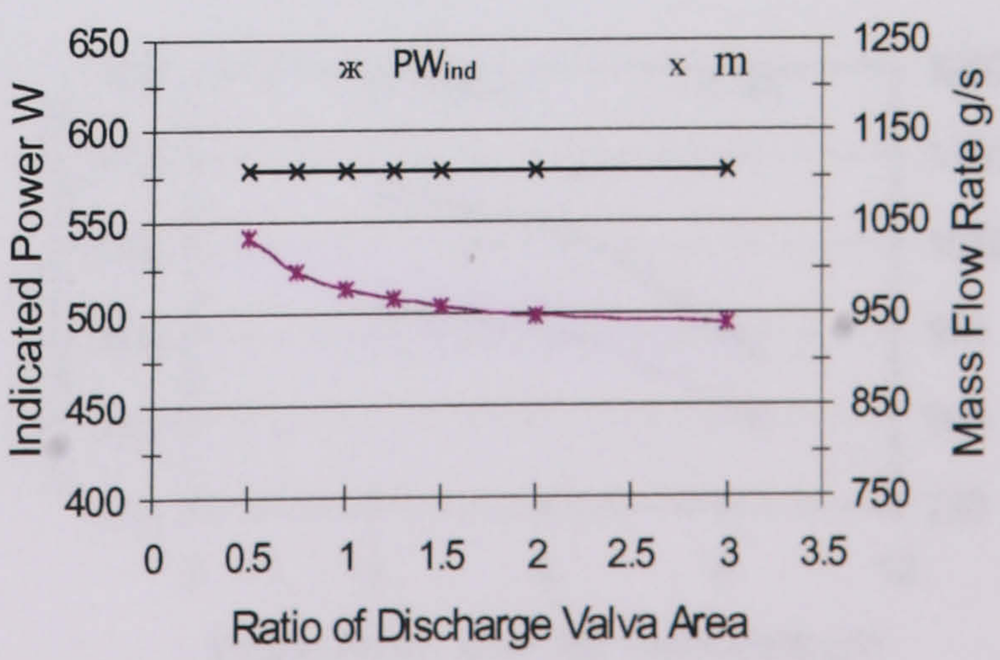

Figure 4.17 Effect of discharge valve equivalent surface area variation

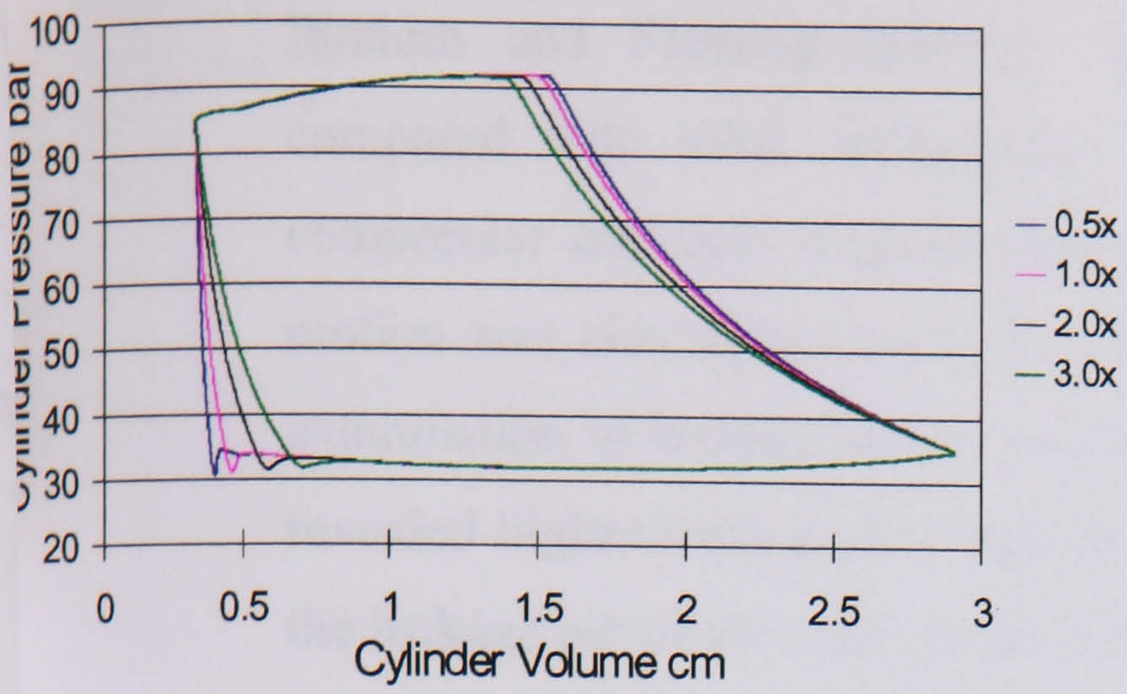

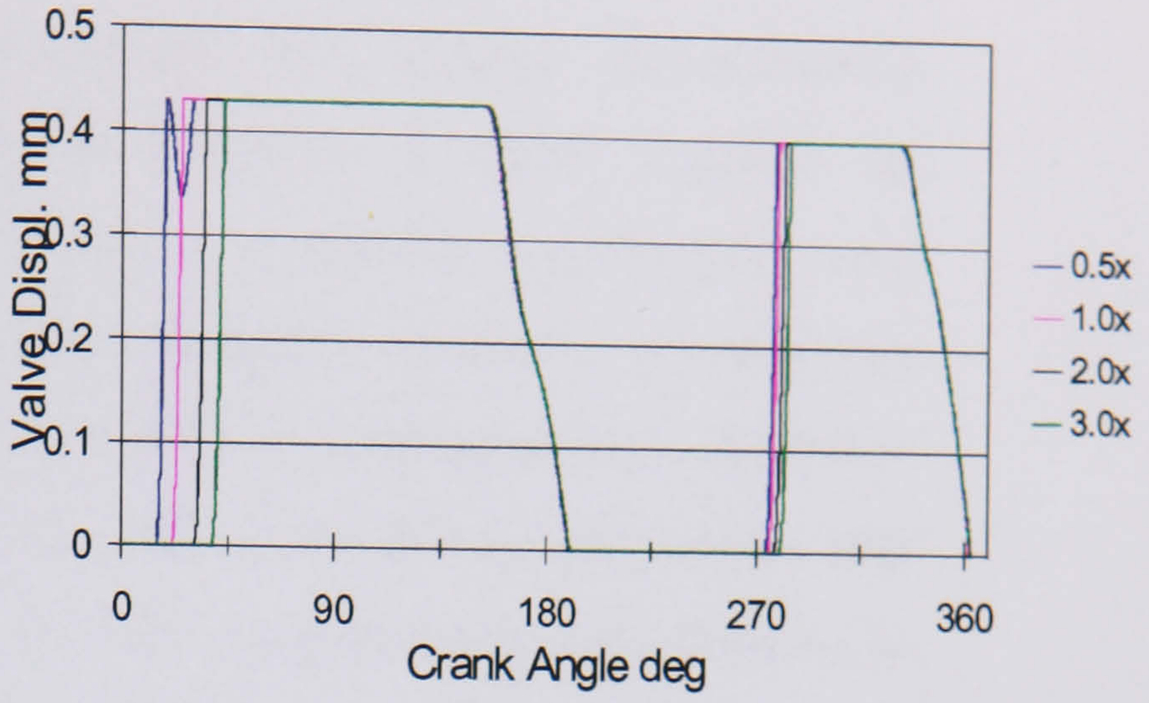

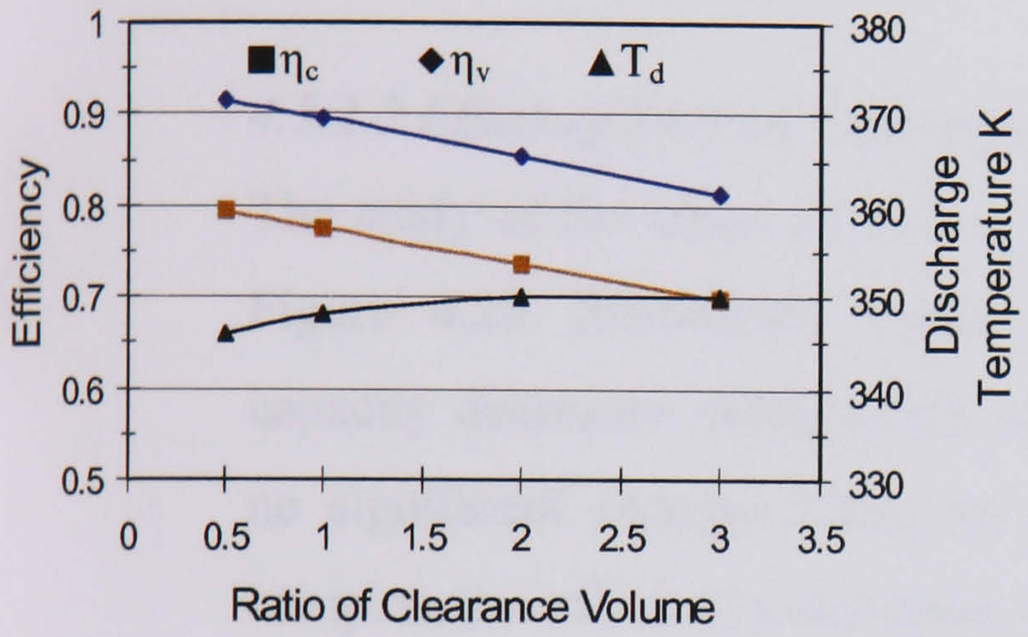

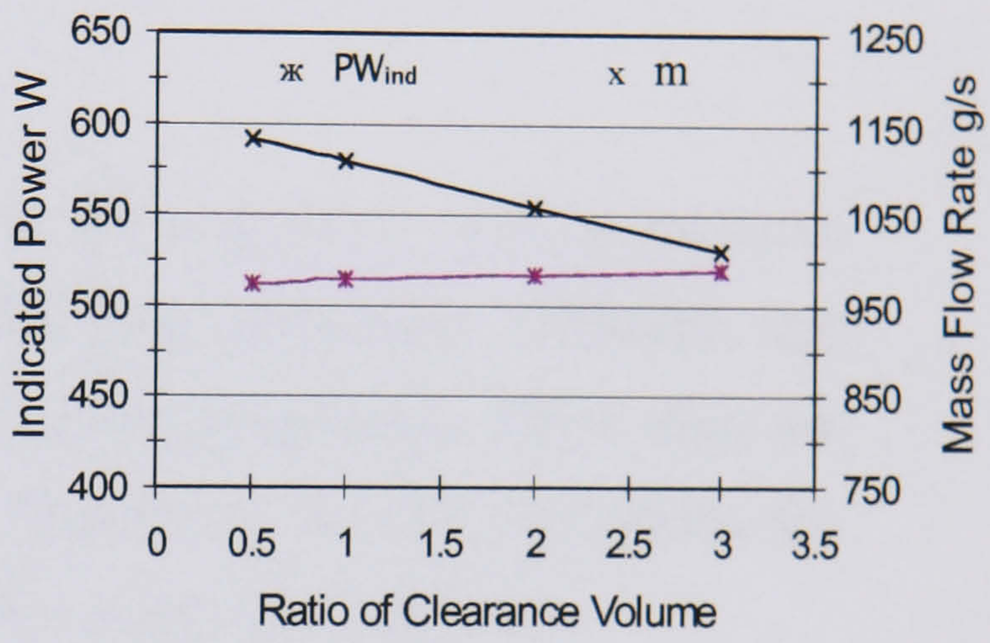

Figure 4.18 Effect of clearance volume variation

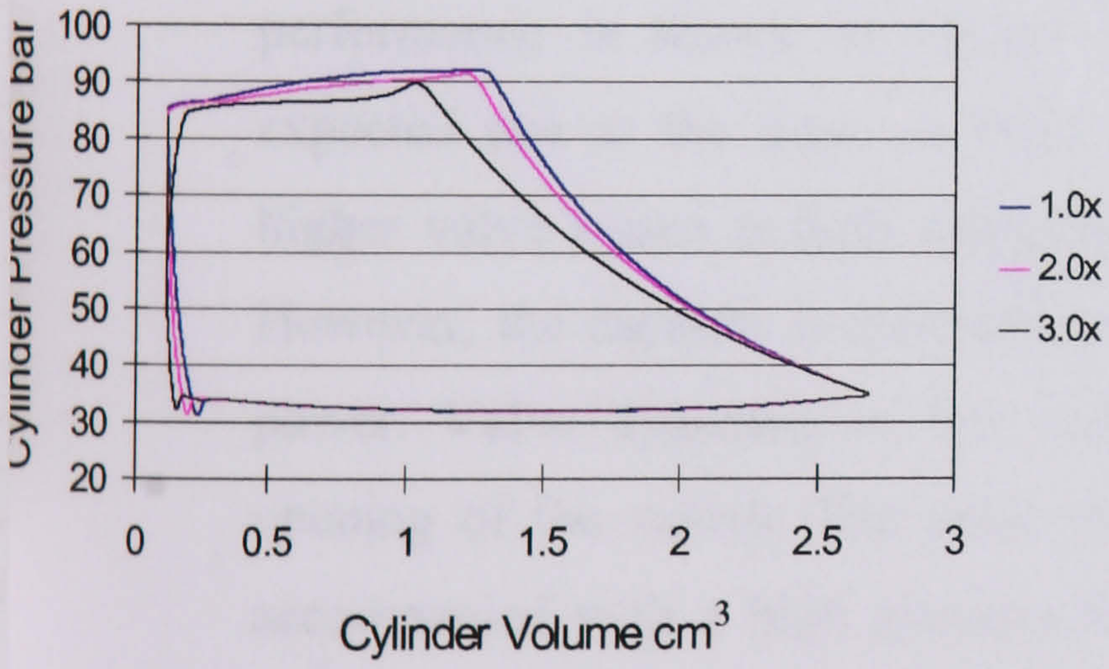

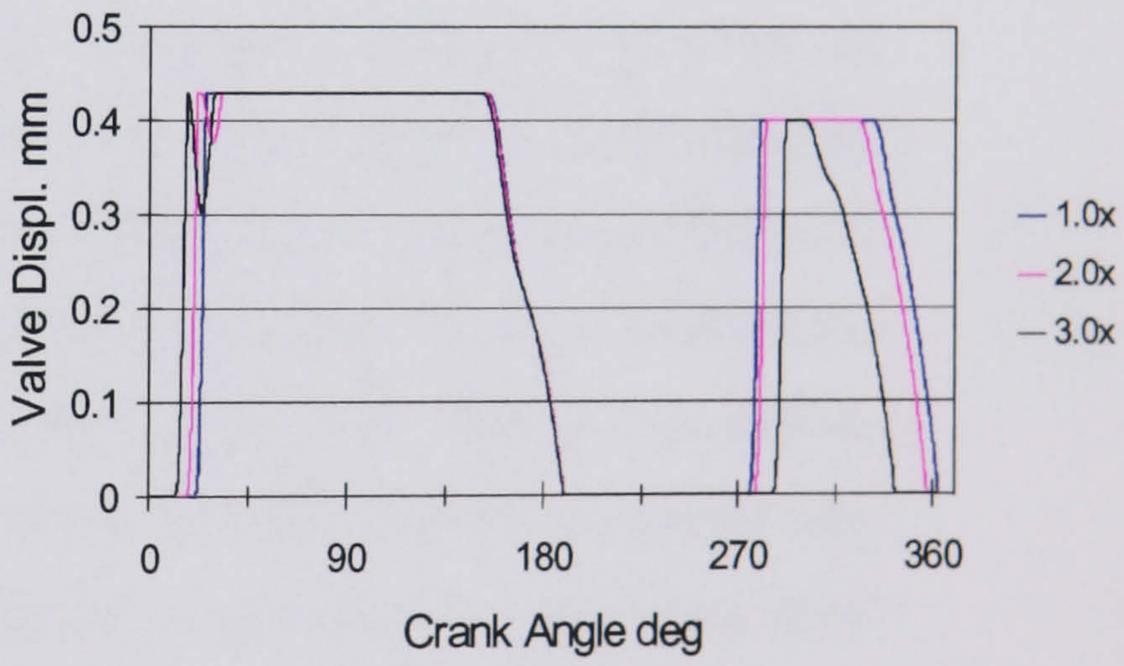

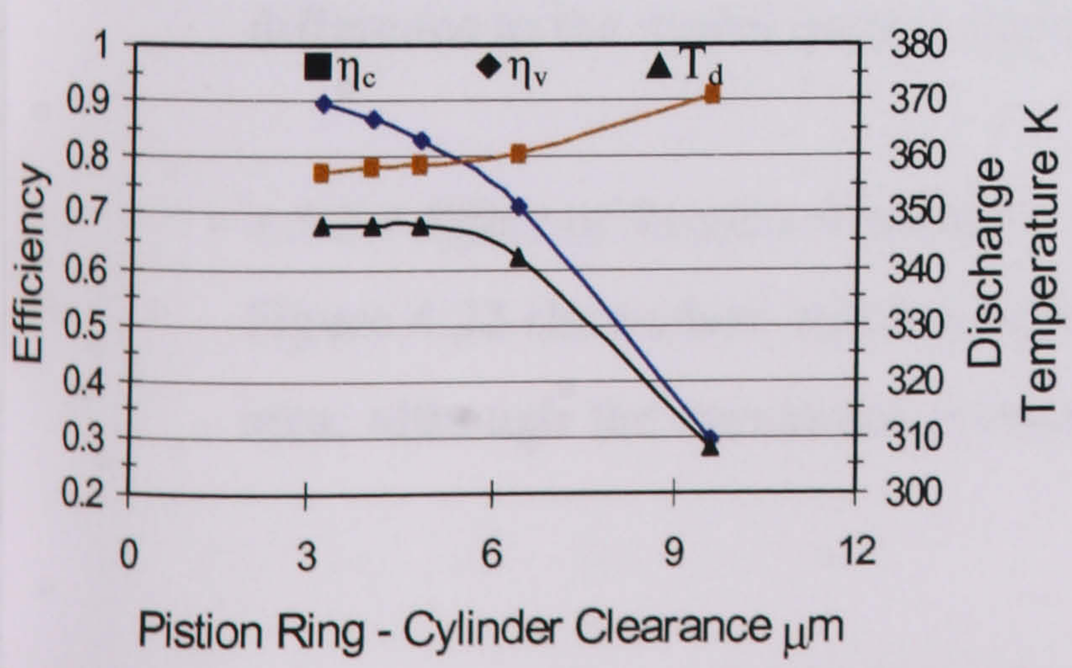

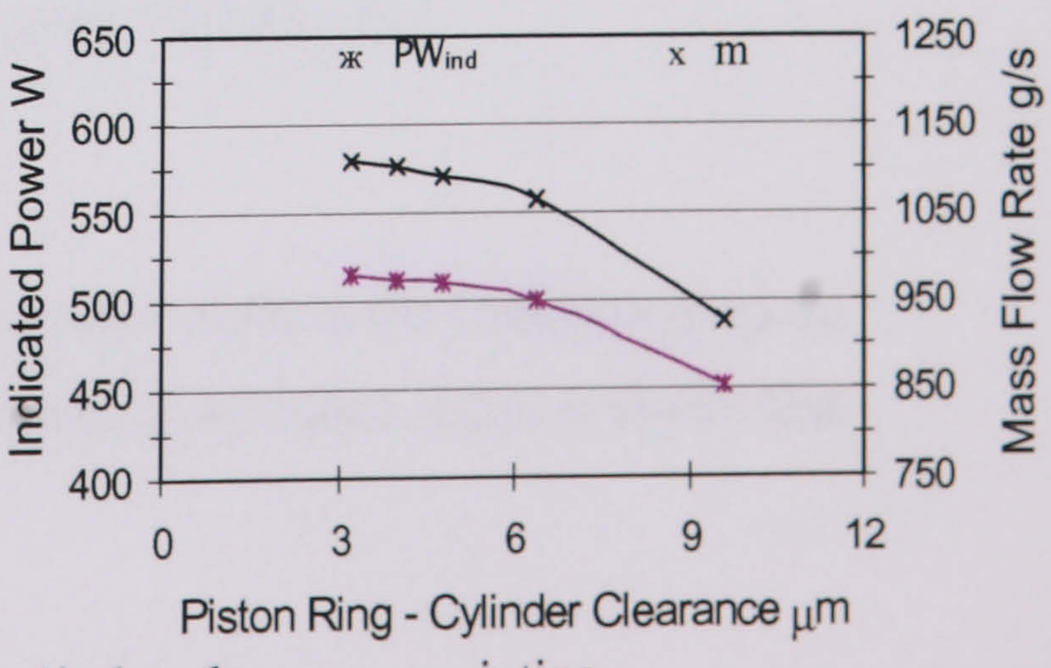

Figure 4.19 Effect of piston ring-cylinder clearance variation

Detailed study for the leakage characteristics of CO_2 compressors was reported by Ibrahim and Fleming (2003a). They investigated CO_2 leakage characteristics compared with other refrigerants. The strong influence of piston clearance on compressor indicator diagram was shown. However, somewhat surprisingly, valve motion was also shown to be sensitive to piston clearance variations. A theoretical examination of leakage due to piston blow-by of CO_2 in a reciprocating compressor revealed higher leakage rate than HCFC-22 and HFC-134a. The results showed that the leakage out of the compression chamber for CO_2 compressors is more sensitive to piston clearance variations than for HCFC-22 and HFC-134a compressors.

4.5.2.2 Effect of Suction Temperature

The study of the effect of suction temperature in the range of 0 - 30 ^{0}C is shown in Figure 4.20. Simulation results show that discharge temperature increases and capacity decreases sharply with an increase in suction temperature. While there are no significant changes either to the indicator diagram or the valve dynamics, the compression efficiency decreases with the increase in suction temperature.

4.5.2.3 Effect of Compressor Speed

A significant effect of compressor speed on valve dynamics and compressor performance is shown in Figure 4.21. The volumetric efficiency increases as expected due to the time available for piston blow-by is reduced. Unfortunately, higher valve losses at high compressor speeds reduce the compression efficiency. However, the capacity is increased sharply, but at the expense of high compression power. Valve dynamics at low compressor speeds are poor due to incomplete opening of the valves. The good valve dynamics at high compressor speeds was accompanied with a high pressure drop across the valves due to large mass flow rates. Reducing the calculation step size below 0.1^0 of crank angle made no difference to the model output; hence 0.1^0 was chosen for all runs.

4.5.2.4 Effect of Suction Pressure

Figure 4.22 shows how increasing the suction pressure reduces the indicator diagram area, although the maximum pressure is maintained in all cases. Also, it shows that

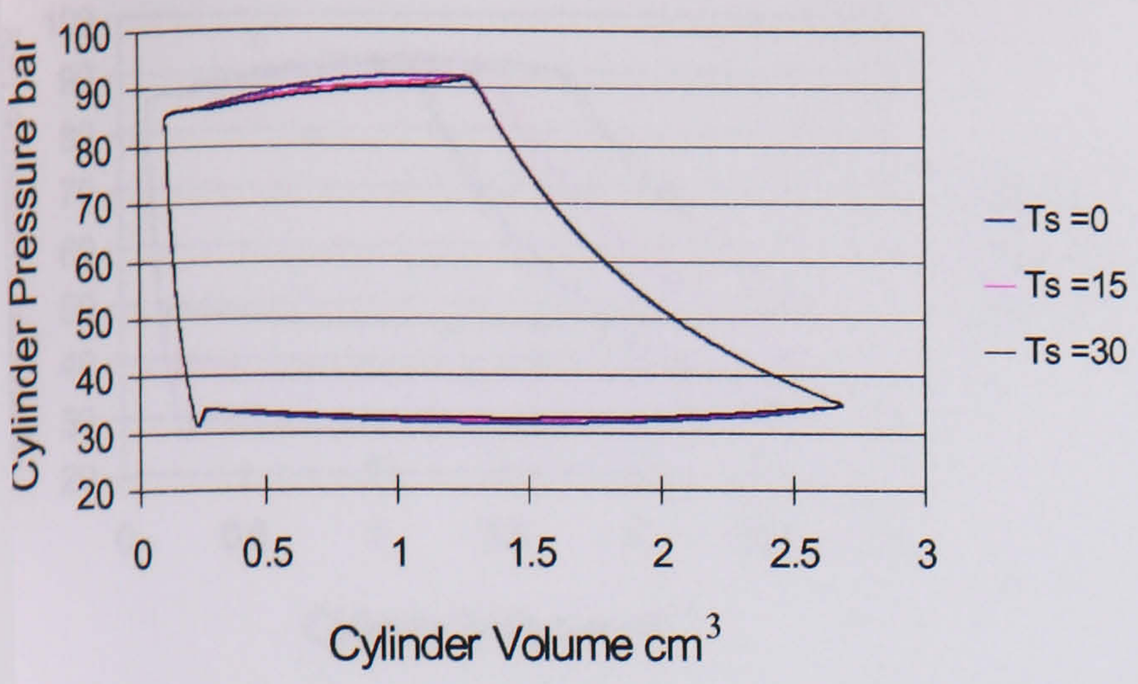

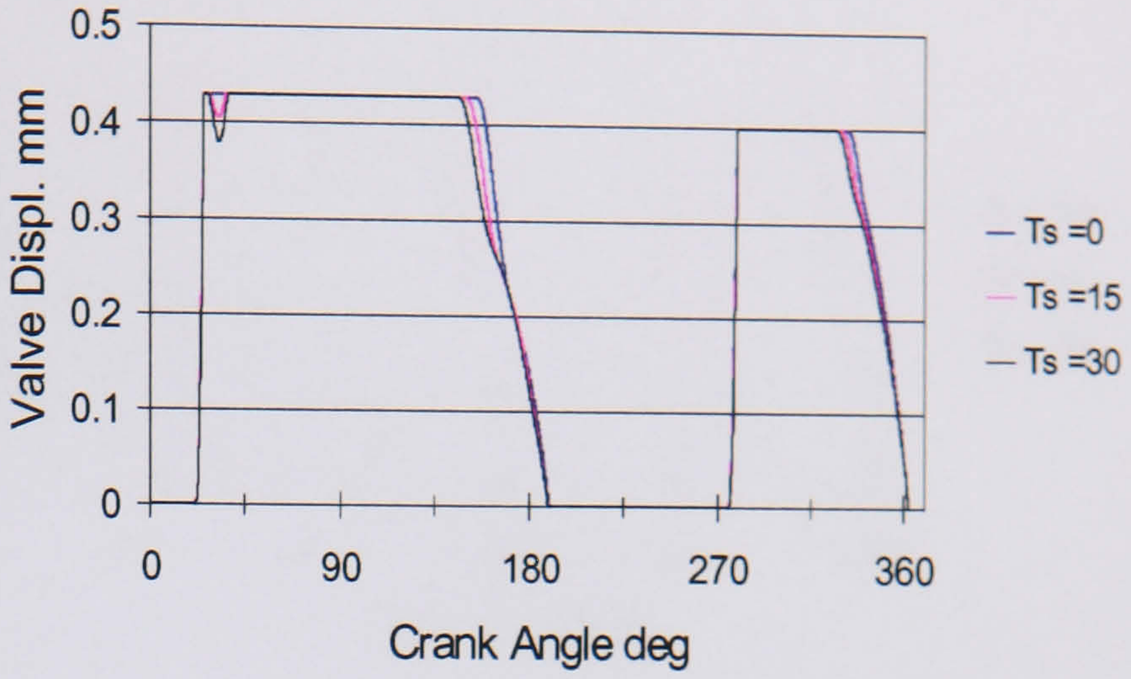

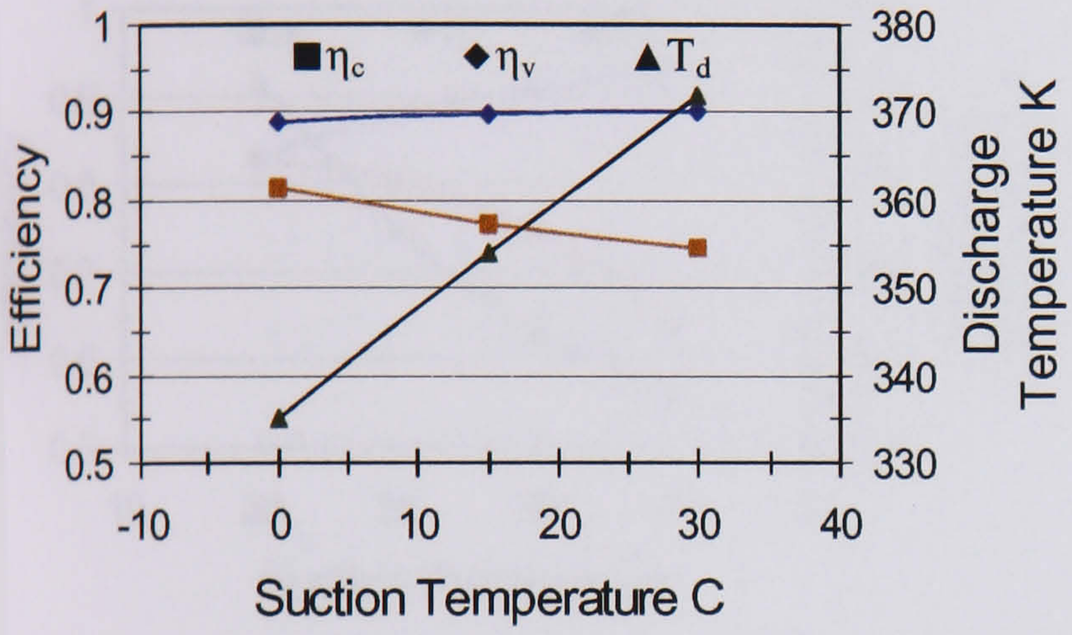

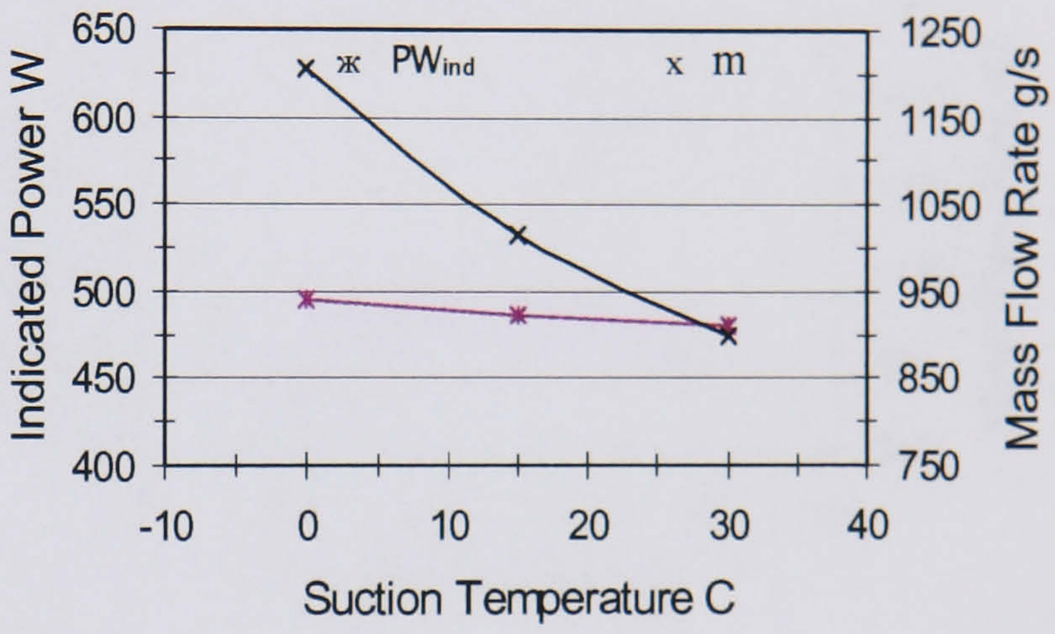

Figure 4.20 Effect of suction temperature variation

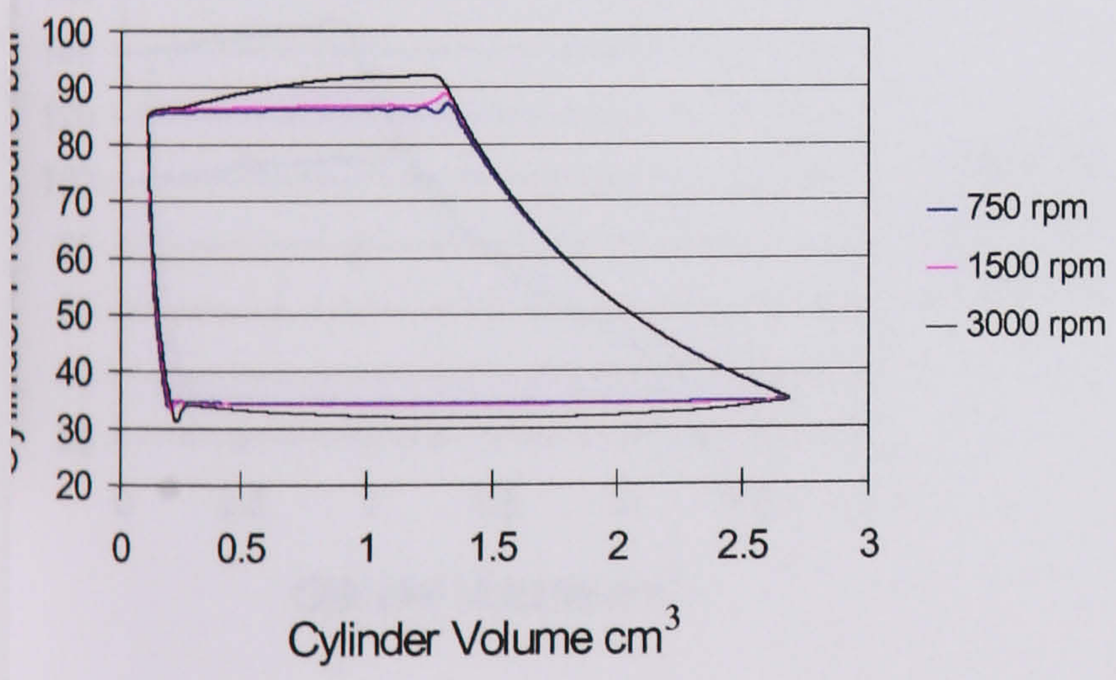

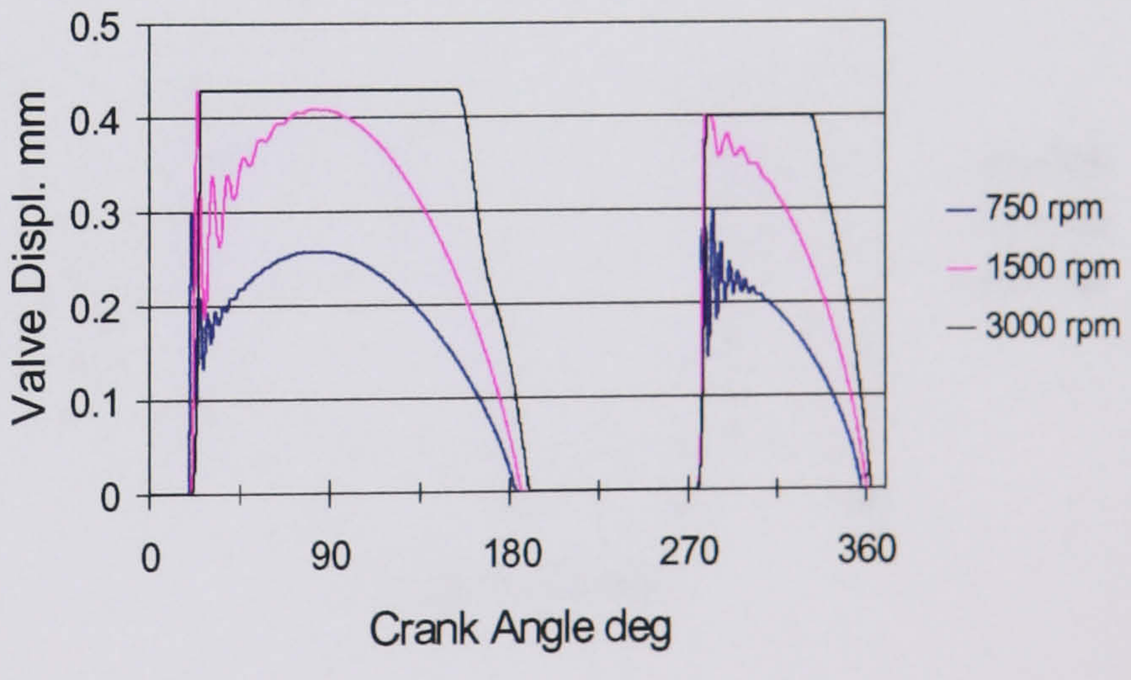

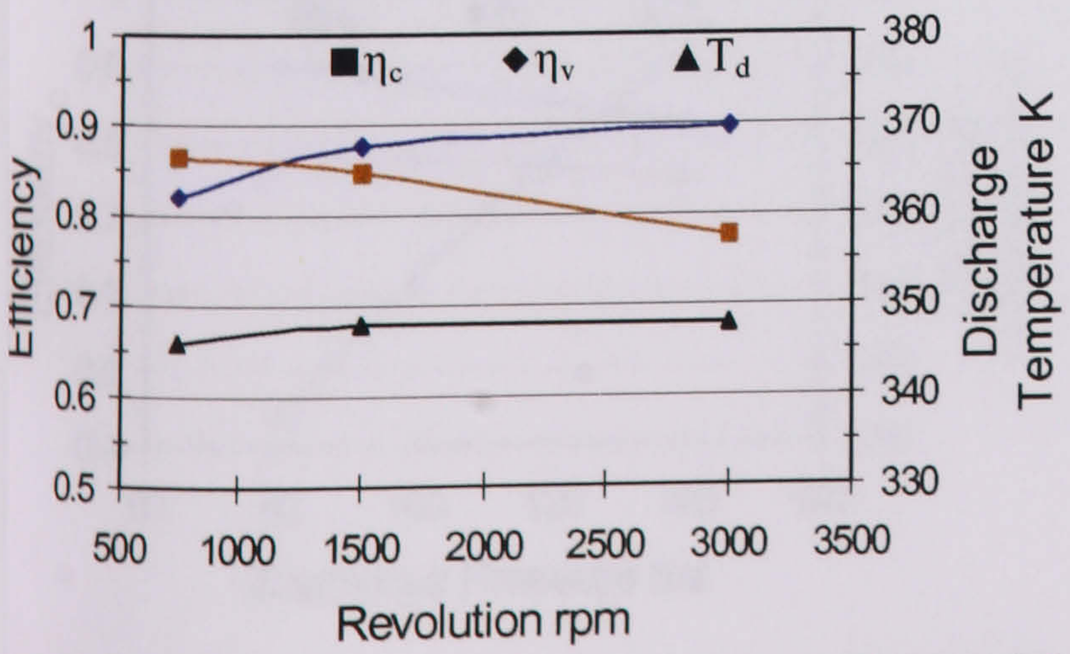

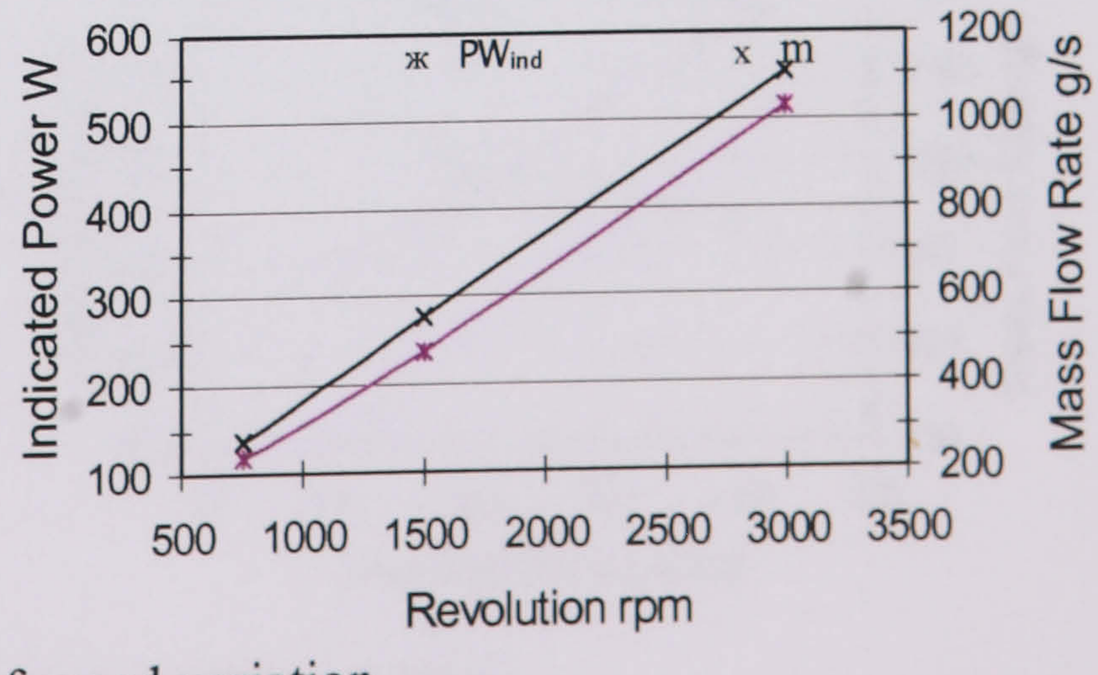

Figure 4.21 Effect of speed variation

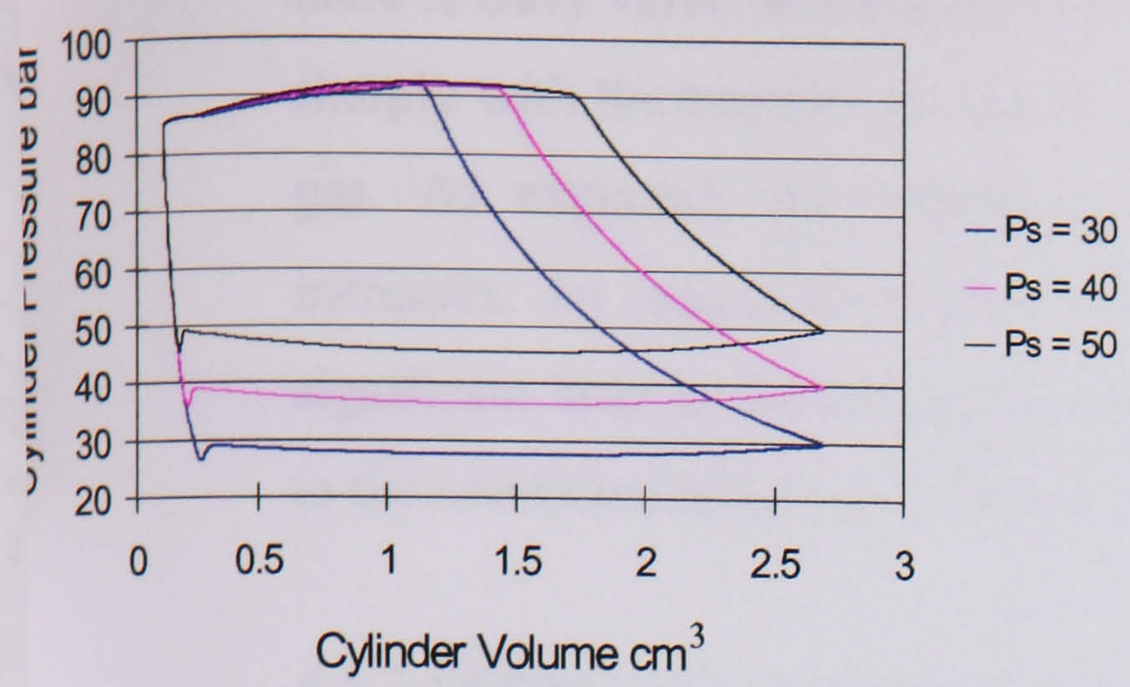

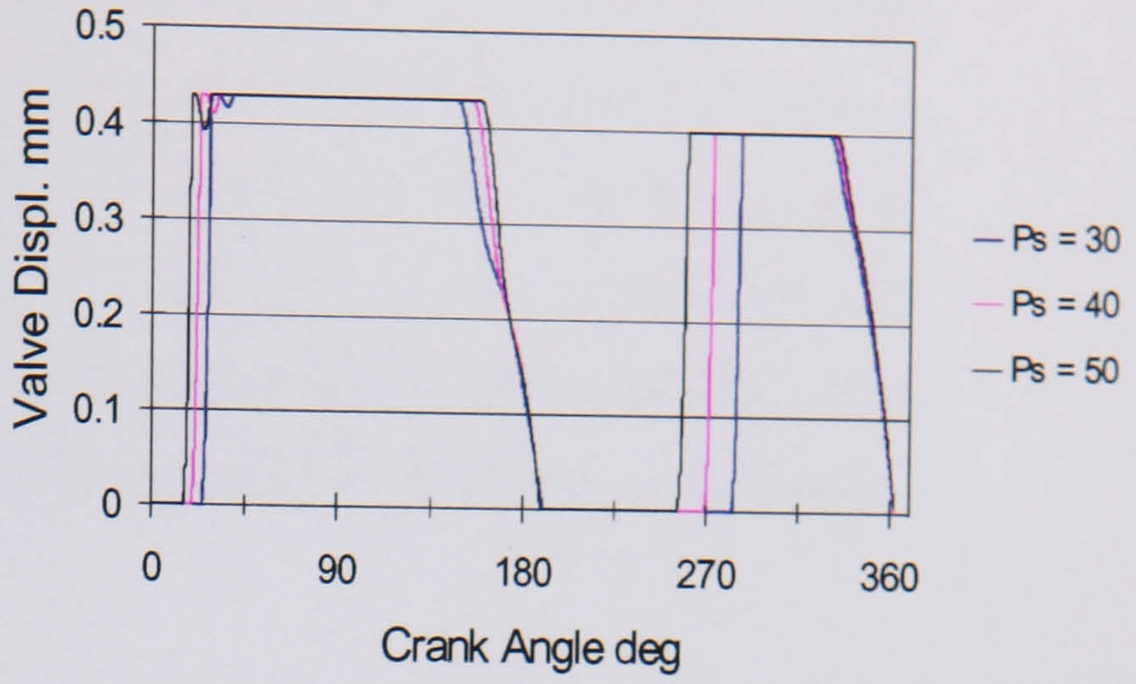

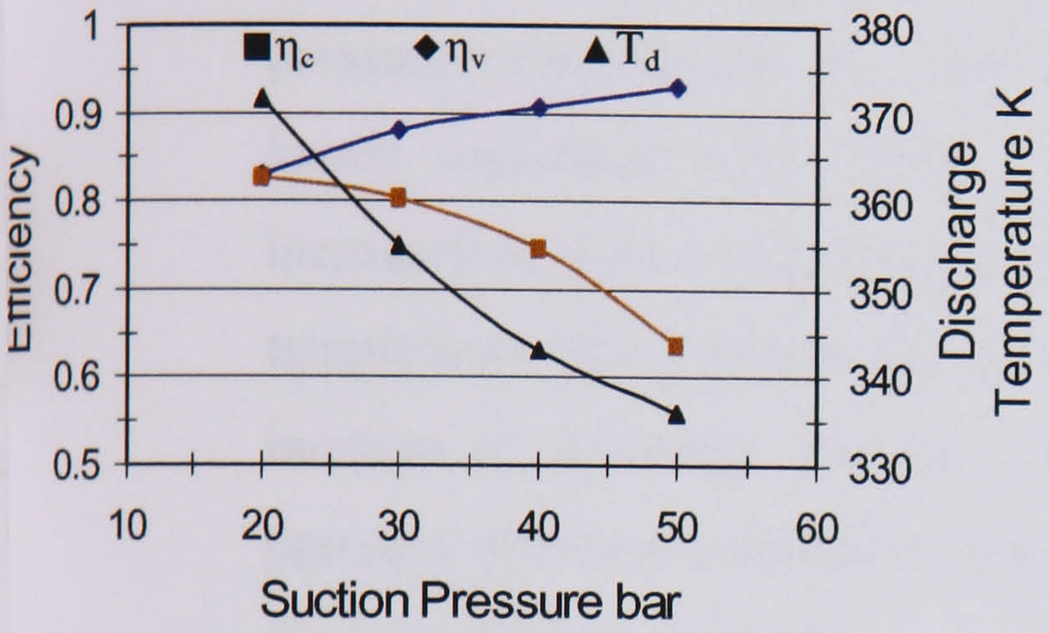

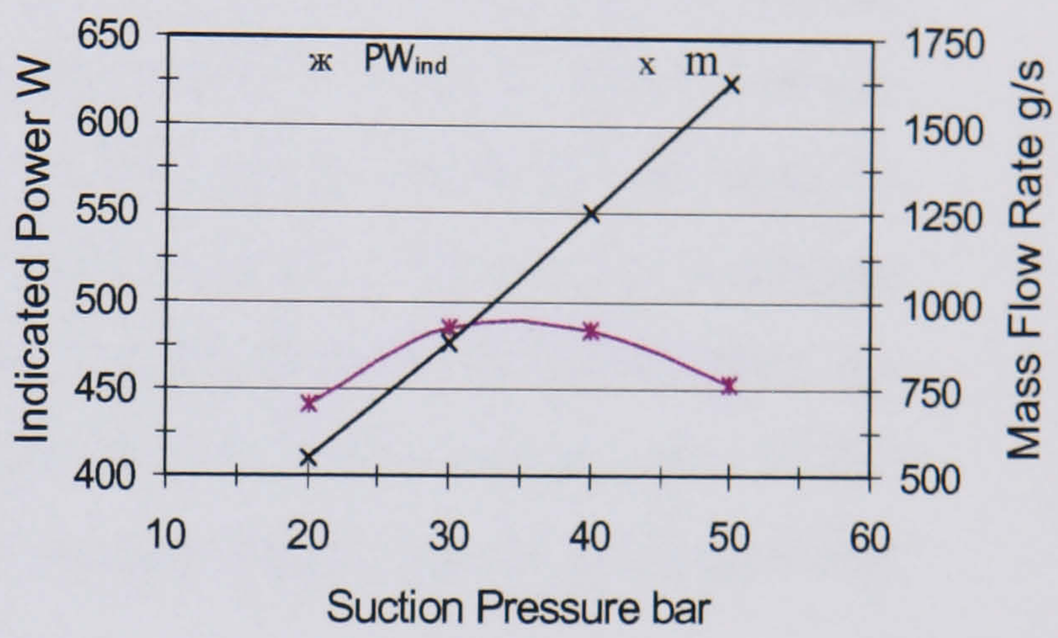

Figure 4.22 Effect of suction pressure variation

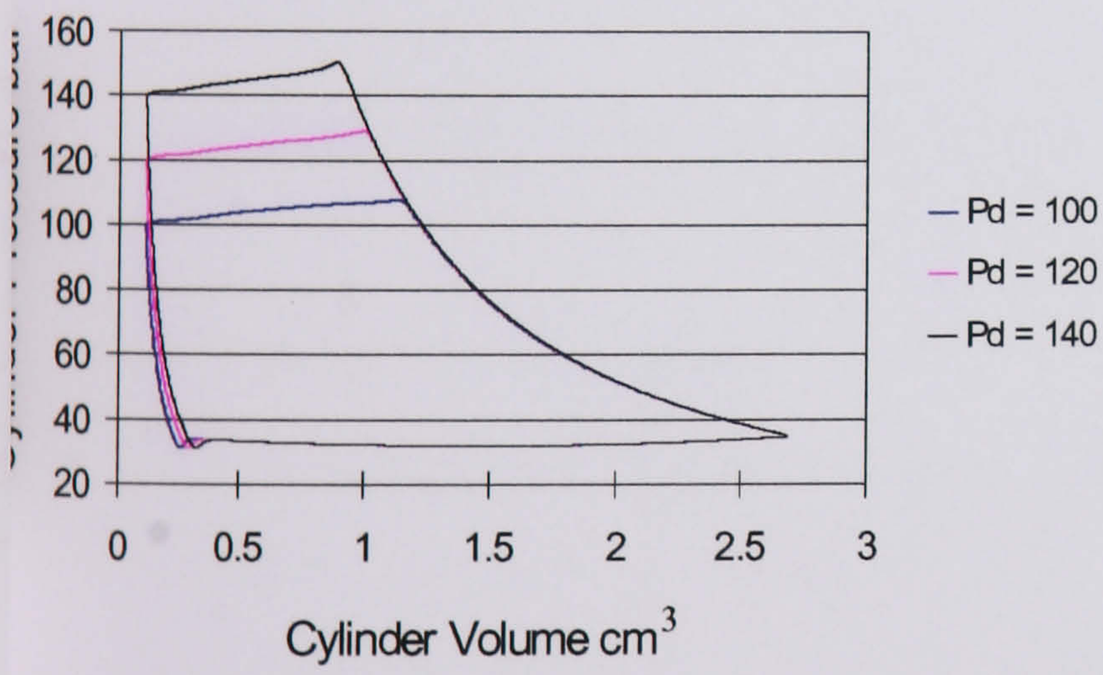

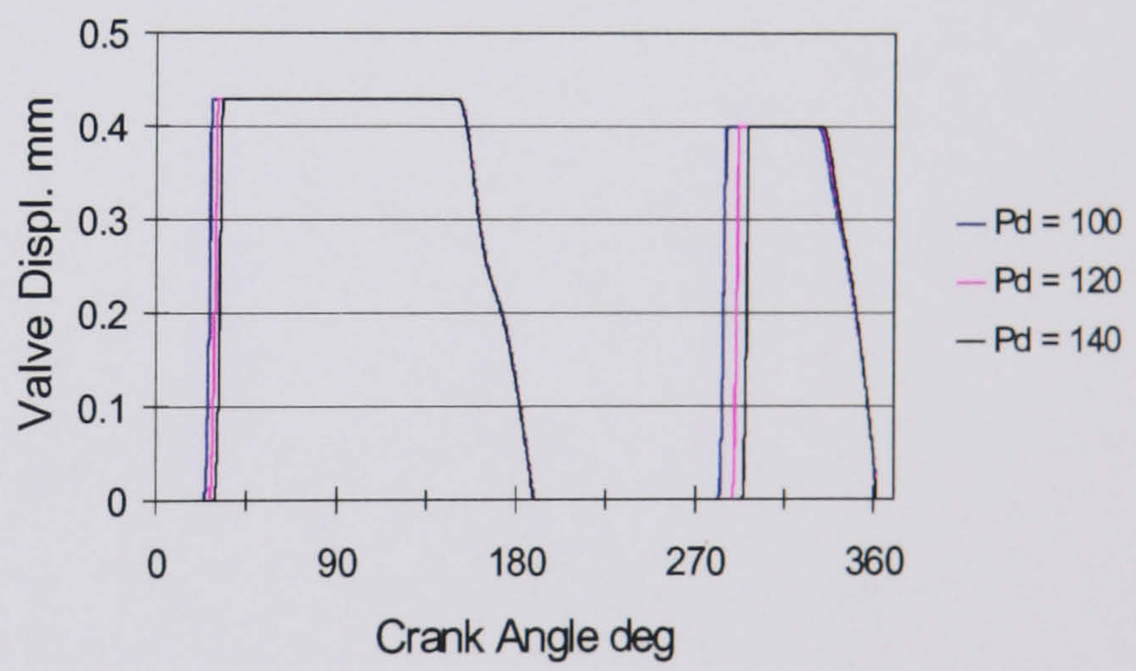

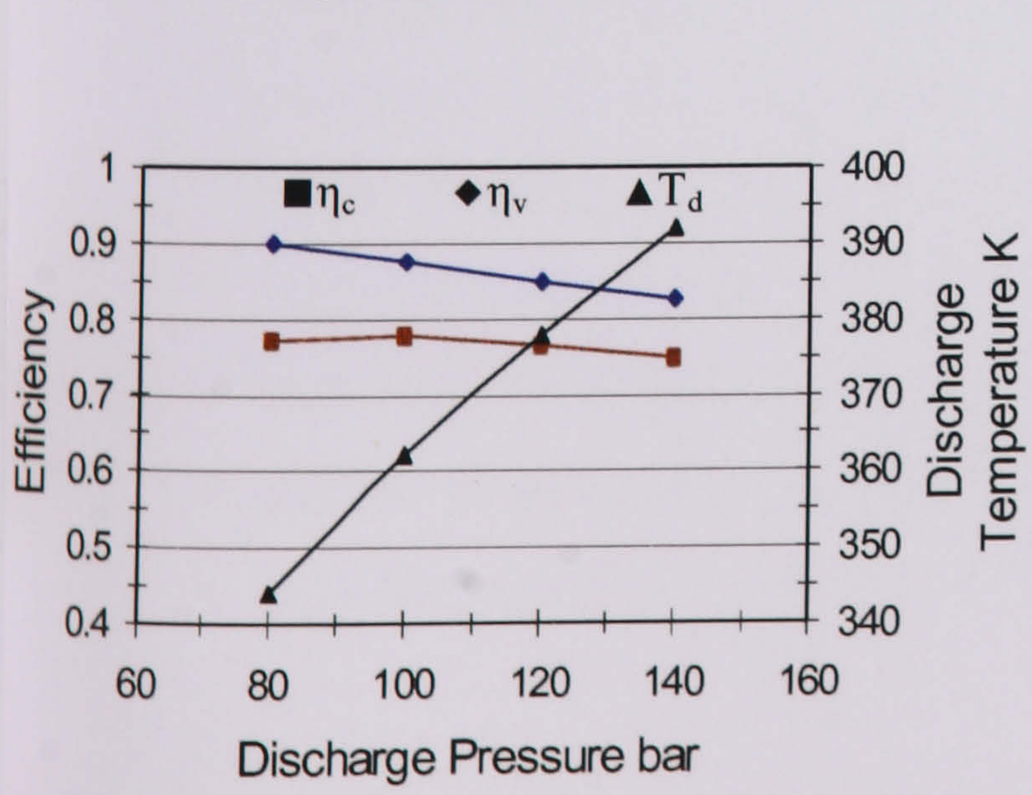

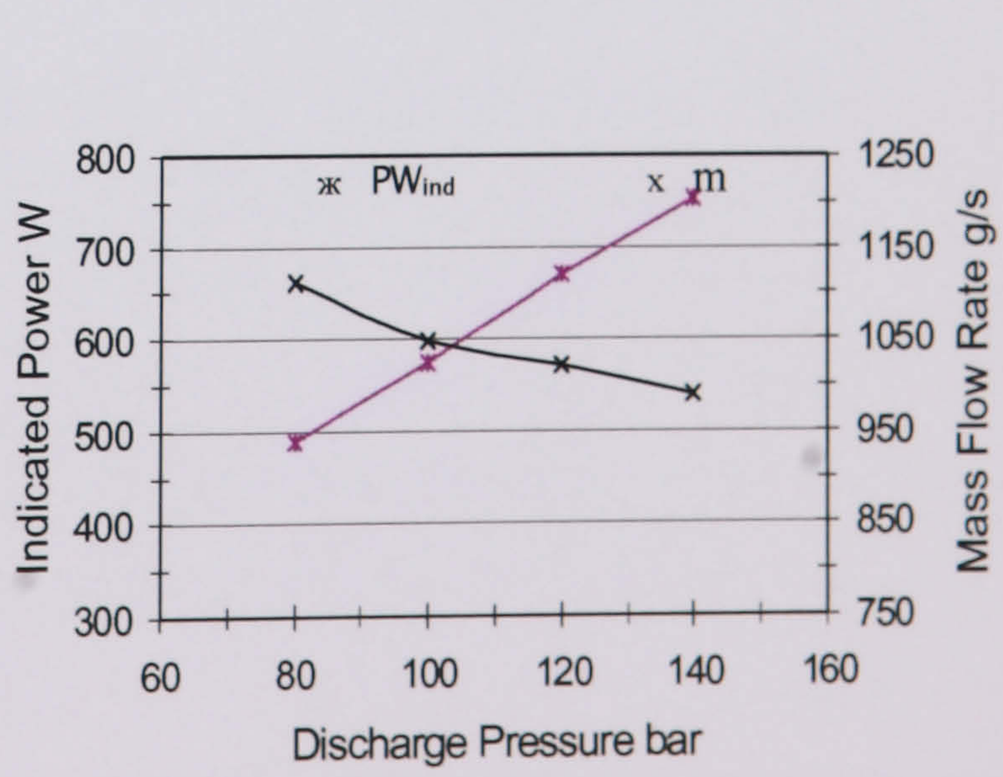

Figure 4.23 Effect of discharge pressure variation

there is early valve opening as the suction pressure increases. The capacity increases sharply with the increase of suction pressure due to the higher density of the suction gas. As expected, the volumetric efficiency improves as the suction pressure increases. An associated drop of pressure ratio occurs. This is also associated with significant drop in discharge temperature. The indicated power has a peak value due to the combined effects of a decrease in indicated efficiency and a capacity increase.

4.5.2.5 Effect of Discharge Pressure

Figure 4.23 shows that the compression efficiency changes a little as discharge pressure increases but the volumetric efficiency decreases, due to higher leakage losses associated with higher discharge pressure. As the discharge pressure is increased to give a very high pressure ratio, capacity drops off fast while discharge temperature and compression power increase significantly, as expected. Also, an increase of discharge pressure causes a slight delay in valve opening due to the pressure difference needed to open the valve taking a longer time to generate when the mass flow is reduced.

Chapter 5

Single-Stage Transcritical CO_2 Heat Pump

5.1 Introduction

A feature of heat pumps in general is that the temperature difference between the hot and cold sinks is likely to vary over a greater range than is the case for refrigeration or air conditioning systems. The load can also vary widely, i.e. from summer to winter, resulting in a wider range of operating conditions. It is therefore desirable to develop an analytical method of predicting the performance of transcritical CO_2 heat pumps under differing conditions of operation.

This chapter addresses the physical system of a transcritical CO_2 heat pump and how the components models were developed. In addition, a simulation model for the overall transcritical CO_2 heat pump cycle is developed. For a given geometry and set of operating conditions, the model is usable to predict system performance.

5.2 System description

5.2.1 Components

A typical transcritical heat pump system is shown in Figure 5.1. The purpose of a heat pump is to pump heat from the low temperature reservoir to the high temperature reservoir. In the practical residential application, the high and low reservoirs may be either indoors or outdoors depending on heat pump operation mode. Both heating and cooling modes do exactly the same thing. They pump heat from one location to another. A heat pump is essentially an air conditioner with a few additions. From the thermodynamic point of view, the basic heat pump components needed to make heat transfer feasible are: two heat exchangers (gas cooler and evaporator) and a compressor. A heat pump has two expansion devices and two

bypass valves. This allows the unit to provide both A/C and heat. In addition, there are other components in an actual heat pump system, the most important of which are: a 4-way valve enabling refrigerant flow reversal for the defrost period and cooling mode and an accumulator which acts as a protective device by limiting the liquid flow into the compressor and stores excess refrigerant during part load operation. Another feature of this system is an internal heat exchanger (IHX) which improves the thermodynamic efficiency and ensures that the compressor suction gas always has some superheat, a desirable condition when a reciprocating compressor is used.

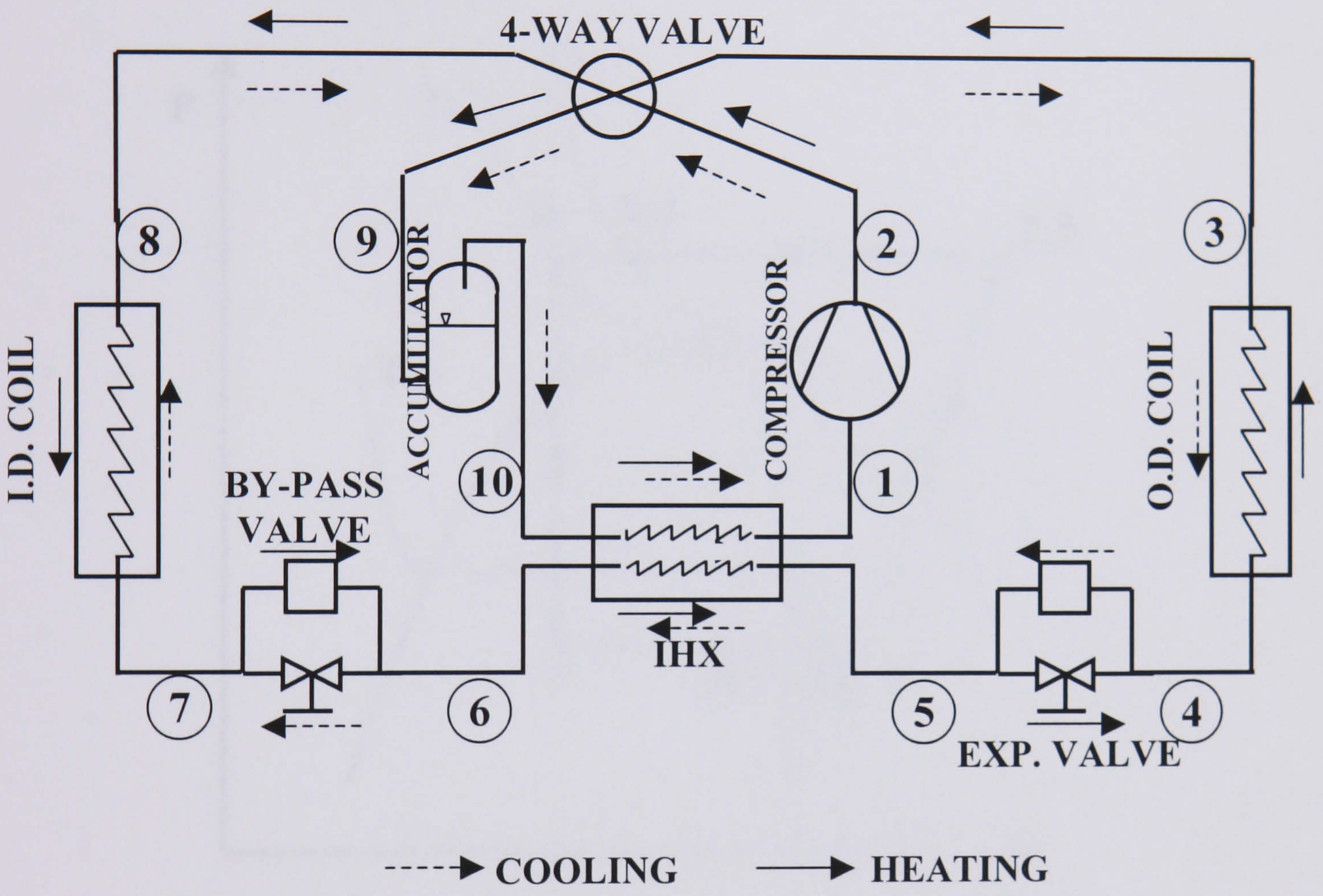

Figure 5.1 Scheme of CO_2 heat pump

In general, the thermodynamic states of the refrigerant at key locations of a heat pump circuit as well as the heat pump performance are functions of many factors. They are: the individual performance of the heat pump components, the compatibility of components in the system, the properties of the refrigerant, the outdoor and indoor air conditions and the refrigerant charge. The manufacturers establish the optimum refrigerant charge for a given heat pump during a prototype test. In general, the criterion of this charge is usually a degree of refrigerant

superheat measured at the compressor inlet at specified test conditions. For the CO_2 system, finding an optimal refrigerant charge is not a critical issue. The basic idea is that the refrigerant outlet of the evaporator is always kept in the wet region (quality around 0.9-0.95) and that the receiver will act as a buffer for varying refrigerant levels (Aarlien and Frivik 1998).

5.2.2 Heating/cooling modes of operation

The thermodynamic cycle in the cooling mode and heating mode are illustrated in Figures 5.2 and 5.3, respectively.

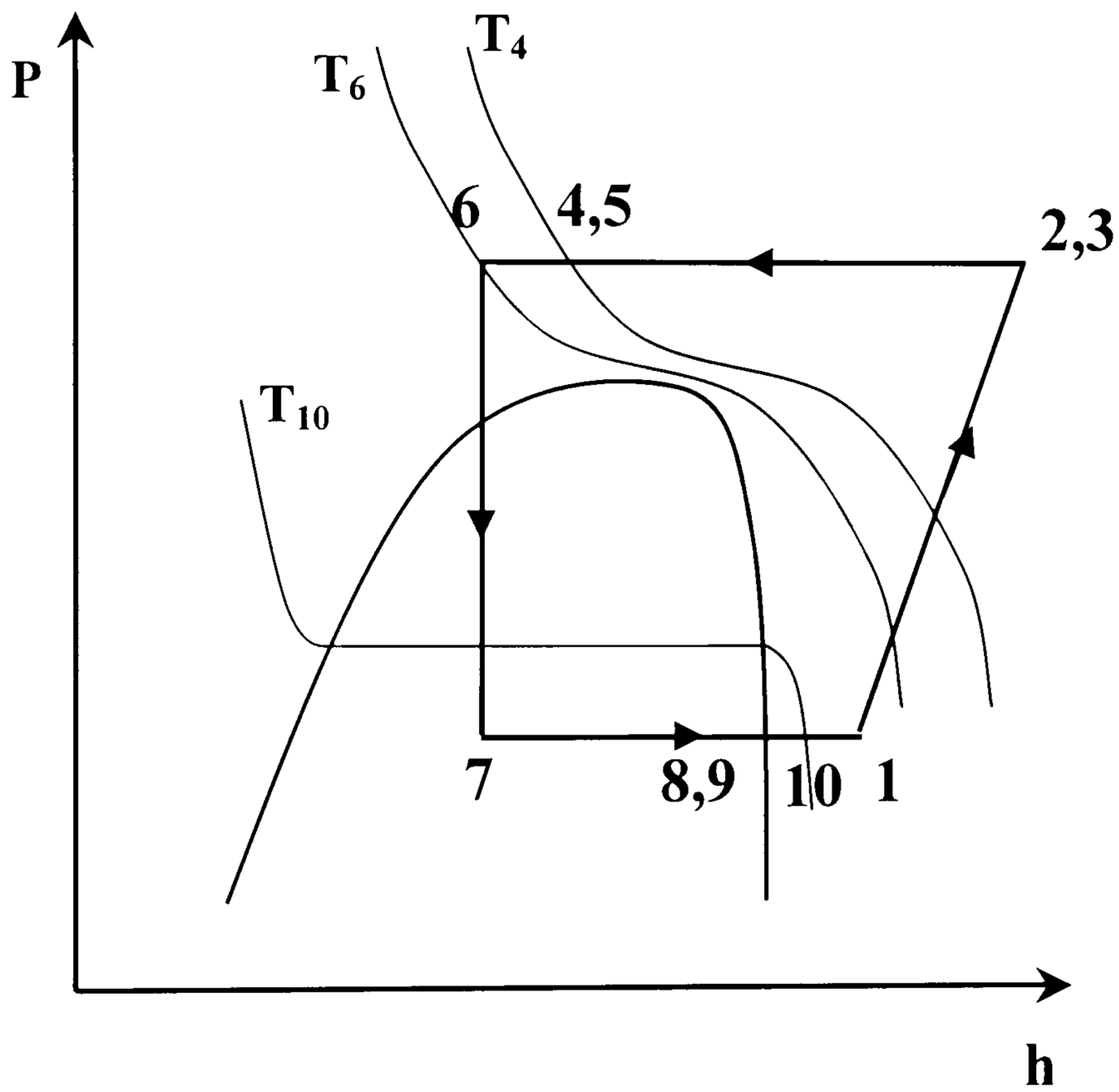

Figure 5.2 Thermodynamic cycle of heat pump in cooling mode

The heat pump cycle in the cooling mode is as follows:

1. (1-2) The compressor pumps the refrigerant to the 4-way valve.
2. (2-3) The 4-way valve directs the flow to the outdoor coil (gas cooler) where the refrigerant is cooled.
3. (3-4) The air flowing across the coil and removes heat from the refrigerant. This is the air that blows into the atmosphere.
4. (4-5) The refrigerant bypasses the first expansion device

5. (5-6) The refrigerant flows through the IHX and gives up heat to the suction gas at compressor inlet.
6. (6-7) The refrigerant flows to the second expansion device situated before the indoor coil (evaporator) where it is expanded.
7. (7-8) Here refrigerant picks up heat from the air blowing across the indoor coil (evaporator) and the air comes out cooler. This is the air that blows into the dwelling.
8. (8-9) The refrigerant vapor then travels back to the 4-way valve to be directed to the IHX through the accumulator (9-10).
9. (10-1) The refrigerant is superheated in the IHX and compressor suction line to start the cycle all over again.

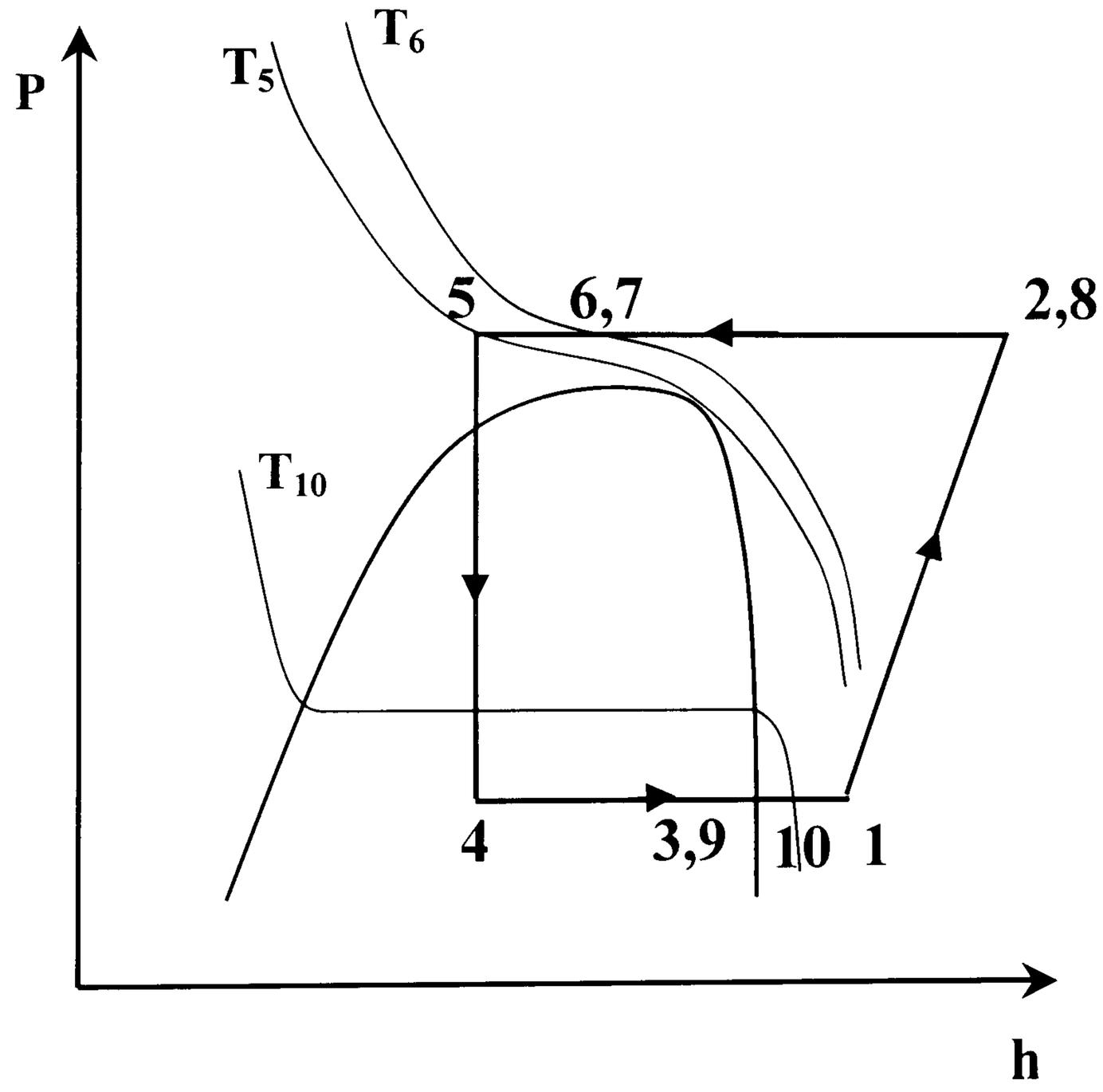

Figure 5.3 Thermodynamic cycle of heat pump in heating mode

Figure 5.3 shows the heat pump in heating mode. The difference from Figure 5.2 is that the 4-way valve directs the compressed refrigerant to the indoor coil first. This makes the indoor coil the gas cooler and releases the heat energy. This heated air

blows to the dwelling. The outdoor coil is used to collect the heat. This now becomes the evaporator.

5.2.3 Control

Controls on a refrigeration or heat pumping system allow the system to modulate for varying environmental conditions or provide means by which the operator may specify a certain type of operation. Controls may be categorized into three basic groups: (1) operating, (2) primary and (3) limit. Operating controls, such as thermostats, turns systems on and off. Primary controls, such as floats, provide safe continuous operation. Limit controls, such as cut-out switches, protect a system from unsafe operation. The controls suggested for the operation of a CO_2 transcritical heat pump fall into the primary category, since a transient system is not considered here (eliminating the need to discuss operating controls) and limiting controls will be similar to those on current vapor compression systems.

Current simple vapor compression cycles based on conventional refrigerants can be implemented in devices using little or no refrigerant flow control (other than the compressor speed). Many HFCs systems of small capacity operate with no active flow control, where refrigerant expansion is accomplished by a needle valve or a capillary tube. While simple in operation, one significant disadvantage of this design is the lack of ability to modulate the evaporation pressure. This causes a problem when

air inlet temperatures to the heat rejection heat exchanger (condenser) are low, because frost can form on the air side of the evaporator since the evaporation pressure will be low due to capillary tube flow characteristics. In addition to a potential frost problem, without the ability to regulate the amount of refrigerant superheating, the compressor will operate less efficiently when the amount of superheating is high (due to reduced volumetric efficiency).

Therefore, on many HFCs units, a thermal expansion valve (TXV) or an electronic expansion valve (which serves the same purpose) regulates the refrigerant mass flow rate, and also sets the evaporation pressure. This is accomplished by adjusting the

refrigerant flow area of the orifice through which expansion is accomplished based on the difference between the evaporator refrigerant exit temperature and the refrigerant evaporation temperature. For most HFCs systems, a TXV is the only form of primary control required, since the heat rejection pressure is fixed by the air temperature entering the condenser (for a fixed air flow rate). This is due to the fact that most of the heat rejection process occurs while the refrigerant is condensing at a constant temperature and pressure. However in a CO_2 transcritical system, no such natural heat rejection pressure control exists, since the refrigerant temperature changes throughout the entire heat rejection process.

The concept of an optimal heat rejection pressure for maximum COP was discussed in chapter two. Therefore, if it could be suitably controlled, the heat rejection pressure may be set to provide a maximum COP for the given environmental conditions. On the other hand, it may be desirable to maximize the capacity of the CO_2 cycle at the expense of COP. Such an instance might occur when a dwelling occupant would like to cool a hot dwelling as quickly as possible. To accomplish this, the heat rejection pressure should be raised above the heat rejection pressure which is optimal for maximum COP. Raising the heat rejection pressure will cause the gas cooler exit enthalpy of the CO_2 to decrease and assuming isenthalpic expansion, the evaporator inlet enthalpy will also decrease, allowing for the opportunity of more latent heat transfer of CO_2 and thus more cooling capacity.

In the present work, a control system for the transcritical CO_2 heat pump shown in Figure 5.1 is suggested. A controllable system requires an accumulator to optimize the refrigerant charge. Two back pressure valves connected to the system via two by-pass valves to regulate the heat rejection pressure in cooling or heating mode are also needed. The control unit switches the 4-way valve into the requested position according to the desired mode of operation.

In addition to a traditional back pressure valve control system, other devices can be used. Section 3.5 lists different techniques as reported in the studies by Rieberer et al. (2000) and Casson et al. (2003).

5.3 Past modelling efforts

5.3.1 General

Subcritical vapor compression heat pumps and chillers have been the target of a large number of simulation models. Herbas et al. (1993) presented a classification scheme on simulation models for heat pumps with three categories. At one end of the spectrum are models based simply on empirical curves describing the performance of the components. Simulation, in such cases, consists in finding the balance point between the condensing unit (condenser and compressor) and the evaporator. This can be accomplished graphically or mathematically, with equations representing the performance data of the components. This method lacks, of course, the necessary generality that a proper simulation model should have.

At the other end are detailed models based on applying thermodynamic laws and fundamental heat and mass transfer relations to individual components. Components now are modelled in much a greater detail. Heat transfer zones (superheated vapour, two-phase region, subcooled liquid), each with different heat transfer characteristics and balance equations, are created for the condenser and evaporator. The local analysis approach can also be applied to the expansion device when a capillary tube is used. The compressor simulation can either be derived from a steady-state integral model taking into account all existing energy flows or even consider all processes that take place within the compressor that can be quantified, including valve movement and instantaneous pressure and volume variation.

Complete thermodynamic and transport property data are needed as well as a detailed description of the modelled equipment. These models can provide system performance information very close to that which would be obtained from a system test. Results from these simulations can be used to compare the performance of different refrigerants in identical hardware or to evaluate the impact of hardware modifications on system performance.

In the second category of simulation models, comprising the majority of existing models, equations are established to describe the behaviour of each component and of the system as a whole. The number of equations for each component is generally small and the result is a system of algebraic non-linear equations (dynamic modelling, i.e. the simulation of the transient behaviour, was not considered in this review). The way the system of equations is solved also varies. It can be solved simultaneously, with an appropriate numerical method, such as successive substitutions or the Newton-Raphson method for multiple variables. The model can also be solved in a modular-sequential manner. Estimates are made for a starting point and each component is solved at a time, the output variables of the upstream component becoming the input values for the next one. Complete cycle calculations are carried out until convergence is obtained.

The evaluation methods in the second category model the performance of refrigerants in a specified cycle and require a complete set of refrigerant thermodynamic properties. This level of evaluation ranges from a theoretical cycle composed of idealized thermodynamic processes to a practical cycle that would include effects such as refrigerant subcooling at the condenser, refrigerant superheat at the evaporator, pressure drops in heat exchangers and representation of the temperature difference between fluids exchanging heat.

Transport properties are not involved in the second category of cycle simulations and this is their major shortcoming. This shortcoming affects the performance predictions at different operating conditions of a heat pump.

5.3.2 Transcritical systems

Steady state modelling of transcritical systems has received comparatively little attention. To date, a limited number of simulation models for CO_2 systems have been developed and a few models exist which implement detailed empirical component models into an overall cycle model.

Neksa (1994) developed the CO_2 simulation model "OptiPro" which has a thermodynamic compressor routine based on the given isentropic efficiency and UA heat exchanger routine based on given heat transfer and pressure drop characteristics.

Also, Pettersen and Skaugen (1994) developed a computer simulation program "MACSIM" for the transcritical CO_2 cycle to generate realistic steady state system characteristics. The simulation program consists of a graphical user-interface, a process simulator based on a general equation solver and a library of thermophysical data for CO_2. The simulations are based on component performance characteristics derived from lab prototype tests, including compressor performance curves at varying speeds and pressure ratios and heat transfer and pressure drop correlations for the heat exchangers at varying internal and external conditions.

Rieberer et al. (1997b) developed a model "HPSIM" for the purpose of simulating a CO_2 heat pump designed to heat water with a heating capacity of 20 kW. The model offered an easy change of modules for the calculation of heat transfer, pressure drop and heat exchanger flow type. The compressor was simulated assuming constant volumetric and isentropic efficiencies. Two temperature ranges were investigated. In addition, the use of an internal heat exchanger was also investigated.

In a later paper, Rieberer and Halozan (1998b) developed a steady state CO_2 heat pump model "HPSTAT" to simulate an air heating system for low-heating-energy houses. The heat transfer coefficients and the pressure drops on the refrigerant- and air-side are calculated for cross-counter flow heat exchangers. Regarding the compressor model, the volumetric and isentropic efficiencies are derived from the experimental data of a CO_2 compressor.

Another CO_2 water heater heat pump model "CO2SIM" was developed by Hwang and Radermacher (1997a). The model accounted for heat transfer processes and pressure drops in each heat exchanger. The simulation incorporated heat exchanger models which simulated the performance of shell-and-tube heat exchangers for both heat absorption and heat rejection. For a fixed compressor isentropic efficiency, no

subcooling or superheating and isenthalpic expansion, they concluded that a CO_2 heat pump could produce hot water at a higher temperature and with 15% higher COP than an HCFC-22 heat pump could. Simulation results are verified against their own experimental data.

Hafner et al. (1998) developed a simple simulation program to predict the performance of a mobile HVAC system. The overall heat transfer coefficient and surface area of heat exchangers was determined from prototype measurements for microchannel heat exchangers. The overall heat transfer coefficient of the internal heat exchanger (IHX) was assumed as a function of the CO_2 mass flow rate. Characteristic curves for the volumetric and isentropic efficiencies of the compressor were assumed to vary with the pressure ratio, speed and displacement. Simulation results were compared to the published data for a CO_2 mobile air conditioning system from the European RACE Project. Good agreement of COPs was obtained.

Robinson and Groll (2000) used a detailed simulation model "ACCO2" to predict the performance of a transcritical CO_2 environmental control unit. Regarding the hermetic compressor model, they curve-fitted the isentropic and volumetric efficiencies curves presented by Rieberer and Halozan (1998b) for a CO_2 compressor.

Brown and Domanski (2000) described a semi-theoretical simulation model "CYCLE11_CO2" for a transcritical CO_2 vapor compression refrigeration cycle. The simulation model is based on a subcritical vapor compression simulation model developed by Domanski et al. (1992) and (1994). The model capabilities include different heat exchanger configurations and the implementation of transport properties of CO_2 to predict overall heat transfer coefficients of heat exchangers on relative bases. However, compressor characteristics were presented by empirical equations based on the isentropic and volumetric efficiencies curves presented by Rieberer and Halozan (1998b). In later papers, Brown et al. (2002a) and (2002b) applied "CYCLE11_CO2" for the evaluation of CO_2 as a substitute for HCFC-22

and HFC-134a in residential air conditioning and mobile air conditioning applications, respectively.

A new model for a CO_2 air conditioner has been developed by Ortiz and Groll (2002). The model can simulate the operation of microchannel heat exchangers. The compressor simulation was similar to the compressor model used by Robison and Groll (2000). The model was validated against experimental data. Compressor power, mass flow rate and COP were predicted within 2%, 10% and 5%, respectively.

The aforementioned studies revealed that, recent modelling efforts have generally focused on heat exchanger performance. In contrast, accurate compressor modelling was not included. Most of studies assumed constant values for compressor performance. Only a few models accounted for compression process characteristics. This was accomplished graphically by Pettersen and Skaugen (1994), or mathematically, with equations representing the performance data of a specific compressor by Rieberer and Halozan (1998b). These methods lack, of course, the necessary generality that a proper simulation model should have. For system performance prediction and design, it is valuable to investigate the performance of individual components and the influence they have on the overall system. In addition due to wide variation of heat pump operating conditions, it is of primary importance to consider the compression characteristics.

Ibrahim and Fleming (2003b) presented an initial simulation model to assess the performance of a trans-critical CO_2 heat pump using a reciprocating compressor. The influence of compressor speed and internal leakage on cycle efficiency were examined quantitatively and discussed. The results presented in this study were generated using a detailed simulation model of a reciprocating compressor. Though the CO_2 system normally would include an internal heat exchanger to increase the superheat of the compressor suction gas, this was omitted in this initial model. However, a major shortcoming of this study was that the performance of heat exchangers, i.e. gas cooler and evaporator, was not considered.

The approach in this study has chosen to focus on the influence of the reciprocating compressor performance on the cycle performance at various operating conditions. With this in mind, a detailed compressor simulation is considered in developing the transcritical CO_2 heat pump model. This is a way of investigating the influence of compression characteristics on the overall performance of heat pump. In addition, an approach similar to the semi-theoretical models of Domanski et al. (1994) and Brown and Domanski (2000) was employed to develop the heat exchanger models. The developed semi-detailed heat exchanger models were used to simulate the performance of the gas cooler and evaporator.

5.4 Modelling approach

The individual component processes of the cycle other than the physics-based compressor model have been modelled using correlations and methods available in the literature. The individual component models have been incorporated into a framework determined by the state points around the cycle. The heat exchanger (gas cooler and evaporator) models take into account local heat transfer coefficients inside the tubes as well as the refrigerant pressure drop.

Each of the five components is modelled separately and then combined to form the overall system model. The model provides simulations for user-specified temperature profiles of the heat source and heat sink. The simulated system includes the compressor, evaporator, gas cooler, isenthalpic expansion device and IHX.

The evaporator and gas cooler are represented by their *UA* values, which is product of the overall heat transfer coefficient *U* and heat transfer area *A*. The IHX is represented by its effectiveness. The user must specify either cross-flow, counter flow or parallel flow configuration for the evaporator and gas cooler. For transcritical operation, the input to the model includes the gas cooler pressure. The model employs REFPROP 5.0 to calculate refrigerant thermophysical properties.

Model employs a convergence logic to establish a thermodynamic loop with respect to the heat sink and source temperatures while satisfying constrains imposed by the input data. For the evaporator and gas cooler, the model aims to obtain agreement between the ΔT calculated using refrigerant properties and the ΔT calculated from the basic heat transfer relation given as:

$$Q_{hx} = \dot{m}_r \Delta h_r = UA_{hx} \Delta T_{hx} \qquad \text{Eqn. 5.1}$$

The ΔT_{hx} calculated using refrigerant and heat transfer fluid (HTF) properties is a harmonic mean of the average effective temperature difference (*LMTD*) for the individual sections. Non-linearity in the refrigerant properties and/or temperature profiles is accounted for by dividing individual sections into smaller segments as necessary.

5.4.1 Heat transfer formulation of heat exchangers

The performance of the heat exchanger is specified in terms of *LMTD* and refrigerant pressure drop. In addition, the heat exchanger input data include the inlet and outlet temperature of the heat transfer fluid for the evaporator and gas cooler. The heat exchanger average effective temperature difference, ΔT_{hx}, is defined by the equation

$$\Delta T_{hx} = \frac{Q_{hx}}{UA_{hx}} \qquad \text{Eqn. 5.2}$$

Evaluation of the average effective temperature based on the inlet and outlet temperatures of heat exchangers could be highly inaccurate if the heat exchange process exhibits either a non-linear temperature profile or an abrupt change of thermophysical properties. Thus ΔT_{hx} is calculated by considering individual heat exchanger sections. An effective average temperature difference for each section is calculated as a log mean temperature difference using the fluid temperatures at the ends of each section. For the evaporator, two sections may exist: superheated vapor and two-phase heat exchange. For transcritical heat exchange in the gas cooler, the simulation model splits the gas cooler into a number of equal enthalpy segments and computes the log mean temperature for each of them. This subdividing continues up to a limit of 128 divisions.

5.4.1.1 Log Mean Temperature Difference

Calculation of the log mean temperature difference for an individual section/segment depends on the heat exchanger configuration.

(1) Counter-flow and Parallel-flow:

The log mean temperature difference for the considered section/segment $LMTD_i$ is evaluated by the relation

$$LMTD_i = \frac{(T_{i,out} - t_{i,in}) - (T_{i,in} - t_{i,out})}{\ln\left(\frac{T_{i,out} - t_{i,in}}{T_{i,in} - t_{i,out}}\right)} \qquad \text{Eqn. 5.3}$$

where, T refrigerant temperature (K)

t HTF temperature (K)

This equation was derived for constant specific heat and heat transfer coefficient in the segment as the method requires the temperature of both fluids to be known at the section/segment inlet and outlet.

(2) Cross flow

The above relations for calculating a counter flow $LMTD_i$ are applicable to pure cross-flow heat transfer only if the temperature of one of the fluids stays constant. In other cross-flow cases, the following equation is used (Threlkeld 1970)

$$LMTD_i = \frac{t_{i,out} - t_{i,in}}{\ln\left(\frac{r}{r + \ln(1 - rp)}\right)} \qquad \text{Eqn. 5.4}$$

where, $r = (T_{i,in}\text{-}T_{i,out})/(t_{i,out}\text{-}t_{i,in})$

$p = (t_{i,out}\text{-}t_{i,in})/(T_{i,in}\text{-}t_{i,in})$

5.4.1.2 Implementation Of Transport Properties

The simulation model was developed to include the effects of transport properties. Both viscosity and thermal conductivity influence cycle performance through their impact on the heat transfer coefficient and pressure drop in the heat exchangers. The simulation model does not have provision for detailed heat exchanger data as input, since detailed modelling of different evaporator and gas cooler configurations is not

intended. The simple heat exchanger elements used in the cycle may be regarded as providing a 'mark I' heat pump. Improvements to heat exchanger performance by changing to a more sophisticated geometry for example may be expected to improve cycle efficiency. Hence, mark I has the virtue of not overstating the performance.

(1) Heat transfer coefficient

The total resistance to heat transfer in a heat exchanger can be represented as a summation of the resistance on the refrigerant side and the combined resistance of the heat exchanger material and the resistance on the HTF side:

$$\frac{1}{UA_{hx}} = R_{hx} = R^* + R_r \qquad \text{Eqn. 5.5}$$

where R^* is defined as

$$R^* = R_{tube} + R_{HTF} \qquad \text{Eqn. 5.6}$$

Consequently,

$$R^* = \frac{1}{UA_{hx}}\left(1 - \frac{UA_{hx}}{h_r A_r}\right) \qquad \text{Eqn. 5.7}$$

The resistance R^* is independent of the refrigerant, and is assumed to be independent of the operating conditions. The value of R^* is evaluated by conducting a reference simulation (for the reference, i.e. design, conditions) using values for A_r and UA_{hx} as input data. The inside tube heat transfer coefficient, h_r, is then calculated for the actual refrigerant conditions. The value of R^* is stored and used in subsequent simulations at different operating conditions to calculate the overall conductance by the following equation:

$$UA_{hx} = \frac{1}{R^* + \dfrac{1}{h_r A_r}} \qquad \text{Eqn. 5.8}$$

The refrigerant side heat transfer coefficient for each heat exchanger is calculated using relevant correlations available in the literature.

To account for the sensitivity of the heat transfer coefficient to the refrigerant mass flow rate, the program calculates the refrigerant mass flux for the reference simulation based on a prescribed tube diameter and number of passes in the heat exchanger. This coil circuitry is used during the subsequent calculation runs, which

may have different mass flow rates resulting in different mass fluxes and associated heat transfer rates.

(2) Pressure drop

Since the gravitational and momentum components are small, the model calculates only the frictional pressure drop. Pressure drop in the evaporator and gas cooler is simulated using the correlation available in literature for each flow regime. The value of the equivalent tube length is calculated for the reference simulation with a specified pressure drop and used in subsequent runs. A single mid-enthalpy point is used for each segment for pressure drop calculations. Refrigerant pressure drop, if specified as an input for a heat exchanger, is distributed by the simulation model in proportion to the enthalpy change within each section/segment.

Now, the mathematical description of each of the heat pump component model and the logic make up the model of the complete cycle will be described in sections 5.5 to 5.10 inclusive.

5.5 Gas cooler

During the cooling of supercritical CO_2 there is no phase transition, by definition. The fluid will remain supercritical while being cooled above the critical pressure. However, during the cooling process, when the temperature of CO_2 drops below the 'pseduo-critical' temperature (the temperature at which the fluid experiences maximum specific heat for a given pressure above critical), the CO_2 properties shift suddenly from those of a gas-like substance to those of a liquid-like substance.

A literature review on the nature of in-tube cooling of supercritical CO_2 has been done. Relevant topics include: friction factor of supercritical CO_2 and empirical correlations developed to predict the rate of cooling heat transfer. The efforts of this author will focus on choosing an appropriate correlation to represent the CO_2 cooling process in the gas cooler from among correlations found in the literature.

5.5.1 Pressure drop

The total pressure drop in a section can be calculated by

$$\Delta p = \frac{G^2}{2\rho}(f_h \frac{L}{D} + \xi) \qquad \text{Eqn. 5.9}$$

where the hydraulic drag coefficient f_h is

$$f_h = f + f_i \qquad \text{Eqn. 5.10}$$

where, G the mass flux (kg/m^{2}s)

ξ local pressure drop (-)

f friction factor (-)

f_i inertia factor (-)

f is caused by the shear stress at the inner tube wall, while f_i is caused by the change of flow geometry and direction. For incompressible fluid flow, f_i = 0. Eqn 5.11 is reduced to the commonly used Darcy-Weisbach equation,

$$\Delta p = \frac{G^2}{2\rho}(f \frac{L}{D} + \xi) \qquad \text{Eqn. 5.11}$$

Since the gravitational and momentum components are small, only the frictional pressure drop will be considered. Many equations have been developed for the Darcy-Weisbach friction factor. The Blasius (1913) and Filenenko (1954) equations are widely used for the turbulent flow in smooth tubes (Fang 2001). Smooth here means that the wall roughness elements are so small that their influence does not extend beyond the laminar sublayer.

Moody (1944) introduced Colebrook's (1939) equation. Colebrook, in collaboration with White, developed an equation that agrees with two extremes of roughness in the transition zone: Prandtl's formula for smooth pipes and von Kármán's formula for the fully rough regime (Haaland 1983). Since Colebrook's equation cannot be solved explicitly for f, various approximate explicit formulae were developed as substitutes for Colebrook's equation, e.g. Moody (1947), Swamee and Jain (1976) and Haaland (1983). Churchill (1977) proposed a more complicated equation for all flow regimes and all relative roughness, which agrees with the Moody diagram.

Kuraeva and Protpopov (1974) proposed a new correlation for determining the friction coefficient for supercritical fluids and verified their correlation against their own experimental data. In the absence of free convection effects, they found that for $Re < 10^5$, the friction coefficient, f, agrees with the value given by the Filenenko equation (1954). For $Re > 10^5$, the authors suggest that $f = 0.02$.

Later, Petrov and Popov (1985) calculated the friction factor of CO_2 cooled in supercritical conditions in the range of $Re_{wall} = 1.4\times10^4$-$7.9\times10^5$ and $Re_{bulk} = 3.1\times10^4$-$8\times10^5$. They obtained an interpolation equation of the friction coefficient,

$$f = f_{0,wall}\frac{\rho_{wall}}{\rho_{bulk}}\left(\frac{\mu_{wall}}{\mu_{bulk}}\right)^{s} \qquad \text{Eqn. 5.12}$$

where, $f_{o,wall}$ is the friction coefficient given by either the Blasius (1913) or Filenenko (1954) equations at tube wall temperature and

$$s = 0.023\left(\frac{|q_{wall}|}{G}\right)^{0.42} \qquad \text{Eqn. 5.13}$$

where, q_{wall} is the heat flux density through tube wall to fluid

Pettersen et al. (2000a) recorded the pressure drop along the microchannel tube as a part of their experiments on transcritical cooling of CO_2. The comparison between their experimental data and calculated results according to conventional single-phase correlations for a smooth tube and turbulent flow regime showed a satisfactory agreement. So, it seems reasonable to make use of the single-phase pressure drop correlation.

Hence, the model applies the most widely used correlation for determining the friction coefficient for the internal smooth tube flow of a single-phase Newtonian fluid proposed by Filenenko (1954)

$$f = (0.\ 79\ ln\ (Re)\text{-}1.64)^{-2} \qquad \text{Eqn. 5.14}$$

The simulation model calculates the pressure drop for each of the 128 gas cooler equally spaced segments (on the enthalpy scale). The total pressure drop is then simply the sum of these individual pressure drops.

5.5.2 Correlations for in-tube cooling of supercritical CO_2

Any mode of convective heat transfer is dependent on the properties of the flowing fluid in question. The CO_2 transcritical heat pump cycle presents a unique situation. As mentioned previously, the heat rejection process in the CO_2 cycle (for most applications) occurs entirely above the critical pressure and temperature. This situation introduces effects such as wide property variation as a function of temperature and near critical heat transfer effects which are not normally observed during internal single-phase convective heat transfer.

The open literature on CO_2 heat transfer is limited. Many studies of forced convective heat transfer of constant thermophysical property fluids in the turbulent regime are widely quoted by heat transfer textbooks, e.g. Kakac et al. (1987). However, all of these formulae are direct modifications of either the Dittus-Boelter equation (1930), e.g. Ghajar and Asadi (1986), or Prandtl's equation (1944), e.g. Petukov and Kirilov (1958), Petukhov and Popov (1963), Petukhov et al. (1973) and Gnielinski (1976).

In order to apply the conventional, constant property approach to this problem successfully, attempts have been made to introduce terms in the equation that take into account the property variation of the fluid along the radial co-ordinate, e.g. Krasnoshchekov et al. (1969), Baskov et al. (1977) and Petrov and Popov (1985, 1988). These terms, which are needed to correct the discrepancies, are substantially empirical, and were developed over the years by "trial-and-error", resulting in a long series of successive modifications.

A comprehensive survey of single-phase in-tube heat transfer correlations of CO_2 supercritical heat transfer was presented by Petukhov (1970), Polykaov (1991), Pitla et al. (1998) and Fang et al. (2001). Based on these literature surveys a limited number of experimental and theoretical investigations have been carried out to study the in-tube cooling of supercritical CO_2. Various heat transfer correlations based on the results of each study have been produced. All of these correlations are based on

Petukov and Kirilov (1958) correlation for the circumferentially averaged, local Nusselt number:

$$Nu_{PK} = \frac{(f/8)\,\mathrm{Re}\,\mathrm{Pr}}{1.07 + 12.7(f/8)^{1/2}(\mathrm{Pr}^{2/3} - 1)} \qquad \text{Eqn. 5.15}$$

The above equation is applicable to the flow of a single-phase fluid where the thermophysical properties are either constant or weakly varying.

Krasnoshchekov and Protopopov (1966) carried out an experimental study of the heat transfer characteristics of CO_2 during turbulent flow in a round tube under cooling conditions. Based on their experimental results, Krasnoshchekov et al. (1969) proposed the following correlation:

$$Nu_{wall} = Nu_{PK,wall}\left(\frac{\rho_{wall}}{\rho_{bulk}}\right)^{n}\left(\frac{\bar{c}_p}{c_{p,wall}}\right)^{m} \qquad \text{Eqn. 5.16}$$

where, m and n are empirically determined constants and ρ_{wall}, $c_{p,wall}$ and transport properties to be used with $Nu_{PK,wall}$ are evaluated at the inside tube wall temperature, ρ is evaluated at the fluid bulk temperature and $\bar{c}_p$ is defined as follows:

$$\bar{c}_p = \frac{(h_{bulk} - h_{wall})}{(T_{bulk} - T_{wall})} \qquad \text{Eqn. 5.17}$$

Baskov et al. (1977) investigated the variation of local heat transfer coefficients at high Reynolds numbers in cooling conditions with CO_2 ascending flow cooled in a long vertical tube through the use of experimentation. They concluded that the correlation proposed by Krasnoshchekov et al. (1969) was valid for horizontal tubes. Thus, they proposed the following correlation for vertical tubes:

$$Nu_{wall} = Nu_{PK,wall}\left(\frac{\rho_{bulk}}{\rho_{wall}}\right)^{n}\left(\frac{\bar{c}_p}{c_{p,wall}}\right)^{m} \qquad \text{Eqn. 5.18}$$

where the value of the exponents m and n are determined from the tabular data provided in their paper, $\bar{c}_p$ is defined by Eqn 5.17 and the other variables are defined in the same manner as the variables in Eqn 5.16

Petrov and Popov (1985) performed numerical studies for the cooling of in-tube supercritical CO_2. They solved the governing equations (continuity, energy and momentum) numerically and developed the following formula:

$$Nu_{wall} = Nu_{PK,wall}\left(1 - 0.001\frac{q_{wall}}{G}\right)\left(\frac{\bar{c}_p}{c_{p,wall}}\right)^n \qquad \text{Eqn. 5.19}$$

where, $\bar{c}_p$ is defined by Eqn 5.17

Later, Petrov and Popov (1988) presented a generalized formula to account for heat transfer of supercritical cooling for water, helium and CO_2,

$$Nu = \left(\frac{f}{8}\right)\mathrm{Re}\,\mathrm{Pr}\Bigg/\left(1.07 + 12.7\left(\frac{f}{8}\right)^{1/2}\left\{\mathrm{Pr}^{2/3}\left(\frac{\rho_{wall}}{\rho_{bulk}}\right)^{1/2} \times \left(1 - A_1\sqrt{\frac{|f_i|}{f}}\right) - \left(1 - A_2\sqrt{\frac{|f_i|}{f}}\right)\right\}\right) \qquad \text{Eqn. 5.20}$$

where, $Pr = \dfrac{\bar{c}_p \mu_{bulk}}{k_{bulk}}$

For CO_2, A_1 =0.9 and A_2 =1.0

Zingerli and Groll (2000) discussed the influence of oil on the heat transfer and pressure drop of supercritical CO_2 during in-tube cooling. However, no existing correlations were compared against this data nor were any correlations developed.

Recently, a new correlation was proposed by Pitla et al. (2000). The numerically developed correlation is based on the "mean Nuselt number" defined as:

$$Nu = \left(\frac{Nu_{wall} + Nu_{bulk}}{2}\right)\frac{k_{wall}}{k_{bulk}} \qquad \text{Eqn. 5.21}$$

where Nu_w and Nu_b are the Nusselt numbers relative to wall and bulk conditions, respectively, which are both evaluated through the Gnielinski (1976) correlation. They claimed that the new correlation is the most accurate available for predicting the heat transfer coefficient. However, a recent work of Yoon et al (2003) conducted experiments on the heat transfer and pressure drop characteristics for supercritical CO_2 under cooling conditions. They compared their experimental results with four

existing correlations including Pitla et al. (2000). Krasnoshchekov et al. (1969) showed a good agreement with experimental data while the Pitla et al. (2000) correlation predicted a different peak location and moreover showed rather poor prediction. They explain this by saying that the bulk and wall conditions do not equally influence the heat transfer coefficient.

Pettersen et al. (2000a) measured the heat transfer coefficient in a flat microchannel aluminium tube under cooling conditions. They compared the measured heat transfer coefficients with those predicted by different calculations models, e.g. Dittus-Boelter (1930), Ghajar and Asadi (1986), Gnielinski (1976) and Petrov and Popov (1988). They asserted that the Gnielinski (1976) correlation showed a satisfactory correspondence. Also, Rieberer (1999) found the Gnielinski (1976) correlation to be the best for single phase CO_2 at supercritical and subcritical conditions after comparing six correlations for smooth tubes with inner diameters of 7.8 mm. Moreover, the experimental results of Olson (2000) confirm that the Gnielinski model (1976) calculated at bulk fluid temperature outperforms the older one by Krasnoshchekov et al. (1969).

Based on the above discussion, the heat transfer coefficient for the gas cooler is evaluated through the Gnielinski (1976) correlation,

$$Nu = \frac{(f/8)(\mathrm{Re}-1000)\,\mathrm{Pr}}{1.0+12.7(f/8)^{1/2}(\mathrm{Pr}^{2/3}-1)} \qquad \text{Eqn. 5.22}$$

The friction coefficient is determined by the formula proposed by Filenenko (1954) for isothermal flows in smooth tubes.

Once the Nusselt number has been obtained, the heat transfer coefficient can be computed. The gas cooler is divided into 128 equal-enthalpy interval segments for which the local CO_2 heat transfer coefficient is calculated. The mean of these values is used as an average CO_2 heat transfer coefficient in the gas cooler.

5.6 Evaporator model

The nature of the two-phase heat absorption process of CO_2 is fundamentally similar to that of any other single fluid refrigerant. However, the literature review has revealed that few experiments have been performed to evaluate the two-phase heat transfer coefficient for a circular tube inside which CO_2 is boiling. Moreover, the experiments have indicated that the two-phase heat transfer coefficient's correlations commonly used for HFCs under-predict heat transfer by 50% or more (Pettersen et al. 1998). Similarly to gas cooler modelling, the approach used here in the construction of a simulation model has been to choose among established correlations found in the literature, selecting those based on large experimental data.

5.6.1 Pressure drop

So far the pressure drop in two-phase flow in pipes has often been predicted by empirical correlations. Tong and Tang (1997) reported that Lockhart and Martinelli (1949) and Martinelli and Nelson (1948) were the first to define the pressure drop of two-phase flows in terms of a single-phase pressure drop,

$$\Phi^2_{LO} = \frac{(\Delta P / \Lambda L)_{TP}}{(\Delta P / \Lambda L)_{LO}} \qquad \text{Eqn. 5.23}$$

where, the two-phase pressure drop $(\Delta P/\Delta L)_{TP}$ is related to the "liquid only" pressure drop $(\Delta P/\Delta L)_{LO}$ by a two phase multiplier Φ_{LO}. Most correlations relate Φ_{LO} to properties such as quality, liquid and vapor density and viscosities.

Bredesen et al. (1997) measured pressure drop which occurred during the in-tube evaporation of carbon dioxide. They found that the correlation developed by Fuchs (1975) rendered satisfactory results. Rieberer and Halozan (1997a) used pressure drop data generated by Bredesen et al. (1997) to compare with three other correlations. The correlation given by Friedel (1979) and recommended by Collier and Thome (1994) proved to fit the experimental results rather well.

Pettersen et al. (2000b) presented experimental data for evaporation heat transfer and pressure drop of CO_2 in microchannel tubes. The measured pressure drops were

compared with values calculated using four different correlations including: Fuchs (1975), Friedel (1979) and a single-phase model from Colebrook equation. The Friedel (1979) correlation gave the best results. The mean deviation was nevertheless 22%.

Later, Kim and Bullard (2001) compared four different pressure drop correlations with the experimental data for a CO_2 microchannel evaporator. They reported that due to the uncertainty of the experimental data as a result of the port blockage and diameter reduction of the heat exchanger used, The Friedel (1979) correlation would provide a better prediction of the pressure drops than others.

The Friedel (1979) correlation is considered to be one of the most accurate two phase pressure drop correlations when the viscosity ratios between liquid and gas is less than 1000 (Collier and Thome 1994). Since, the viscosity ratio of CO_2 is approximately 10 the Friedel (1979) correlation was chosen for the pressure drop calculation.

$$\Phi_{LO}{}^2 = A_1 + \frac{3.24 A_2}{Fr^{0.045} We^{0.035}} \qquad \text{Eqn. 5.24}$$

where, $A_1 = (1-x)^2 + x^2 \left(\frac{\rho_L}{\rho_V}\right)\left(\frac{f_V}{f_L}\right)$

$$A_2 = x^{0.78}(1-x)^{0.24}\left(\frac{\rho_L}{\rho_V}\right)^{0.91}\left(\frac{\mu_V}{\mu_L}\right)^{0.19}\left(1-\frac{\mu_V}{\mu_L}\right)^{0.7}$$

and Fr is the Froude Number, $\frac{G^2}{gD\rho_{TP}}$, and We is the Weber Number, $\frac{G^2 D}{\rho_{TP}\sigma}$

where, $\rho_{TP} = \left(\frac{x}{\rho_V} + \frac{1-x}{\rho_L}\right)^{-1}$

For a semi-detailed model of the evaporator, both gravitational pressure drop and momentum (or local) pressure drop are neglected as was the case in the gas cooler model; i.e. only friction pressure drop was calculated.

5.6.2 Correlations for in-tube evaporative heat transfer of CO_2

Several correlations are available for two-phase evaporative heat transfer but none specially developed for use with CO_2. Review of the existing literature indicates that previous work on experimental investigation of CO_2 evaporative heat transfer and its modeling is limited. Kundsen and Jensen (1997) conducted internal heat transfer measurements of in-tube evaporation using CO_2 as a refrigerant. The results indicated that the measured heat transfer coefficients correlated to within 14% of 1.9 times the value given by the Shah (1982) correlation for in-tube evaporation over the range of test matrix values. A similar result was found in a different experimental study on 7.0 mm round tube by Bredesen et al. (1997). Rieberer and Halozan (1997a) also evaluated the experimental in-tube CO_2 evaporative heat transfer coefficients of Bredesen et al. (1997) and compared the data set to heat transfer coefficients generated by two other boiling correlations. As with the other correlations, the calculated values under-predict the measured evaporative heat transfer. Zhao et al. (1997) conducted experiments of CO_2 in-tube evaporation. However, no existing correlations were compared against the experimental data nor were any correlations developed.

Based on the experimental results of Bredesen et al. (1997), Hwang et al. (1997b) investigated the applicability of six commonly used empirical correlations reported by Chen (1966), Bennett-Chen (1980), Gungor-Winston (1987), Shah (1976), Schrock-Grossman (1959), and Liu-Winteron (1991). It was found that the correlations had a large deviation (from 20% to 80%) when predicting the boiling heat transfer coefficient of CO_2. Hwang et al. proposed a new empirical model, the Modified Bennett-Chen correlation, for CO_2 flow boiling in horizontal smooth tubes. They claimed that the new correlation could predict the heat transfer coefficients, consistent with Bredesen's results, to within a mean deviation of 14%. The new correlation is given by

$$h_E = h_{nb} + h_{cv} \qquad \text{Eqn. 5.25}$$

where $h_{cv} = h_l F Pr_l^{0.6}$

$F = 1.0$ for $X_{tt} \geq 10$

$F = 2.0\,(0.2113 + 1/X_{tt})^{0.736}$ for $X_{tt} < 10$

$$X_{tt} = \left(\frac{1-x}{x}\right)^{0.9}\left(\frac{\rho_v}{\rho_l}\right)^{0.5}\left(\frac{\mu_v}{\mu_l}\right)^{0.1}$$

$$h_{nb} = 0.0012S\left(\frac{{k_l}^{0.79}{c_{pl}}^{0.5}{\rho_l}^{0.49}}{\sigma^{0.6}{\mu_l}^{0.29}{h_{lv}}^{0.24}{\rho_v}^{0.24}}\right)\left[T_w - T_{sat}(P_l)\right]^{0.4}\left[P_{sat}(T_w) - P_l\right]^{0.75}$$

$$S = \frac{1-\exp(-Fh_l X_0 / k_l)}{Fh_l X_0 / k_l}$$

$$X_0 = 0.05\left(\frac{\sigma}{g(\rho_l - \rho_v)}\right)^{0.5}$$

Evaporation tests by Pettersen et al. (2000b) for smaller diameter round tubes proved that the conventional correlations severely over-predict the evaporation heat transfer coefficient.

Recent microchannel heat transfer studies of CO_2 were reported by Zhao et al (2000) and Hihara and Tanaka (2000). They reported experimental results of heat transfer and pressure drop for the flow boiling of CO_2 in microchannel heat exchangers and characterized the effects of heat flux, mass flux and vapor quality on the heat transfer coefficients. Later, Zhao (2002) presented a study focus on measuring the flow boiling heat transfer coefficients of CO_2 in microchannels in the presence of a miscible oil at various oil concentrations and as a function of such operational conditions as mass flux, saturation temperature and vapor density. Unfortunately, no existing correlations were compared against the experimental data nor were any correlations developed.

Since the modified Bennet-Chen correlation proposed by Hwang et al. (1997b) is the only available correlation so far verified against experimental data for CO_2 evaporation, it has been applied to simulate the two-phase heat transfer process in the CO_2 heat pump evaporator. The Gnielinski (1976) correlation has been used to predict the single-phase heat transfer coefficient in the superheat section of the evaporator when this is needed.

5.7 Compressor model

The compressor model developed in chapter four is applied. The compressor model is used to generate the mass flow rate through the system. A user-specified mechanical efficiency and electric motor efficiency could be used in conjunction with the indicated power generated by compressor model to predict the total electrical power consumption needed for the compression process.

5.8 Internal heat exchanger

The IHX is of a counter-flow configuration and employs a user-specified effectiveness to model its thermal performance. Hence, no heat transfer correlation is needed. The IHX effectiveness is defined as,

$$\varepsilon_{IHX} = \frac{h_{L,e} - h_{L,i}}{h_L(P_{L,e}, T_{H,i}) - h_{L,i}} \qquad \text{Eqn 5.26}$$

where, h is the refrigerant specific enthalpy

L refers to the low pressure and H to the high pressure side.

The IHX is assumed to be externally adiabatic, i.e. no heat loss to the ambient. The pressure drops on both the high- pressure and low-pressure sides of the IHX are simulated in the same manner as for the gas cooler.

5.9 Expansion device

The model treats the expansion process as isenthalpic. Changes in kinetic and potential energies are neglected. The refrigerant state at the exit of the high pressure side of the IHX is considered to be the inlet to the expansion device. The exit state of the expansion valve is the refrigerant state at the evaporator inlet.

5.10 Overall cycle simulation

The individual components models are incorporated in an overall cycle model framework that identifies state points throughout the cycle. The simulation model is written in Visual C++®. The heat exchanger models take the local heat transfer coefficients into account as described earlier. Each heat exchanger model also accounts for the refrigerant side pressure drop. The cycle model may or may not include the IHX, depending on the choice of the user. The user may simply input the effectiveness of the internal heat exchanger equals zero to exclude the IHX from the cycle/system. The pressure drop and heat transfer in the connecting lines are not considered; therefore, the outlet state of one component becomes the inlet state of the next component.

Similarly to the approach developed by Domanski et al. (1994) and Brown and Domanski (2000), the simulation model can account for transport properties in representing performance of the heat exchangers on relative bases. To use this option, the user first has to execute a simulation run with imposed pressure drops and *UA* values to allow the program to calculate pressure drop and heat transfer parameters for use in subsequent simulation runs. The program comprises three main segments: (a) Input, (b) Simulation algorithm and (c) Output. The following discussion presents details of each of the simulation segments.

5.10.1 Inputs

The input data file includes the same compressor data prescribed in the last chapter and similar to that given in Appendix A. In addition, values for mechanical efficiency and electric motor efficiency are required. However, the user can neglect the effect of friction and electric power loss by assuming those values equal unity. The evaporator and gas cooler can be either of the counter-flow, parallel-flow or cross-flow type. Both are described by their *UA* values and by the refrigerant pressure drops through the respective heat exchangers. The input data include the inlet and outlet temperatures of the HTF for each heat exchanger, the temperature rise in evaporator and the high side (i.e. outlet of the gas cooler) pressure. The

internal heat exchanger is of the counter-flow type and is described by the pressure drop in each side of the heat exchanger and by its effectiveness.

The user has the option of involving transport properties. The transport properties are used to calculate results at a reference condition. That is, the reference results, along with transport properties, are used to simulate other operating conditions, e.g. different HTF temperatures or different compressor speeds. The user input should include the number of the refrigerant circuits and the tube inner diameter for each heat exchanger. A sample of model inputs is given in Appendix B.

5.10.2 Simulation algorithm

The purpose of the simulation algorithm is to determine the operating point, i.e. the thermodynamic states of the CO_2 at circuit key locations, corresponding to pre-specified operating conditions for a transcritical CO_2 heat pump. In general, both successive substitution and simultaneous solution techniques are used to solve the unknown variables resulting from the simulation of steady-state models of thermal systems. Whereas successive substitution involves a number of iterations within many internal loops to satisfy specified conditions to reach convergence, the simultaneous solution method solves a set of non-linear equations in a global manner. Although there are several algorithms available, the Newton-Raphson method is the most popular. General information about the successive substitution and Newton-Raphson methods is given in Stoecker (1989) and Jung and Radermacher (1991). Successive substitution is adopted in this study to simulate the transcritical CO_2 heat pump.

The successive substitution method involves a number of loops in which certain specified conditions such as energy balance are to be satisfied to reach a converged solution. It starts with an innermost loop with an assumed value. Unless this set of solutions satisfies a specified condition within the loop, the old guess is modified and substituted until convergence is achieved at the outermost loop.

Here, the simulation of the steady state model applied an iterative convergence algorithm. However, the algorithm is not guaranteed to converge for all sets of input data. For example, convergence cannot be achieved if unrealistically small *UA* values are specified in relation to the compressor swept volume. Also, unrealistic inlet and outlet temperatures of HTF may result in a simulation crash. A flow chart giving the sequence of operations in the transcritical CO_2 heat pump simulation program is shown in Figure 5.4. The convergence is established when calculations agree within 0.1 kW, hence the iteration is terminated. The Iterative convergence algorithm is presented below.

The algorithm consists of three main convergence loops as summarized below:

1. Specify the initial guess of the gas cooler temperature approach (CTA).
2. Specify the refrigerant exit state of gas cooler.
3. Specify the initial guess of temperature drop ($\Delta T_{IHX,H}$) inside the high-pressure side of the IHX.
4. Specify the refrigerant state at the inlet of the expansion device.
5. Specify the initial guess of the evaporation pressure.
6. Specify the refrigerant inlet state of the evaporator.
7. Specify the refrigerant state at the exit of the two-phase and superheat vapor sections of evaporator.
8. Specify the initial guess of the compressor volumetric efficiency.
9. Simulate the evaporator. Updates guess the evaporation pressure and repeat steps 6 to 9 until the calculated evaporator capacity based on refrigerant properties converges to the actual capacity based on the known UA_E within a pre-specified error tolerance. This is the innermost convergence loop of the simulation algorithm.
10. Specify the superheat of the refrigerant leaving the IHX.
11. Simulate the compressor and update the compressor volumetric efficiency.
12. Specify the compression power and the gas cooler capacity.
13. At this point, all of the states in the heat pump cycle are known and the thermodynamic energy balance could be satisfied. Otherwise, update $\Delta T_{IHX,H}$ and repeat steps 4 to 13 until the thermodynamic energy balance are satisfied

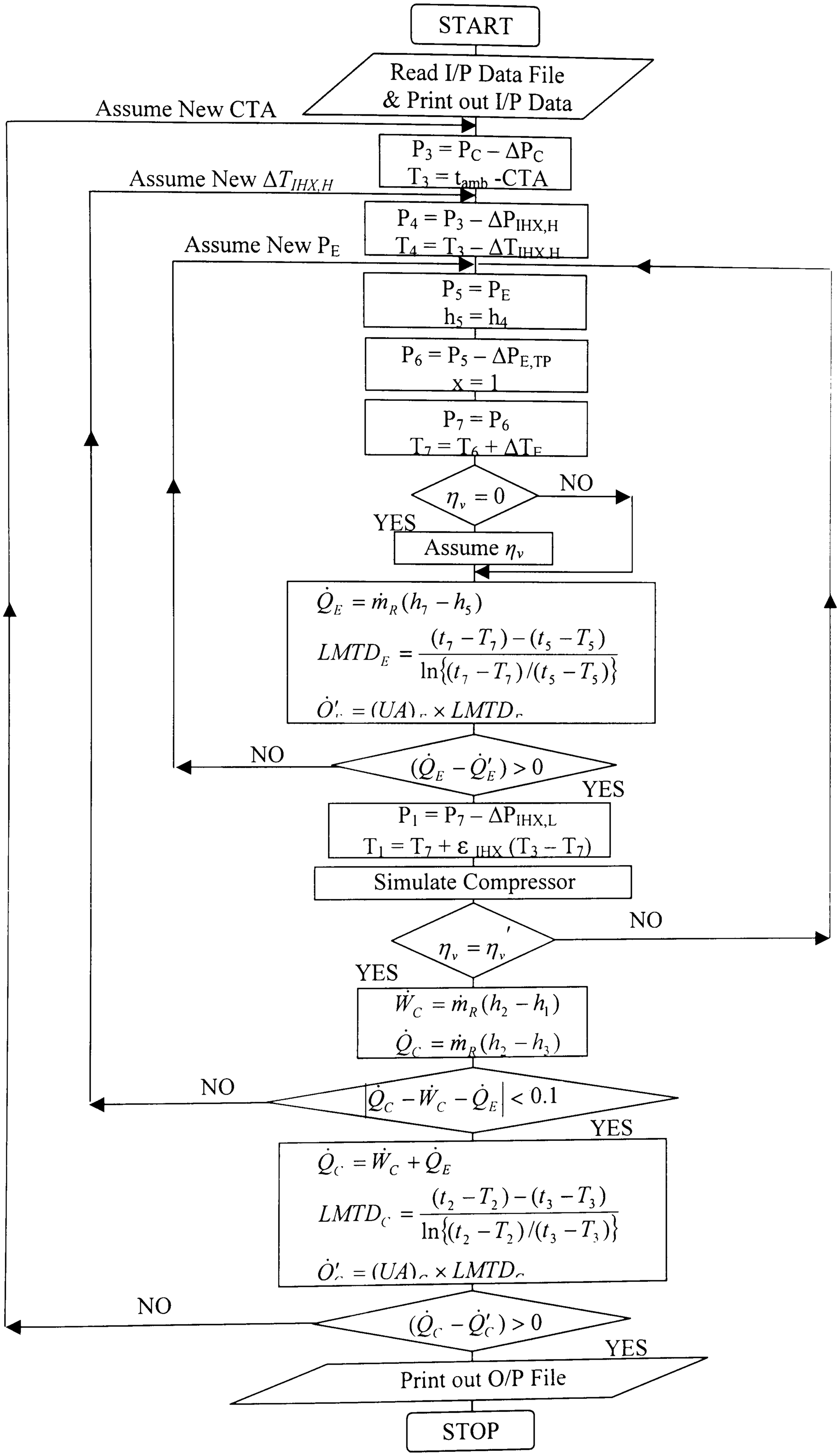

Figure 5.4 Flow chart of transcritical CO_2 heat pump simulation program

within a pre-specified error tolerance. This is the middle convergence loop of the simulation algorithm.

14. Simulate the gas cooler. If the calculated gas cooler capacity using refrigerant properties is within a pre-specified error tolerance of the actual capacity based on a known UA_C then the operating point of the heat pump has been found, so go to step 15. Otherwise Updates guess CTA and repeat steps 2 to 14 until the convergences is obtained. This is the outermost convergence loop of the simulation algorithm.
15. Calculate the output results

5.10.3 Outputs

The simulation output includes calculations for the heat exchangers, the compressor, key refrigerant state points and the overall system performance. A sample of model outputs is given in Appendix C. The refrigerant pressure, temperature, specific volume, enthalpy and entropy are given at each key location.

For the gas cooler and evaporator the outputs include: the average effective temperature difference, the UA, ΔP and the average heat transfer coefficient. For the compressor the outputs are similar to that generated by the compressor simulation model developed in chapter 4.

The system performance parameters calculated are: the compression power, capacity of each heat exchanger, refrigerant mass flow rate and COP.

5.11 Heat Pump model validation

The validation of the simulation model for the transcritical CO_2 heat pump is achieved by comparing experimental records with those predicted by the simulation program. This assessment was made to judge the correctness of the theoretical computation. In the following, the experimental results published in open literature for CO_2 heat pumps working either in cooling or heating modes under steady state conditions are presented.

5.11.1 Experimental studies

5.11.1.1 CO_2 Mobile Heat Pumps

The experimental studies found in the literature for CO_2 mobile heat pumps compared the performance of a prototype CO_2 system with conventional CFC-12 and HCFC-134a systems.

In successive studies, Lorentzen and Pettersen (1993) and Pettersen (1994) developed and tested a prototype CO_2 automotive air conditioning system. They used, as a reference, a commercially available CFC-12 automotive air-conditioning system and built a prototype CO_2 system of comparable cooling capacity. The CO_2 system had an IHX to transfer heat between the high-pressure CO_2 leaving the gas cooler and the low-pressure CO_2 leaving the evaporator. The expansion valve was controlled manually.

From 1994 to 1997, five European automotive manufacturers and four European automotive suppliers participated in the RACE (refrigeration and automotive climate systems under environmental aspects) project to investigate the feasibility of CO_2 as a refrigerant in automotive air conditioning systems. Gentner (1997) presented some results of this experimentally based project showing that CO_2 systems give acceptable cooling capacity, fuel consumption, and lower TEWI, when compared to an HCFC-134a system.

McEnaney et al. (1998) and (1999) presented experimental results for a prototype CO_2 system and a commercially available HCFC-134a automotive air conditioner. The CO_2 system employed an IHX and a manual metering valve. The CO_2 evaporator and gas cooler were new generation microchannel heat exchangers developed by Pettersen et al. (1998) while the HCFC-134a heat exchangers were of conventional technology. The external volumes of the evaporators were identical for both systems with the CO_2 evaporator having 20% larger air-side surface area. The CO_2 gas cooler had 23% lower external volume and 28% lower air-side surface than the HCFC-134a condenser.

Preissner et al. (2000) presented experimental results for prototype CO_2 and HCFC-134a automotive air conditioners. The major difference between this study and previous ones is that the HCFC-134a evaporator and condenser were prototype heat exchangers based on the latest technology (similar technology to the CO_2 heat exchangers), and an IHX was employed in the HCFC-134a system (not just in the CO_2 system as in previous studies).

Experimental studies on heating mode operation of prototype CO_2 automobile air conditioning system were reported. The first results of the experimental runs of a prototype CO_2 automobile air conditioning system operating in heating mode were presented by Bullard and Hrnjak (2000) and Giannavola et al. (2000). Data were presented for a moderately cold ambient weather. Ambient temperatures were varied in the range –10 ^{0}C to 20 ^{0}C with a compressor speed of 950 rpm representing idling condition. Heat rejection was in the supercritical region and the ambient air was dehumidified using glycol coil to minimize risk of frost formation on the evaporator.

Hafner (2000) tested a prototype CO_2 air conditioning system in heating mode. The heating capacity was between 2 and 6 kW at ambient temperatures of 5 ^{0}C and –5 ^{0}C and the relative humidity was 80%. Frost formation on the exterior heat exchanger surface was the limiting factor of the system.

5.11.1.2 CO_2 Residential Heat Pumps

There are a very few studies in the open literature on the use of CO_2 in residential heat pump applications as compared to the number of studies on the use of CO_2 in other applications. The experimental studies found in the literature for CO_2 residential heat pumps compared the performance of a prototype CO_2 system with conventional HCFC-22 and HFC-410A systems.

Aarlien and Frivik (1998) compared the performance of a prototype CO_2 system with a baseline HCFC-22 system in the cooling and heating modes. The CO_2 system consisted of microchannel heat exchangers with the same core volumes as the finned-tube heat exchangers used in the baseline system.

Beaver et al. (1999) presented experimental results for a prototype CO_2 system and a commercially available HFC-410A heat pump in the cooling mode. The CO_2 system utilized microchannel heat exchangers, while the HFC-410A system used fin-tube heat exchangers having the same core volume as the CO_2 heat exchangers. As a follow-up to this study, Richter at al. (2000) measured the performance of the CO_2 and HFC-410A systems in heating mode.

Culter et al. (2000) designed and built a prototype transcritical CO_2 ECU for the U.S. Army. Details of system design were presented but test results were not available. Later, Connaghan (2002) investigated experimentally a breadboard model of a CO_2 U.S. Army ECU. The unit was tested under high outdoor ambient temperature range from 32.2 ^{0}C up to 51.7 ^{0}C, while indoor conditions were 32.2 ^{0}C and 50% relative humidity. Discharge pressures ranged from 10 to 13 MPa when stable conditions were maintained. Also, Manzione et al. (2002) evaluated experimentally a transcritical CO_2 using an open compressor in a packaged unitary military ECU.

5.11.2 Validation

While many prototypes of CO_2 systems were developed, except for McEnaney et al. (1998) and (1999), Beaver et al. (1999) and Richter at al. (2000), few details of the thermodynamic states of the CO_2 in key locations are presented. On the other hand more details were available for hardware construction, especially heat exchangers' physical characteristics, and the testing conditions of each system. Most of the experimental studies were mainly concerned with the overall performance parameters of the system, e.g. COP and capacity.

The simulation model was verified by comparing its predictions to laboratory measurements for CO_2 systems. The model components and systems were selected to match the systems studied experimentally by McEnaney et al. (1998) and (1999) for a mobile air conditioner and by Richter et al. (2000) for a residential heat pump in heating mode operation. These experimental studies were selected to fulfil the following objectives:

(1) Validation of the predictions of the simulation model at different operation modes of the heat pump; cooling and heating, and different applications; mobile and residential systems.

(2) Availability of data needed for input data file, e.g. HTF temperatures, gas cooler pressure, etc.

(3) The thermodynamic states of CO_2 in key locations throughout the system are known at a given testing condition.

The third objective is to generate an accurate value for *UA* of each heat exchanger. The selection of *UA* is based on trial-and error technique. The *UA* values that best fit the thermodynamic states of CO_2 in key locations throughout the system at a given, i.e. reference, testing condition are used to predict the system performance at different operating conditions.

Since the detailed data of compressors used was not available, for simulation purposes the CO_2 hermetic compressor developed by Fagerli (1997) was adopted to have the same displacement volume. The gas cooler and evaporator had the same physical characteristics, e.g. refrigerant passage diameter and number of circuits of original hardware units. In general, good agreement was obtained based on the assumptions made. The model predictions for each system are given below.

Figures 5.5a, 5.5b and 5.5c show the comparison of simulation model predictions and experimental measurements at different operating conditions for a mobile air conditioning system studied experimentally by McEnaney et al. (1998) and (1999). Here, M3 testing condition was selected as a reference state. Figures 5.5b and 5.5c show the comparison of measured and simulated results of the COP and cooling capacity, respectively. The agreement is consistently better than ±12% for COP and ±7% for capacity, which is satisfactory for an exercise of this kind.

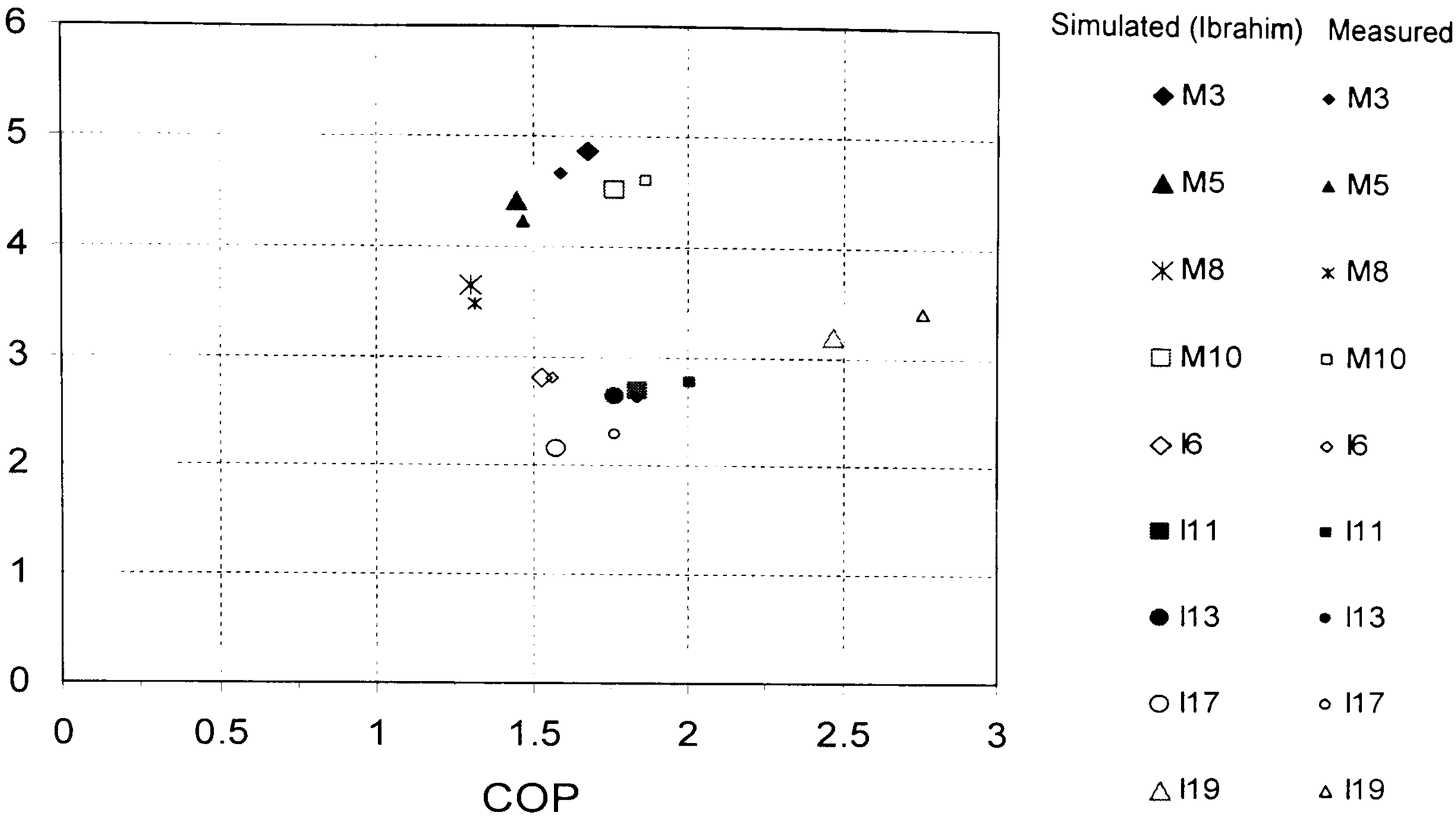

Figure 5.5a Comparison of simulation results and measurements for CO_2 mobile a/c system at different testing conditions (McEnaney et al. 1998)

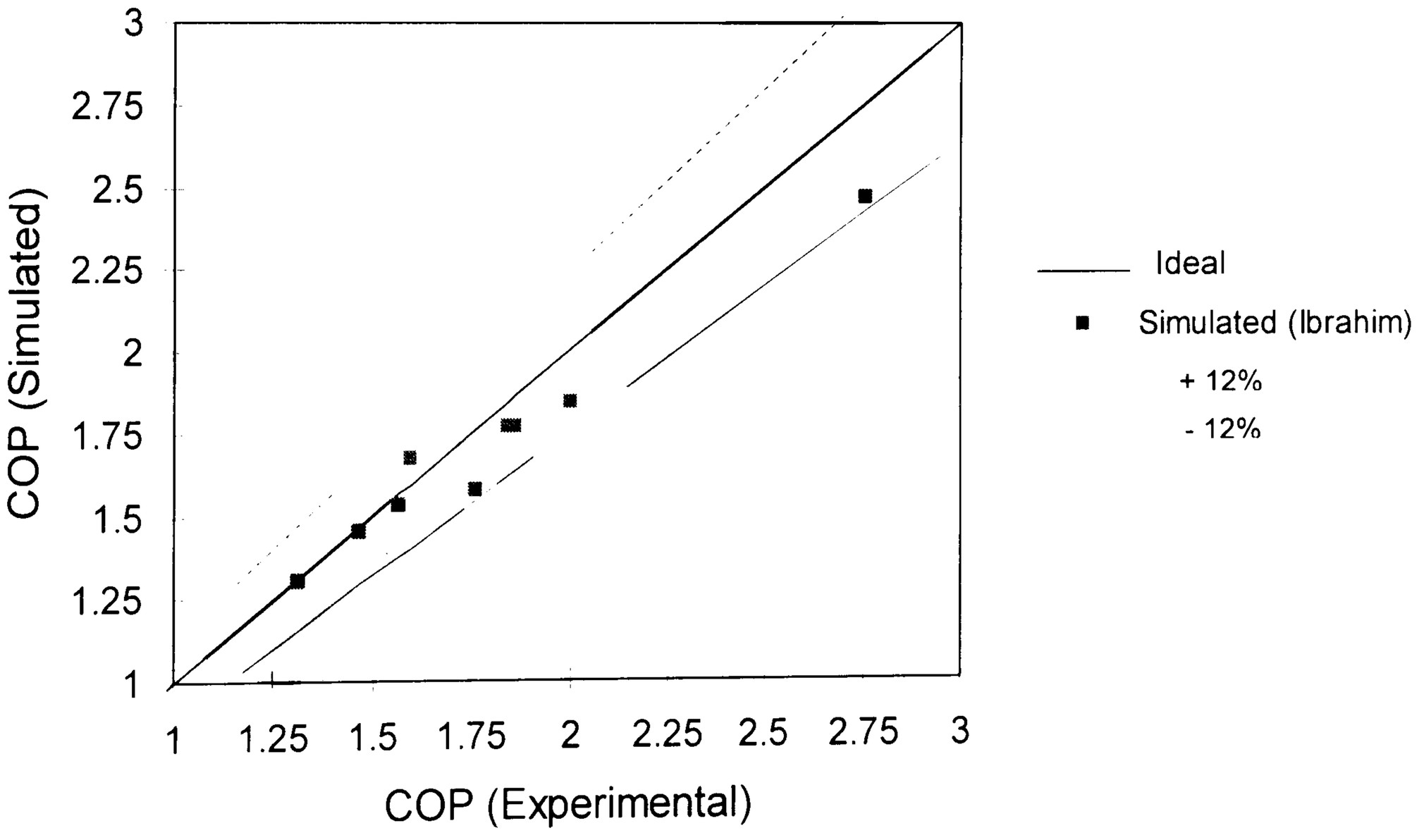

Figure 5.5b Comparison of simulated Vs measured COP for CO_2 mobile a/c (McEnaney et al. 1998)

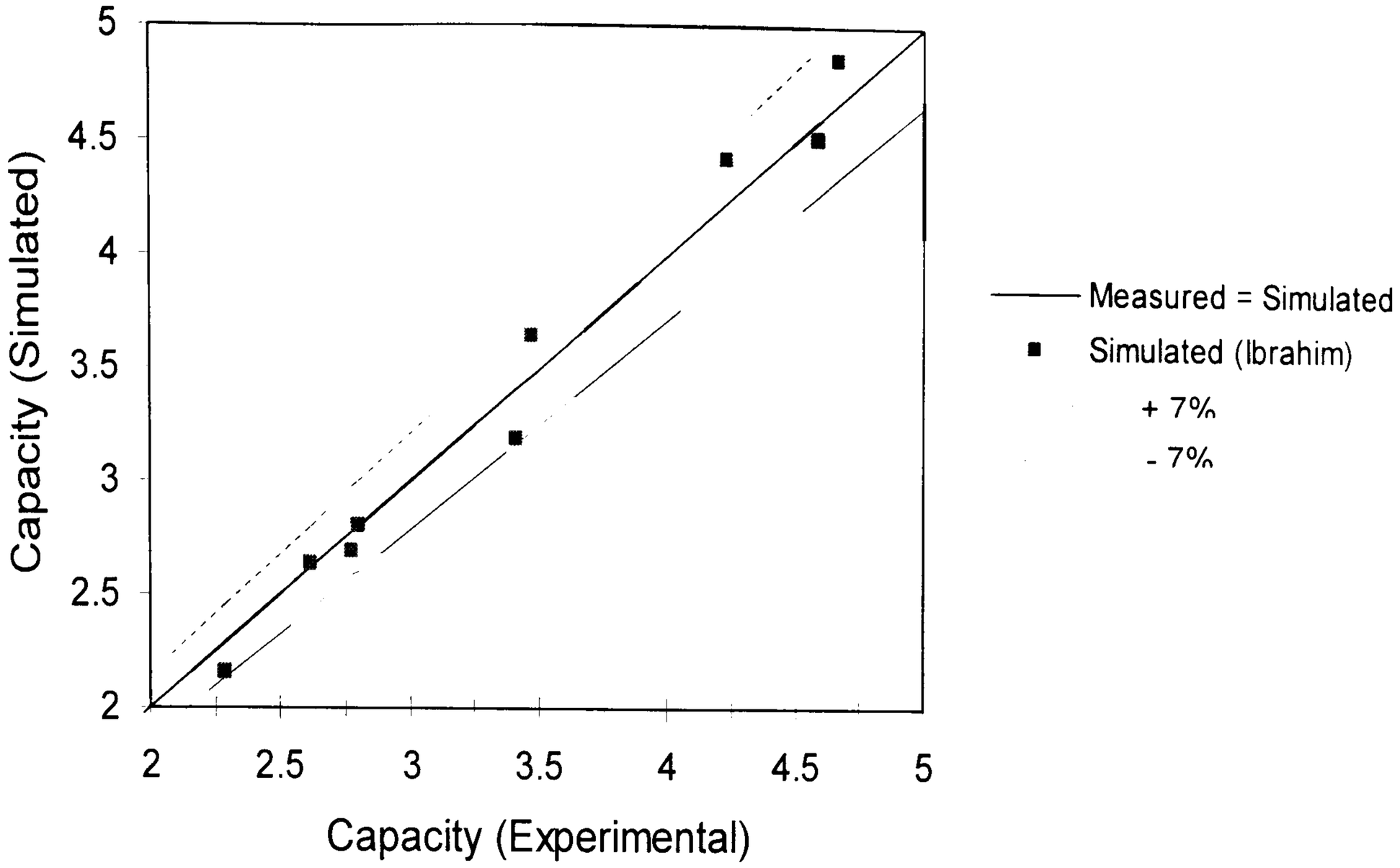

Figure 5.5c Comparison of simulated Vs measured capacity for CO_2 mobile a/c (McEnaney et al. 1998)

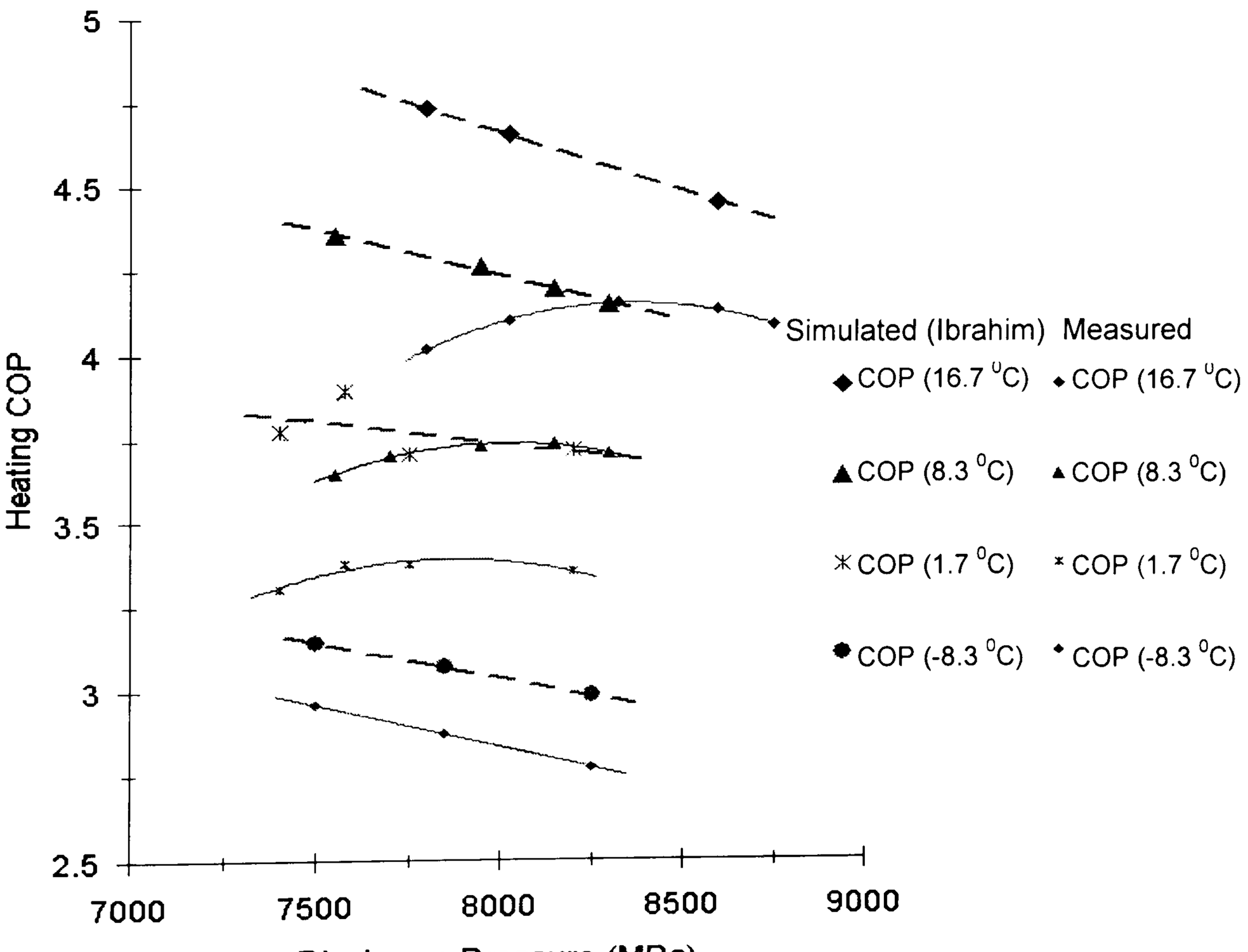

Figure 5.6a Comparison of simulation results and measurements for CO_2 residential heat pump in heating mode at different outdoor temperatures (Richter et al. 2000)

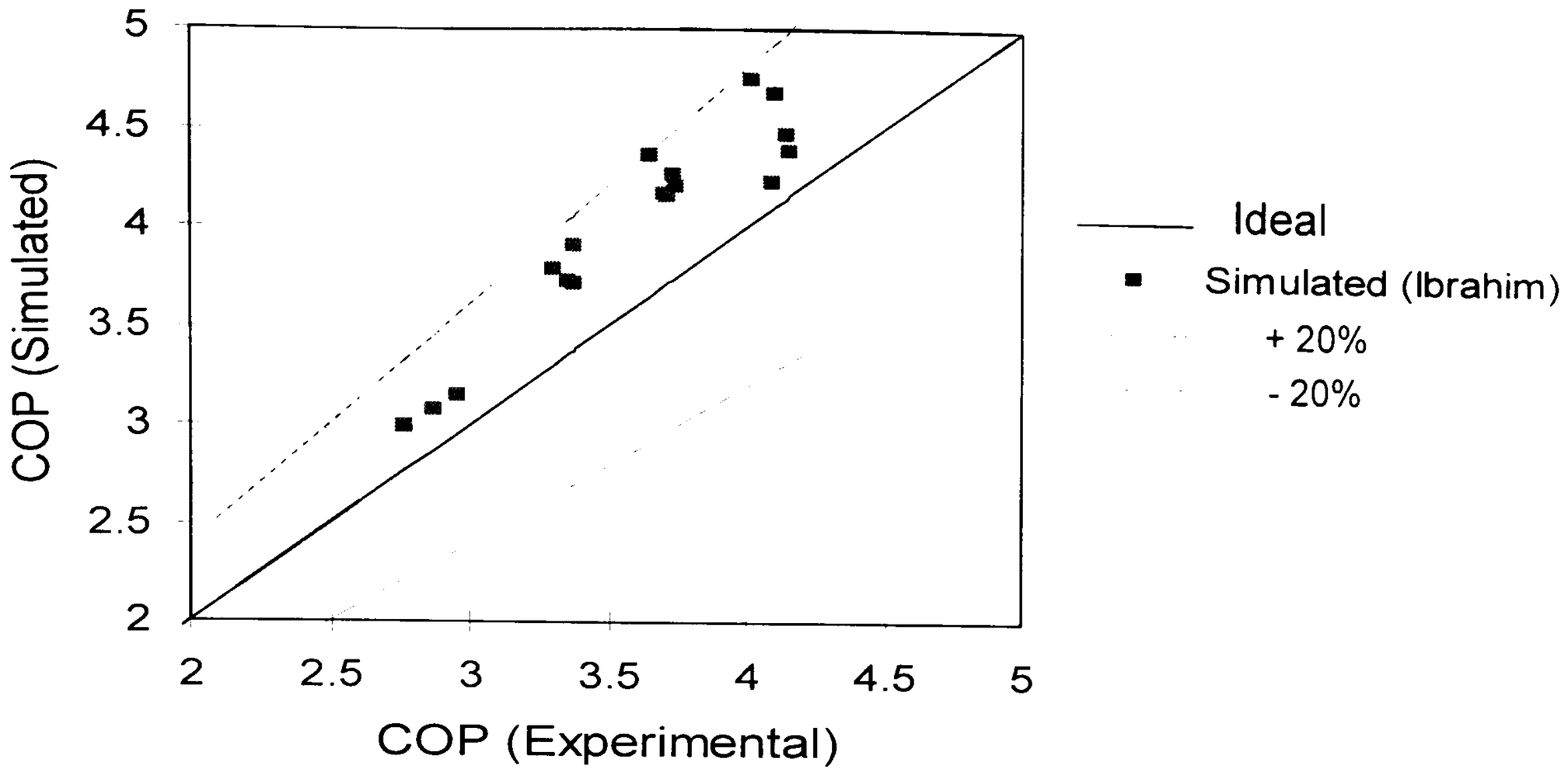

Figure 5.6b Comparison of simulated Vs measured COP for CO_2 residential ECU (Richter et al. 2000)

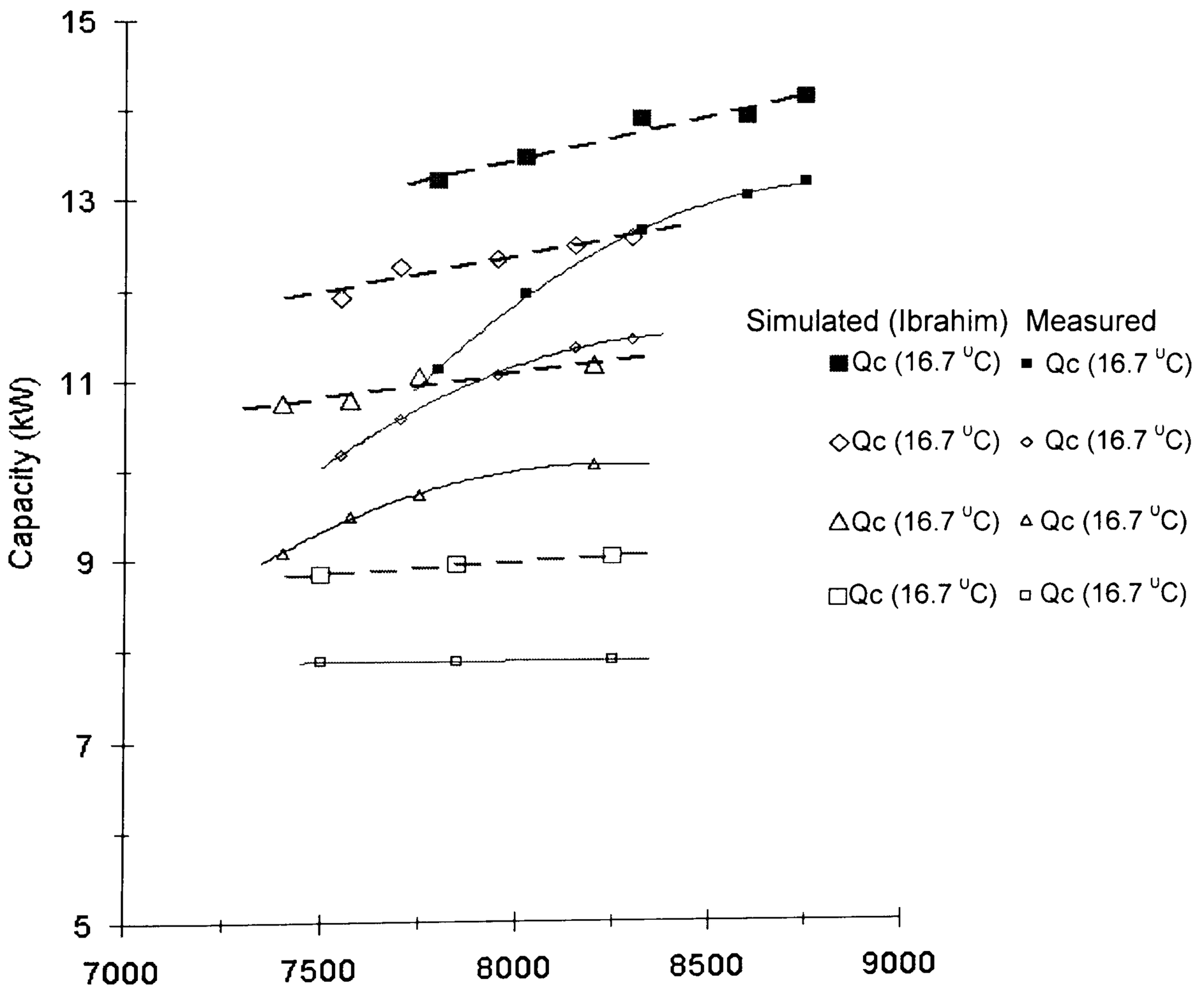

Figure 5.6c Comparison of simulation results and measurements for CO_2 residential heat pump in heating mode at different outdoor temperatures (Richter et al. 2000)

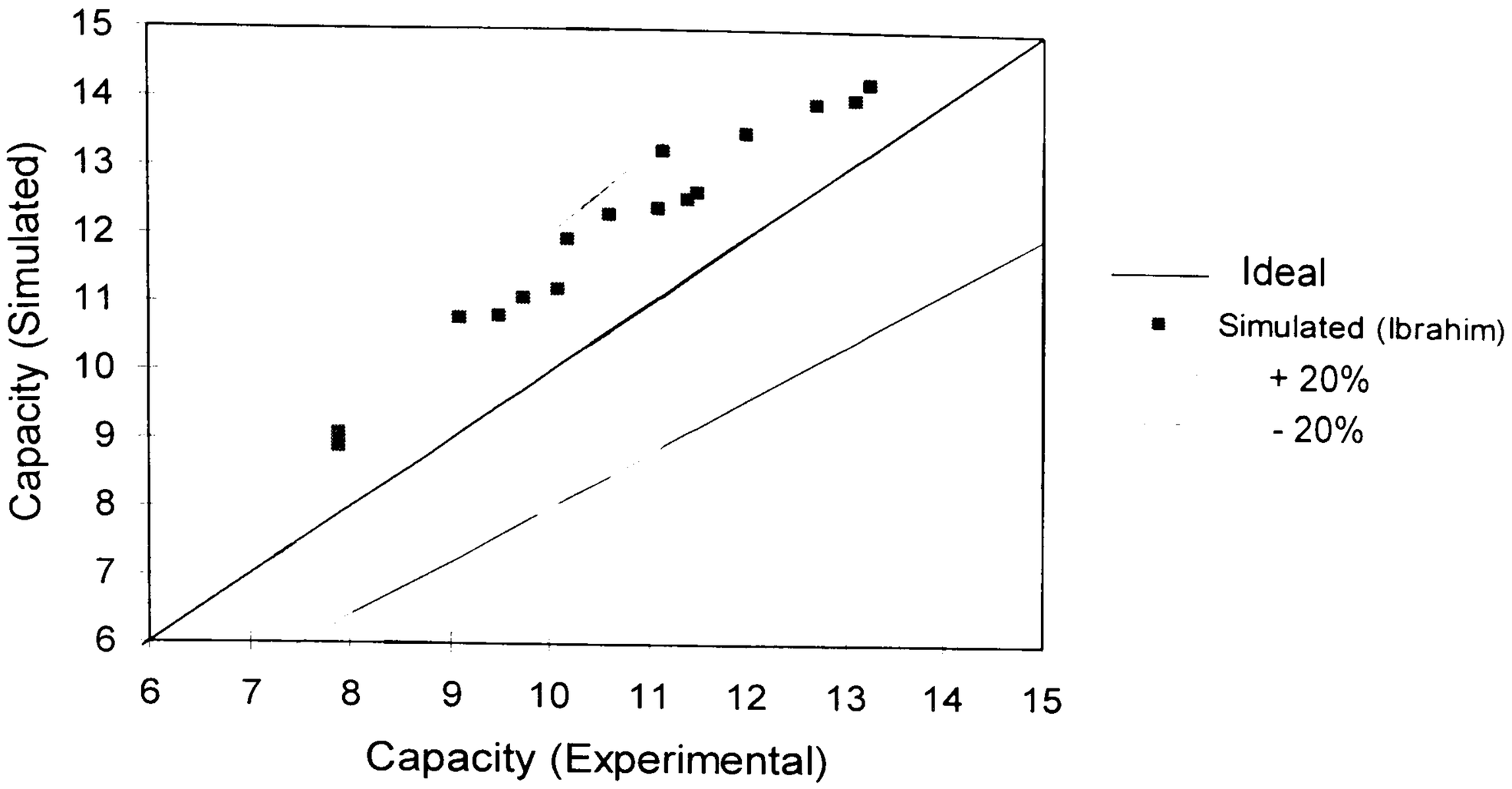

Figure 5.6d Comparison of simulated Vs measured capacity for CO_2 residential ECU (Richter et al. 2000)

Figures 5.6a, 5.6b, 5.6c and 5.6d present the comparison between performance predictions and experimental measurements for a residential heat pump operating in heating mode studied experimentally by Richter et al. (2000). The reference condition was a 9.8 kW nominal heating capacity at 8.3 ^{0}C outdoor temperature and 21.8 ^{0}C indoor temperature. The simulated results for COP and heating capacity are consistently 20% higher than the measured values. Based on the assumptions made for the compressor and a semi-detailed simulation of the heat exchangers, these results are acceptable. However, the simulated trends of COP at higher OD temperatures (above 1.7 ^{0}C) do not agree with measured trends. Richter, unfortunately, gives insufficient compressor details for representative modeling. Hence, the manner in which the model is misrepresenting the COP is unknown. An explanation of the COP curves, which fail to agree on trend above 1.7 ^{0}C OD temperature, may be possible when more system details are known.

5.12 The simulation model application

5.12.1 System configuration and rating conditions

The transcritical CO_2 heat pump was evaluated at conditions approximating two cooling and heating rating points for residential heat pumps. These conditions, represented by temperatures of the heat transfer fluid (air), are shown in Table 5.1.

The indoor and outdoor coils and IHX are similar to the prototype units used by Richter et al. (2000). The hermetic reciprocating compressor developed by Fagerli (1997) is used. However, the displacement of the compressor is changed to 2.7 m^3/h at 1400 rpm to match the rate of prototype compressor. Appendix C presents the relevant geometrical parameters for the compressor and various heat exchangers as the inputs to simulation model.

Table 5.1 Temperatures of HTF used for rating the residential CO_2 heat pump

	Cooling	Heating
Gas cooler inlet ^0C	35	21.1
Gas cooler outlet ^0C	43.2	32.7
Evaporator inlet ^0C	26.7	8.3
Evaporator outlet ^0C	14.4	2.7

5.12.2 Performance predictions at different operating conditions

The simulation model is a valuable tool to assess the performance of a transcritical heat pump at different operating conditions, e.g. summer to winter, different setting of indoor temperatures and different combinations of indoor/outdoor temperatures (ID/OD).

Figure 5.7 compares the COP and capacity of the CO_2 heat pump operating in heating mode at four outdoor temperatures of 16.7, 8.3, 1.7 and –8.3 ^0C. In each case, the indoor temperature is kept constant (21.1 ^0C). The simulation results show that, at constant gas cooler pressure, the COP and capacity decrease as the outdoor

temperature decreases. On the other hand at constant indoor/outdoor temperatures increasing the gas cooler pressure increases the capacity at the expense of higher compression power and lower COP. The COP falls steadily and capacity rises steadily as the gas cooler pressure rises, the trend being the same for different outdoor temperatures. Also, it is noted that there is no optimum operating point corresponding to maximum COP in the range of operating conditions. Given that the cycle has five elements, each with its own individual characteristics, its behaviour is difficult to predict. This of course the reason that an automated model is needed for the investigation of behaviour.

Though a higher COP could be obtained by sub-critical (condensing cycle) operation at room temperature around 21 ^{0}C, raising the high side pressure to increase the delivered heat from the gas cooler reduces the need for expensive extra electric heating when heating and cooling are both required on the site. Also, the heat rejection pressure is a convenient control variable for achieving optimum conditions for system operation.

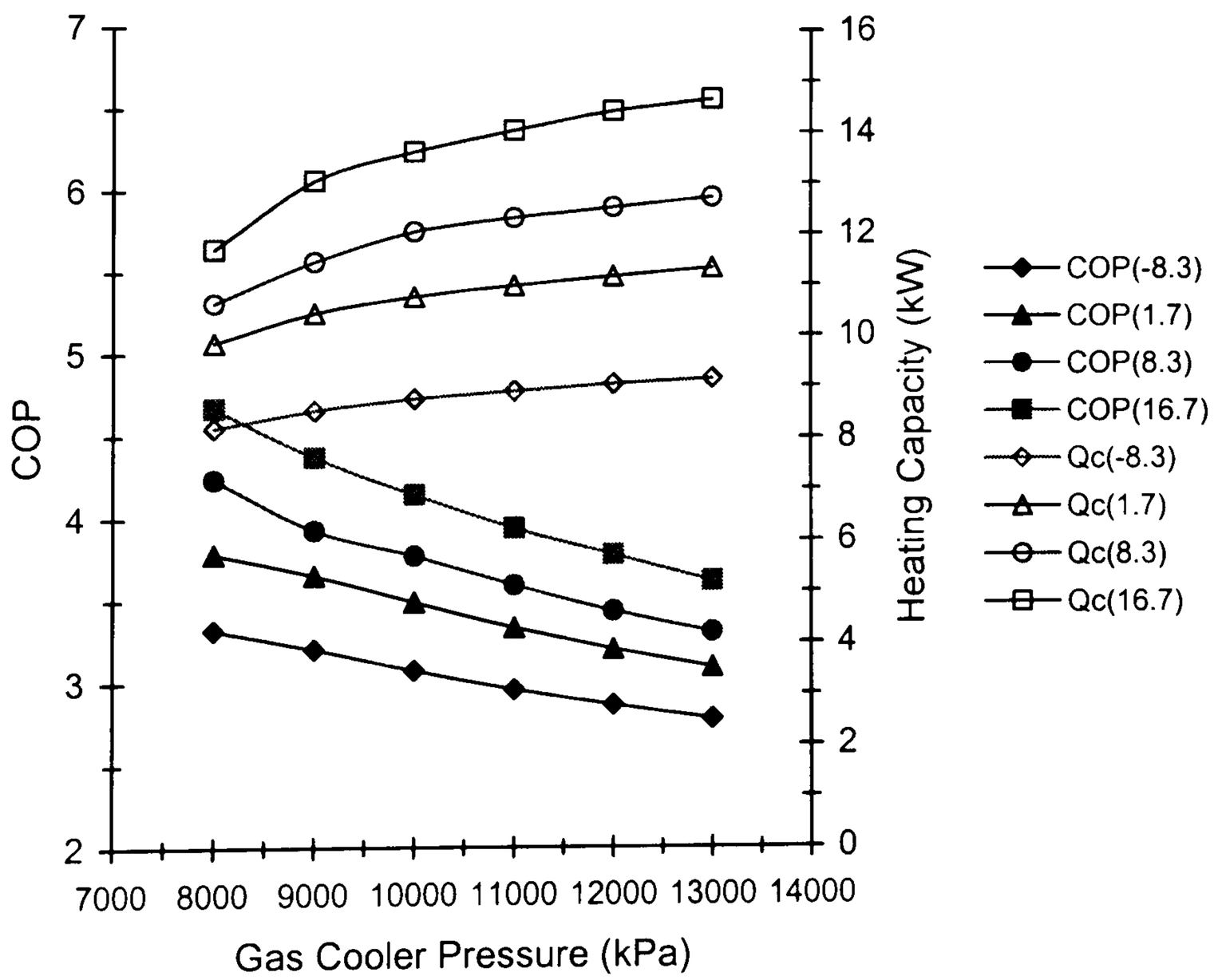

Figure 5.7 Performance of transcritical CO_2 heat pump in heating mode at different outdoor temperatures (^{0}C)

To explore the performance of the CO_2 heat pump at different settings of indoor temperatures, the outdoor temperature is kept constant (8.3 ^{0}C) and the indoor temperature has the values of 21.1 ^{0}C and 26.7 ^{0}C. Figure 5.8 shows that increasing the heat pump temperature head, e.g. difference between ID and OD temperatures, results in a lower COP and capacity.

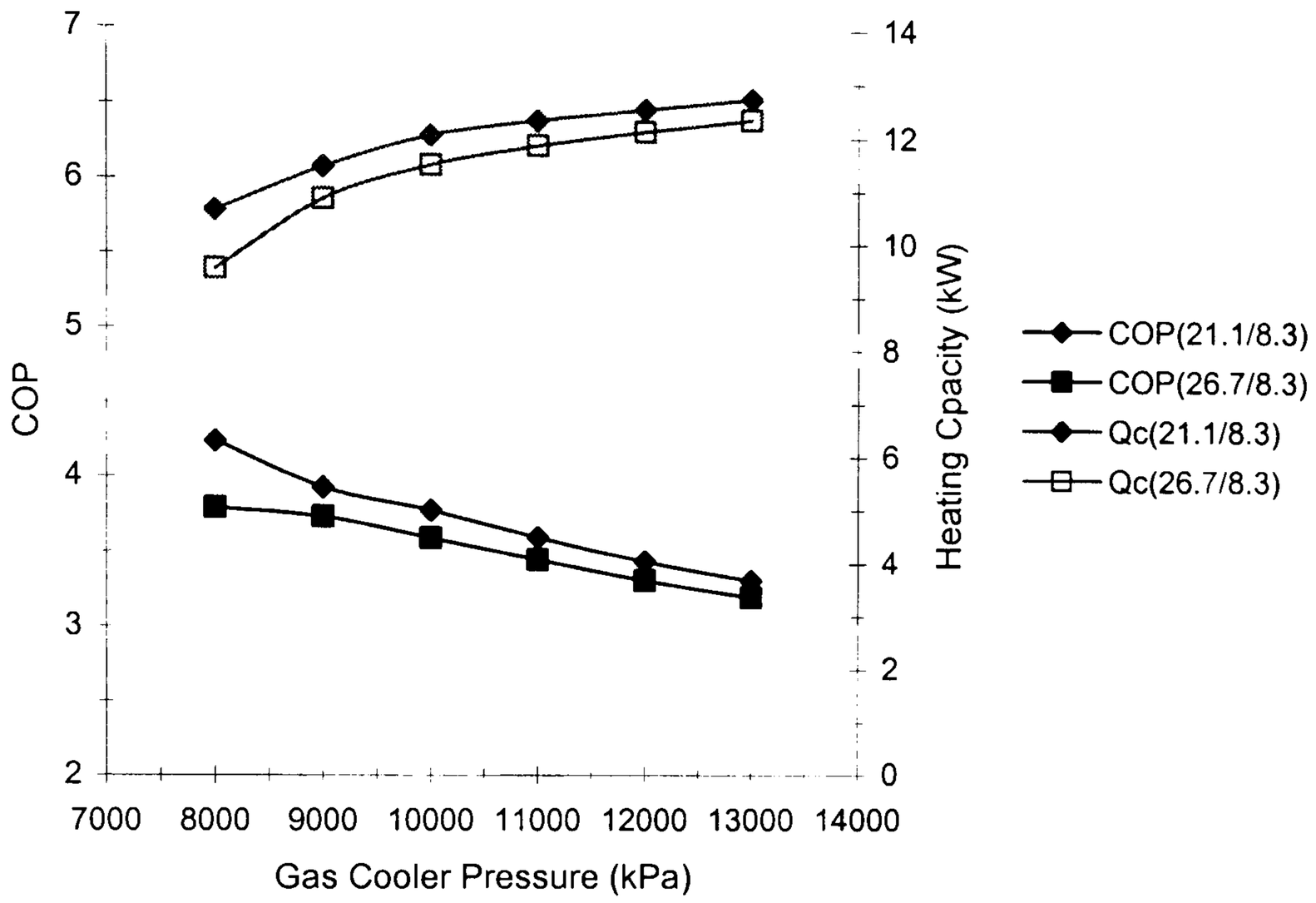

Figure 5.8 Performance of transcritical CO_2 heat pump in heating mode at different indoor temperatures (ID ^{0}C/ OD ^{0}C)

Figures 5.9 and 5.10 illustrate the heat pump performance working in cooling mode. Figure 5.9 represents the COP and capacity at constant indoor temperature (26.7 ^{0}C) and different cooling loads. The simulation results reveal that the optimal COP has been shifted to higher values of gas cooler pressure as the outdoor temperature increases. Also, the influence of gas cooler pressure on COP decreases as the outdoor temperature increases. As observed, the curves of COP tend to be less concave at higher outdoor temperatures. On the other hand, a similar trend of capacity increase for higher gas cooler pressures is observed at different outdoor temperatures. The broad behaviour of COP and capacity is in accordance with that indicated by basic thermodynamics. However, more detailed behavioural features are difficult to explain by inspection. Indeed, the purpose of the simulation is to reveal features which are not obvious and to reveal them quantitatively.

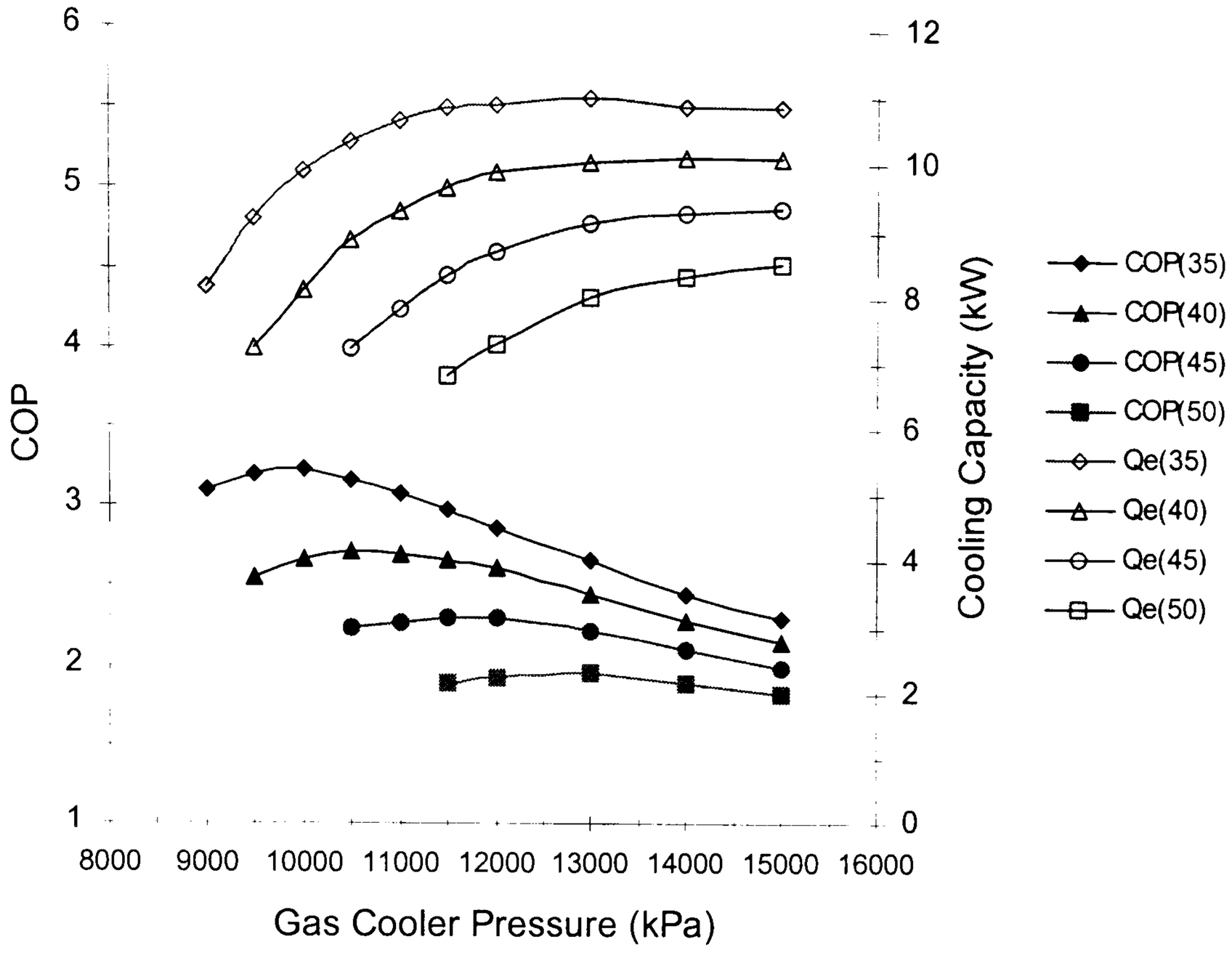

Figure 5.9 Performance of transcritical CO_2 heat pump in cooling mode at different outdoor temperatures (^{0}C)

Insight into behaviour of CO_2 cycles such those discussed here may be gained by examining the shapes of the isotherms on the pressure-enthalpy chart. They have S-like shapes turned 90^0 anticlockwise. Each curve has a different rate of slope change from its neighbours. Close inspection shows that increasing the heat rejection temperature, which shifts the isotherms right, has a greater influence on system capacity than the increase in compression work due to higher heat rejection pressure, which shifts the horizontal isobar up. Hence, the curvature of the COP graphs changes.

Figure 5.10 shows insignificant influence of decreasing indoor temperature setting on CO_2 heat pump performance. This is true especially at lower gas cooler pressure. Also, the effect of indoor temperature change is comparatively small for the cooling mode compared with the heating mode. Furthermore, the optimal COP is fulfilled at the same gas cooler pressure regardless indoor temperature.

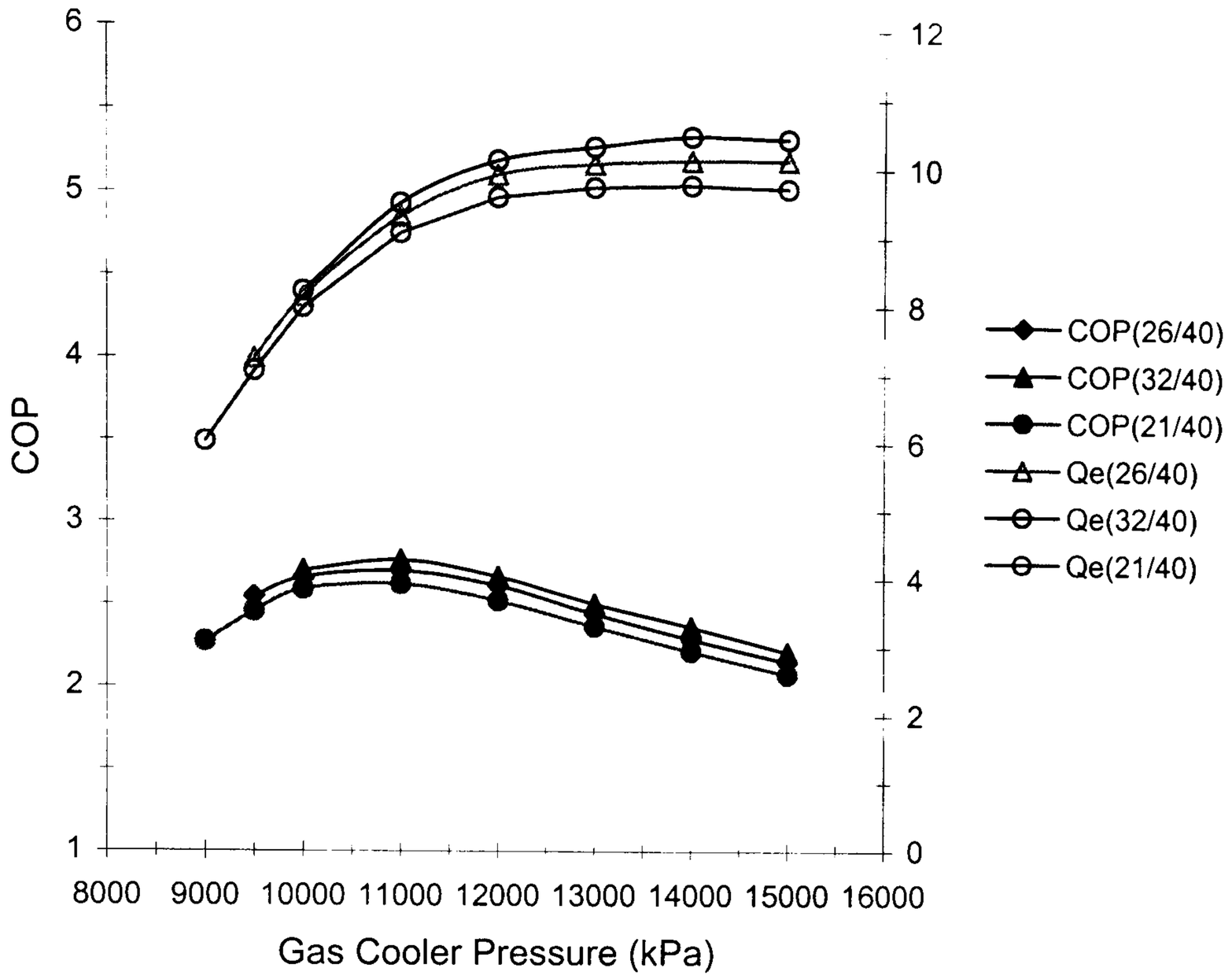

Figure 5.10 Performance of transcritical CO_2 heat pump in cooling mode at different indoor temperatures (ID ^{0}C/OD ^{0}C)

5.12.3 Performance predictions at different compressor parameters

It is interesting to investigate the direct influence of compressor parameters on the CO_2 heat pump performance. No simulation study on the CO_2 vapor compression systems carried out to date incorporate the effect of common compressor faults like weak valve springs or leaking piston rings. One of the major advantages of the author's simulation model is the facility for monitoring the overall performance of the heat pump with respect to different, i.e. design and/or operating, parameters of the compressor. This subsection gives the results of the simulation model for different compressor parameters on the abovementioned CO_2 heat pump working in cooling mode at ID/OD of 26.7/35 ^{0}C and for 100 bar gas cooler pressure.

Figure 5.11 shows the significant influence of valve spring pre-load on performance. The influence of suction valve pre-load is more pronounced than discharge valve pre-load. In general, the pre-load depends on the stiffness and the initial compression

of the spring. However, the value of pre-load could be altered to some extent by tolerance build-up and different thermal expansions of compressor parts. The relatively large drop in the cooling capacity and consequently the COP at higher suction valve pre-load is due to the decrease of compressor flow rate as was shown in Figure 4.12. While, the decrease of the COP at higher discharge valve pre-load is a result of the increase of compression power as was shown in Figure 4.13.

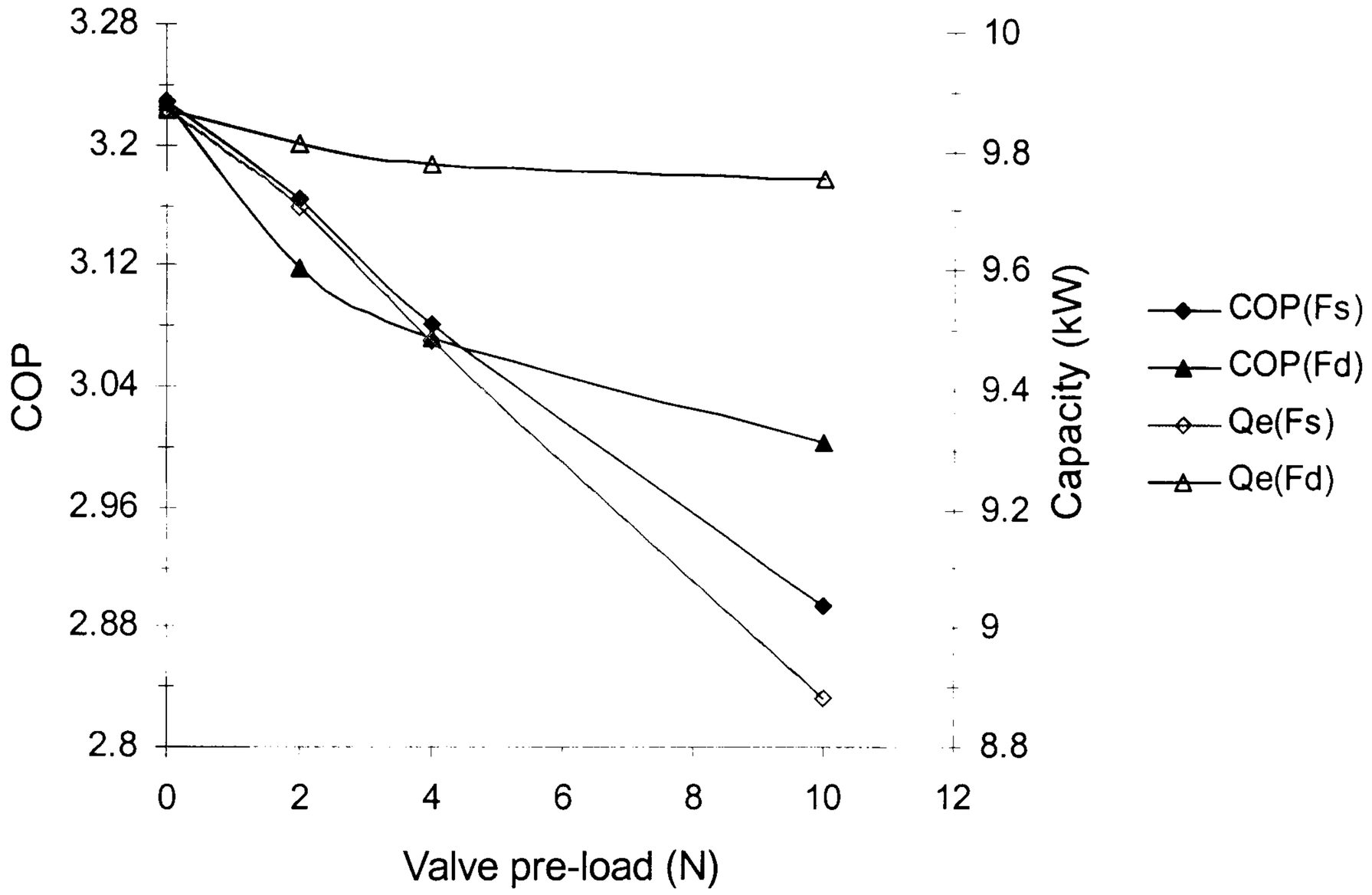

Figure 5.11 Performance of transcritical CO_2 heat pump at different pre-loads of compressor valves (s=suction, d=discharge)

Figure 5.12 illustrates the influence of increasing maximum lifts for suction and discharge valves. The simulation results indicate a considerable influence of increasing the maximum lift of the valves on COP. The maximum COP occurs at a ratio of 1.25 approximately. The influence of suction valve is more significant than discharge valve. Insight into the trend of the COP and cooling capacity may be gained by examining the curves of compression power and mass flow rate at different maximum valve lifts as were shown in the Figures 4.14 and 4.15. Approximately 6% improvement in COP could be obtained by proper selection of valve maximum lift. However, the influence on heat pump capacity is not significant.

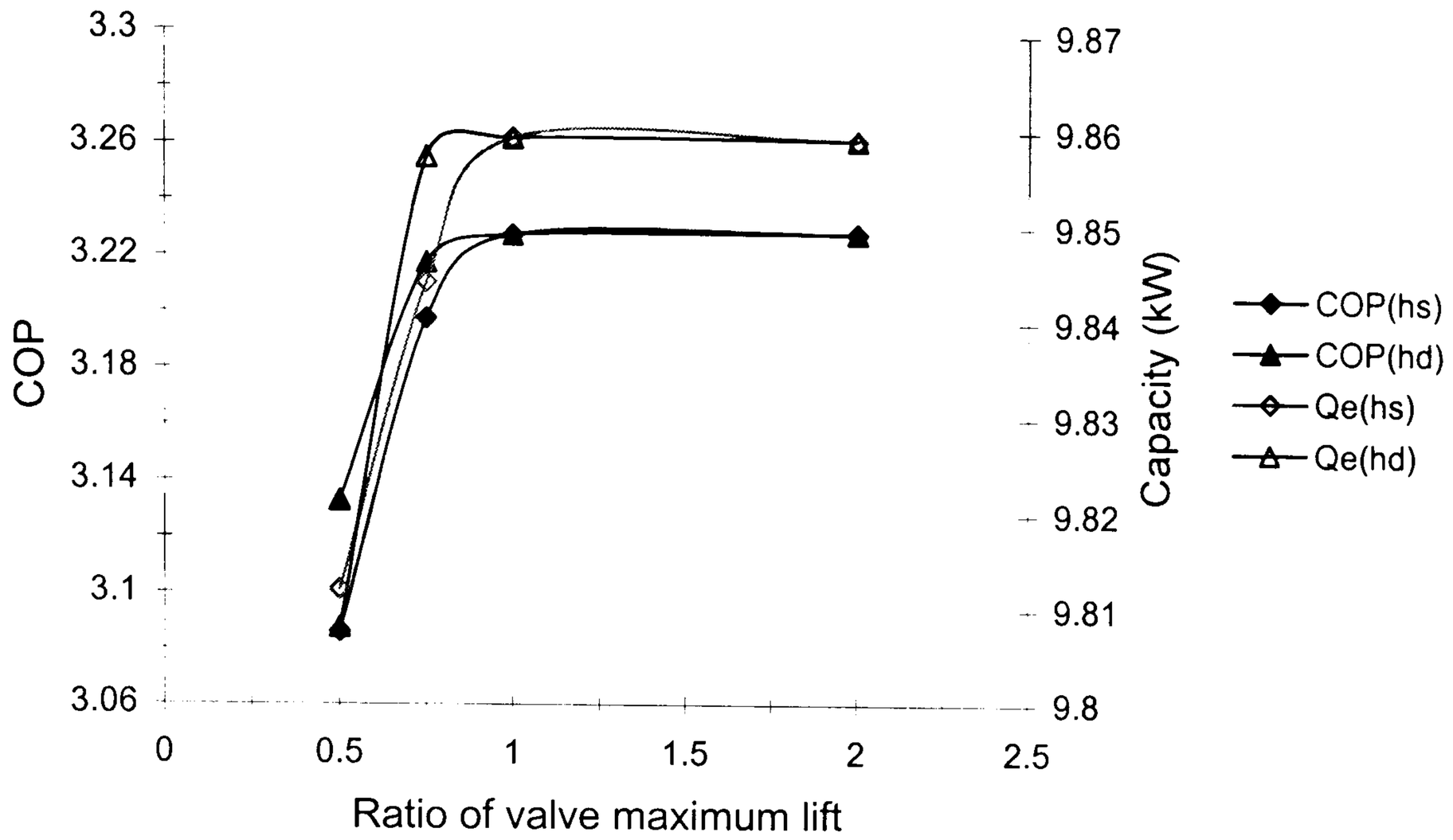

Figure 5.12 Performance of transcritical CO_2 heat pump at different maximum lift of compressor valves (s=suction, d=discharge)

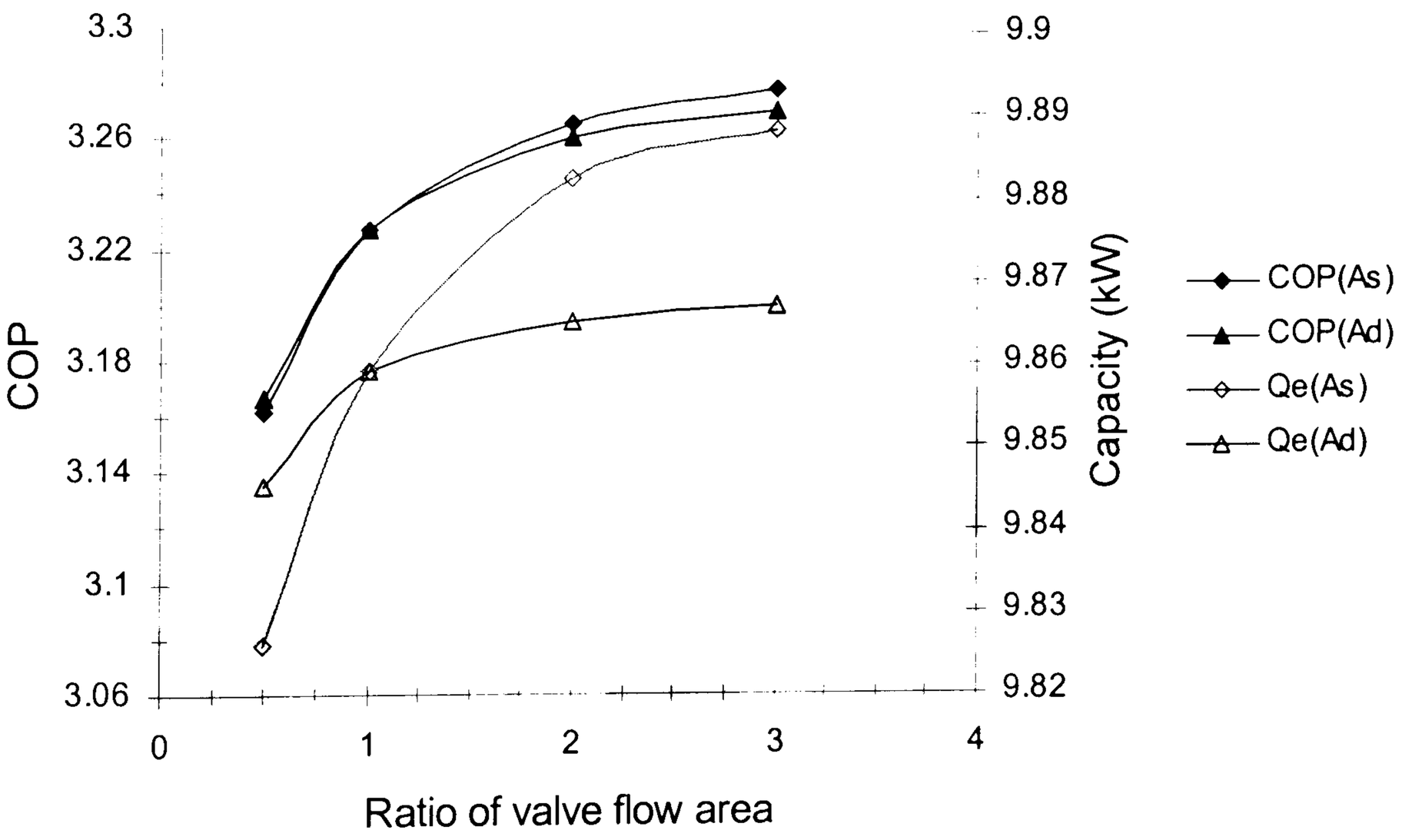

Figure 5.13 Performance of transcritical CO_2 heat pump at different valve flow area of compressor valves (s=suction, d=discharge)

Figure 5.13 shows that the increasing of valve flow area 3 times results in a slight increase of COP (2% approximately). On the other hand the relative increase of capacity could be ignored.

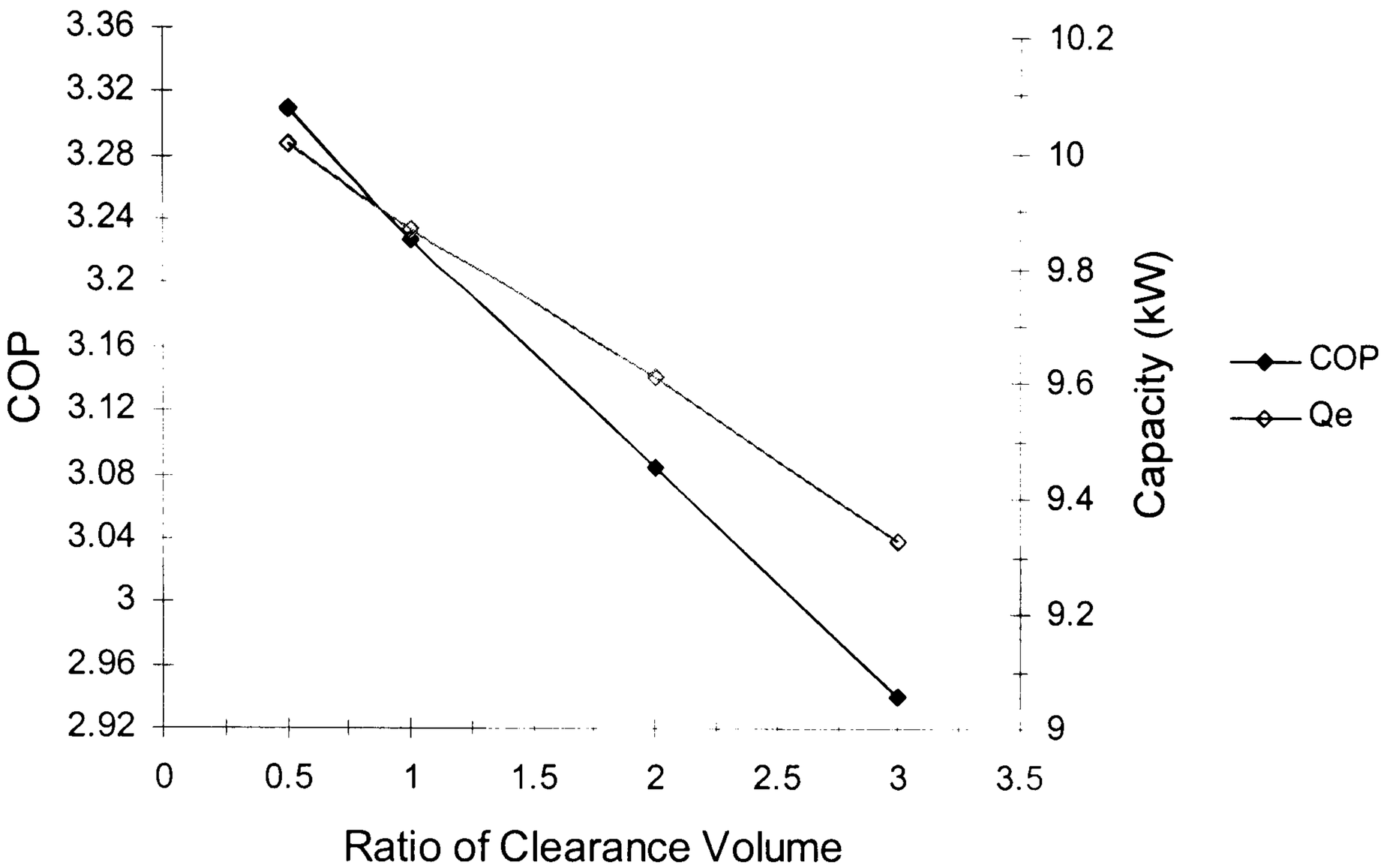

Figure 5.14 Performance of transcritical CO_2 heat pump at different clearance volume of compressor

Figure 5.14 reveals the significant negative influence of increasing clearance volume. Increasing the clearance volume 3 times results in 10% and 6% drop of COP and capacity, respectively. The heat pump model is needed to quantify these influences which are of course not surprising, given that the drastic effect on compressor performance of a large clearance volume is well known.

The influence of piston ring clearance is shown in Figure 5.15. It is interesting to note the significant influence of piston ring clearance on the CO_2 heat pump performance. The clearance between the piston rings and cylinder wall is due to ring end butting clearance, ring bending stiffness and its value is altered by wear and differential thermal expansion of different materials at high temperatures. As indicated, the COP and capacity both drop sharply if the piston ring clearance is

doubled. These results are expected due to the large drop of compressor volumetric efficiency caused by the increase of piston ring clearance as was shown in chapter 4. These results highlight the pronounced influence of piston ring leakage on the overall performance of a transcritical CO_2 heat pump.

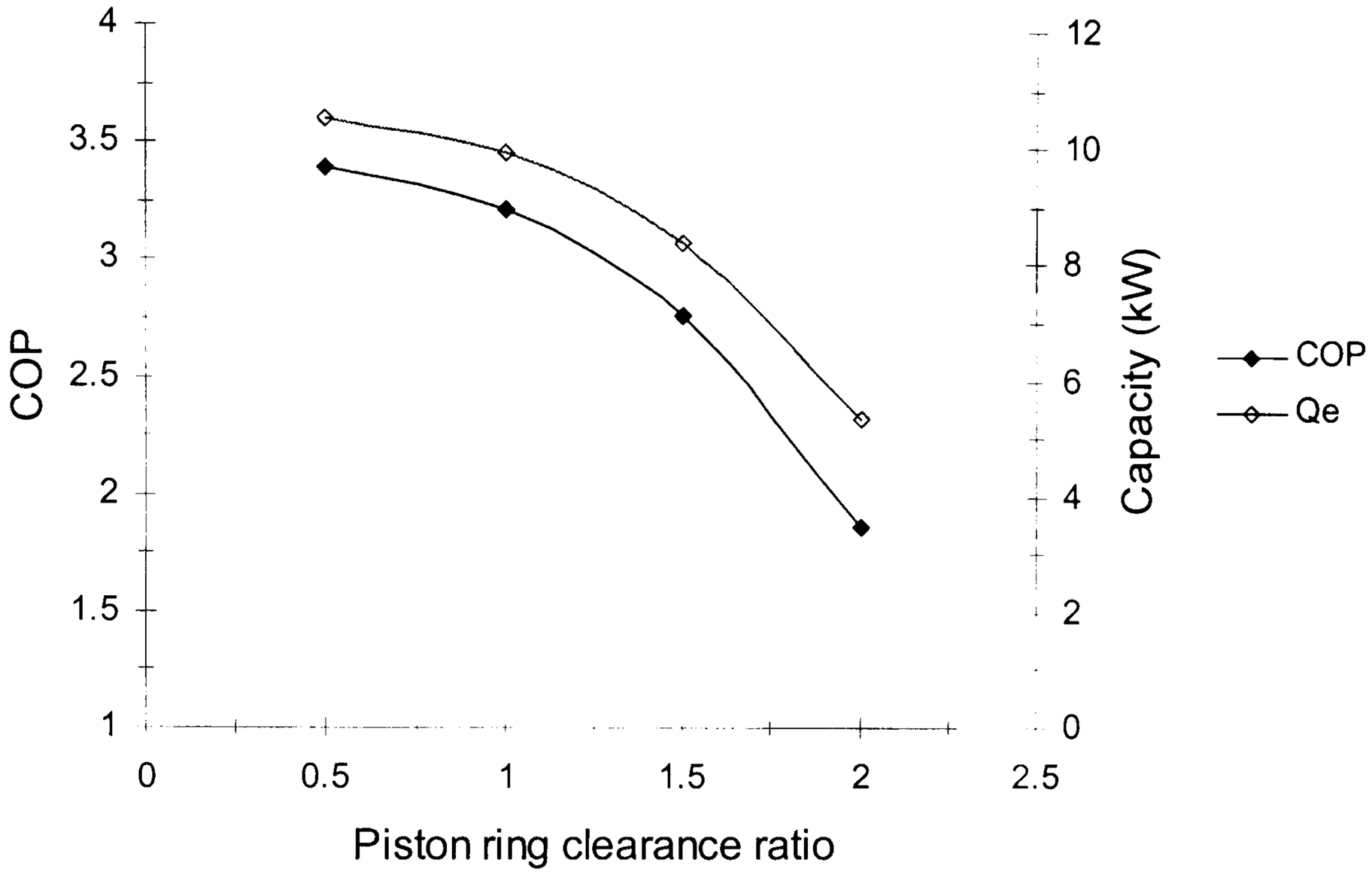

Figure 5.15 Performance of transcritical CO_2 heat pump at different piston ring clearance of compressor

In Figure 5.16, the effects of compressor speed variations on the heat pump performance are examined. The availability of a speed control technique is presumed. As shown, the capacity is linearly related to compressor speed, i.e. approximately 20% increase of capacity is gained due to the increase of compressor speed by 20%. However, this capacity gain is accomplished at the expense of a 10% drop in the COP value.

It is worth noting that the simulation results showed that capacity modulation achieved by varying the compressor speed is more efficient than the change of gas cooler pressure at constant compressor speed. For example, simulation results at ID/OD of 26.7/35 ^{0}C presented in Figures 5.16 and 5.9 show that the COP is 3.07 for

a cooling capacity of 10.8 kW when the gas cooler pressure is 10000 kPa and the compressor speed is 1600 rpm. This should be compared with a COP of 2.99 for the same cooling capacity when the gas cooler pressure is 11500 kPa and the speed is 1400 rpm. Hence, from an energetic viewpoint it is better to fulfil certain load demands by changing compressor speed rather than adjusting the gas cooler pressure.

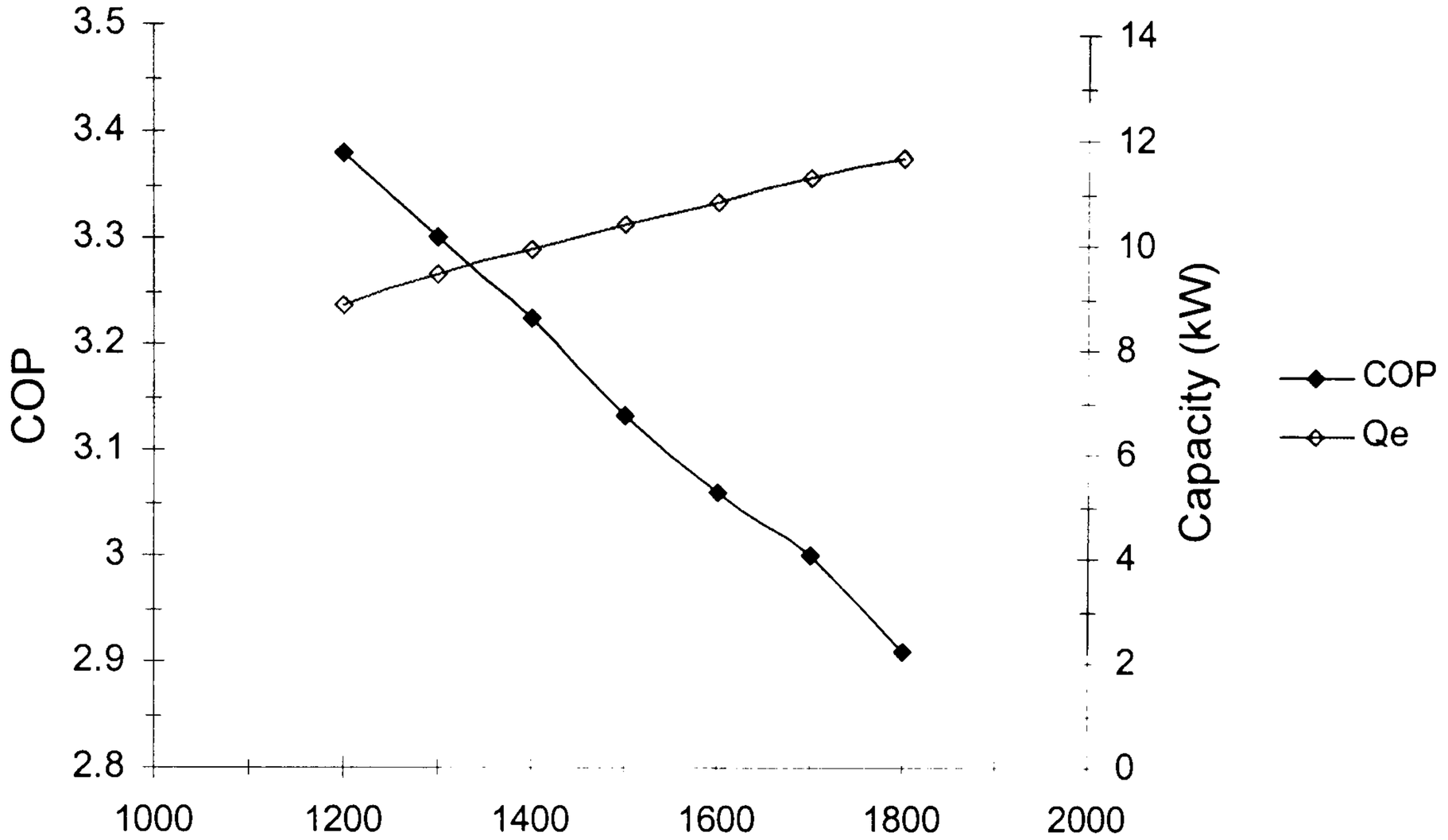

Figure 5.16 Performance of transcritical CO_2 heat pump at different compressor speeds

Finally, the effects due to different values of stiffness and mass of compressor valves are examined. Considerable influences on valve dynamic behaviour are indicated (Figures 4.8 to 4.11), but they have little effect on the overall performance of the heat pump. Since the range of values of stiffness and mass entered into the model is small, a further investigation using a wider range of values is necessary before more general conclusions can be drawn.

Chapter 6

Two-Stage Transcritical CO_2 Heat Pump

6.1 Introduction

The performance of a transcritical carbon dioxide cycle is typically poorer than that of a HFC or HCFC vapor compression cycle. Decreasing the power required by the transcritical CO_2 system can be approached in various ways. One way is to increase the system operating efficiency by modifying the cycle configuration. Likewise, system capacity can be addressed in the same manner.

Using two-stage compression gives a larger flexibility in system design than exists for a system with one-stage of compression. One possibility of increasing the efficiency of the process is by subcooling the high-pressure gas/liquid before throttling by means of a heat exchanger supplied with gas throttled to intermediate pressure. By controlling the mass flow to intermediate pressure, this can also be used as a means of capacity control, however with a certain loss in efficiency (Lorentzen 1995).

A computer simulation model was developed and applied to analyze the system performance of the transcritical CO_2 cycle with two-stage compression and subcooling. Performance prediction for a wide range of configuration parameters and operating conditions is presented. In particular, the effects of different values of intermediate pressure and swept volume ratio (SVR) on heat pump performance were investigated.

A literature survey on open publications revealed that no simulation models of transcritical multi-stage CO_2 vapor compression systems have been carried out to date. In the absence of such simulation models, the author's two-stage model represents a forward step in the design and simulation of transcritical CO_2 systems.

6.2 Selection of cycle configuration

In a two-stage cycle, the total flow after the condenser/gas cooler is split into two parts: the larger flow passes through the low pressure evaporator, while the smaller flow works only between an intermediate pressure level and the gas cooler pressure. The two-stage process is an attempt to bring the compression closer to the ideal (isothermal) compression. A large number of stages would bring it closer still to isothermal, but would be impractical. A two-stage system configuration was chosen for investigation since two-stage cycles fulfill the following objectives:

(1) For the same heat pump capacity, the flow compressed all the way from the low pressure is reduced, which results in a decrease of the compression work and higher COP.

(2) The throttling loss is reduced since the flashed fluid developed in the expansion process is wetter at the evaporator inlet.

(3) Improved compressor volumetric efficiency; by working at smaller pressure difference across piston rings, ring leakage is reduced.

(4) Higher compressor mechanical efficiency results from reduced friction associated with a smaller pressure difference acting on the crank mechanism and the bearings.

(5) Reduced compressor discharge temperature especially in the heating mode operation at low outdoor temperatures.

6.2.1 Two-stage system arrangements

6.2.1.1 Two-stage Compressor

In general, the two stages can be achieved in different ways for use in the refrigeration cycles. A multi-cylinder (compound compressor) having cylinders of different geometry can be used with the cylinder sizes chosen to suit the low and high pressure stages. Or the more common arrangement could be used, namely two separate compressors with different swept volumes chosen appropriately.

Regarding two-stage reciprocating compound compressors, none were found in the literature for use with CO_2. An automobile two-stage compressor based on the swash

plate design was developed by the company Denso (Inagaki et al. 1997). Later, Neksa et al. (2000) and Dorin et al. (2000) described the development of a semi-hermetic two-stage compressor series by Officine Mario Dorin company. Also, Tadano et al. (2000) reported on the development of a rotary two-stage hermetic compressor for small capacities (750 W) from the company Sanyo. Most recently, another prototype rotary two-stage hermetic compressor was developed by Tecumseh Products Company (Deriman and Bunch 2003).

However, in principle there is no difference between separate stages and compound operation. In both cases gas cooling as close as possible to the saturation line is necessary between the LP- and HP-stages.

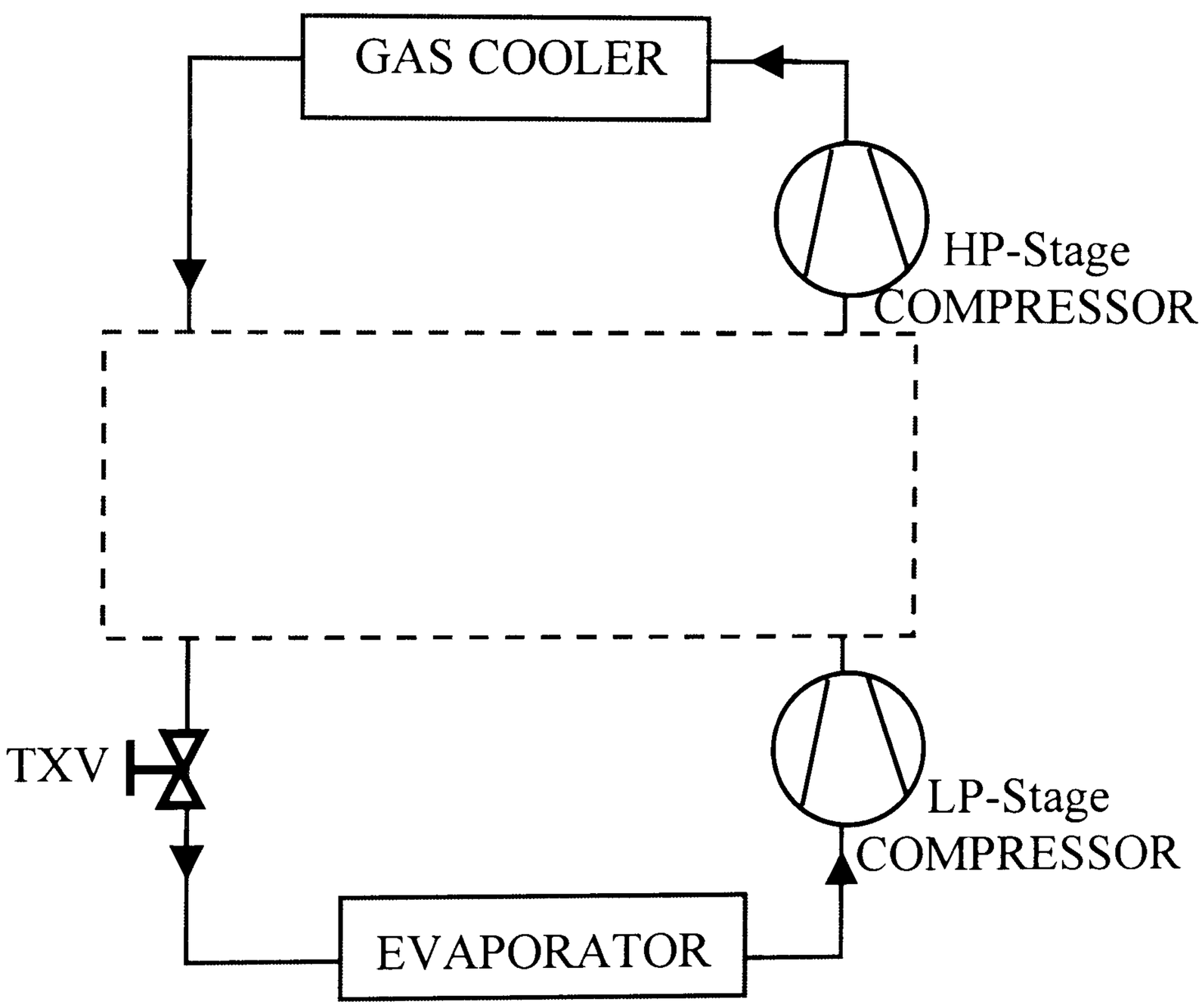

Figure 6.1 Simplified two-stage cycle

6.2.1.2 Interstage Cooling Systems

In practice, the intercooling between the stages is achieved directly by means of the refrigerant, but there are different ways to achieve this. Threlkeld (1970), Stoecker and Jones (1982) and Koelet (1992) have already shown that there are several ways

to construct interstage cooling systems, each having its own advantages. Figure 6.1 shows a diagram of simplified two-stage cycle only containing the main components and where the dotted square represents the interstage cooling section. The most common types of intercooling configurations for two-stage cycle are shown schematically in Figures 6.2 to 6.5 whereby each figure should be pictured successively into Figure 6.1.

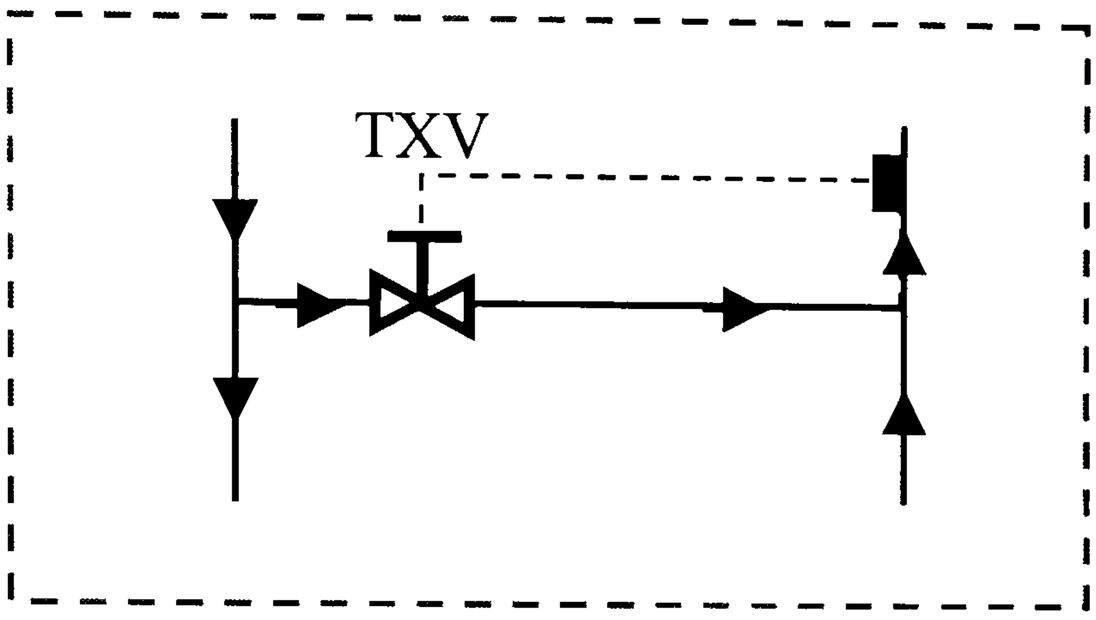

Figure 6.2 Injection interstage gas cooling, (Configuration A)

The simplest way to achieve intercooling for the two-stage cycle is to use a thermostatic expansion valve (TXV) to inject wet refrigerant between the outlet of the LP stage and the inlet of the HP stage. Configuration A, as shown in Figure 6.2, is a simple mixing pipe mounted between the LP discharge and HP suction connection of the compressor. This interstage cooler is very simple and inexpensive; no need for additional isolation stop valves, oil separators in the LP discharge line or suction filter in the HP suction line. Configuration A is used in small to medium-large systems and can be built onto the compound compressor. However, TXV operation requires gas cooler pressure control, to ensure a minimum pressure-difference across the TXV. Too low pressure differences result in hunting. If the gas cooler pressure is uncontrolled to obtain the lowest possible head-pressure and thus the highest COP, an electronic expansion valve control (EXV) must be used.

The major disadvantage of this method is that there is no increase in evaporator enthalpy difference compared with single-stage operation due to expansion in one stage without subcooling. Therefore, a small capacity results in a relatively high specific power consumption and a rather expensive compressor per unit of capacity.

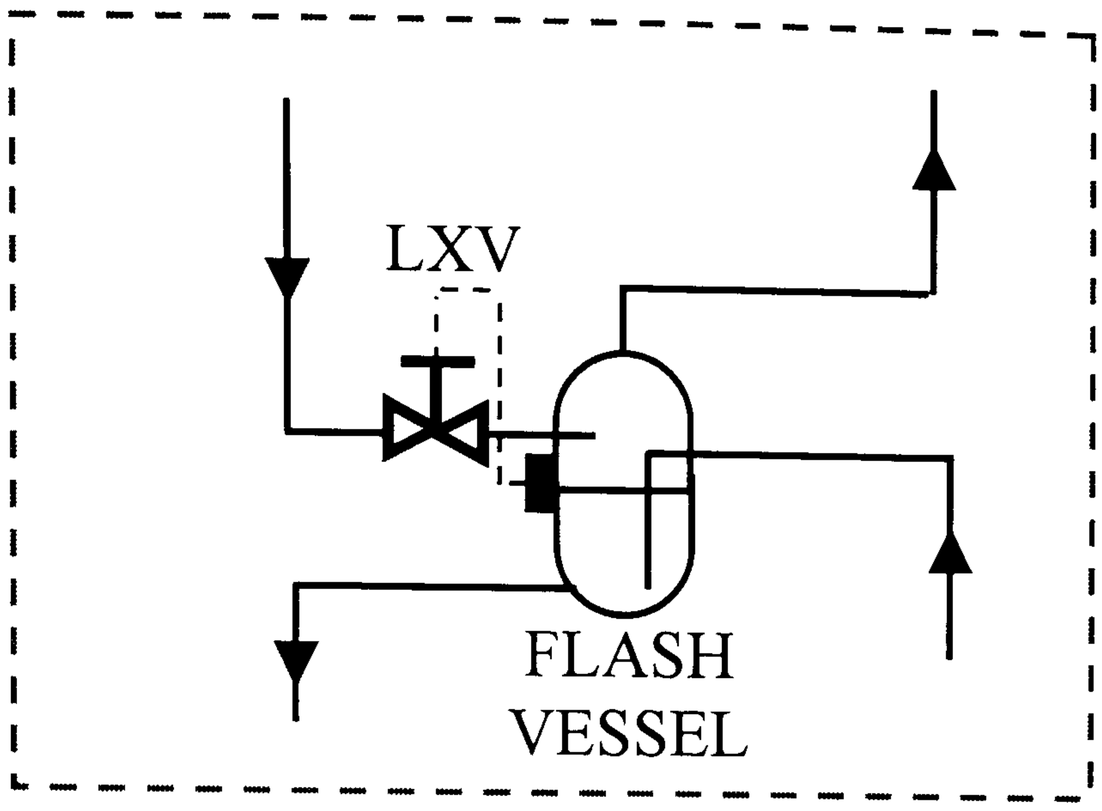

Figure 6.3 Open flash interstage cooling, (Configuration B)

Figure 6.3 shows configuration B that is called flash (or open) intercooling. The open intercooler can be thought of as a supplementary evaporator placed between the LP- and HP-stage, fed by refrigerant from the condenser/gas cooler and maintained at an operating level by a float-valve. It removes heat from the LP-stage vapor as it bubbles through the bath of liquid refrigerant, while cooling the main supply of liquid refrigerant to the evaporator and acting as a "flash vessel" for the flash gas generated in the first stage of the expansion process. The vapor refrigerant is aspirated at intermediate pressure by the HP-stage compressor. The full liquid refrigerant flow is passed through this vessel. The refrigerant at the gas cooler exit undergoes a double expansion: first from high to intermediate pressure of the flash vessel via a level-controlled expansion valve (LXV) and then the saturated liquid at intermediate pressure is fed from this vessel to the evaporator via a second TXV.

Flash interstage cooling achieves maximum possible enthalpy difference, and hence maximum capacity, across the evaporator for a given operating condition. However, it requires extra space and is rather complicated and expensive due to the necessity of isolation stop valves, an oil separator in the LP discharge line and a suction filter in the HP suction line. Configuration B is more suitable for medium-large to very large systems. Further, low pressure difference across the TXV for evaporator feeding results in a risk of forming flash gas in the feeding line between the interstage cooler and the evaporator.

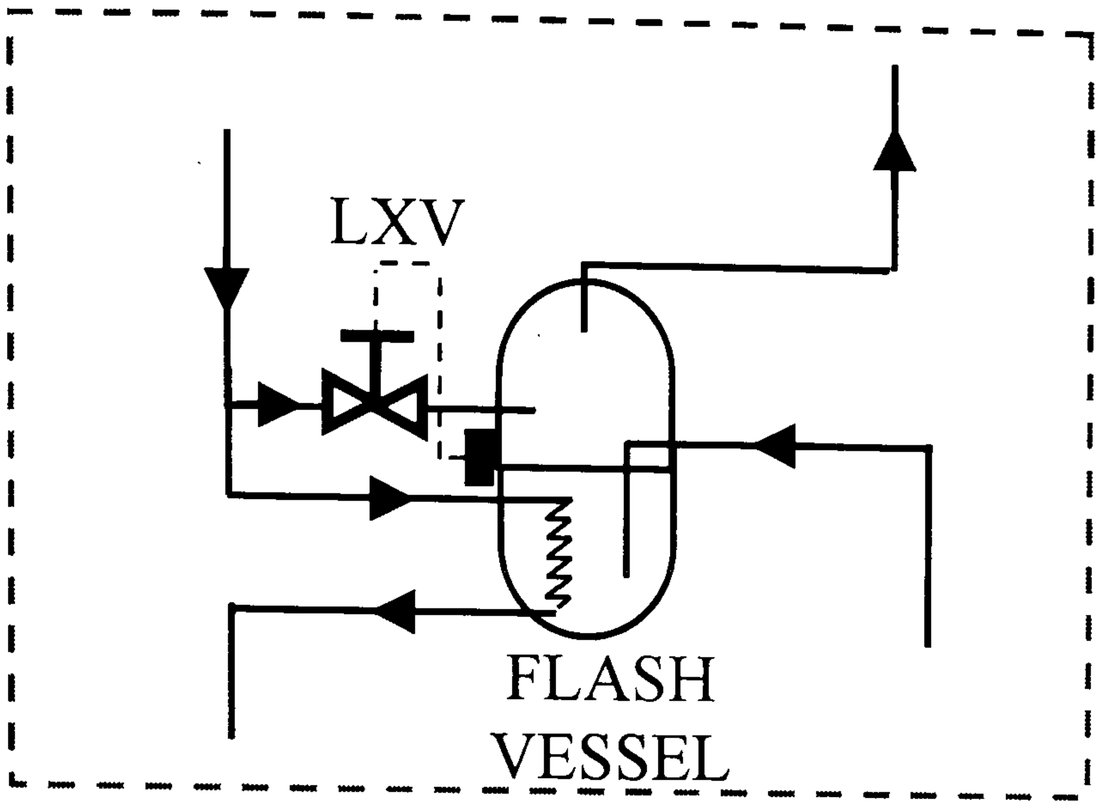

Figure 6.4 Closed flash interstage cooling, (Configuration C)

Configuration C is a variant of configuration B. As shown in Figure 6.4, the interstage cooling takes place in a similar manner, but the refrigerant at the gas cooler exit flows under HP-stage via a closed cooling coil in the interstage cooler vessel to the expansion valve of the evaporator. So, the HP refrigerant expansion is singular. The other LXV for feeding the interstage cooler vessel only has the function to inject just that amount of HP refrigerant required for the interstage gas cooling. At the same time, the major stream of HP refrigerant flow through the coil is subcooled. The degree of subcooling achieved in a closed intercooler is not so great as that obtained in an open intercooler, usually 10 K above the liquid bath temperature.

One advantage of the closed system lies in the fact that the refrigerant is at HP and that there is hardly any risk of flash gas bubbles forming in the feeding line from interstage cooler vessel to the evaporator; this provides for a more satisfactory operation of the TXV. A closed intercooler is suitable for medium-large to very large systems and is more universal, i.e. without restrictions regarding connection of the different components to one another. On the other hand, refrigeration capacity at given conditions is somewhat lower than that of an open intercooler due to a higher enthalpy of the liquid-vapor mixture at the evaporator inlet. Also, a closed intercooler is more complicated, more expensive and needs an LP oil separator.

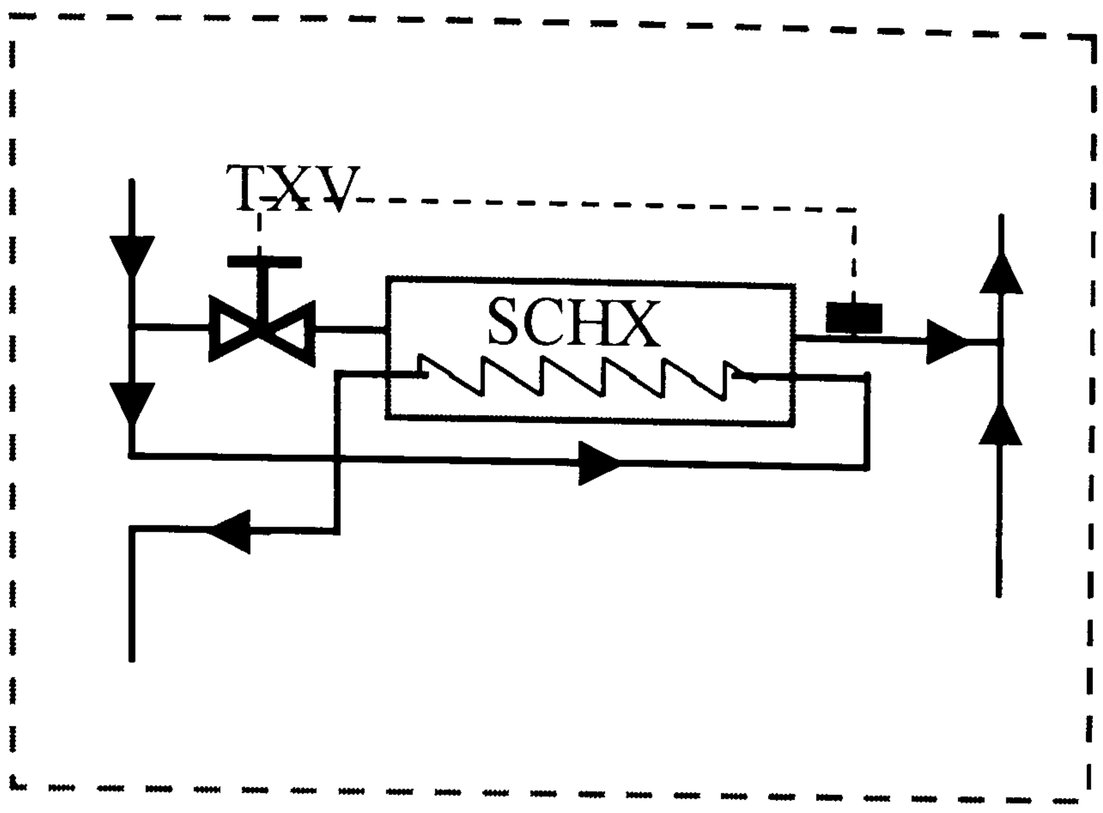

Figure 6.5 Injection interstage gas and gas/liquid cooling, (Configuration D)

Configuration D, as shown in Figure 6.5, is an extension of configuration A. It employs a direct expansion intercooler (henceforth called a subcooling heat exchanger, SCHX) in which a subcooling coil is cooled by direct expansion from TXV; refrigerant vapor leaves the SCHX and is injected into the line between the LP- and HP-stage in such a condition as to desuperheat the LP-stage vapor to a reasonable state.

Configuration D is a thermodynamically identical alternative to configuration C but is characterized by a much smaller liquid content of the interstage cooler and trouble free oil return to the HP stage. In addition, it is smaller, simpler, less expensive and more convenient. In principle, a complete interstage cooler built onto a compound compressor is possible, resulting in space saving. Configuration D is applied in small and medium-large installations and there is no need for additional isolation stop valves, LP oil separator or HP suction filter (direct piping between LP discharge and HP suction). Similar to configuration A, TXV operation requires gas cooler pressure control, to ensure a minimum pressure-difference over the TXV. If the gas cooler pressure is uncontrolled, an EXV must be used.

6.2.1.3 IHX Connections

A common way to avoid wet gas entering the compressor is to use an IHX. In two-stage systems, at least three possible connections exist:

(1) On the total flow before the flash vessel/SCHX

(2) On the large flow after the split and before the SCHX

(3) On the large flow after the split and after the flash vessel/SCHX

The first connection lowers the temperature into the SCHX/flash vessel expansion valve, and thus reduces the amount of gas in the flash vessel for configuration B and C or the flow it is possible to evaporate in the SCHX for configuration D. Both connections (1) and (2) decrease the temperature of the liquid at high pressure going into the SCHX, which restricts the flow it is possible to evaporate in the SCHX.

One other aspect is that the area of IHX is highly dependent on how the heat exchanger is connected. The area needed to achieve the same amount of superheating is less for an IHX placed according to connection (1) or (2) than for an IHX placed according to connection (3). The reason for this is that the temperature difference between liquid refrigerant and suction gas is larger for connections (1) and (2).

6.2.1.4 SCHX Sizing Parameters

The SCHX is a key component. Figure 6.6 shows the parameters for sizing the SCHX for optimum cycle performance and cost. The maximum cooling that can be derived from the SCHX is to produce liquid refrigerant at the saturation temperature associated with the intermediate pressure saturation temperature. Obviously, the minimum effect would be no change in the refrigerant temperature as it passes through the SCHX. At this minimum point, there would be no mass flow through the intermediate section and no heat transfer in the SCHX, as the system becomes equivalent to a conventional single-stage system. The ratio of the actual subcooling to the maximum possible is referred to as the effectiveness.

The SCHX can be viewed simply as the evaporator of the second-stage cycle, and is generally better configured as counter-flow instead of parallel-flow. The key parameter is its saturated injection temperature (SIT), which is the saturated refrigerant temperature at its outlet interstage pressure. The SIT is a function of the

evaporator and gas cooler pressures, and the HP- and LP- SVR as defined by the designer.

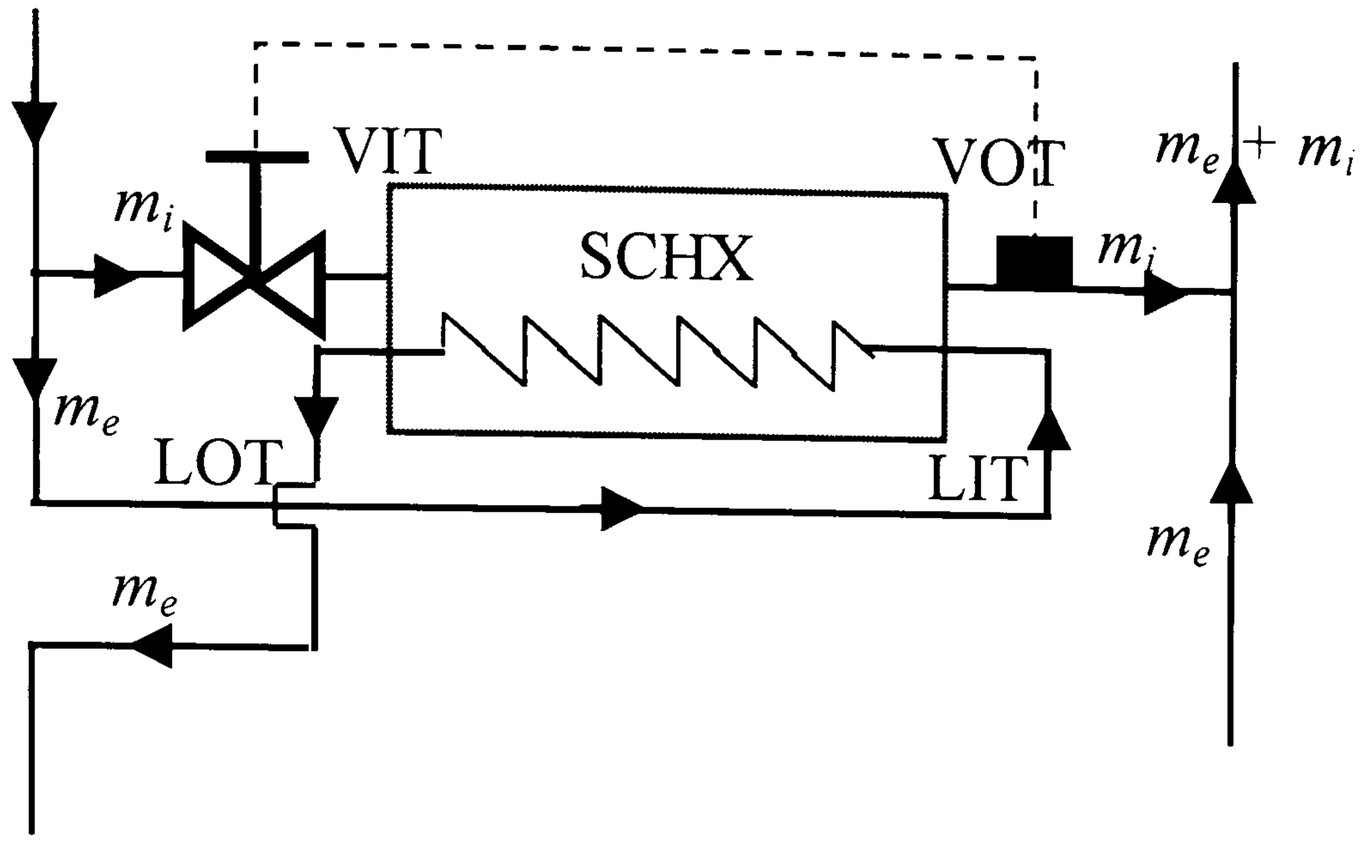

Figure 6.6 Parameters of SCHX

In practice, the capacity gain calculation is a function of the SCHX size, so it is important to define the sizing criteria. A simple approach to sizing the SCHX is to consider the temperature difference (TD) between its liquid outlet temperature (LOT) and SIT. The smaller the TD is, the larger the SCHX will be and vice versa. In the model, LOT is derived based on an assumed TD and the derived SIT.

The SCHX capacity is determined as the product of the evaporator mass flow (m_e) and the enthalpy difference across the SCHX liquid side. Thus, the injection mass flow (m_i) can then be determined from the energy balance equation for the SCHX. The last parameter is the SCHX vapour out temperature (VOT), which is governed by the superheat (SH) control of the TXV.

A simplified approach is to use the 5 K design guideline as recommended by Beeton and Pham (2003). They reported that 5 K TD is a good balance between SCHX performance and cost, typically in the range of 90%+ SCHX effectiveness. Higher TD results in underperformance. Lower TD requires a larger area resulting in higher cost. Also, 5 K SH is generally a good balance to ensure stable TXV control. Excessive SH means starved SCHX performance. A flooded SCHX would provide wet suction into the HP-stage. However it is known that true 0 K SH is optimum, this

is difficult to achieve in practice without TXV hunting The TXV should be sized to deliver Q_{SCHX}. The system designer might be able to size a fixed expansion orifice to achieve 0 K, but not for all conditions. The ideal flow control is an EXV, but its added costs and controls/sensors cannot always be justified.

Using this 5 K guideline for TD and SH, the only key parameter remaining is the SIT, which is determined experimentally or using simulation analysis as function of gas cooler and evaporator pressures for a given hardware design.

6.2.1.5 Optimum Intermediate Pressure/Temperature

Thermal efficiencies of multi-stage systems depend mainly upon the intermediate pressures. For two-stage vapour compression cycles, the interstage pressure (corresponding to the minimum compressor work) is commonly taken as the geometric mean of the refrigerant condensation and evaporation pressures, which is only applicable for a perfect gas with complete intercooling between the stages. However, Threlkeld (1970) demonstrated that for two-stage refrigeration cycles, the optimum interstage pressure is different from the geometric mean pressure.

The optimum interstage pressure for the subcritical multi-stage vapor compression systems has been obtained by various authors. Behringer (1928) as described by Gosney (1982) carried out extensive calculations for a two-stage ammonia cycle with liquid subcooling and desuperheating between the stages to the saturation temperature, the optimum interstage temperature is given by: Topt = T_m + 5, where T_m is the saturation temperature in K corresponding to the pressure for equal pressure ratios in the first- and second-stage. However for more realistic cycles, that is, allowing for compressor and motor efficiencies, Baumann and Blass (1961) found that an optimum occurred at a point quite close to equal pressure ratios in the stages (Rundle et al. 1995).

Arora and Dhar (1971) have given a general expression for the optimum interstage pressure allocation in ideal multi-stage compression systems, with and without intercooling between the stages, on the basis of the minimum work. The results

showed that the optimum interstage pressure approximately equals the geometric mean of the condensation and evaporation pressures. However, when the flash inter-cooler was incorporated, they found a considerable difference between the geometric mean and the optimal pressure values.

Prasad (1981) found that the interstage temperature of a two-stage refrigeration cycle is given by the geometric mean of the condensation and evaporation temperatures.

Gupta and Prasad (1983) developed correlations to predict the optimum interstage temperatures when the effects of compressor efficiency, condenser subcooling and evaporator superheating are involved. The optimum results were found on the basis of maximum COP rather than minimum work.

Later, Prasad and Prasad (1987) adopted the cost criteria to obtain the optimum interstage pressure based on a more realistic (commercial) methodology. In their study, the costs of components, compressor electrical energy and condenser cooling water are considered. The variations of optimum values of condensing temperature, interstage pressure, compressors power and cooling water rate with the evaporation temperature are presented graphically for the CFC-12.

Zubair et al. (1995) showed that the optimum performance of the refrigeration system with mechanical subcooling occurred when the subcooler compressor (saturation suction) temperature corresponds to the arithmetic mean of the condensation and evaporation temperatures (in degree Kelvin).

Rundle et al. (1995) carried out thermodynamic analysis of an actual two-stage cycle with an open intercooler. They found that the intermediate pressure that corresponded to maximum system efficiency was higher than that generally predicted by the prevalent formulae.

The key difference between the CO_2 system and above-mentioned literature examples is due to the transcritical operation of a CO_2 system. Baek et al. (2002b)

conducted a theoretical analysis to investigate the effect of intermediate pressure on the performance of the transcritical CO_2 cycle with two-stage compression and intercooling. Simplified assumptions included (1) isentropic compression, (2) an ideal combination of the gas cooler and the intercooler so that the CO_2 temperature at the outlet of the gas cooler and the external coolant temperature at the outlet of the intercooler equals the environmental temperature, which is 35 ^{0}C (3) A 20 ^{0}C constant temperature of CO_2 at the inlet of LP-stage compressor was imposed. Their theoretical results indicated that for a constant gas cooler pressure of 10 MPa and various evaporation pressures, 2.5 up to 4.5 MPa, a maximum COP was achieved at an intermediate pressure of 8 MPa regardless of the evaporation pressure. They concluded that the optimum intermediate pressure of the transcritical cycle deviated from the well-known geometric mean pressure criterion. However, this conclusion should be reconsidered due to the simplifying assumptions used in the derivation.

6.2.2 Description of the selected two-stage heat pump cycle

The two-stage system functions with three levels of pressure, which will be referred to as low, intermediate and high. The two-stage circuit is chosen based on configuration D and connection 3 for the IHX. This two-stage heat pump cycle is characterized by: simple construction, less expensive, compact size and suitability for small and medium capacity heat pump units. In addition, a complete interstage cooler built onto compound compressor is possible.

The two-stage heat pump cycle consists of a two-stage compressor, a gas cooler, two expansion valves, an evaporator, IHX and SCHX. The circuit diagram of the system is shown in Figure 6.7. The state points shown on Figure 6.7 correspond to the state points on the P-h diagram in the Figure 6.8. The description of the cycle process is given below.

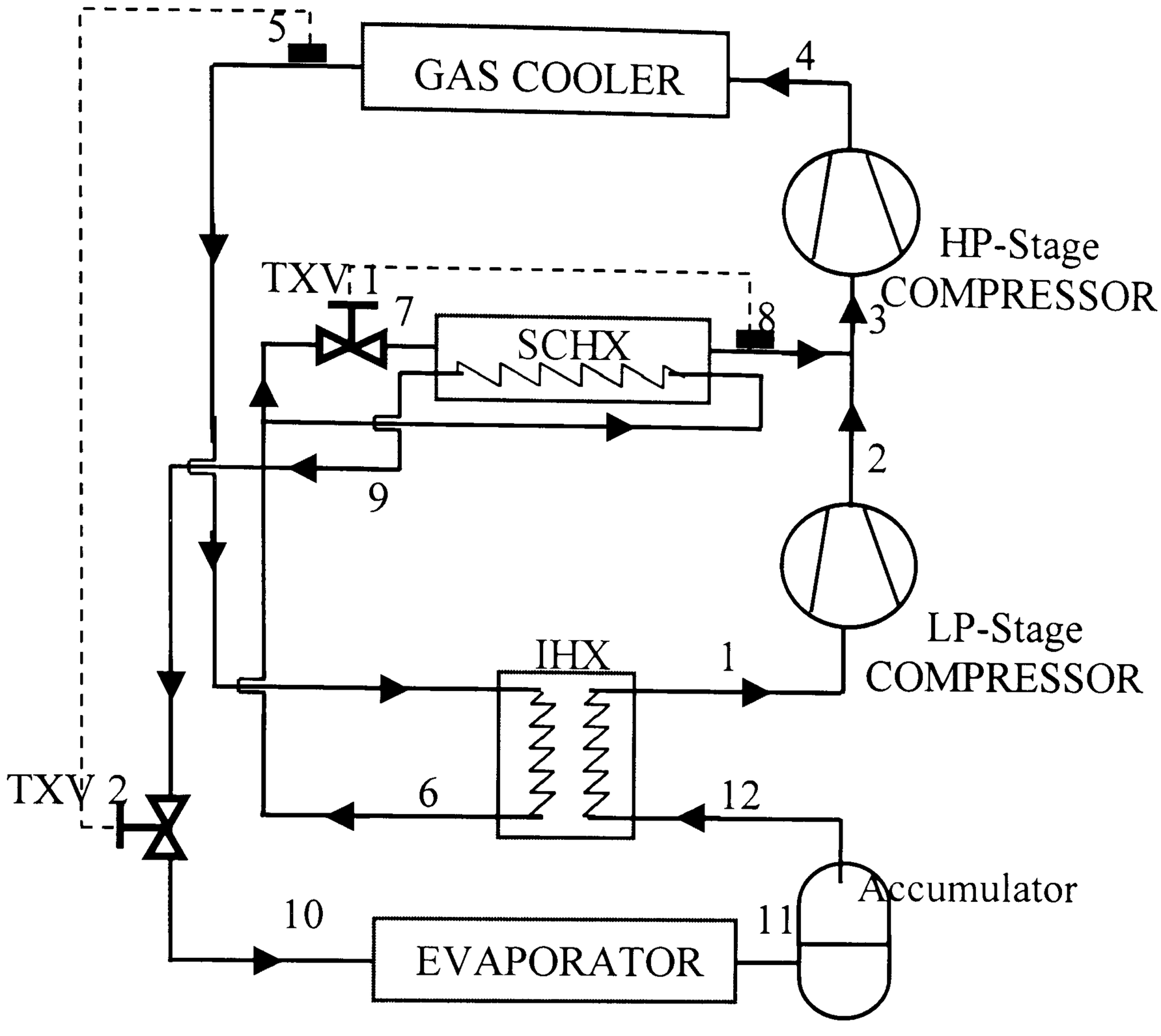

Figure 6.7 Diagram of transcritical two-stage CO_2 heat pump

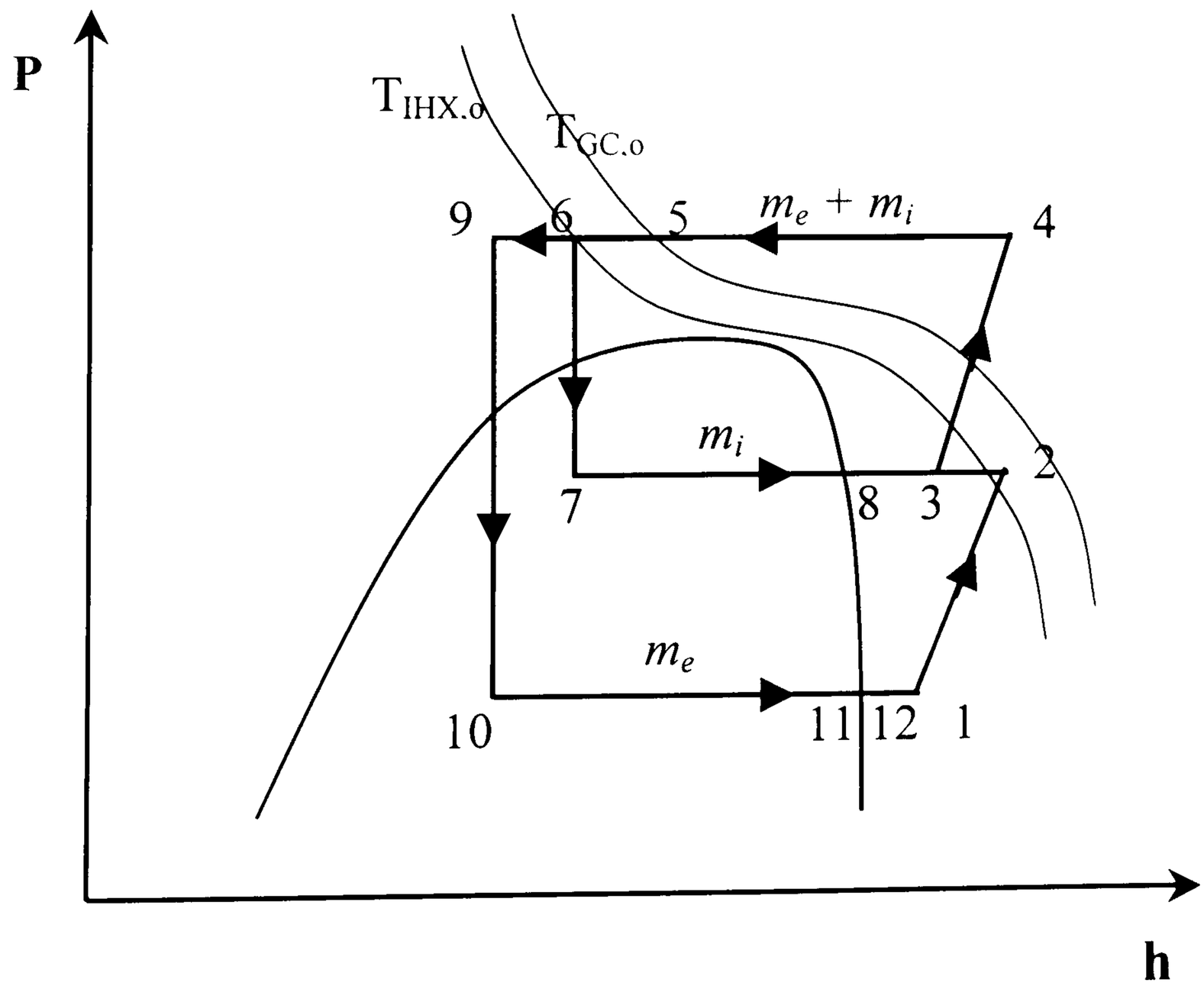

Figure 6.8 P-h diagram of transcritical two-stage CO_2 heat pump

From the evaporator outlet (12) the refrigerant is lead through the IHX to the suction line (1) of the low stage part of the two-stage compressor. From the discharge of the low stage of the two-stage compressor (2) the refrigerant is mixed with the refrigerant vapor from the SCHX (8).

From state point (3) the mixed refrigerant is compressed by the high stage of the two-stage compressor and discharged into the high stage discharge line that will lead the refrigerant to the inlet of the cooler (4). The liquid-like refrigerant leaving the cooler (5) is fed to the IHX. The highly cooled refrigerant leaving the IHX (6) is then split into two parts:

- The major part is led through the high-pressure side of the SCHX.
- A minor part is expanded (7) into the SCHX where it will evaporate (8) and thereby further cool refrigerant for the evaporator (9).

The refrigerant vapor from the SCHX (8) is mixed with the superheated refrigerant from the low stage of the two-stage compressor (4) before it is drawn into the high stage (5). The highly cooled refrigerant leaving the SCHX (9) is then expanded (10) into the evaporator.

6.3 Two-stage cycle simulation

In order to predict the performance of the two-stage transcritical CO_2 heat pump for a wide range of configurations and operating conditions, a steady-state simulation model is needed. The single-stage heat pump simulation model presented in Chapter 5 was adopted to account for multi-stage compression and accompanied intercooling.

The two-stage heat pump simulation model includes sub-models for key components: two-stage compressor, gas cooler, evaporator, expansion valve, IHX and SCHX. A Successive substitution technique is used to solve for the unknown variables resulting from the steady-state simulation of key component sub-models.

6.3.1 Performance indices

This section details the equations describing the parameters relevant to the performance criteria of the two-stage heat pump.

6.3.1.1 Compressor Performance

The compression power is the sum of indicated compressor power of each stage. PW_{ind} is calculated at each stage using the equation:

$$PW_{ind} = W_{ind} \times \frac{N}{60} \qquad \text{Eqn 6.1}$$

where, W_{ind} indicated cycle work corresponds to the area enclosed by pressure/volume curve.

The compression or indicated efficiency based on indicated work calculated from indicator diagram is described as:

$$\eta_{ind} = \frac{\Delta h_s}{\frac{m_e}{m_e + m_i} W_{ind,1} + W_{ind,2}} \qquad \text{Eqn 6.2}$$

where, Δh_s specific isentropic compressor work for LP- and HP-stages combined

The total compression power is calculated as follows,

$$PW = PW_{ind} / (\eta_{mech} \times \eta_{elec}) \qquad \text{Eqn 6.3}$$

where, η_{mech} and η_{elec} are user-specified mechanical and electrical efficiencies of the compressor and motor, respectively

6.3.1.2 Heat Pump Performance

The assessment of the heat pump is based on the derived performance data: COP and capacity. The capacity is calculated based on refrigerant actual mass flow rate and enthalpy change within the indoor heat exchanger. The COP is the ratio of the indoor heat exchanger capacity to the total compression power of the two-stage compressor.

6.3.2 Program structure

The structure of the program is similar to that developed in Chapter 5. However, some modifications were necessary to accommodate the multi-stage compression process. In the following a brief description of these modifications is outlined:

1. The evaporator mass flow rate and injected mass are initially calculated based on pre-specified swept volumes and assumed volumetric efficiencies for LP- and HP-stage compressors. The final values are calculated in subsequent steps through the compressor sub-model.
2. The intermediate pressure is a user-specified parameter.
3. The mixing process of the refrigerant vapor from the SCHX with the superheated refrigerant from the LP-stage compressor before it is drawn into the HP-stage compressor is assumed to be adiabatic and isobaric.
4. The main program calls the compressor sub-model twice to simulate the multi-stage compression. The input parameters for each call characterize the geometric parameters and relevant suction and discharge pressures of LP- and HP-stage compressors.
5. The pressure drops in the IHX and SCHX were ignored.
6. The recommendations of Beeton and Pham (2003) are assumed in the SCHX simulation. 5 K SH is assumed for proper operation of the TXV at the inlet of the SCHX. Also, 5 K TD limits the minimum LOT at the exit of the SCHX. However, the SCHX capacity calculations are based on mass flow rates generated using the compressor sub-model.

6.3.3 Simulation model validation

In order to verify the output of the simulation model experimental measurements should be applied for comparison, but data was not available. Though some descriptions have been published on the use of CO_2 as a refrigerant in low temperature stage of cascade systems, e.g. Pearson (2001), and as a secondary fluid for commercial refrigeration, there are no experimental studies found in the open literature for multi-stage vapor compression systems with CO_2 as the sole refrigerant.

In addition, no simulation models on the transcritical CO_2 vapor compression systems carried out to date account for multi-stage compression. Hence, the developed simulation model considered here represents a first attempt to assess the performance of a transcritical multi-stage CO_2 heat pump under a wide spectrum of system design parameters and different operating conditions. Through this analysis, useful data can be provided for the design of energy efficient transcritical CO_2 heat pump systems, which will positively contribute to the development of environmentally safe heat pump systems.

6.4 The simulation model application

6.4.1 System hardware construction

The hardware construction of the simulated two-stage system consists of components developed mainly for single-stage transcritical CO_2 heat pump systems. The physical characteristics of ID, OD coils and IHX are similar to the prototype units used by Richter et al. (2000) for single-stage residential heat pump. Otherwise, the hermetic reciprocating compressor developed by Fagerli (1997) is used for HP- and LP-stage compression. The displacement of the compressor is chosen to be 2.7 m^3/h at 1400 rpm. The geometrical parameters of the LP- and HP-stage compressors are similar, but the cylinder diameter of the HP-stage compressor is altered to account for a different swept volume. The details for the compressor and various heat exchangers necessary for the input data file corresponds to the relevant geometrical parameters presented in Appendix C.

6.4.2 Simulation strategy

For given HTF temperatures, the simulation strategy is based on selecting the swept volume of the HP-stage compressor. Then, the intermediate pressure is altered. As long as convergence is fulfilled for SCHX presumed design considerations, the heat pump performance indices, e.g. capacity and COP, are calculated.

In the cooling mode of heat pump operation, the gas cooler pressure corresponds to the optimum gas cooler pressure of the single-stage system derived, for the given HTF temperatures, in Chapter 5. In heating mode operation, a constant value of gas cooler pressure of 9 MPa is assumed. The effectiveness of the IHX is assumed to be 72% through out the simulation model runs. The compressor mechanical and motor electrical efficiencies are set at unity in these calculations. The option of entering more realistic values is available.

Finally, the effect of different gas cooler pressures on the heat pump performance is examined, at the given HTF temperatures.

6.4.3 Simulation results

In this section the effect of SVR and intermediate pressure on the performance of the two-stage CO_2 heat pump is discussed. The SVR is defined as the ratio of the HP-stage compressor swept volume to the LP-stage compressor swept volume. The search for optimum values of intermediate pressure/temperature and SVR is also considered. In the following, the simulation results for the transcritical two-stage CO_2 heat pump working either in cooling or heating modes under steady-state conditions are presented.

For different operating conditions the SVR was varied from 0.8 up to 1.0. The effect of intermediate pressure, related to SIT, upon COP and capacity is shown in Figures 6.9 to 6.11 for cooling mode and Figures 6.12 to 6.13 for heating mode. The upper limit of intermediate pressure is determined based on 5 K design criteria for TD. On the other hand, as the intermediate pressure decreases the evaporator mass flow increases and the refrigerant mass decreases. The lower limit of intermediate pressure is determined to ensure a positive refrigerant injected mass for intercooling.

In cooling mode operation, simulation results showed that the COP decreases linearly as the intermediate pressure increases, regardless of SVR or ID/OD temperatures. As the intermediate pressure increases the refrigerant injected mass for intercooling increases which improves the compression efficiency. Though the

compression efficiency is improved the total compression power is increased. As the intermediate pressure becomes higher the rate of compression power increase for the LP-stage compressor overcomes rate of compression power decrease for the HP-stage compressor. The variation of COP is influenced mainly by compression power.

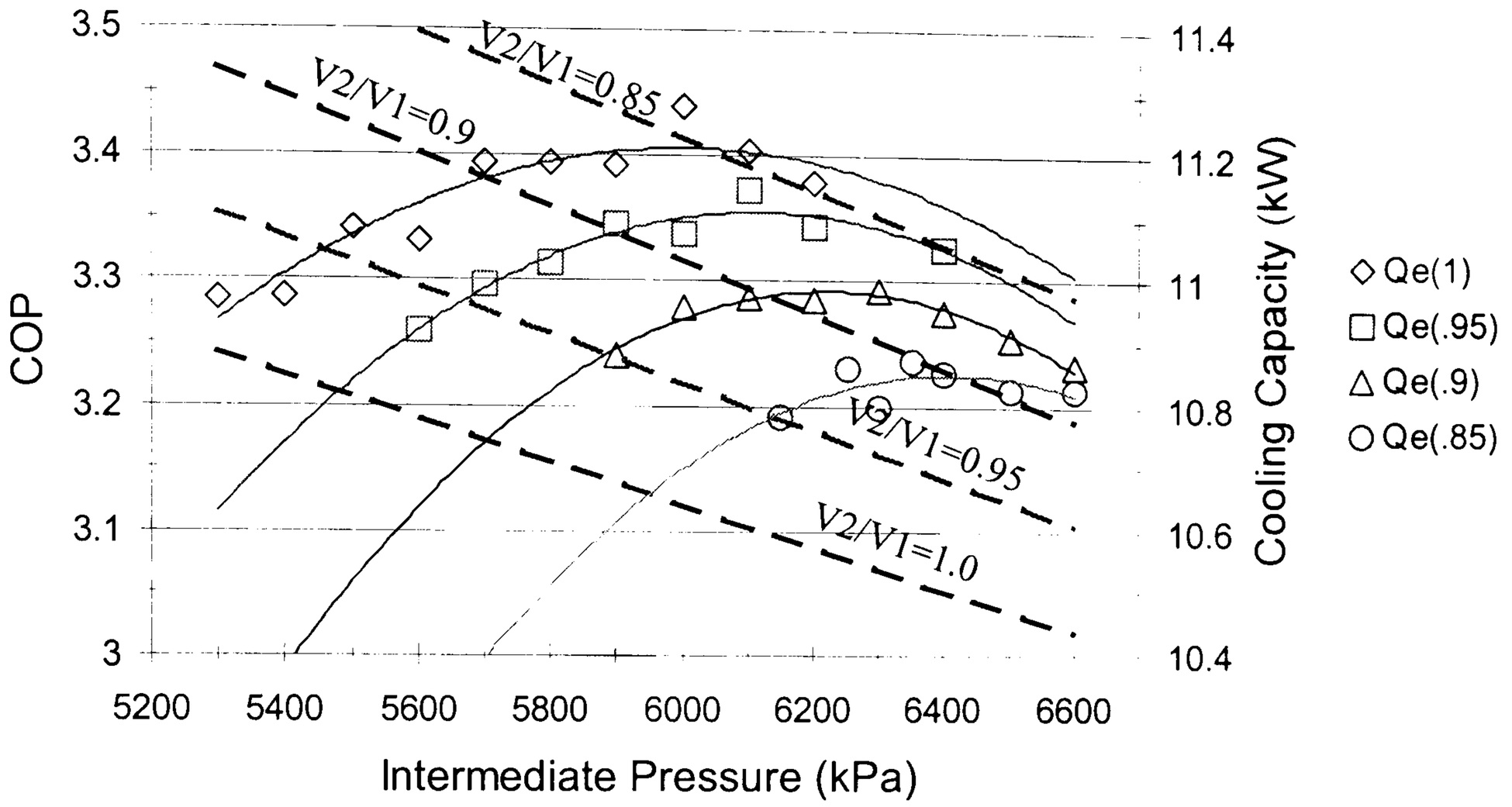

Figure 6.9 Two-stage CO_2 heat pump performance, cooling mode at ID/OD of 26.7/35 ^{0}C

Figure 6.10 Two-stage CO_2 heat pump performance, cooling mode at ID/OD of 26.7/40 ^{0}C

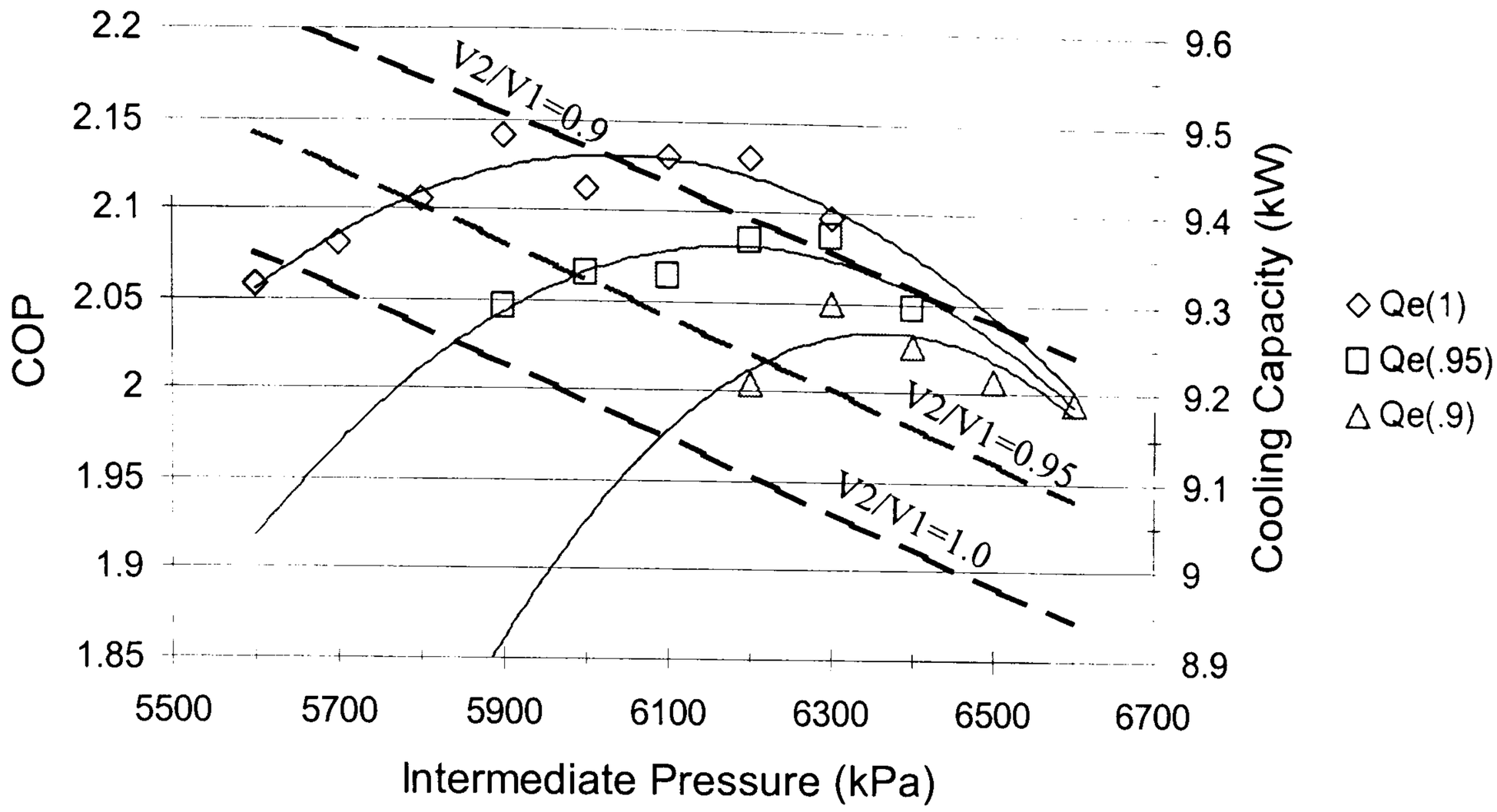

Figure 6.11 Two-stage CO_2 heat pump performance, cooling mode at ID/OD of 26.7/50 ^{0}C

In general, the cooling capacity is less sensitive, than COP, to variation of intermediate pressure. The SCHX reduces the expansion loss by decreasing the flash gas at the evaporator inlet. The increase of enthalpy change across the evaporator results in an increase of cooling capacity. However, as the intermediate pressure increases the refrigerant mass evaporated in the evaporator decreases to such an extent that the cooling capacity starts to decrease.

Unlike the cooling mode, the maximum COP for the heating mode operation is attained at the upper limit of intermediate pressure. The performance of the heat pump in the heating mode could be interpreted as follows. The increase of intermediate pressure results in a higher refrigerant mass circulating in the gas cooler. As a consequence, the heating capacity increases which leads to a higher COP even as the compression power increases.

Simulation results in Figures 6.12 and 6.13 showed that the COP is more sensitive to the variation of intermediate pressure at lower outdoor temperatures. Also, capacity increases as intermediate pressure increases, nevertheless SVR. Both COP and capacity have a linear trend with respect to variation of intermediate pressure.

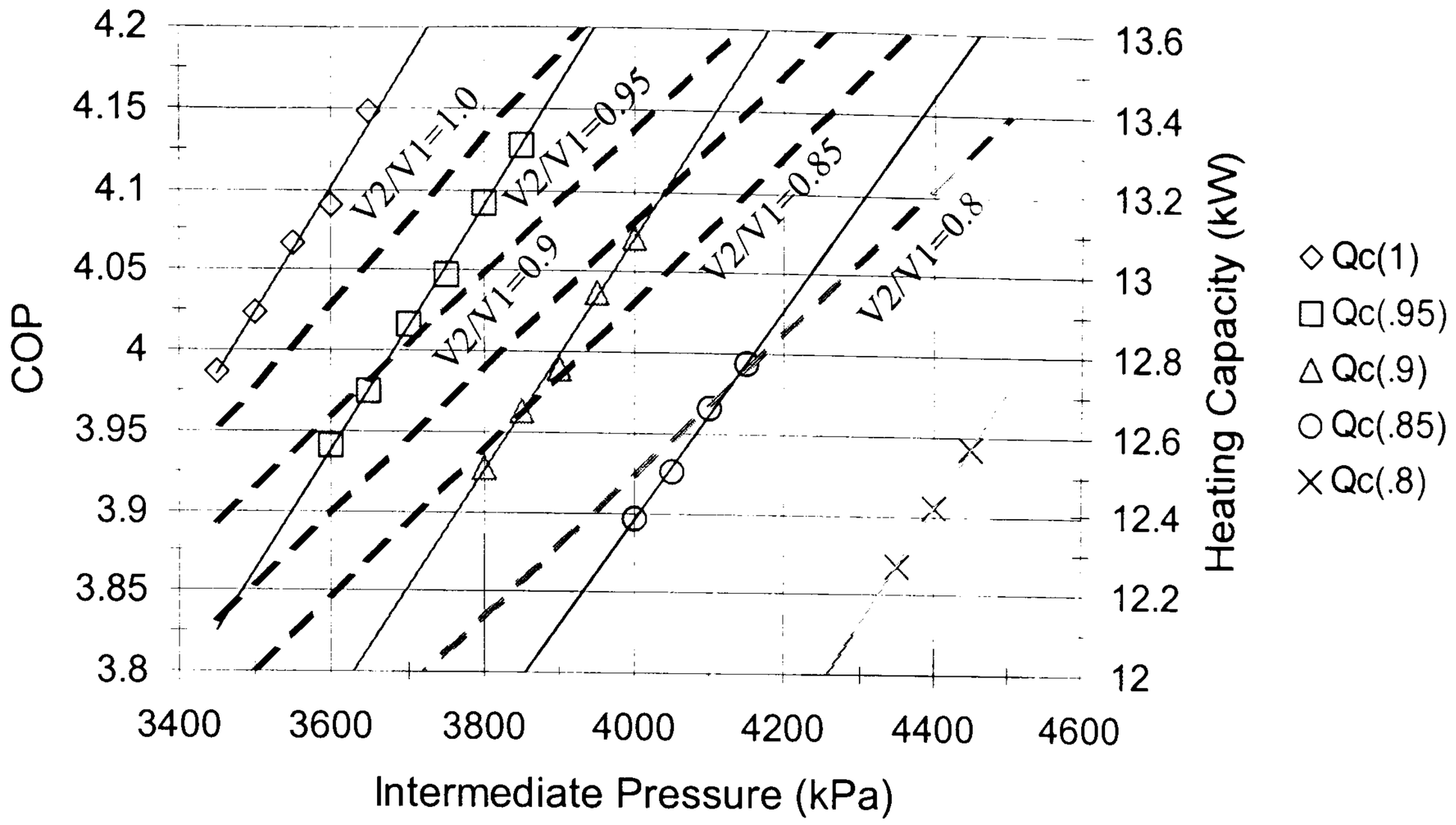

Figure 6.12 Two-stage CO_2 heat pump performance, heating mode at ID/OD of 21.1/1.7 ^{0}C

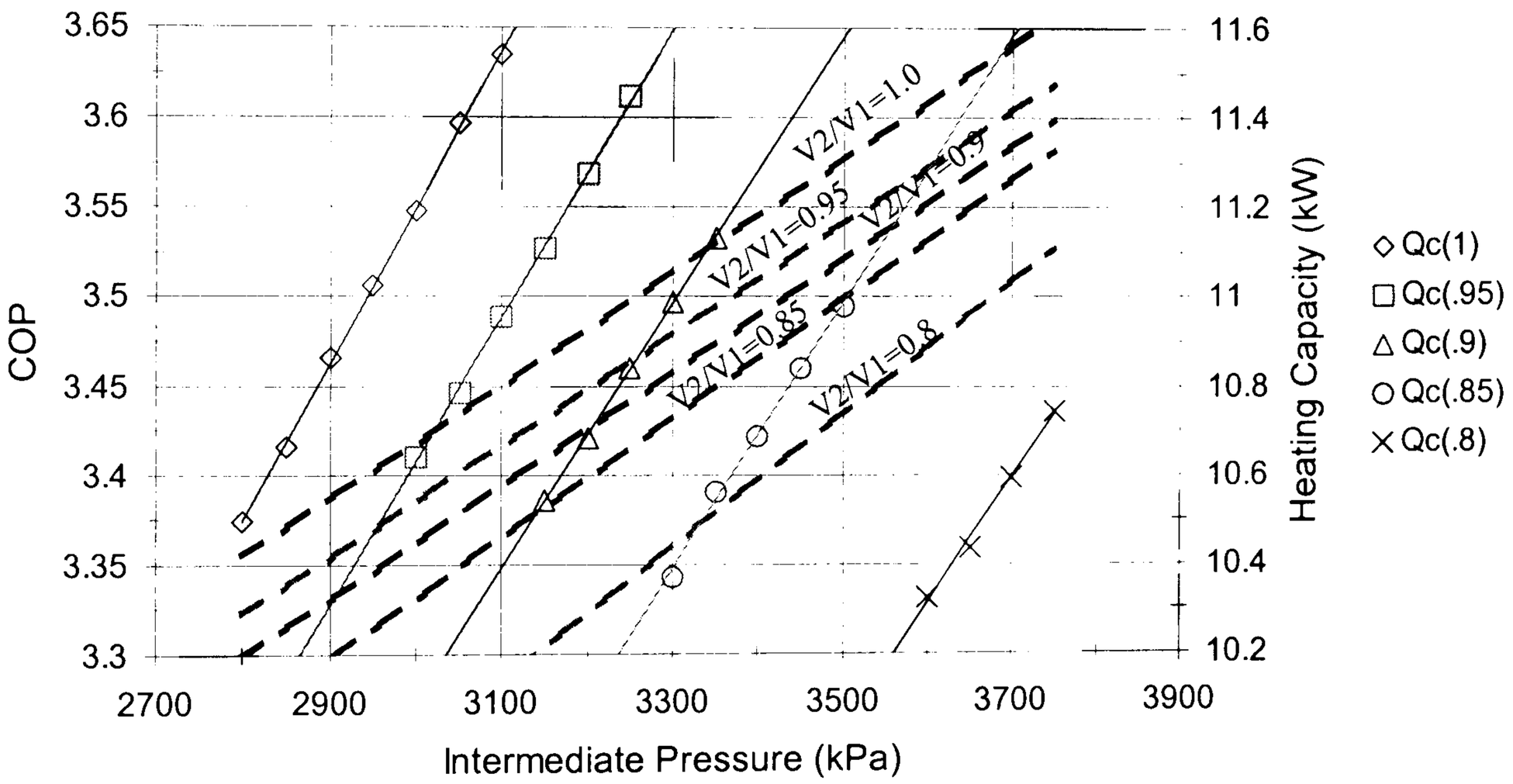

Figure 6.13 Two-stage CO_2 heat pump performance, heating mode at ID/OD of 21.1/-8.3 ^{0}C

Simulation results revealed that the optimum intermediate pressure, i.e. regarding energy efficiency depends on the operating conditions and the system design, i.e. SVR. Figures 6.14 and 6.15 shows optimum intermediate pressure for different outdoor conditions and SVR. In general, the optimum intermediate pressure increases as SVR decreases. This trend is preserved for both cooling and heating modes of operation.

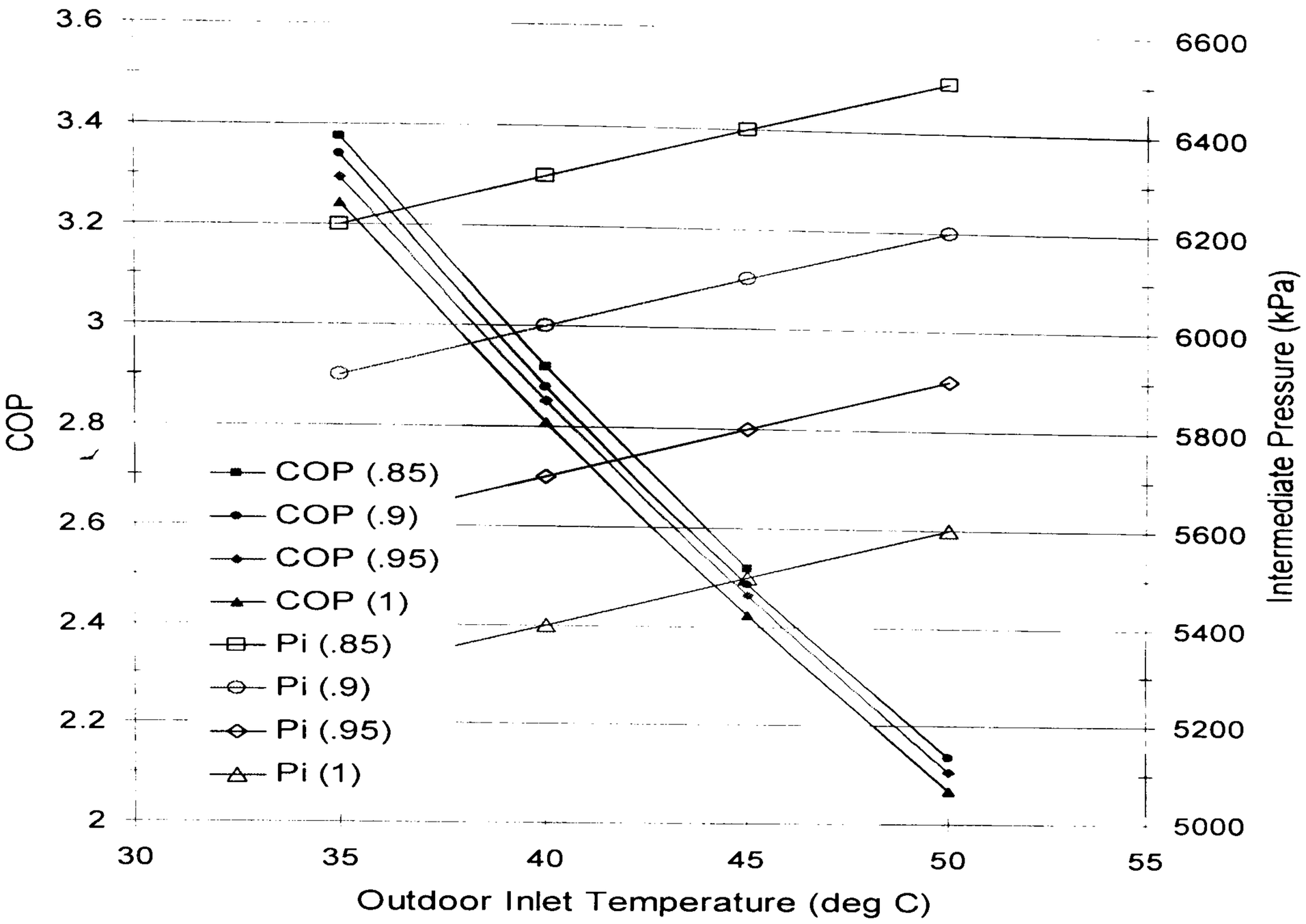

Figure 6.14 Optimum COP of two-stage CO_2 heat pump in cooling mode

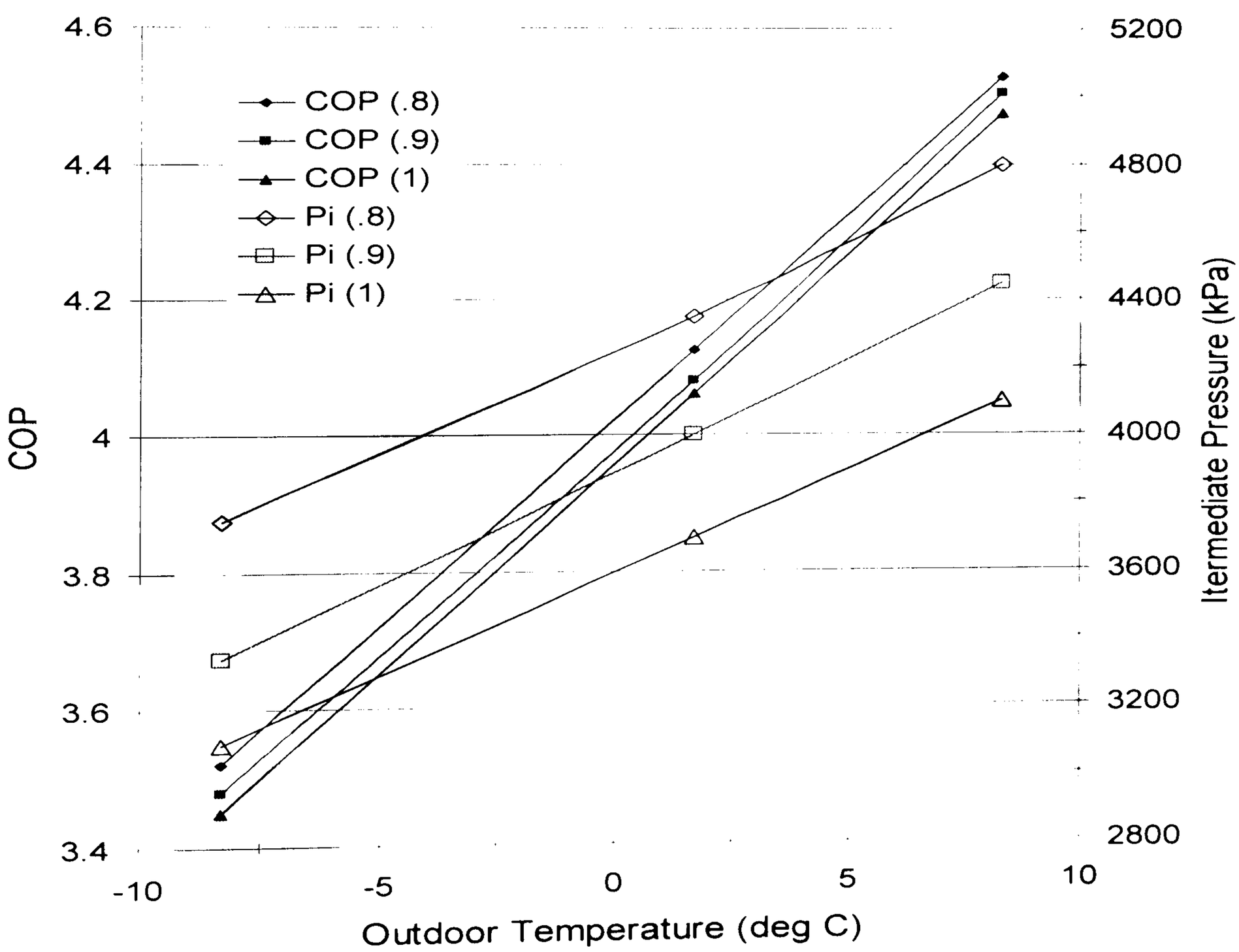

Figure 6.15 Optimum COP of two-stage CO_2 heat pump in heating mode

The most interesting of these results is the linear trend of optimum intermediate pressure with respect to outdoor temperature at different SVR. Based on these results, it is possible to determine a control function. This function is used to adjust the intermediate pressure such that the system can be run with a maximum COP. The simplest correlation for this function is a linear relation. Also, this function could be generalized to account for different SVR and OD temperatures. Moreover, the maximum COP of such systems at different OD temperatures could be expressed as a function of intermediate pressure and SVR.

The simulation of a SCHX type two-stage heat pump circuit has shown impressive changes in system performance compared with a conventional, i.e. single-stage, system. In general, simulation results showed a significant increase in COP and capacity while using the gas cooler, evaporator and compressor components from the conventional system.

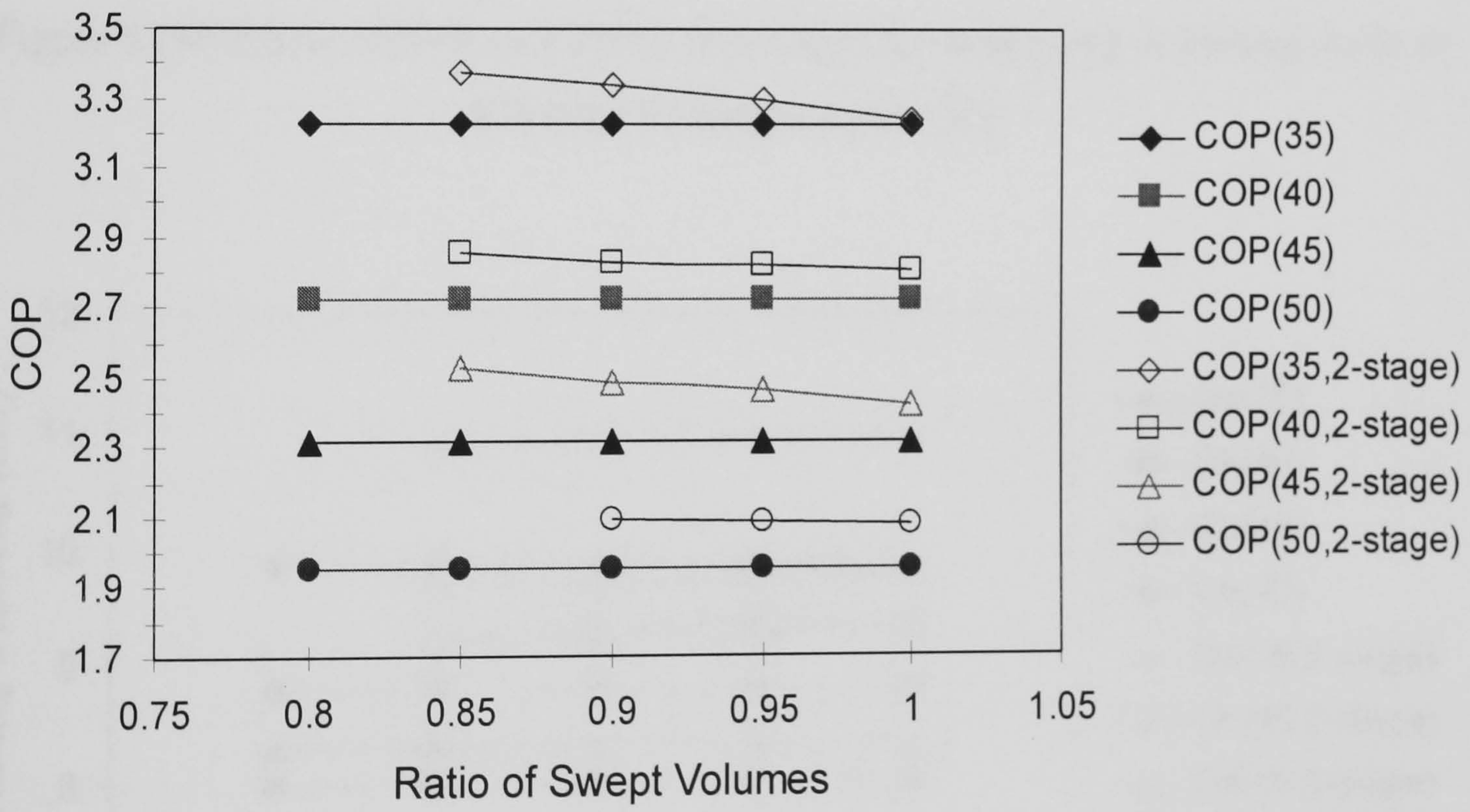

Figure 6.16a Effect of SVR on COP of two-stage CO_2 heat pump in cooling mode at different OD temperatures (^{0}C)

Figures 6.16a and 6.16b show that COP improvement due to multi-staging is less significant at high SVR. Maximum COP is achieved at lower SVR. COP

improvement in heating mode is more pronounced than that in cooling mode. However, COP of the two-stage system operating with SCHX surpasses that of the conventional single-stage system.

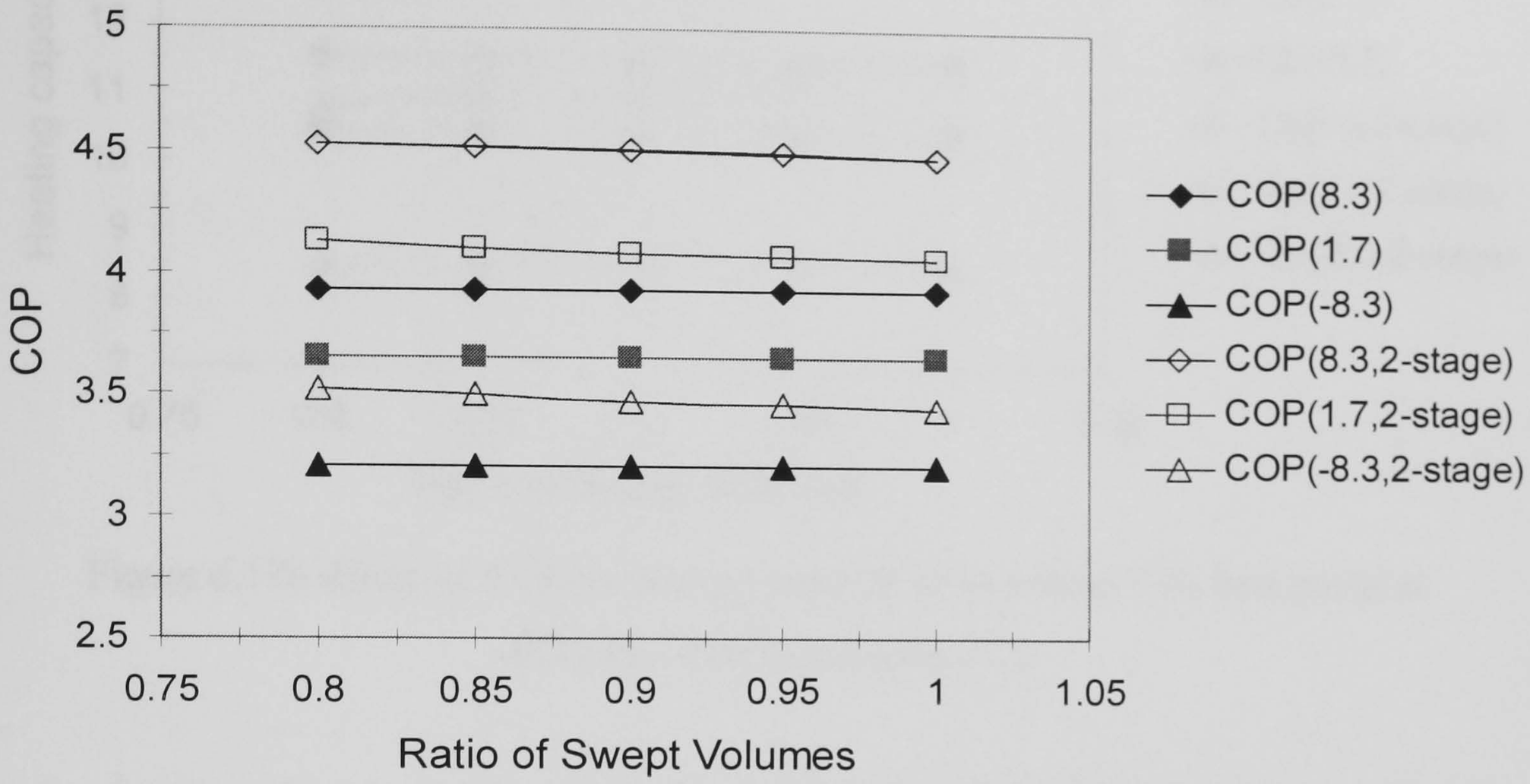

Figure 6.16b Effect of SVR on COP of two-stage CO_2 heat pump in heating mode at different OD temperatures (^{0}C)

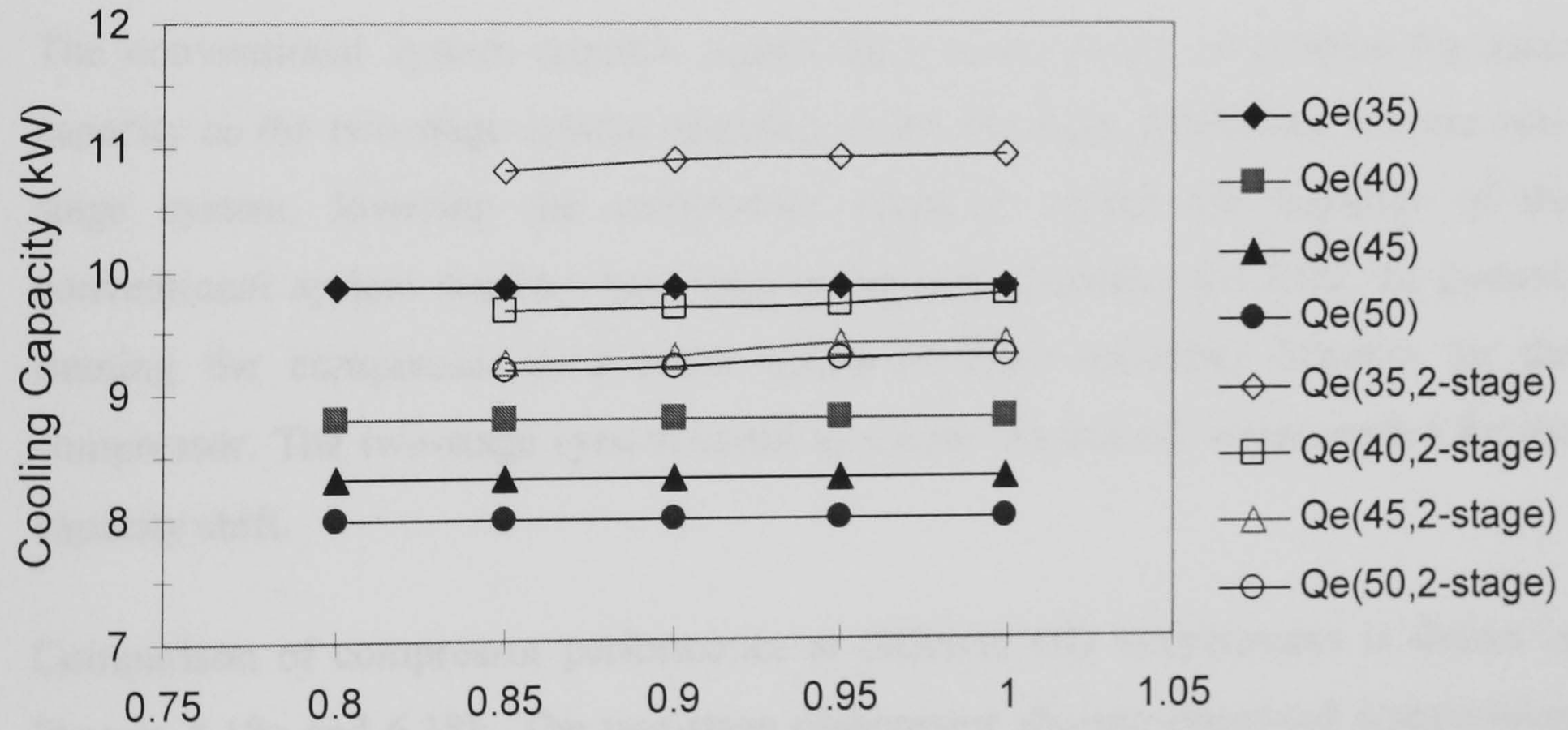

Figure 6.17a Effect of SVR on cooling capacity of two-stage CO_2 heat pump at different OD temperatures (^{0}C)

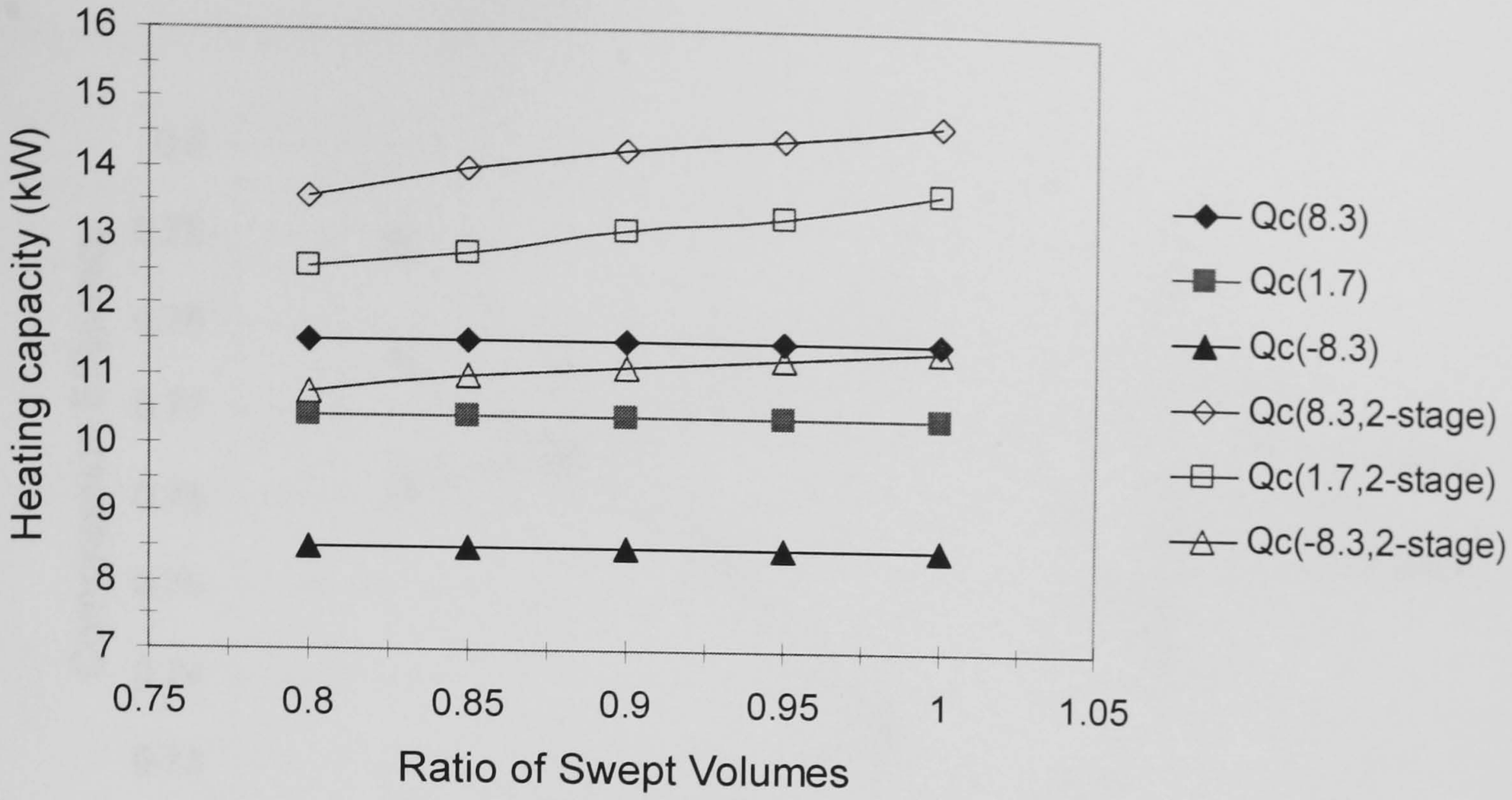

Figure 6.17b Effect of SVR on heating capacity of two-stage CO_2 heat pump at different OD temperatures (^{0}C)

As shown in Figures 6.17a and 6.17b, the SCHX will increase the capacity of the system apparently. The greater the SVR is, the higher the capacity will be. However, it does this at the expense of higher input power requirements even with improved compression efficiency.

The conventional system requires significantly more power to produce the same capacity as the two-stage system operating under the same conditions. For the two-stage system, lowering the compressor speed to match the capacity of the conventional system requires less input power and increases the COP. In general, running the compressor at a lower speed provides reliability benefits for the compressor. The two-stage system could be cycled on and off when needed for the capacity shift.

Comparison of compressor performance at different OD temperatures is shown in Figures 6.18a and 6.18b. The two-stage compressor showed improved compression efficiency throughout the operating range. This is true especially at low outdoor temperature. The compression efficiency of the two-stage compressor drops at higher OD temperature due to increasing pressure ratio and absolute decrease of refrigerant injected mass for intercooling.

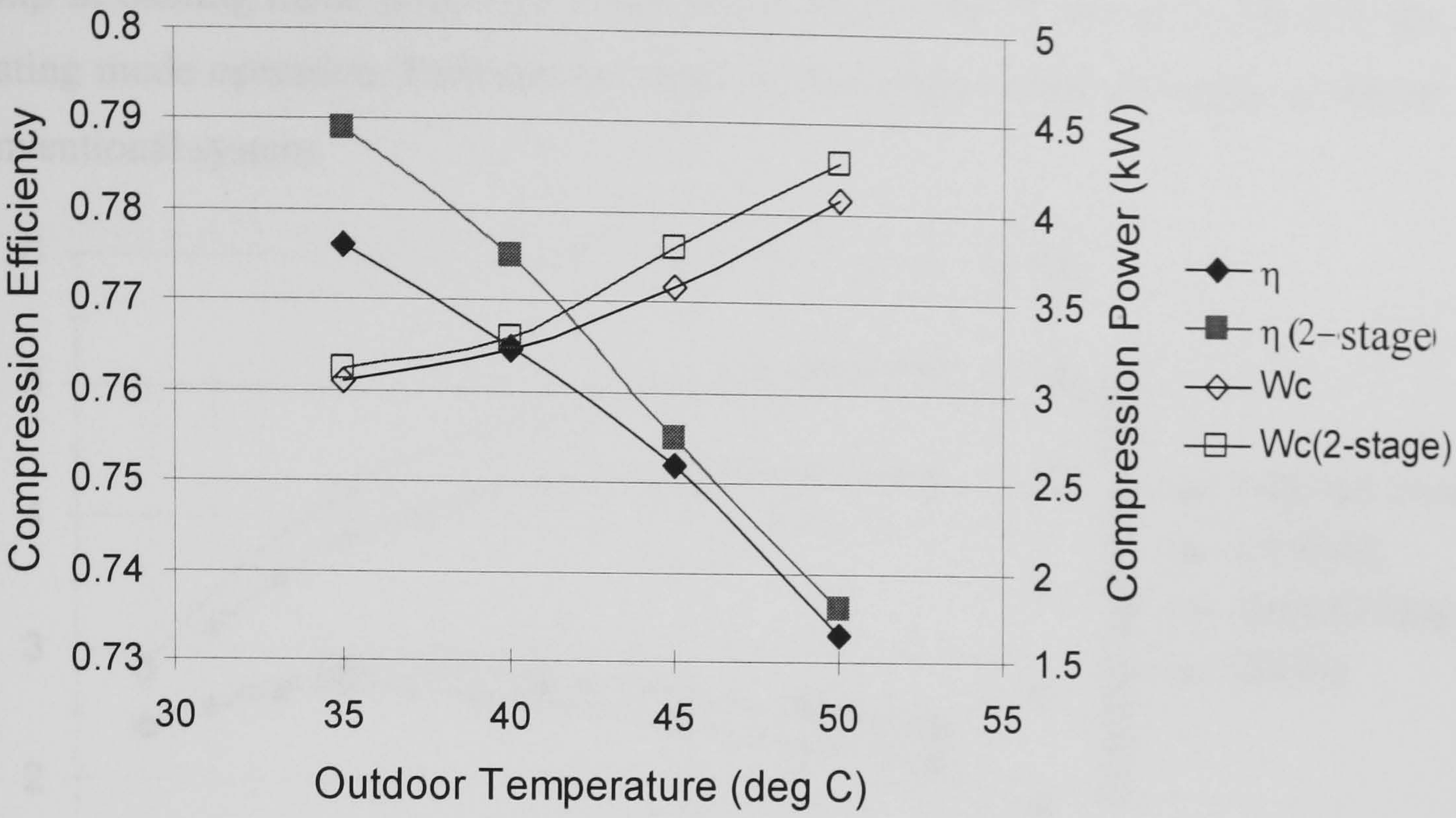

Figure 6.18a Compression efficiency and compression power of single- and two-stage CO_2 heat pump, cooling mode

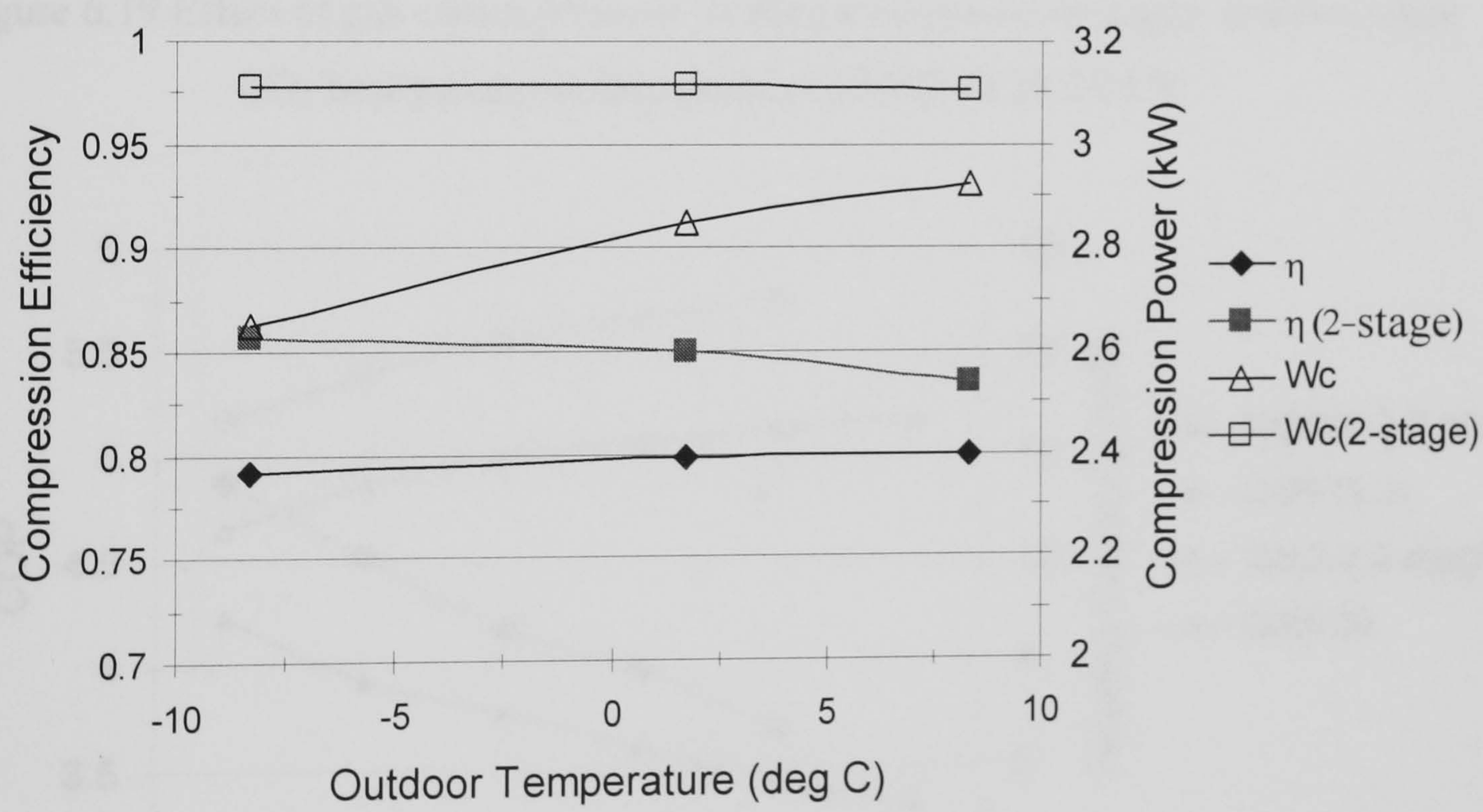

Figure 6.18b Compression efficiency and compression power of single- and two-stage CO_2 heat pump, heating mode

Figures 6.19 and 6.20 show the influence of gas cooler pressure variations for heat pump in cooling mode at ID/OD temperatures of 26.7/40 ^{0}C and at 21.1/8.3 ^{0}C for heating mode operation. Performance trend of two-stage system is similar to that of conventional system.

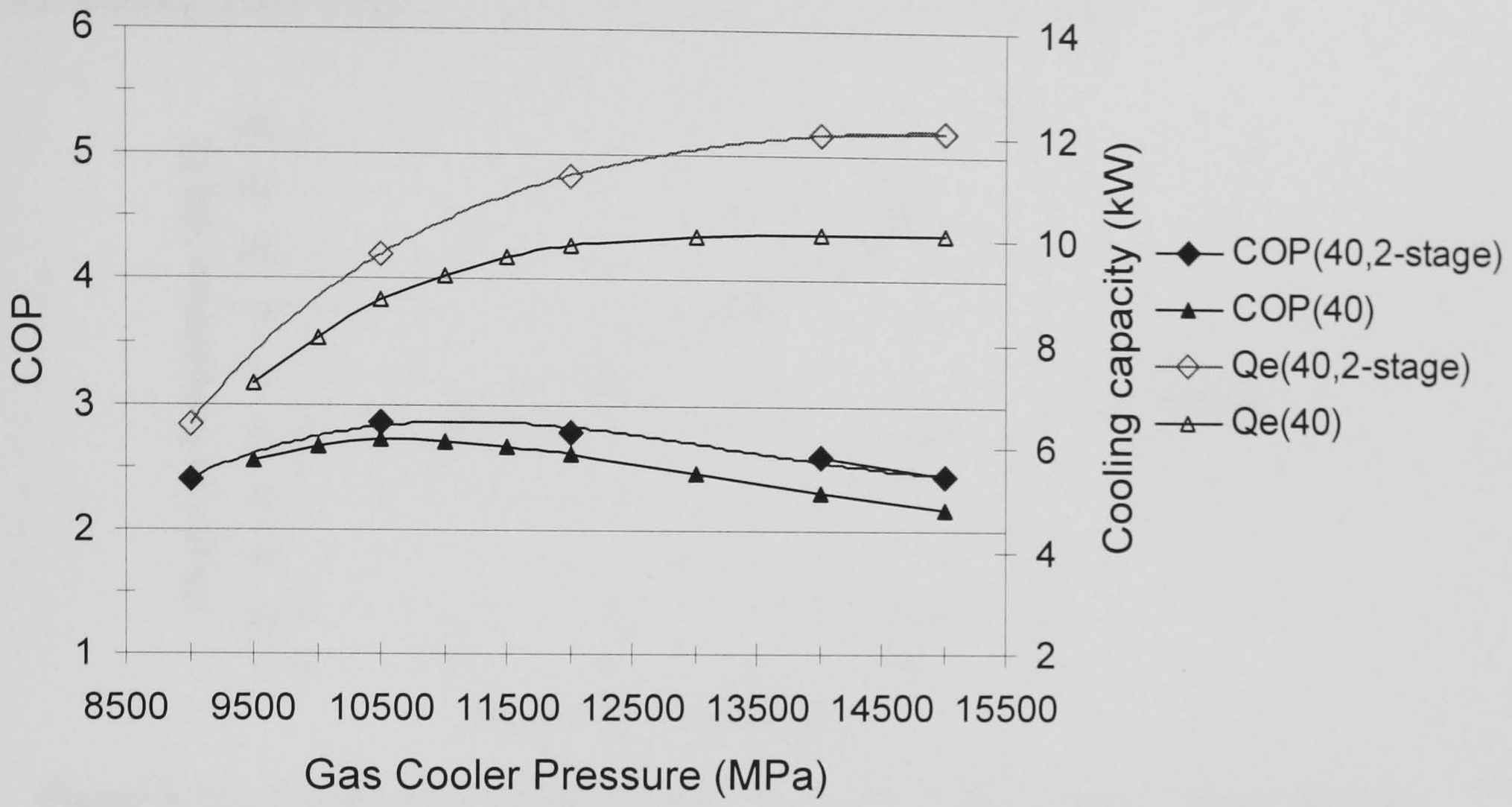

Figure 6.19 Effect of gas cooler pressure on the performance of single- and two-stage CO_2 heat pump, cooling mode at ID/OD of 26.7/35 ^{0}C

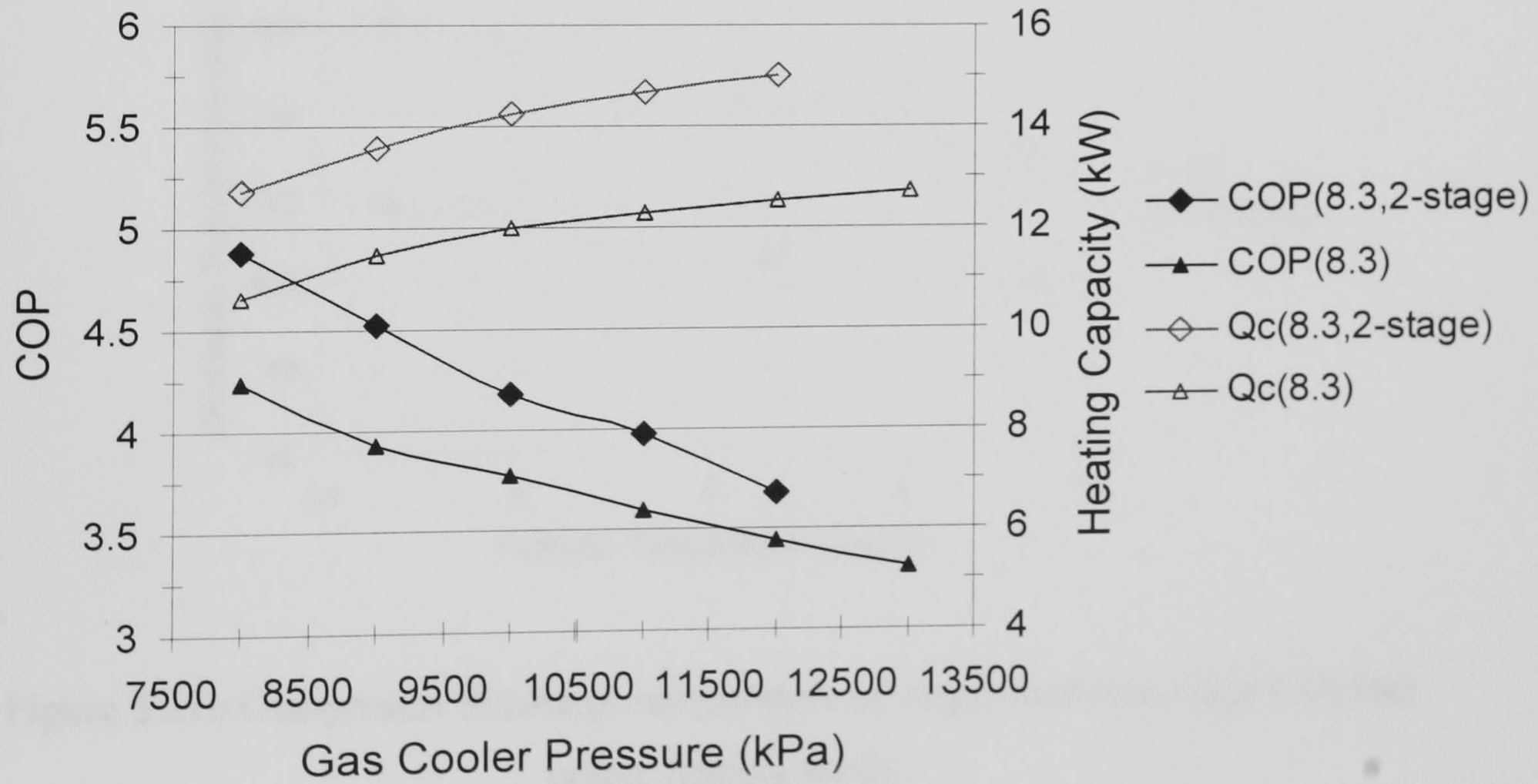

Figure 6.20 Effect of gas cooler pressure on the performance of single- and two-stage CO_2 heat pump, heating mode at ID/OD of 21.1/8.3 ^{0}C

Further benefits for the two-stage system are shown in Figures 6.21 and 6.22. Figure 6.21a and 6.21b show the decrease in compressor discharge refrigerant temperature observed with the two-stage system. This was a larger shift for the heating mode than for the cooling mode. The benefit of two-stage compression is more pronounced for the heating mode where an overall higher pressure ratio is needed.

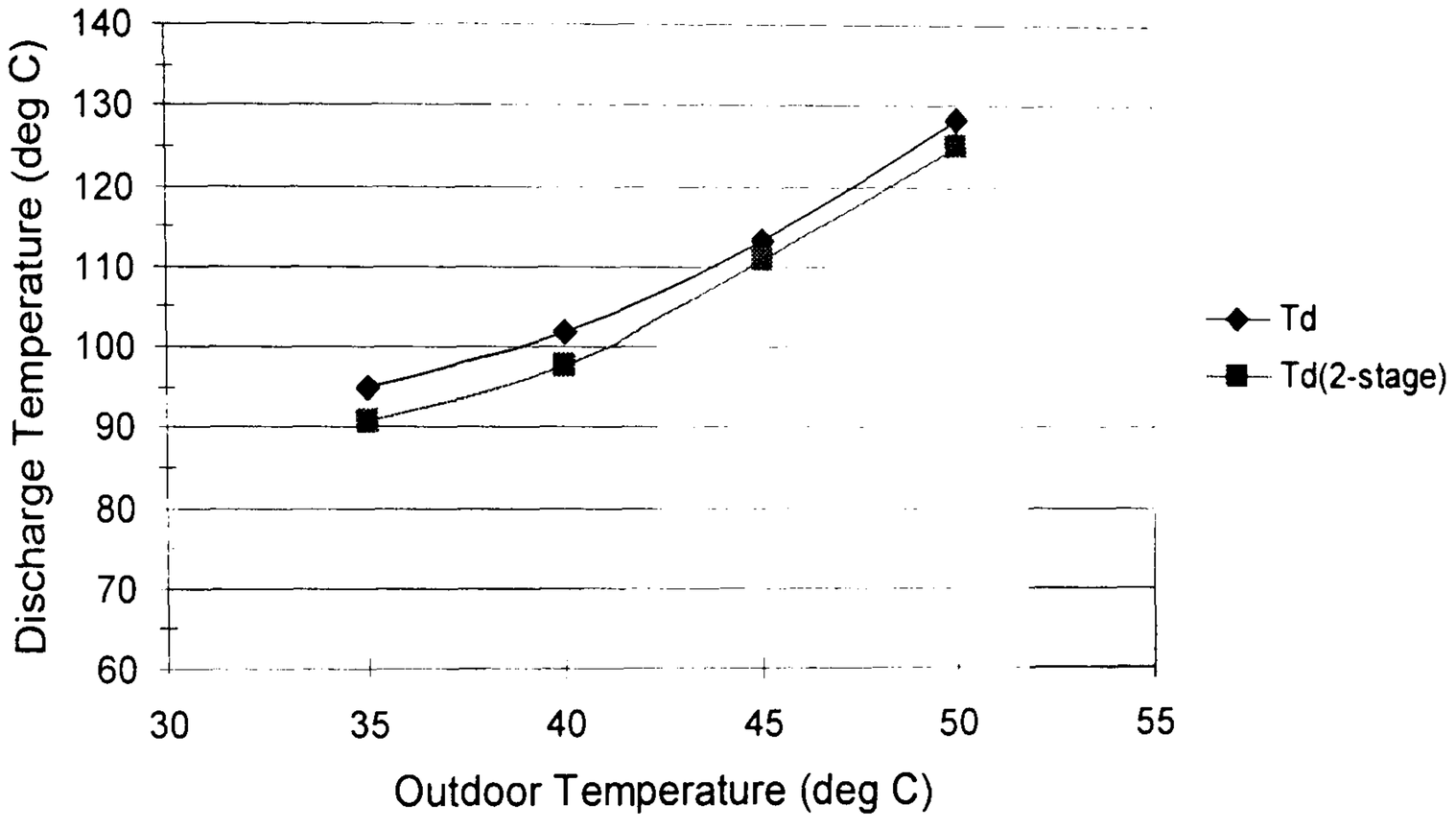

Figure 6.21a Compressor discharge temperature of single- and two-stage CO_2 heat pump, cooling mode

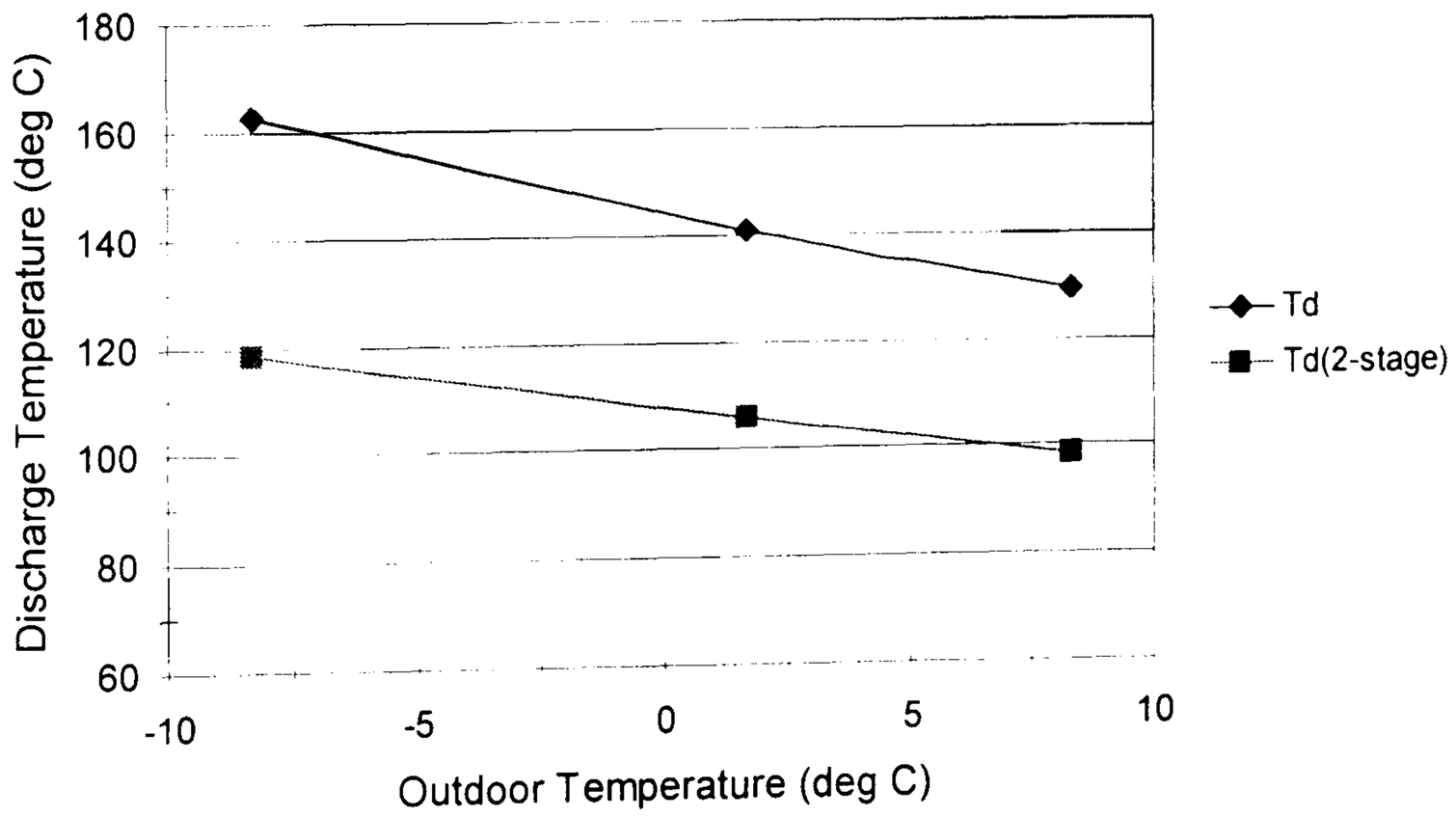

Figure 6.21b Compressor discharge temperature of single- and two-stage CO_2 heat pump, heating mode

The simulation results for a two-stage transcritical CO_2 heat pump at various piston ring clearances show that benefit over the single stage system can be attained. Figure 6.22 shows that the capacity of two-stage system was found to be 7-60% higher than capacity of the conventional single-stage system as it simultaneously provides 2-30% improvement in COP. Maximum difference was obtained at higher clearance. The comparison was made at ID/OD temperatures of 26.7/35 ^{0}C.

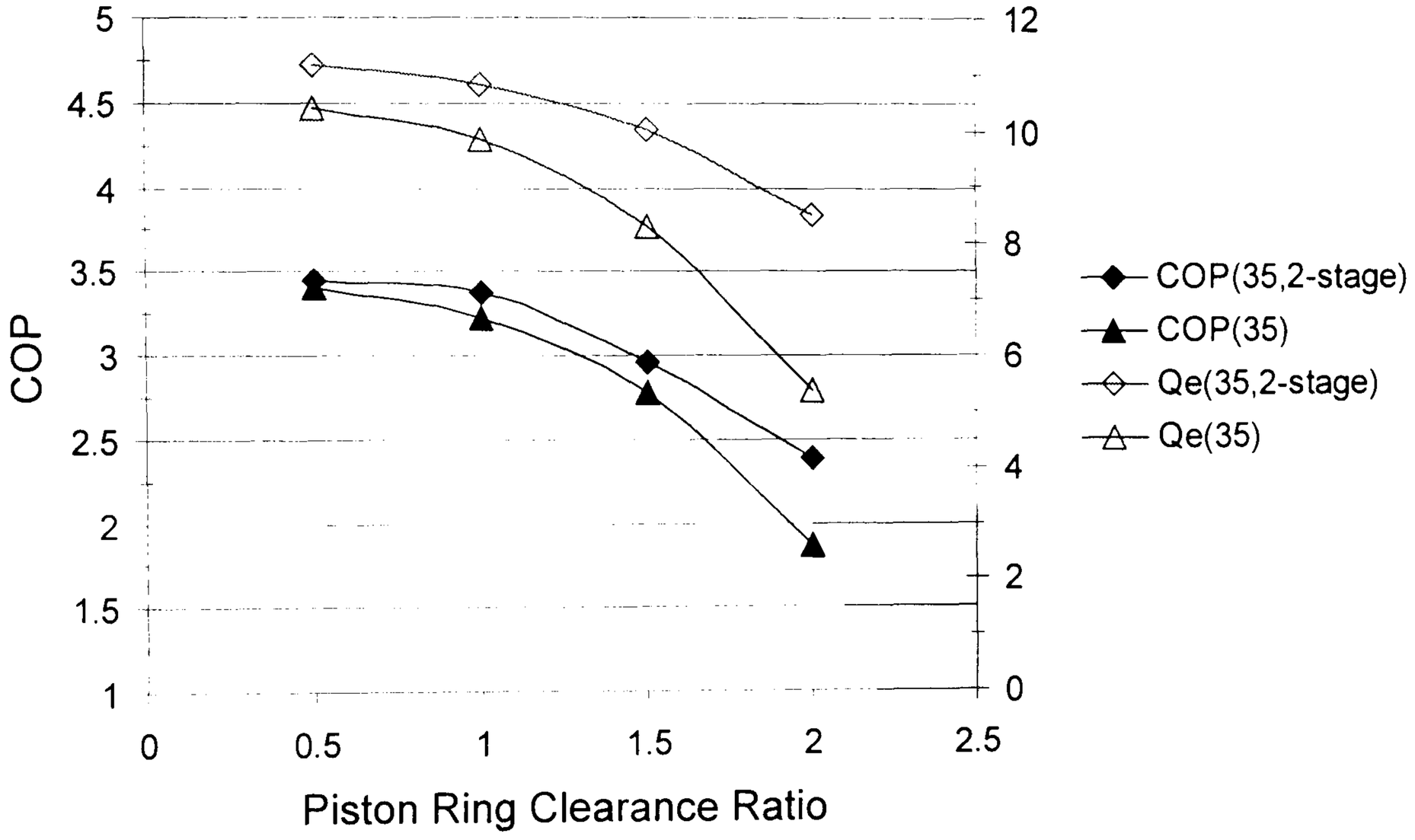

Figure 6.22 Effect of piston ring clearance on the performance of single- and two-stage CO_2 heat pump, cooling mode at ID/OD of 26.7/35 ^{0}C

Chapter 7

Conclusions

& Recommendations For Future Work

7.1 General

Prior to this study, there were no models known to the author for CO_2 heat pumps which simulate the compression process using a detailed reciprocating compressor model. Furthermore, there were no models for CO_2 heat pumps incorporating multi-stage compression, with or without detailed compressor models.

The author believes that the work reported here is a contribution to knowledge in the field of heating / cooling systems which have CO_2 as the working fluid. In addition, the models presented will be of value to other research workers and plant designers. Plant operators may also find the models valuable for the study of behaviour trends.

7.2 Conclusions

7.2.1 Compressor model

- The behaviour indicated by the compressor model is broadly in accord with that expected of a reciprocating compressor and reported by many other workers.
- Due to the high pressure differences at which carbon dioxide compressors operate, the study of piston ring-cylinder leakage is particularly important.
- Ring-cylinder clearance represents the influences of ring geometry, manufacturing tolerances and/or wear. Increasing the clearance had a large effect on the pressure-volume diagram as expected, but the effect on the valve motion was also significant. The model should be of value in investigating the influence of manufacturing tolerances and ageing, i.e. wear.

7.2.2 Single-stage transcritical CO_2 heat pump model

- The model is a useful tool for investigating the characteristics of such systems for design and performance purposes (chapter 5). Given that it incorporates a detailed compressor simulation, it is particularly useful for investigating the influence of compressor design and operational features.
- Suction valve maximum lift has a greater effect on COP than discharge maximum lift, but the effect of either on capacity, is insignificant.
- Valve moving mass, spring stiffness and flow area have a large influence on valve dynamics but very little on thermodynamic performance.
- Thermodynamic behaviour, particularly COP, is very sensitive to piston ring-cylinder clearance.

7.2.3 Two-stage transcritical CO_2 heat pump model

- The cooling mode COP decreases linearly with increasing intermediate pressure, regardless of swept volume ratio or ID/OD temperatures; capacity is less sensitive.
- Heating mode COP rises with intermediate pressure, reaching a maximum at high values; its sensitivity to changes in the intermediate pressure is greater at lower values of OD temperatures than at higher values.
- The intermediate pressure at which energy efficiency in general is highest depends on the operating conditions and swept volume ratio. The model could be used to determine a control function by means of which the intermediate pressure is adjusted to seek maximum energy efficiency. The function could be generalised to take into account OD temperatures and swept volume ratios for example.
- The two-stage system requires less power for the same conditions and capacity than the single stage system. However, the improvement reduces as the swept volume ratio increases.
- Compressor efficiency is greater for the two-stage system for the same range of OD temperatures, particularly at low OD temperatures.
- For a given range of piston ring-cylinder clearances the loss of efficiency and capacity are considerably less for the two-stage than for the single-stage system;

the two-stage system was 7 to 60% higher in capacity and 2 to 30% higher in COP. The difference between the two systems was greatest at the highest clearance. Hence it may be concluded that two-stage systems, being less sensitive to wear than single stage systems, will have a longer service life.

7.3 Recommendations for future work

7.3.1 Compressor model

Similarly detailed models for other compressor types such as scroll, rotary etc would be an advantage so that other workers could make compressor comparisons and also heat pump comparisons with other compressor types in use.

7.3.2 Single-stage heat pump

Single-stage CO_2 water heaters are already successful in the marketplace. To make this cycle competitive for other applications, development is needed. Work recovery from the expansion process should be given attention, in combination with improved internal heat exchange. Work recovery from the expansion is particularly attractive because it simultaneously reduces the power needed for compression while improving evaporator efficiency and capacity by supplying wetter gas at the evaporator inlet.

7.3.3 Two-stage heat pump

The two-stage cycle is of course an alternative to the single-stage cycle and could compete with conventional systems if improved in efficiency, reliability and first cost. Hence future work is required in these areas. Benefit could be obtained by paying attention to the following areas of concern:

- More effective internal heat exchange, including other configuration concepts for intercooling.
- More realistic simulations for the external heat exchangers; in the models presented here for the heat transfer to/from the fluids (air and water) providing

the hot/cold sinks, simple concepts are used. Closer attention to the physics of these processes could provide benefits.

- There is a pressing need for experimental work on trial two-stage cycles. The creation and testing of different cycle configurations conveniently and quickly would greatly assist general progress and, of course, provide much need validation for the models. A cycle is proposed and discussed in chapter 6.

REFERENCES

Aarlien R, Frivik P E. Comparison of practical performance between CO_2 and R-22 reversible heat pumps for residential use. *Proc Int Conf IIR. Natural working fluids '98,* Oslo Norway, 1998, p.341.

Aarlien R, Pettersen J, Skaugen G, Neksa P. Residential air conditioning with CO_2 – preliminary results. *Proc Int Conf IIR, Applications for natural refrigerants*, Aarhus, Denmark, 1996, p.659.

Adair R P, Qvale E B, Pearson J T. Instantaneous heat transfer to the cylinder wall in reciprocating compressors. *Proc Int Compressor Eng Conf at Purdue,* West Lafayette USA, 1972, p.521.

Adolph U. Possibilities and limits of using natural refrigerants in air conditioning systems for railway cars. *Proc Int Conf IIR, New applications for natural working fluids in refrigeration and air conditioning,* Hanover, Germany, 1994, p.477.

Annand W J. Heat transfer in the cylinders of reciprocating internal combustion engines. *Proc IMechE*, 1963; 117: 973.

Arora C P, Dhar P L. Optimization of multi-stage refrigerant compressors. *Proc IIR/IIF 13th Int Congress of refrigeration,* Paris, France, 1971, Vol II, p.693.

Arzano-Daurelle C, Clodic D, Hivet B. Compressor model for open reciprocating compressor, application to cylinder wall cooling study. *Proc Int Compressor Eng Conf at Purdue,* West Lafayette USA, 1998, p.865.

Baek J S, Groll E A, Lawless P B. Development of a piston-cylinder expansion device for the transcritical carbon dioxide cycle. *Proc Int Refrigeration Conf at Purdue,* West Lafayette USA, 2002a.

Baek J S, Groll E A, Lawless P B. Effect of pressure ratios across compressors on the performance of the transcritical carbon dioxide cycle with two-stage compression

and intercooling. *Proc Int Refrigeration Conf at Purdue,* West Lafayette, USA. 2002b.

Baskov V L, Kurave I V, Protopopov V S. Heat transfer with turbulent flow of a liquid under supercritical pressure in tubes under cooling conditions. *High Temperature,* 1977; 15 (1): 81.

Bauer F. The influence of liquids on compressor valves. *Proc Int Compressor Eng Conf at Purdue,* West Lafayette USA, 1990, p.647.

Baumann H, Conzett M. Small oil free piston type compressor for CO_2. *Proc Int Compressor Eng Conf at Purdue,* West Lafayette USA, 2002.

Beaver A, Yin J, Bullard C W, Hrnjak P S. Experimental and model study of the heat pump/air conditioning systems based on transcritical cycle with R 744. *Proc IIR/IIF 20th Int Congress of refrigeration,* Sydney, Australia, 1999.

Beeton W L, Pham H M. Vapor-injected scroll compressors. *ASHRAE J,* April 2003, p. 22.

Bennett D L, Chen J C. Forced convective boiling in vertical tubes for saturated pure components and binary mixtures. *AIChE J.* 1980; 26: 454.

Blackhurst D R. CO_2 v NH_3, a comparison of two systems. *Proc Institute of Refrigeration,* London, UK, 2002.

Blankespoor H J, Touber S. Computer simulation of a one-cylinder reciprocating compressor using a hybrid computer. *Proc Int Compressor Eng Conf at Purdue,* West Lafayette USA, 1972, p.506.

Boewe D E, Bullard C W, Yin J M, Hrnjak P S. Contribution of internal heat exchanger to transcritical R-744 cycle performance. *ASHRAE Transactions*: Research 4473, 2001.

Böswirth L. A model for valve flow taking non steady flow into account. Part I, II *Proc Int Compressor Eng Conf at Purdue,* West Lafayette USA, 1984, p.227.

Böswirth L. A new valve dynamics simulation program and its use for the design of valves. *Proc Int Compressor Eng Conf at Purdue,* West Lafayette USA, 1996, p.365.

Böswirth L. Non steady flow in valves. *Proc Int Compressor Eng Conf at Purdue,* West Lafayette USA, 1990, p.664.

Boyle R J. Valve design optimisation for a 3-cylinder semi-hermetic reciprocating refrigeration compressor. *PhD Thesis*, Department of Thermodynamics and Fluid Mechanics, University of Strathclyde, 1985.

Brablik J. Computer simulation of the working process in the cylinder of a reciprocating compressor with piping system. *Proc Int Compressor Eng Conf at Purdue,* West Lafayette USA, 1974, p.151.

Braendgaard T. Test of an open reciprocating compressor operating as low-stage compressor in a R744/R717 cascade system. *Proc Int Conf IIR, Applications for natural refrigerants,* Aarhus, Denmark, 1996, p.623.

Bredesen A M et al. Heat transfer and pressure drop for in-tube evaporation of CO_2. *Proc Int Conf, Heat transfer issues in 'natural' Refrigerants.* Maryland, USA, Vol. 1, 1997a, p. 1.

Bredesen A M. Computer simulation of valve dynamics as an aid to design. *Proc Int Compressor Eng Conf at Purdue,* West Lafayette USA, 1974, p.171.

Brendeng E. CO_2 in the low temperature stage of large industrial refrigerating plants. *Workshop Proc IEA/IIR, CO_2 technology in refrigeration, heat pump and air conditioning systems,* Trondheim, Norway, 1997, p.103.

Brok S W, Touber S, van der Meer J S. Modelling of cylinder heat transfer-large effort, little effect? *Proc Int Compressor Eng Conf at Purdue,* West Lafayette USA, 1980, p.43.

Brown J, Lough A, Pringle S, Karll B. Oil stiction in automatic compressor valves. *Proc IIR 14th Congr of Refrigeration,* Moscow Russia, 1975.

Brown J, Pearson S F. Piston leakage in refrigeration compressors. *J Refrig.* 1963; 7:104.

Brown S J, Domanski P A. Semi-theoretical simulation model for a transcritical carbon dioxide mobile A/C system. *Proc SAE Int Congress and Exposition.* 2000. paper 2000-01-0985.

Brown S J, Kim Y, Domanski P A. Evaluation of carbon dioxide as R-22 substitute for residential air-conditioning. *ASHRAE Transactions*: Symposia. HI-02-13-3. 2002a.

Brown S J, Yana-Motta S F, Domanski P A. Comparative analysis of an automotive air conditioning systems operating with CO_2 and R134a. *Int J Refrig.* 2002b; 25 (1): 19.

Bukac H. Optimum piston bore fit for maximum compressor efficiency. *Proc Int Compressor Eng Conf at Purdue.* West Lafayette USA, 2000, p.523.

Bullard C W, Hrnjak P S. Comparing CO_2 to HFCs for mobile a/c and residential heat pumps. *Workshop Proc IEA/IIR, CO_2 technology in refrigeration heat pump and air conditioning systems,* Trondheim, Norway, 1997, p.33.

Bullard C W, Yin J M, Hrnjak P S. Compact counterflow gas cooler for R-744. *ASHRAE Transactions*: Symposia. AC-02-1-3, 2002.

Bullard C W, Yin J M, Hrnjak P S. Transcritical CO_2 mobile heat pump and a/c system experimental and model results. *Proc SAE automotive alternative refrigerant systems symposium,* Arizona, USA, 2000.

Bullock C E. Theoretical performance of carbon dioxide in subcritical and transcritical cycles. *ASHRAE/NIST Refrigerants Conf*, Gaithersburg, USA, 1997, p.20.

Casson V et al. Optimisation of the throttling system in a CO_2 refrigerating machine. *Int J Refrig.* 2003; 26 (8): 926.

Cavallini A, et al. Thermal analysis of a hermetic reciprocating compressor. *Proc Int Compressor Eng Conf at Purdue,* West Lafayette USA, 1996, p.535.

Cavallini A. Working fluids for mechanical refrigeration. *Int J Refrig.* 1996; 19 (8): 485.

Cengel Y A, Boles M A. Thermodynamics: an engineering approach. 2nd ed., McGraw-Hill Inc., 1994.

Chen J C. A correlation for boiling heat transfer to saturated fluids in vertical flow. *Ind Eng Chem Process Design Develop.* 1966; 5 (3): 322.

Chong M S, Watson H C. Prediction of heat and mass transfer during compression in reciprocating compressors. *Proc Int Compressor Eng Conf at Purdue,* West Lafayette USA, 1976, p.466.

Christensen K G. Use of CO_2 as primary and secondary refrigerant in supermarket applications. *Proc IIR/IIF 20th Int Congress of refrigeration,* Sydney, Australia, 1999.

Chumak I G et al. Thermodynamic appraisal of heat pumps with CO_2 refrigerant. *Proc Int Conf IIR. Applications for natural refrigerants,* Aarhus, Denmark, 1996. p.633.

Churchill S W. Friction factor equation spans all fluid-flow regimes. *Chemical Engineering,* 1977; (7): 91.

Colebrook C F. Turbulent flow in pipes with particular reference to the transition region between smooth and rough pip laws. *J Inst Civil Eng.* 1939; 11: 133.

Collier J G, Thome J R. Convective boiling and condensation, 3rd ed, Oxford University Press, 1994.

Collings D A et al. Compressor mechanism comparison for R744 application. *Proc Int Compressor Eng Conf at Purdue,* West Lafayette USA, 2002.

Connaghan M. Experimental investigation of a breadboard model of a carbon dioxide U.S. army environmental control unit. *Proc Int Refrigeration Conf at Purdue,* West Lafayette, USA, 2002.

Corberán J M, et al. Modelling of refrigeration piston compressors. *Proc Int Compressor Eng Conf at Purdue,* West Lafayette USA, 2000, p.571.

Culter B, Hwang Y, Bogdanic L, Radermacher R. Development of a transcritical environmental control unit. *Proc 4th IIR – Gustav Lorentzen Conference at Purdue,* West Lafayette, USA, 2000, p.91.

Dechamps C J, Ferreira R T, Prata A T. The effective flow and force areas in compressors valves. *Proc Int Compressor Eng Conf at Purdue,* West Lafayette USA, 1988, p.104.

DeSantis R, Gironi F, Marrelli L. Vapor–liquid equilibrium from a hard-sphere equation of state. *Ind Eng Chem Fund,* 1976; 15:183.

Dittus F W, Boelter L M K. Heat transfer in automobile radiators of the tubular type. *University of California Publications Of Engineering,* 1930; 2: 443.

Domanski P A, Didion D A, Mulroy W J, Parise J. A simulation model and study of hydrocarbon refrigerants for residential heat pump systems. *Proc Int Conf IIR, New applications of natural working fluids in refrigeration and air conditioning,* Hanover, Germany, 1994, p.339.

Domanski P A, McLinden M O. A simplified cycle simulation for the performance rating of refrigerants and refrigerant mixtures. *Int J Refrig.* 1992; 15 (2): 81.

Dorin F, Neksa P. CO_2 compressors and equipment, use and availability. *Proc Inst of Refrig, Beating the ban – is CO_2 available alternative,* London, UK, 2000, p.1

Dreiman N, Bunch R. Concept of hermetic rotary compressor with carbon dioxide as working fluid. *Proc IMechE Conf, Compressors and Their Systems at City University,* London, UK, 2003, p.451.

Driver R W. Applications for the hinge-vane positive displacement compressor-expander. *Proc IMechE Conf, Compressors and Their Systems at City University,* London, UK, 1999, p.339.

Eggen G, Aflekt K. Commercial refrigeration with ammonia and CO_2 as working fluids. *Proc Int Conf IIR, Natural working fluids '98,* Oslo, Norway, 1998, p.237.

Eggen G, Rosvik S. Commercial refrigeration with ammonia and CO_2 as working fluids. *Workshop Proc IEA ANNEX 22, Compression systems with natural working fluids,* Torndheim, Norway, 1995, p. 189.

Eichelberg G. Some new investigations on old combustion engine problems. *Engineering*, 1939; 148: 547.

Ely J F, Hanley H J M. Prediction of transport properties. 1. Viscosity of fluids and mixtures. *Ind Eng Chem Fund,* 1981; 20: 323.

Ely J F, Hanley H J M. Prediction of transport properties. 2. Thermal conductivity of pure fluids and mixtures. *Ind Eng Chem Fund,* 1983; 22: 90.

Enkemann T, Arnemann M. Investigation of CO_2 as a secondary refrigerant. *Proc Int Conf IIR, New applications of natural working fluids in refrigeration and air conditioning,* Hanover, Germany, 1994, p.721.

Enkemann T, Kruse H, Ostendorp P A. CO_2 as heat pump working fluid for retrofitting hydronic heating systems in Western Europe. *Workshop Proc IEA/IIR, CO_2 technology in refrigeration, heat pump and air conditioning systems,* Trondheim, Norway, 1997, p.79.

Fagerli B E. A theoretical comparison of the mechanical control behaviour of a R744 and R134a automotive a/c compressor. *Proc Int Compressor Eng Conf at Purdue,* West Lafayette USA, 2002.

Fagerli B E. An investigation of possibilities for CO_2 compression in a hermetic compressor. *Proc IIR Int Conf, Applications for natural refrigerants,* Aarhus Denmark, 1996a, p.489.

Fagerli B E. CO_2 compressor development. *Workshop Proc IEA/IIR, CO_2 technology in refrigeration, heat pump and air conditioning systems,* Trondheim, Norway, 1997, p.295.

Fagerli B E. Development and experiences with a hermetic CO_2 compressor. *Proc Int Compressor Eng Conf at Purdue,* West Lafayette USA, 1996b, p.229.

Fagerli B E. On the feasibility of compressing CO_2 as working fluid in scroll compressors. *Proc Int Refrigeration Conf at Purdue,* West Lafayette USA, 1998, p.165.

Fagerli B E. Theoretical analysis of compressing CO_2 in scroll compressors. *Proc Int Conf IIR, Natural working fluids '98,* Oslo, Norway, 1998, p.204.

Fagotti F et al. Heat transfer modelling in a reciprocating compressor. *Proc Int Compressor Eng Conf at Purdue,* West Lafayette USA, 1994, p.605.

Fagotti F, Prata A. A new correlation for instantaneous heat transfer between gas and cylinder in reciprocating compressors. *Proc Int Compressor Eng Conf at Purdue,* West Lafayette USA, 1998, p.871.

Fang X, Bullard C W, Hrnjak P S. Heat transfer and pressure drop of gas coolers. *ASHRAE Transactions*: Research. 4440, 2001.

Ferreira R T, Driessen J L. Analysis of the influence of valve geometric parameters on the effective flow and force areas. *Proc Int Compressor Eng Conf at Purdue,* West Lafayette USA, 1986, p.632.

Ferreira R T, Lilie D E. Evaluation of the leakage through the clearance between piston and cylinder in hermetic compressors. *Proc Int Compressor Eng Conf at Purdue,* West Lafayette USA, 1984, p. 1.

Filonenko G K. Hydraulic resistance in pipes. *Teploenergetika.* 1954; 1 (4): 40.

Fleming J S, Brown J, Shu P C. The influence of oil stiction on compressor valve performance. *Proc 16th Int Congr of Refrigeration*, Paris France, 1983

Fleming J S, et al. The economics of compressor modelling. *Proc IMechE Conf, Compressors and Their Systems at City University,* London UK, 2001, p.359.

Fleming J. Carbon dioxide as the working fluid in heating and/or cooling systems. *International Institute of Refrigeration Bulletin,* . , 2003.

Försterling S, Tegethoff W, Köhler J. Theoretical an experimental investigation on carbon dioxide compressors for mobile air conditioning systems and transport refrigeration. *Proc Int Refrigeration Conf at Purdue,* West Lafayette USA, 2002.

Friedel L. Improved friction pressure drop correlations for horizontal and vertical two phase pipe flow. *Proc European Two Phase Flow Group Meeting, Ispra Italy,* Paper 2, 1979.

Friley J R, Hamilton J F. Characterization of reed type compressor valves by the finite element method. *Proc Int Compressor Eng Conf at Purdue,* West Lafayette USA, 1966, p.295.

Fukuta M, Radermacher R, Lindsay D, Yanagisawa T. Performance of vane compressor for CO_2 cycle. *Proc 4thIIR – Gustav Lorentzen Conference at Purdue,* West Lafayette, USA, 2000, p.339.

Fukuta M, Yanagisawa T, Ogi Y, Radermacher R. Cycle performance of CO_2 cycle with vane compressor-expander combination. *Proc IMechE Conf, Compressors and Their Systems at City University,* London, UK, 2001, p.315.

Fushs P H. Heat transfer and pressure drop during flow of evaporating liquid in horizontal tubes and bends. *PhD thesis.* Norwegian Institute of Technology. 1975.

Garimella S. Conduction effects in cross-counter flow supercritical gas coolers for natural refrigerants. *21st IIR Int Congr of Refrigeration,* Washington D.C., USA, 2003.

Gentner H. Passenger car air conditioning using carbon dioxide as refrigerant. *Proc Int Conf IIR, Natural working fluids '98,* Oslo, Norway, 1998, p.259.

Gerlach R C, Berry R A. Effect of heat transfer and related variables on compressor performance. *Proc 4th Annual Int Reciprocating Machinery Conf,* San Antonio USA, 1989.

Ghajar A J, Asadi A. Improved forced convective heat-transfer correlations for liquids in the near-critical region. *AIAA J.* 1986; 24 (12): 2030.

Giacomelli E, Giorgetti M. Investigation on oil stiction in ring valves. *Proc Int Compressor Eng Conf at Purdue,* West Lafayette USA, 1974, p.167.

Giannavola M S et al. Experimental investigations of an automotive heat pump prototype for military, SUV and compact cars. *Proc 4thIIR – Gustav Lorentzen Conference at Purdue,* West Lafayette, USA, 2000, p.115.

Gnielinski V. New equations for heat and mass transfer in turbulent pipe and channel flow. *Int Chem Eng.* 1976; 16(2): 359.

Gosney W B. Principles of refrigeration. Cambridge University Press. 1982.

Griner G C, Gatecliff G W, Richardson H. Static and dynamic analysis of reed valves using a minicomputer based finite element system. *Proc Int Compressor Eng Conf at Purdue,* West Lafayette USA, 1980, p.172.

Groll E A. Absorption/compression cycle using working pair CO_2/acetone. *19th Int Congr of Refrigeration,* The Hague, The Netherlands, 1995, p.812.

Groll E A. Modelling of absorption/compression cycles using working pair carbon dioxide/acetone. *ASHRAE Transactions*, Vol. 103, 2002, p. 863.

Guilpart J, Leducq D, Belance R. Computer subroutines for rapid evaluation of natural refrigerants thermodynamic properties. *Proc IIR Int Conf, Natural working fluids '98,* Oslo Norway, 1998, p.449.

Gungor K E, Winterton H S. Simplified general correlation for saturated flow boiling and comparisons of correlations with data. *Chem Eng Res Des.* 1987; 65 (2): 148.

Gupta V K, Prasad M. Optimum thermodynamic performance of three-stage refrigeration systems. *Int J Refrig.* 1983; 6 (2): p 103.

Haaland S E. Simple and explicit formulas for the friction factor in turbulent pipe flow. *J Fluids Eng.* 1983; 105 (1): 89.

Hafner A, Pettersen J, Skaugen G, Neksa P. An automobile HVAC system with CO_2 as the refrigerant. *Proc Int Conf IIR, Natural working fluids '98,* Oslo, Norway, 1998, p. 335.

Hafner A. Experimental study on heat pump operation of prototype CO_2 mobile air conditioning system. *Proc 4thIIR – Gustav Lorentzen Conference at Purdue,* West Lafayette, USA, 2000, p.177.

Halozan H, Rieberer R. CO_2 as refrigerant – possible applications. *Proc 4thIIR – Gustav Lorentzen Conference at Purdue,* West Lafayette, USA, 2000, p.43.

Hamilton J F. Extensions of mathematical modelling of positive displacement type compressors. *Ray W. Herrick Laboratories, Purdue University*, West Lafayette USA, 1974.

Hartmann D L. Global Physical Climatology. *Academic Press*,1994, p. 319-330.

Hasengawa H et al. Experimental and theoretical study of hermetic CO_2 scroll compressor. *Proc 4thIIR – Gustav Lorentzen Conference at Purdue,* West Lafayette, USA, 2000, p.347.

Herbas T B, Berlinck E C, Uriu A T, Marques R P, Parise A R. Steady-state simulation of vapour compression heat pumps. *Int J Energy Research.* 1993: 17 (9): 801.

Hesse U, Arenmann H. Carbon dioxide-hydrocarbon mixtures as alternative fluids in refrigeration systems. *Proc Int Conf IIR, New applications of natural working fluids in refrigeration and air conditioning,* Hanover, Germany, 1994, p.711.

Hesse U, Spauchus H O. Lubricants for carbon dioxide. *Proc Int Conf IIR, Applications for natural refrigerants,* Aarhus, Denmark, 1996, p.605.

Hesse U. Secondary refrigerant systems for supermarket application with brine or carbon dioxide. *Proc Int Conf at Purdue*, West Lafayette, USA, 1996, p.369.

Heyl P et al. Expander-compressor for a more efficient use of CO_2 as refrigerant. *Proc Int Conf IIR, Natural working fluids '98,* Oslo, Norway, 1998, p.195.

Heyl P, Preussner S, Kraus W E. The CO_2 heat pump project at the TU Dresden. *Workshop Proc IEA/IIR, CO_2 technology in refrigeration, heat pump and air conditioning systems,* Trondheim, Norway, 1997, p.217.

Heyl P, Quack H. Free piston expander-compressor for CO_2 – design, applications and results. 20^{th} *IIR/IIF Int Congr of Refrigeration,* Sydney, Australia, 1999.

Hihara E, Tanaka S. Boiling heat transfer of carbon dioxide in horizontal tubes. *Proc 4^{th}IIR – Gustav Lorentzen Conference at Purdue,* West Lafayette, USA, 2000, p.279.

Hiller C C, Glicksman L R. Detailed modelling and computer simulation of reciprocating refrigeration compressors. *Proc Int Compressor Eng Conf at Purdue,* West Lafayette USA, 1976, p.12.

Hirao T et al. Development of air conditioning system using CO_2 for automobile. *Proc 4^{th}IIR – Gustav Lorentzen Conference at Purdue,* West Lafayette, USA, 2000, p.193.

Hirata T, Fujiwara K. Improvement of mobile air conditioning system from point of global warming problems. *Proc Int Conf IIR, Natural working fluids '98,* Oslo, Norway, 1998, p.269.

Hiwata A. et al. Performance investigation with oil injection to compression chambers on CO_2 scroll compressor. *Proc Int Compressor Eng Conf at Purdue,* West Lafayette USA, 2002.

Holst J. Test rig for CO_2 automotive air conditioning compressor. *Proc Int Conf IIR. Applications for natural refrigerants,* Aarhus, Denmark, 1996, p.651.

Howard H. Non-dimensional parameter development for transcritical cycles. *Proc Int Refrigeration Conf at Purdue,* West Lafayette USA, 2002.

Huber M L, Ely J F. A predictive extended corresponding states model for pure and mixed refrigerants including an equation of state for R-134a. *Int J Refrigeration,* 1994; 17(1): 18.

Huber M, Gallagher J, Mclinden M, Morrison G. Standard Reference Database 23: Thermodynamic and transport properties of refrigerants and refrigerant mixtures-REFPROP, Ver 5.0. *NIST*, 1996

Huff H J, Hwang Y, Radermacher R. High-side pressure optimisation in transcritical CO_2 cycles with work extracting expansion devices. *Proc SAE automotive alternative refrigerant systems symposium,* Arizona, USA, 2002a.

Huff H J, Lindsay D, Radermacher R. Positive displacement compressor and expander simulation. *Proc Int Compressor Eng Conf at Purdue,* West Lafayette USA, 2002b.

Hughes J M, Qvale E B, Pearson J T. Experimental investigation of some thermodynamic aspects of refrigeration compressors. *Proc Int Compressor Eng Conf at Purdue,* West Lafayette USA, 1972, p.516.

Hwang Y, Radermacher R. Boiling heat transfer correlation for carbon dioxide. *Proc Int Conf, Heat transfer issues in 'natural' Refrigerants.* Maryland, USA, Vol. 1, 1997b, p. 44.

Hwang Y, Radermacher R. Carbon dioxide refrigeration system. *Workshop Proc IEA/IIR, CO_2 technology in refrigeration, heat pump and air conditioning systems,* Trondheim, Norway, 1997a, p.71.

Hwang Y, Radermacher R. Development of hermetic carbon dioxide compressor. *Proc Int Refrigeration Conf at Purdue,* West Lafayette USA, 1998a, p.171.

Hwang Y, Radermacher R. Evaluation of carbon dioxide heat exchanger. *Proc Int Conf, Heat transfer issues in 'natural' Refrigerants.* Maryland, USA, Vol. 1, 1997c, p. 83.

Hwang Y, Radermacher R. Experimental evaluation of CO_2 water heater. *Proc Int Conf IIR, Natural working fluids '98,* Oslo, Norway, 1998b, p.368.

Hwang Y, Radermacher R. Experimental investigation of the CO_2 refrigeration cycle. *ASHRAE Transactions*: Symposia. CH-99-22-2, 1999.

Ibrahim A, Fleming J S. Leakage characteristics of CO_2 reciprocating compressors at off design conditions. *Proc IMechE Conf, Compressors and Their Systems at City University,* London UK, 2003a, p.111.

Ibrahim A, Fleming J S. Performance assessment of a trans-critical co_2 heat pump using a reciprocating compressor. *Proc IIR/IIF 21st Int Congress of refrigeration,* Washington, USA, 2003b.

Imaichi K, Ishii N, Saito S., Imasu K. Leakage effects on indicator diagrams at stopping of reciprocating compressors. *Proc Int Compressor Eng Conf at Purdue,* West Lafayette USA, 1978, p.283.

Inagaki M et al. Pointing to the future: two-stage CO_2 compression. *Proc Int Conf, Heat transfer issues in 'natural' Refrigerants.* Maryland, USA, Vol. 1, 1997, p. 58.

Infante Ferreira C A, Boukens R A. Carbon dioxide – secondary coolant or refrigerant for cascade systems? *Proc Int Conf IIR. Applications for natural refrigerants,* Aarhus, Denmark, 1996, p.185.

Infante Ferreira C A, Soesanto S. CO_2 in comparison with R404A. *Proc Int Conf, Heat transfer issues in 'natural' refrigerants,* Maryland, USA, Vol. I, 1997, p.108.

Infante Ferreira C A. Potential of carbon dioxide in two refrigeration applications commonly encountered in the Netherlands. *Proc Int Refrigeration Conf at Purdue,* West Lafayette, USA, 1998, p.127.

Jacobs J. Analytical and experimental techniques for evaluating compressor performance losses. *Proc Int Compressor Eng Conf at Purdue*, West Lafayette USA, 1976, p.116.

Jakobsen A. Improving efficiency of trans-critical CO_2 cycles using an ejector driven by heat rejected in the gas cooler. *Proc IIR/IIF 20th Int Congress of refrigeration,* Sydney, Australia, 1999.

Jörgensen S H. Variable automotive CO_2 compressor. *Proc Int Refrigeration Conf at Purdue,* West Lafayette USA, 1998, p.159.

Jung D S, Radermacher R. Performance simulation of single-evaporator domestic refrigerators charged with pure and mixed refrigerants. *Int J Refrig.* 1991; 14 (4): 223.

Kakac S, Shah R, Aung W. Handbook of single-phase convective heat transfer. John Wiley & Sons, Inc., 1987.

Karll B. Computer simulation of the cylinder process in a compressor based on the First Law of Thermodynamics. *Proc Int Compressor Eng Conf at Purdue,* West Lafayette USA, 1972, p.18.

Kauf F. Determination of the optimum high pressure for transcritical CO_2 refrigeration cycles. *Int J Therm Sci.* 1999; 38 (4): 325.

Kauffeld M, Christensen K G. Reefer 2000, a new energy-efficient reefer container concept using carbon dioxide as refrigerant. *Proc Int Conf IIR, Natural working fluids '98,* Oslo, Norway, 1998, p.351.

Keribar R, Morel T. Heat transfer and component temperature prediction in reciprocating compressors. *Proc Int Compressor Eng Conf at Purdue,* West Lafayette USA, 1988, p.454.

Khalifa H E, Liu X. Analysis of stiction effect on the dynamics of compressor suction valve. *Proc Int Compressor Eng Conf at Purdue,* West Lafayette USA, 1998, p.87.

Kim M S, Bullard C W. Development of a microchannel evaporator model for a CO_2 air-conditioning system. *Energy.* 2001; 26 (10): 931.

Kim S G, Kim M S. Experiment and simulation on the performance of an autocascade refrigeration system using carbon dioxide as a refrigerant. *Int J Refrig.* 2002; 25 (8): 1093

Kim S T, Min T S. Computer simulation for a small hermetic compressor. *Proc Int Compressor Eng Conf at Purdue,* West Lafayette USA, 1984, p.148.

Knudsen H J, Jensen P H. Heat transfer coefficient for boiling carbon dioxide. *Workshop Proc IEA/IIR, CO_2 technology in refrigeration, heat pump and air conditioning systems,* Trondheim, Norway, 1997, p.319.

Koelet P C, Gray T B. Industrial refrigeration: principles, design and applications. Hampshire [England], 1992.

Kohler J, Sonnekalb M, Kaiser H, Koecher W. Carbon dioxide as a refrigerant for vehicle air-conditioning with application to bus air-conditioning. *Int CFC and Halon Alternatives Conf & Exhibition,* 1995, p.376.

Kohler J. Kaiser H, Lauterbach B. CO_2 as refrigerant for bus air conditioning and transport refrigeration. *Workshop Proc IEA/IIR, CO_2 technology in refrigeration, heat pump and air conditioning systems,* Trondheim, Norway, 1997, p.139.

Kohler J. Sonnekalb M, Kaiser H. A transcritical refrigeration cycle with carbon dioxide for bus air conditioning and transport refrigeration. *Proc Int Refrig Conf at Purdue,* West Lafayette USA, 1998, p.121.

Kornhauser A, Smith J L. Application of a complex Nusselt number to heat transfer during compression and expansion. *ASME J Heat Transfer,* 1994; 116: 536.

Krasnoshchekov E A, Kuraeve I V, Protopopov V S. Local heat transfer of carbon dioxide under super-critical pressure under cooling conditions. *High Temperature.* 1969; 7 (5): 922.

Kruse H, Heidelck R, Suss J. The application of CO_2 as a refrigerant. *International Institute of Refrigeration Bulletin,* 99.1, 1999.

Kuraeve I V, Protopopov V S. Mean friction coefficients for turbulent flow of a liquid at a supercritical pressure in horizontal circular tubes. *High Temperature.* 1974; 12 (1): 218.

Kusakari K et al. Innovative hot water supply technology conducive to arresting global warming – development and significance of CO_2 heat pump water heater. *Proc 18th Congress of World Energy Council,* Buenos Aires, Argentine, 2001.

Lawton B. Effect of compression and expansion on instantaneous heat transfer in reciprocating internal combustion engines. *Proc IMechE,* 1987; 201: 175.

Lee J P, Hwang Y, Radermacher R. An experimental investigation of oil retention characteristics in CO_2 air conditioning systems. *Proc Int Refrigeration Conf at Purdue,* West Lafayette USA, 2002.

Lee K P. A simplistic model of cyclic heat transfer phenomena in closed spaces. *Proc18th Intersociety Energy Conversion Eng Conf,* 1983, p.720.

Lee S, Singh R, Moran M J. First law analysis of a compressor using a computer simulation model. *Proc Int Compressor Eng Conf at Purdue,* West Lafayette USA, 1984, p.577.

Lemke N et al. Stratified tap water storage system for carbon dioxide heat pumps. *Proc IIR/IIF 20th Int Congress of refrigeration,* Sydney, Australia, 1999, p.

Li D, Baek J S, Groll E A, Lawless P B. Thermodynamic analysis of vortex tube and work output expansion devices for the transcritical carbon dioxide cycle. *Proc 4th IIR – Gustav Lorentzen Conference at Purdue,* West Lafayette, USA, 2000, p.433.

Li H et al. Field and laboratory evaluation of lubricants for CO_2 refrigeration. *Proc Int Refrigeration Conf at Purdue,* West Lafayette USA, 2002.

Li H, Rajewski T E. Experimental study of lubricant candidates for the CO_2 refrigeration systems. *Proc 4th IIR – Gustav Lorentzen Conference at Purdue,* West Lafayette, USA, 2000, p.409.

Liang H, Kuehn T H. Irreversibility analysis of a water-to-water mechanical compression heat pump. *Energy,* 1991; 16 (6): 883.

Liao S M, Zhao T S, Jakobsen A. A correlation of optimal heat rejection pressures in transcritical carbon dioxide cycles. *Appl Therm Eng.* 2000; 20 (9): 831.

Liao S, Jakobsen A. Optimal heat rejection pressure in transcritical carbon dioxide air conditioning and heat pump systems. *Proc Int Conf IIR, Natural working fluids '98,* Oslo, Norway, 1998, p.346.

Liu R., Zhou Z. Heat transfer between gas and cylinder wall of refrigerating reciprocating compressor. *Proc. Int Compressor Eng Conf at Purdue*, West Lafayette USA, 1984, p.110.

Liu Y, Yu Y. Prediction for the sealing characteristics of piston rings of a reciprocating compressor. *Proc Int Compressor Eng Conf at Purdue*, West Lafayette USA, 1986, p.973.

Liu Z, Winterton R H S. A general correlation for saturated and subcooled flow boiling in tubes and annuli based on a nucleate pool boiling. *Int J Heat and Mass Transfer.* 1991; 34 (11): 2759.

Lockhart R W, Martinelli R C. Proposed correlation of data for isothermal two-phase, two-component flow in pipes. *Chem Eng Prog.* 1949; 45 (3): 39.

Lorentzen G, Pettersen J. A new, efficient and environmentally benign system for car air-conditioning. *Int J Refrig.* 1993; 16 (1): 4.

Lorentzen G. Natural refrigerants, a complete solution. *Proc IIR Conf CFCs*, Padua, Italy, 1994a, p. 317-328.

Lorentzen G. On the performance of automatic compressor valves. *Proc 9th Int Congr of Refrigeration,* 1955.

Lorentzen G. Revival of carbon dioxide as a refrigerant. *Int J Refrig.* 1994c; 17 (5): 292.

Lorentzen G. The use of natural refrigerants: a complete solution to the CFC/HCFC predicament. *Int J Refrig.* 1995; 18(3): p 190.

Lorentzen G. Trans-critical vapor compreeioncycle device. Patent WO 90/07683, 1990.

Lorentzen G. Use of CO_2 in commercial refrigeration – an energy efficient solution. *Proc Int Conf IIR, New applications of natural working fluids in refrigeration and air conditioning,* Hanover, Germany, 1994b, p.703.

Machu E H. Valve dynamics of reciprocating compressor valves with more than one degree of freedom. *Proc IMechE Conf, Compressors and Their Systems at City University,* London, UK, 2001, p.503.

MacLaren J F T et al. A model of a single stage reciprocating gas compressor accounting for flow pulsations. *Proc Int Compressor Eng Conf at Purdue,* West Lafayette USA, 1974, p.144.

MacLaren J F T, Kerr S V. An analytical and experimental study of self-acting valves in a reciprocating air compressor. *Proc IMechE*, 1969; 184: 24.

Manepatil S, Yadava G S, Nakra B C. Theoretical study of design and operating parameters on the reciprocating compressor performance. *Proc Int Compressor Eng Conf at Purdue,* West Lafayette USA, 1998, p.821.

Manzione J A, Calkins P E. Evaluation of transcritical CO_2 using an automotive compressor in a packaged unitary military ECU. *ASHRAE Transactions*: Symposia. HI-02-13-1, 2002.

Manzione J A. Development of carbon dioxide environmental control unit for the US army. *Proc Int Conf IIR, Natural working fluids '98,* Oslo, Norway, 1998, p.251.

Mars H, van Son A, Touber S. Improvement of compressor valve design by the use of hybrid simulation. *Proc 15th Int Congr of Refrigeration,* Venezia, Italy, 1979, B2 94.

McEnaney R P et al. Experimental comparison of mobil a/c systems when operated with transcritical CO_2 versus conventional R134a. *Proc Int Refrig Conf at Purdue,* West Lafayette USA, 1998, p.145.

McEnaney R P et al. Performance of the prototype of a transcritical R744 mobile a/c system. *Proc SAE Int Congress and Exposition,* 1999, paper 99-01-0872.

Mclinden M O, Lemmon E W, Jacobsen R T. Thermodynamic properties for the alternative refrigerants. *ASHRAE/NIST Refrigerants Conf*, Gaithersburg, USA, 1997, p.135.

McMullan J T. Refrigeration and the environment - issues and strategies for the future. *Int J Refrig.* 2002; 25(1): 89.

Meyer J, Seeton C J. Low pressure CO_2 air conditioning system. *Proc SAE automotive alternative refrigerant systems symposium,* Arizona, USA. 2000.

Meyer W A, Thompson H D. An analytical model of heat transfer to the suction gas in a low-side hermetic refrigeration compressor. *Proc Int Compressor Eng Conf at Purdue,* West Lafayette USA, 1990, p.898.

Moody L F. An approximate formula for pipe friction factors. *Mech Eng.* 1947; 69: 1005.

Moody L F. Friction factors for pipe flow. *ASME Transactions.* 1944; 671.

Mozurkewich G et al. Simulated performance and cofluid dependence of a CO_2-cofluid refrigeration cycle with wet compression. *Int J Refrig.* 2002; 25 ( ): 1123.

Mukaiyama H et al. Experimental results and evaluation of residential CO_2 heat pump water heater. *Proc 4thIIR – Gustav Lorentzen Conference at Purdue,* West Lafayette, USA, 2000, p.67.

Neksa P et al. Development of semi-hermetic CO_2 compressors. 20th *IIR/IIF Int Congr of Refrigeration,* Sydney, Australia, 1999.

Neksa P, Aarlien R. Current status of heat pumps with carbon dioxide as working fluid. *Proc Int Refrig Conf at Purdue,* West Lafayette USA, 1998a, p.139.

Neksa P, Dorin F, Bekstad H, Bredesen A. Development of two-stage semi-hermetic compressors. *Proc 4thIIR – Gustav Lorentzen Conference at Purdue,* West Lafayette, USA, 2000, p.355.

Neksa P, Girotto S. Schieloe P A. Commercial refrigeration using CO_2 as refrigerant – system design and experimental results. *Proc Int Conf IIR, Natural working fluids '98,* Oslo, Norway, 1998b, p.227.

Neksa P, Pekstad H, Zakeri G R, Schiefloe P A. CO_2 heat pump water heater: characteristics, system design and experimental results. *Int J Refrig,* 1998c; 21 (3): 172.

Neksa P, Pekstad H. CO_2 heat pump Prototype system – experimental results. *Workshop Proc IEA/IIR, CO_2 technology in refrigeration, heat pump and air conditioning systems,* Trondheim, Norway, 1997, p.201.

Neksa P. CO_2 heat pump systems. *Int J Refrig,* 2002; 25 (4): 421.

Neksa P. Trans-critical vapour compression heat pumps. Proc Int Conf IIR. New Applications of natural working fluids in refrigeration and air conditioning, Hnnover. Germany, 1994, p. 395.

Ng E H, Tramschek A B, McLaren J F T. Computer simulation of a reciprocating compressor using a real gas equation of state. *Proc Int Compressor Eng Conf at Purdue,* West Lafayette USA, 1980, p.33.

Ohkawa T et al. Development of hermetic swing compressors for CO_2 refrigerant. *Proc Int Compressor Eng Conf at Purdue,* West Lafayette USA, 2002.

Olson D A. Heat transfer of super-critical carbon dioxide flowing in a cooled horizontal tube. *Proc 4thIIR – Gustav Lorentzen Conference at Purdue,* West Lafayette, USA, 2000, p.251.

Ortiz T M, Groll E A. Validation of a new model for the performance of carbon dioxide as a refrigerant for residential air conditioners. *Proc Int Refrigeration Conf at Purdue,* West Lafayette, USA, 2002.

Oslen B F. Chemical reactions in ammonia, carbon dioxide and hydrocarbon systems. *Proc Int Conf IIR, Applications for natural refrigerants,* Aarhus, Denmark, 1996, p.593.

Park S N, Kim M S. Performance of autocascade refrigeration system using carbon dioxide and R134a. *Proc Int Conf IIR, Natural working fluids '98,* Oslo, Norway, 1998, p.311.

Parsch W, Brunsch B. CO_2 compressors new technology for cool heads and warm feet. *Proc 7th LuK Symposium,* 2002, p.123.

Patil A S, Manzione J A. US Army CO_2 development program. *Proc IIR/IIF 20th Int Congress of refrigeration,* Sydney, Australia, 1999.

Patil A S. Natural working fluids – military advantages and opportunities. *Proc Int Conf IIR, Natural working fluids '98,* Oslo, Norway, 1998, p.247.

Pearson A B. Carbon dioxide – new uses for an old refrigerant. *Proc IIR/IIF Conf 21st International Congress of Refrigeration*, Washington USA, 2003.

Pearson A B. New developments in industrial refrigeration. *ASHRAE Journal,* March 2001, p. 54.

Pearson S F. Development of improved secondary refrigerants. *Proc Institute of Refrigeration,* London, UK, 1993.

Pearson S F. Natural selection – the struggle for survival in the competitive world of refrigeration equipment. *Proc IIR/IIF 20th Int Congress of refrigeration,* Sydney, Australia, 1999.

Petrov N E, Popov V N. Heat transfer and hydraulic resistance with turbulent flow in a tube of water under supercritical parameters. *Thermal Engineering.* 1985; 35(5), (6): 577.

Petrov N E, Popov V N. Heat transfer and resistance of carbon dioxide being cooled in the supercritical region. *Thermal Engineering,* 1985; 32(3): 131.

Pettersen J et al. A comparative evaluation of CO_2 and HCFC-22 residential air-conditioning systems in a Japanese climate. *Workshop Proc IEA/IIR, CO_2 technology in refrigeration. Heat pump and air conditioning systems*, Trondheim, Norway, 1997, p.177.

Pettersen J et al. Development of compact heat exchangers for CO_2 air-conditioning systems. *Int J Refrig.* 1998; 21 (3): 180.

Pettersen J et al. Recent advances in CO_2 refrigeration. *Proc IIR/IIF 19th Int Congress of refrigeration,* Hague, Netherlands, 1995, p.961.

Pettersen J, Rieberer R, Leister A. Heat transfer and pressure drop characteristics of super-critical carbon dioxide in microchannel tubes under cooling. *Proc 4th IIR – Gustav Lorentzen Conference at Purdue,* West Lafayette, USA, 2000a, p.99.

Pettersen J, Rieberer R, Munkejord S T. Heat transfer and pressure drop characteristics of evaporating carbon dioxide in microchannel tubes under cooling. *Proc 4th IIR – Gustav Lorentzen Conference at Purdue,* West Lafayette, USA, 2000b, p.107.

Pettersen J, Skaugen G. Operation of transcritical CO_2 vapour compression circuits in vehicle air conditioning. *Proc Int Conf IIR, New Applications of natural working fluids in refrigeration and air conditioning,* Hnnover, Germany, 1994, p. 495-506.

Pettersen J. An efficient new automobile air-conditioning system based on co_2 vapour compression. *ASHRAE Transactions*: Symposia. OR-94-5-3, 1994.

Pettersen J. Experimental results of carbon dioxide in compression systems. *ASHRAE/NIST Refrigerants Conf*, Gaithersburg, USA, 1997, p.27.

Petukhov B S, Kirillov V V. On heat exchange at turbulent flow of liquid in pipes. *Teploenergetika.* 1958; 4(4): 63.

Petukhov B S, Kurganov V A, Gladuntsov A I. Heat transfer in turbulent pipe flow of gases with variable properties. *Heat Transfer Sot Res.* 1973; 5(4):109.

Petukhov B S, Popov V N. Theoretical calculation of heat exchange and frictional resistance in turbulent flow in tubes of an incompressible fluid with thermophysical properties. *High Temperature,* 1963; 1(1): 69.

Petukhov B S. Heat transfer and friction in turbulent pipe flow with variable physical properties. *Advances in Heat Transfer,* 1970; 6: 503.

Pfriem H. Periodic heat transfer at small pressure Fluctuations, *NASA TM-1048*, 1943.

Pitla S S, Groll E A, Ramadhayani S. New correlation to predict the heat transfer coefficient during in-tube cooling of turbulent supercritical CO_2. *Int J Refrig.* 2002; 25 (7): 887.

Pitla S S, Groll E A, Ramadhyani S. New correlation for the heat transfer coefficient during in-tube cooling of turbulent supercritical carbon dioxide. *Proc 4th IIR – Gustav Lorentzen Conference at Purdue,* West Lafayette, USA, 2000, p.259.

Pitla S S, Robinson D M, Groll E A, Ramadhyani S. Heat transfer from supercritical carbon dioxide in tube flow: a critical review. *Int J HVAC&R Research.* 1998; 4 (3): 281.

Polyakov A F. Heat transfer under supercritical pressure. *Advances in Heat Transfer,* 1991; 21: 1.

Prakash R, Singh R. Mathematical modelling and simulation of refrigeration compressors. *Proc Int Compressor Eng Conf at Purdue,* West Lafayette USA, 1974, p.274.

Prandtl L. Guide to flow theory. Vieweg und Sohn, Braunschweig. 1944

Prasad M, Prasad R. A new approach to determine optimum operating parameters for multistage refrigeration system. *Proc IIR/IIF 17th Int Congress of refrigeration,* Vienna Austria, 1987, vol B, p.601.

Prasad M. Optimum interstage pressure for 2-stage refrigeration systems. *ASHRAE J,* 1981; 23(1), p. 58.

Preissner M et al. Comparison of automotive air – conditioning systems operating with CO_2 and R134A. *Proc 4thIIR – Gustav Lorentzen Conference at Purdue,* West Lafayette, USA, 2000, p.185.

Quack H, Kraus W E. Carbon dioxide as a refrigerant for railway refrigeration and air conditioning. *Proc Int Conf IIR, New applications of natural working fluids in refrigeration and air conditioning,* Hanover, Germany, 1994, p.489.

Reckenwald G W, Ramsey J W, Patanker S V. Predictions of heat transfer in compressor cylinders. *Proc Int Compressor Eng Conf at Purdue,* West Lafayette USA, 1986, p.159.

Renz H. Semi-hermetic reciprocating and screw compressors for carbon dioxide cascade systems. *20th IIR/IIF Int Congr of Refrigeration,* Sydney, Australia, 1999.

Richter M R, et al. Transcritical CO_2 heat pump for residential application. *Proc 4thIIR – Gustav Lorentzen Conference at Purdue,* West Lafayette, USA, 2000, p.9.

Rieberer R, Gassler M, Halozan H. Control of CO_2 heat pump. *Proc 4thIIR – Gustav Lorentzen Conference at Purdue,* West Lafayette, USA, 2000, p.75.

Rieberer R, Halozan H. Design of heat exchangers for CO_2-heat pump water heaters. *Proc Int Conf, Heat transfer issues in 'natural' Refrigerants.* Maryland, USA, Vol. 1, 1997a, p. 75.

Rieberer R, Halozan H. CO_2 heat pumps in controlled ventilation systems. *Proc Int Conf IIR, Natural working fluids '98,* Oslo, Norway, 1998a, p. 167.

Rieberer R, Halozan H. CO_2 heat pumps water heater: simulation and test results. *Proc Int Conf IIR, Natural working fluids '98,* Oslo, Norway, 1998b, p. 133.

Rieberer R, Kasper G, Halozan H. CO_2 – a chance for once through heat pump heaters. *Workshop Proc IEA/IIR, CO_2 technology in refrigeration, heat pump and air conditioning systems,* Trondheim, Norway, 1997b, p.193.

Rieberer R, Neksa P, Schiefloe P. CO_2 Heat pumps for space heating and tap water heating. *Proc IIR/IIF 20th Int Congress of refrigeration,* Sydney, Australia, 1999.

Rieberer R. CO_2 properties. *IIR Workshop Proc on CO_2 Technology in Refrigeration, Heat Pump and Air Conditioning systems*, Mainz, Germany, 1999.

Rigola J et al. Parametric study of hermetic reciprocating compressors. *Proc Int Compressor Eng Conf at Purdue,* West Lafayette USA, 1996, p.529.

Robinson D M, Groll E A. Efficiencies of transcritical CO_2 cycles with and without an expansion turbine. *Workshop Proc IEA/IIR, CO_2 technology in refrigeration, heat pump and air conditioning systems,* Trondheim, Norway, 1997, p.59.

Robinson D M, Groll E A. Introducing $ACCO_2$ – a public domain air- to-air simulation model of the transcritical carbon dioxide cycle. *Proc 4th IIR – Gustav Lorentzen Conference at Purdue,* West Lafayette, USA, 2000, p.33.

Robinson D M, Groll E A. Using carbon dioxide in a transcritical vapour compression refrigeration cycle. *Proc Int Refrigeration Conf at Purdue,* West Lafayette USA, 1996, p.329.

Rolfsman L. CO_2 and NH_3 in the supermarket ICA- focus. *Proc Int Conf IIR, Applications for natural refrigerants,* Aarhus, Denmark, 1996, p.219.

Rolfsman L. CO_2 experience from Swedish installations. *ASHRAE Transactions*: Symposia. AC-02-7-3, 2002.

Rolfsman L. Plant design considerations for cascade systems using CO_2. *Proc IIR/IIF 20th Int Congress of refrigeration,* Sydney, Australia, 1999.

Röttger W, Kruse H. Analysis of the working cycle of single – stage refrigeration compressors using digital computers. *Proc Int Compressor Eng Conf at Purdue,* West Lafayette USA, 1976, p.18.

Rowland F S, Molina M J. Stratospheric sink for chloroflouromethanes: chlorine atom-catalysed destuction of ozone. *Nature*, 1974, Vol 249, p. 810-812.

Rundle R W, Tarnawski V R, Aittomäki A. The optimum performance of a two stage cycle with an open intercooler. *Proc IIR/IIF 19th Int Congress of refrigeration,* Hague, Netherlands, 1995, vol. IIIa, p.475.

Saikawa M et al. A basic study on CO_2 heat pumps especially for hot tap water supply. *Workshop Proc IEA/IIR, CO_2 technology in refrigeration, heat pump and air conditioning systems*, Trondheim, Norway, 1997, p.53.

Saikawa M et al. Development of prototype of CO_2 heat pump heater for residential use. *Proc 4th IIR – Gustav Lorentzen Conference at Purdue,* West Lafayette, USA, 2000, p.51.

Saikawa M, Hashimoto K. An experimental study on the behaviour of CO_2 heat pump cycle. *Proc Int Conf IIR, Natural working fluids '98,* Oslo, Norway, 1998, p.177.

Sakamoto S, Giese P. SANDEN / LuK cooperation on CO_2 compressors. *Proc SAE automotive alternative refrigerant systems symposium,* Arizona, USA, 2000.

Sasaki M. et al. The effectiveness of a refrigeration system using CO_2 as a working fluid in the trans-critical region. *ASHRAE Transactions*: Research 4537, 2002.

Scheideman F. et al. Thermodynamic and acoustic simulation of positive displacement refrigeration compressors. *Proc Int Compressor Eng Conf at Purdue,* West Lafayette USA, 1978, p.290.

Schmidt E L, Klocker K, Flacke N, Steimle F. A heat pump drier using carbon dioxide as the working fluid. *Proc IIR/IIF 20th Int Congress of refrigeration,* Sydney, Australia, 1999.

Schmidt E L, Klocker K, Flacke N, Steimle F. Applying the transcritical CO_2 process to a drying heat pump. *Int J Refrig,* 1998; 21 (3): 202

Schonfeld H, Kraus W E. Calculation and simulation of a heat exchanger; supercritical carbon dioxide-water. *Proc Int Conf, Heat transfer issues in 'natural' Refrigerants.* Maryland, USA, Vol. 1, 1997, p. 36.

Schrock V E, Grossman L M. Forced convective boiling studies. *Rept No. 73308 – UCX - 2182.* University of California, Berkeley. 1959.

Schwerler D, Hamilton J F. An analytical method for determining effective flow and force areas for refrigeration compressor valving systems. *Proc Int Compressor Eng Conf at Purdue,* West Lafayette USA, 1972, p.30.

Scott T C, Davis G L. Effect of compressor improvements on air-conditioning system performance. *Proc Design and Operation of Industrial Compressors Conf.* University of Strathclyde, Glasgow UK, 1978, p.77.

Seeton C et al. Solubility, viscosity, boundary lubrication and miscibility of CO_2 and synthetic lubricants. *Proc 4thIIR – Gustav Lorentzen Conference at Purdue,* West Lafayette, USA, 2000, p.409.

Seeton C J et al. Reduced pressure carbon dioxide cycle for vehicle climate control. *Proc SAE alternate refrigerant forum,* Arizona, USA, 1999.

Shah M M. A new correlation for heat transfer during boiling through pipes. *ASHRAE Transactions.* 1976; vol 82, part 2: 66.

Shah M M. Chart correlation for saturated boiling heat transfer: equations and further studies. *ASHRAE Transactions.* 1982; vol 88, part 1: 185.

Shiva Prasad B G. Fast response temperature measurements in a reciprocating compressor. *Proc Int Compressor Eng Conf at Purdue,* West Lafayette USA, 1992b, p.1385.

Shiva Prasad B G. Heat transfer in reciprocating compressors – a review. *Proc Int Compressor Eng Conf at Purdue,* West Lafayette USA, 1998, p.857.

Shiva Prasad B G. Regenerative heat transfer in reciprocating compressors. *Proc 7th Annual Int Reciprocating Machinery Conf,* Denver USA, 1992a.

Skaugen G, Svensson M C. Dynamic modeling and simulation of a transcritical CO_2 heat pump unit. *Proc Int Conf IIR, Natural working fluids '98,* Oslo, Norway, 1998, p.183.

Skaugen G. Simulation of extended surface heat exchangers using CO_2 as refrigerant. *Proc 4thIIR – Gustav Lorentzen Conference at Purdue,* West Lafayette, USA, 2000, p.295.

Smith H J. Effect of piston bore clearance in small refrigeration compressors. *Proc IMechE*, 1961; 175: 991.

Soedel W. Introduction to computer simulation of positive displacement type compressors. *Ray W. Herrick Laboratories, Purdue University*, West Lafayette USA. 1972.

Sotecker W F, Jones J W. Refrigeration and air conditioning, 2nd ed, McGraw Hill, Inc., 1982.

Span R, Wagner W. A new equation of state for carbon dioxide covering the fluid region from the triple point temperature to 1100 K at pressure to 800 MPa. *J Phys Chem Ref Data,* 1996; 26: 1509.

Squarer D, Kothman R E. Digital computer simulation of a reciprocating compressor – a simplified analysis. *Proc Int Compressor Eng Conf at Purdue,* West Lafayette USA, 1972, p.502.

Stehr H. Oil stiction-investigations to optimise reliability of compressor valves. *Proc IMechE Conf, Compressors and Their Systems at City University*, London UK, 2001, p.477.

Steimle F, Flacke N, Klocker K. Design and construction of a cascade refrigeration plant for the energetic investigation of natural working fluid combinations. *Proc IIR/IIF 20th Int Congress of refrigeration,* Sydney, Australia, 1999b.

Steimle F, Schmidt E L. Alternative refrigerants for refrigeration and air conditioning. *Proc IIR/IIF Conf 20th International Congress of Refrigeration*, Sydney, 1999a.

Steimle F. CO_2 – drying heat pumps. *Workshop Proc IEA/ IIR, CO_2 technology in refrigeration heat pump and air conditioning systems,* Trondheim, Norway, 1997, p.243.

Stene J. IEA Annex 22 - Compression systems with natural working fluids. Status and outlook for the project. *Proc Int Conf IIR, Applications for natural refrigerants*, Aarhus, Denemark, 1996, p. 65.

Stoecker W F. Design of thermal systems, 3rd ed, McGraw Hill, New York, 1989.

Stokar M, Trepp C. Compression heat pump with solution circuit, part 1: design and experimental results. *Int J Refrig.* 1987; 10 (2): 87.

Stosic N, Smith I K, Kovacevic A. A twin screw combined compressor and expander for CO_2 refrigeration systems. *Proc Int Compressor Eng Conf at Purdue,* West Lafayette USA, 2002.

Strommen I, Bredesen A M, Eikevik T, Neksa P, Pettersen J, Aarlien R. Heat pumping systems for the next century. *Proc IIR/IIF Conf 20th International Congress of Refrigeration*, Sydney, Australia, 1999.

Sun S, Ren T. New method of thermodynamic computation for a reciprocating compressor: computer simulation of working process. *Int J Mech Sci,* 1995; 37(4): 343.

Süss J, Kruse H. Design criteria of CO_2 compressors for vapour compression cycles. *Proc Int Meeting IIR, Heat pump systems, energy efficiency and global warming,* Linz, Austria, 1997, p.139.

Süss J, Kruse H. Efficiency of the indicated process of CO_2 compressors. *Int J Refrig.* 1998; 21 (3): 194.

Süss J, Kruse H. Research on the behaviour of refrigeration compressors using CO_2 as the refrigerant. *Proc Int Compressor Eng Conf at Purdue,* West Lafayette USA, 1996, p.223.

Süss J. Low capacity hermetic type compressor for transcritical CO_2 applications. *Proc Int Compressor Eng Conf at Purdue,* West Lafayette USA, 2002.

Swamee P K, Jain A K. Explicit equations for pipe-flow problems. *J Hydraulic Division ASCE.* 1976; 102 (5): 657.

Tadano M et al. Development of the CO_2 hermetic compressor. *Proc 4th IIR – Gustav Lorentzen Conference at Purdue.* West Lafayette, USA, 2000, p.323.

Taylor C R. Carbon dioxide – based refrigerating systems. *ASHRAE Journal.* September 2002, p.22.

Tegethoff W J, Lemke N, Koehler J. Equation oriented modelling of a/c systems application to R134a and CO_2 a/s systems for buses. *Proc IIR/IIF 20th Int Congress of refrigeration,* Sydney, Australia, 1999.

Threlkeld J L. Thermal environmental engineering, 2nd ed, Prentice-Hall, Inc., NJ. 1970.

Todescat M L, Fagotti F, et al. Thermal energy analysis in reciprocating hermetic compressors. *Proc Int Compressor Eng Conf at Purdue,* West Lafayette USA, 1992, p.1419.

Tong L S, Tang Y S. Boiling heat transfer and two-phase flow, 2nd ed, Taylor& Francis, 1997.

Trella T J, Soedel W. Effect of valve port gas inertia on valve dynamics – Part I, Simulation of poppet valve - Part II, flow retardation at valve opening. *Proc Int Compressor Eng Conf at Purdue,* West Lafayette USA, 1974, p.190.

Villadsen V. Reciprocating compressors for refrigeration and heat pump application. *Int J Refrig,* 1985; 8 (5): 262.

Wertenbach J, Caesar R. An environmental evaluation of an automobile air-conditioning system with CO_2 versus HFC-134a as refrigerant. *Proc Int Conf IIR, Natural working fluids '98,* Oslo, Norway, 1998, p.279.

Wertenbach J, Kauf F. High pressure refrigeration system with CO_2 in automobile air-conditioning. *Workshop Proc IEA/IIR, CO_2 technology in refrigeration heat pump and air conditioning systems,* Trondheim. Norway, 1997, p.127.

White F. M. Fluid Mechanics. McGraw-Hill, 3rd ed., 1994, ISBN 0-07-113765-3

White S D, Yarrall M G, Cleland D J, Hedley R A. Modelling the performance of a transcritical CO_2 heat pump for high temperature heating. *Int J Refrig,* 2002; 25 (4): 479.

Woollatt D. A simple numerical solution for compressor valves with one degree of freedom. *Proc Int Compressor Eng Conf at Purdue,* West Lafayette USA, 1972, p.30.

Woschni G. A universally applicable equation for the instantaneous heat transfer coefficient in the internal combustion engine. *SAE Transactions,* 1967; 76: 3065.

Xin R, Hatzikazakis P. Reciprocating compressor performance simulation. *Proc Int Compressor Eng Conf at Purdue,* West Lafayette USA, 2000, p.1.

Yanagisawa T, Fukuta M, Ogi Y, Ishii D. Performance characteristics of compressors working with carbon dioxide. *Proc 20th Int Congr of Refrigeration,* Sydney Australia, 1999.

Yanagisawa T, Fukuta M, Sakai T, Kato H. Basic operating characteristics of reciprocating compressor for CO_2 cycle. *Proc 4th IIR – Gustav Lorentzen Conference at Purdue*, West Lafayette USA, 2000, p.331.

Yarrall M G et al. Performance of a transcritical CO_2 heat pump for the food processing industries. *Proc Int Conf IIR, Natural working fluids '98,* Oslo, Norway, 1998, p.159.

Yarrall M G. Performance of a transcritical CO_2 heat pump for simultaneous refrigeration and water heating. *Proc IIR/IIF 20th Int Congress of refrigeration,* Sydney, Australia, 1999.

Yin J et al. Experimental and model comparison of transcritical CO_2 versus R 134a and R410 system performance. *Proc Int Conf IIR, Natural working fluids '98,* Oslo, Norway, 1998, p.331.

Yin J M, Bullard C W, Hrnjak P S. Design strategies for R744 gas coolers. *Proc 4th IIR – Gustav Lorentzen Conference at Purdue,* West Lafayette, USA, 2000, p.315.

Yoon S H, Cho E S, Kim M S, Kim Y. Studies on the evaporative heat transfer and pressure drop of carbon dioxide near the critical point. *Proc IIR/IIF 21st Int Congress of refrigeration,* Washington, USA, 2003.

Younglove B A, Mclinden M O. An international standard equation-of-state formulation of the thermodynamic properties of refrigerant 123 (2,2-dihloro-1,1,1-trifluroethane). *J Phys Chem Ref Data,* 1994; 23: 731.

Yu Y, Tan Y. The experiment and analysis of drag coefficient of the ring-type valve. *Proc Int Compressor Eng Conf at Purdue,* West Lafayette USA, 1986, p.632.

Zakeri G R, Neksa P, Pekstad H. Results and experiences with the first commercial pilot plant CO_2 heat pump water heater. *Proc 4th IIR – Gustav Lorentzen Conference at Purdue,* West Lafayette, USA, 2000, p.59.

Zhang Z, Qu T, Yu Y. The study of using carbon dioxide as the alternative of R502 in industrial refrigeration applications. *Proc Int Refrigeration Conf at Purdue,* West Lafayette, USA, 1998, p.115.

Zhao Y et al. Evaporation heat transfer coefficients of ammonia and CO_2 inside a smooth tube. *Proc Int Conf, Heat transfer issues in 'natural' Refrigerants.* Maryland, USA, Vol. 1, 1997, p. 93.

Zhao Y, Molki M, Ohadi M, Dessiatoun S. Flow boiling of CO_2 in microchannels. *ASHRAE Transactions*: Symposia. DA-00-2-1, 2000.

Zhao Y, Molki M, Ohadi M, Franca F, Radermacher R. Flow boiling of CO_2 with miscible oil in microchannels. *ASHRAE Transactions*: Research. 4505, 2002.

Zingerli A, Groll E A. Influence of refrigeration oil on the heat transfer and pressure drop of supercritical CO_2 during in-tubes cooling. *Proc 4th IIR – Gustav Lorentzen Conference at Purdue,* West Lafayette, USA, 2000, p.269.

Zubair S M, Yaqub M, Khan S H. On optimum interstage pressure for two-stage and mechanical-subcooling vapor-compression refrigeration cycles. *J Solar Energy Eng, ASME Trans,* 1995; 117, p.64.

APPENDICES

Appendix A

Compressor Model

Sample of Input Data File

Reciprocating Compressor Input Data File

General Data :

NC	IR[1]	IR[2]	IR[3]	IR[4]	IR[5]
1	35	0	0	0	0
XW[1]	XW[2]	XW[3]	XW[4]	XW[5]	
1	0	0	0	0	
NREFST	IEQN	IHT	NCYC	STEP(deg)	
3	2	2	3	0.1	

R(m)	L(m)	DCYL(m)	LTC(m)	NCYL	RPM	DSL(m)	LSL(m)
0.0064	0.048	0.016	0.00056	1	3000	0.008	0.0

TS(deg C)	PS(kPa)	PD(kPa)
10	3500	8500

Suction Valve Data :

NSV	DSV(m)	DSP(m)	MSV(kg)	HSV(m)	NSSV	MSSV(kg)	KSSV(N/m)	PLSV(N)
1	0.00486	0.00486	0.0001439	0.00043	1	0	3887	0.0

CDSV(-)	PDSV(-)	ZSV(-)	SPSV(-)	STSV(-)
0.68	0.86	0.6	0.0	0.0

Discharge Valve Data :

NDV	DDV(m)	DDP(m)	MDV(kg)	HDV(m)	NSDV	MSDV(kg)	KSDV(N/m)	PLDV(N)
1	0.00444	0.00444	0.0001176	0.0004	1	0	3872	0.0

CDDV(-)	PDDV(-)	ZDV(-)	SPDV(-)	STDV(-)
0.83	0.51	0.6	0.0	0.0

Leakage :

IOIL	NPR	bPR(m)	hl(mm)
1	2	0.002	0.0032

Appendix B

Transcritical CO_2 Cycle Model

Sample Of Input Data File

Residential Heat Pump Input Data File

General Data :

NC	IEQN
1	2

IR[1]	IR[2]	IR[3]	IR[4]	IR[5]
35	0	0	0	0

XW[1]	XW[2]	XW[3]	XW[4]	XW[5]
1	0	0	0	0

Evaporator (OD Coil):

DTE(deg C)	TEIN(deg C)	TEOUT(deg C)	
0.0	8.30	2.7	
RUAE(kW/C)	RDPE(kPa)	ETD(m)	AE(m2)
1.7875	54.0	0.00262	2.73

Reciprocating Compressor :

IHT(-)	NCYC	STEP(deg)	ETAEL(%)	ETAM(%)			
2	3	0.1	100	100			
R(m)	L(m)	DCYL(m)	LTC(m)	NCYL	RPM	DSL(m)	LSL(m)
0.0064	0.048	0.016	0.00056	12	1450	0.008	0.0

Suction Valve Data :

NSV	DSV(m)	DSP(m)	MSV(kg)	HSV(m)	NSSV	MSSV(kg)	KSSV(N/m)	PLSV(N)
1	0.00486	0.00486	0.0001439	0.00043	1	0	3887	0.0

CDSV(-)	PDSV(-)	ZSV(-)	SPSV(-)	STSV(-)
0.68	0.86	0.6	0.0	0.0

Discharge Valve Data :

NDV	DDV(m)	DDP(m)	MDV(kg)	HDV(m)	NSDV	MSDV(kg)	KSDV(N/m)	PLDV(N)
1	0.00444	0.00444	0.0001176	0.0004	1	0	3872	0.0

CDDV(-)	PDDV(-)	ZDV(-)	SPDV(-)	STDV(-)
0.93	0.51	0.6	0.0	0.0

Piston Rings :

IOIL(-)	NPR	bPR(m)	hl(mm)
1	2	0.002	0.0032

Gas Cooler (ID Coil):

PGC(kPa)	TCIN(deg C)	TCOUT(deg C)	
8000	26.7	32.7	
RUAC(kW/C)	RDPC(kPa)	CTD(m)	AC(m2)
0.8625	115	0.00261	4.1

Internal Heat Exchanger :

EFF(-)	DHXHP(kPa)	DHXLP(kPa)
1.0	237	194

Appendix C

Transcritical CO_2 Cycle Model

Sample Of Output Data File

Output Data File

General Performance Data

EVAPORATOR HEAT TRANSFER BALANCE
ITERATION NO: 146.00
QED= 0.033074

SYSTEM ENERGY BALANCE
ITERATION NO: 30.000
BAL= 0.020604

COOLER HEAT TRANSFER BALANCE
ITERATION NO: 6.0000
QCD= -0.00082525

State	Temp (degC)	Pressure (kPa)	Sp Vol (m^3/kg)	Enthalpy (kJ/kg)	Entropy (kJ/kgC)
1	23.907	3232.0	0.013893	185.09	0.025123
2	102.11	8115.0	0.0069921	237.26	0.042099
3	23.850	8000.0	0.0012783	-21.519	-0.76280
4	10.350	7763.0	0.0011131	-59.128	-0.89095
5	-0.0037	3480.0	0.0011749	-59.128	-0.87252
6	-0.5928	3426.0	0.010036	142.59	-0.13253
7	-0.5928	3426.0	0.010036	142.59	-0.13253

Ave. Effective Temp Difference of Cooler: 14.094
Ave. Effective Temp Difference of Evaporator: 5.3118

Thermal Resistance of HTF and tube in Cooler (K/kW): 0.81085
Thermal Resistance of HTF and tube in Evaporator (K/kW): 0.54145

Average Refrigerant Heat Transfer Coefficient in Cooler (kW/m2K): 699.73
Average Refrigerant Heat Transfer Coefficient in Evaporator (kW/m2K): 2036.5

Refrigerant Mass Flow Rate: 0.047052 kg/s

Pressure ratio: 2.5108

Performance	Cycle	System
Work:	52.171 kJ/kg	2.6274 kW
Internal H.EX.:	37.608 kJ/kg	1.7696 kW
Cooling:	201.72 kJ/kg	9.5279 kW
Heating:	258.78 kJ/kg	12.155 kW

COP: 4.6263

Reciprocating Compressor Performance Data

WMOL= 44.010

GAMMA = 1.2634
W_th (kJ/kg) = 42.524
P_th (kW) = 2.1756

THETA1= 21.100
PSVO= 3232.0
VSVO= 2.5199e-006

THETA2= 185.80
PSVC= 3238.4
VSVC= 3.2166e-005

THETA3= 276.80
PDVO= 8115.0
VDVO= 1.5984e-005

THETA4= 360.10
PDVC= 8066.4
VDVC= 1.3512e-006

GAMMA_E= 1.4770

GAMMA_C= 1.3136

MIND (kg/s)= 0.050362
MOUT (kg/s)= 0.047052
BLOWBY (kg/s)= 0.0033103
ETA_VC = 0.95309
ETA_VT = 1.0000
ETA_IND= 0.93818
ETA_V= 0.87652

PMIN (kPa)= 3024.7
PMAX (kPa)= 8461.0

PS_AVE (kPa)= 3156.5
PD_AVE (kPa)= 8250.3

Alpha_s (W/m2 K) = 1936.5
Qs (W)= 0.00000
TSS (K)= 297.06

QNET (W)= 2791.4 (QADD= 4221.5 , QREJ= 7012.9)
PSUC (W)= 648.94
PDIS (W)= 574.25

PIND (kW)= 2.6274
ETAC= 0.81510